

Washington University in St. Louis

Washington University Open Scholarship

McKelvey School of Engineering Theses &
Dissertations

McKelvey School of Engineering

10-30-2024

Impacts of Phosphate and Residual Free Chlorine on the Precipitation, Stability and Dissolution of Lead Corrosion Products

Yao Ma

Washington University – McKelvey School of Engineering

Follow this and additional works at: https://openscholarship.wustl.edu/eng_etds

Recommended Citation

Ma, Yao, "Impacts of Phosphate and Residual Free Chlorine on the Precipitation, Stability and Dissolution of Lead Corrosion Products" (2024). *McKelvey School of Engineering Theses & Dissertations*. 1108.
https://openscholarship.wustl.edu/eng_etds/1108

This Dissertation is brought to you for free and open access by the McKelvey School of Engineering at Washington University Open Scholarship. It has been accepted for inclusion in McKelvey School of Engineering Theses & Dissertations by an authorized administrator of Washington University Open Scholarship. For more information, please contact digital@wumail.wustl.edu.

WASHINGTON UNIVERSITY IN ST. LOUIS

McKelvey School of Engineering
Department of Energy, Environmental & Chemical Engineering

Dissertation Examination Committee:

Daniel E. Giammar, Chair

Peng Bai

Jeffrey G. Catalano

Young-Shin Jun

Fangqiong Ling

Impacts of Phosphate and Residual Free Chlorine on the Precipitation, Stability and Dissolution
of Lead Corrosion Products

by

Yao Ma

A dissertation presented to
the McKelvey School of Engineering
of Washington University in
partial fulfillment of the
requirements for the degree
of Doctor of Philosophy

December 2024
St. Louis, Missouri

© 2024, Yao Ma

Table of Contents

List of Figures	vii
List of Tables	xviii
Acknowledgments.....	xxi
Abstract	xxiv
Chapter 1: Introduction.....	1
1.1 Background	1
1.1.1 Lead Service Lines.....	1
1.1.2 Lead Contamination in Water.....	3
1.1.3 Lead Corrosion Control with Phosphate Inhibitors	4
1.1.4 Lead Corrosion Product Lead Oxide (PbO ₂).....	6
1.2 Research Objectives	10
1.3 Dissertation Overview.....	11
Chapter 2: Improved Control of Lead Release from Boosting Orthophosphate and Removing Polyphosphate from a Blended Phosphate Corrosion Inhibitor.....	15
2.1 Introduction	16
2.2 Material and Methods.....	20
2.2.1 Set-up of Pipe Loops.....	20
2.2.2 Preparation of Water Chemistry.. ..	22
2.2.3 Experiment Stages.....	22
2.2.4 Analytical Methods.....	23
2.3 Results and Discussion.....	26
2.3.1 Phosphate, pH, and Residual Free Chlorine in Lead Pipe Assemblies.	26
2.3.2 Lead Release in the Presence of Blended and Orthophosphate Corrosion Inhibitors.....	28
2.3.3 Comparison of Measured and Predicted Equilibrium Dissolved Lead Concentrations.....	34
2.3.4 Statistical Significance Analysis on Dissolved and Total Lead Concentrations.....	37
2.3.5 Characterization of Scale Morphology and Element Distribution... ..	38
2.3.6 Characterization of Scale Crystalline Phases.....	40
2.3.7 Element Concentrations of Scales on the Pipes of the Pipe Loops during Different Stages...	42

2.3.8	Corrosion Control Implications...	44
2.4	Conclusions	45
2.5	Acknowledgements	46
Chapter 3: Stability of Lead(IV) Oxide in a Lead Pipe Scale and its Potential Role in Corrosion Control		47
3.1	Introduction	48
3.2	Material and Methods.....	53
3.2.1	Materials	53
3.2.2	Formation of PbO ₂ on Lead Coupons..	53
3.2.3	Analytical Methods.....	56
3.2.4	Characterization of PbO ₂ on Lead Coupons.....	57
3.2.5	Impact of Stagnation Time on the Free Chlorine Depletion and Lead Release..	59
3.2.6	Identification of the Threshold Residual Free Chlorine to Maintain the Stability of PbO ₂ in Scale..	60
3.3	Results and Discussion.....	61
3.3.1	Residual Free Chlorine Decay during Water Stagnation...	61
3.3.2	Effect of Residual Free Chlorine and Stagnation Time on Lead Release.....	63
3.3.3	Threshold Residual Free Chlorine that Maintains the Stability of Lead(IV) PbO ₂ Scale...68	
3.3.4	The Corresponding ORP to Threshold Residual Free Chlorine.....	72
3.4	Environmental Implications.	73
3.5	Acknowledgements	75
Chapter 4: Dynamics of Lead Release from Pipes Containing PbO ₂ in response to Free Chlorine Depletion during Water Stagnation		76
4.1	Introduction	77
4.2	Material and Methods.....	80
4.2.1	Set-up of Pipe Loop Reactors	80
4.2.2	Preparation of Water Chemistry.	81
4.2.3	Experiment Design.....	81
4.2.4	Analytical Methods.....	84
4.3	Results and Discussion.....	86
4.3.1	Establishment of PbO ₂ as a Dominant Component in Pipe Scales.....	86
4.3.2	Stability of PbO ₂ Lead Scale during Water Stagnation.....	88
4.3.3	Threshold Residual Free Chlorine to Maintain the Stability of PbO ₂ Lead Scales.....	92

4.4	Implications for Corrosion Control in PbO ₂ -dominated Lead Pipes.....	96
4.4.1	Develop and Preserve PbO ₂ in Pipe Scales.....	96
4.4.2	Threshold Free Chlorine Concentration.....	98
4.4.3	Release of Dissolved Lead and Particulate Lead.....	100
4.5	Conclusions.....	101
4.6	Acknowledgements	102
Chapter 5: Effect of Orthophosphate in Lead Release from PbO ₂ -rich Layers on Elemental Lead		104
5.1	Introduction	105
5.2	Material and Methods.....	110
5.2.1	Materials	110
5.2.2	Lead Coupon Experiments.....	111
5.2.3	Pipe-loop Experiments.....	113
5.2.4	Analytical Methods.....	116
5.2.5	Scale Analysis.....	116
5.3	Results and Discussion.....	118
5.3.1	Lead Coupon Study: Effects of Orthophosphate on Lead Release and Scale Composition... 118	
5.3.2	Pipe-loop Study: Effects of Orthophosphate on Lead Release and Scale Composition... 125	
5.3.3	Pipe-loop and Coupon Study... ..	136
5.3.4	Implications for Lead Corrosion Control.....	139
5.4	Conclusions.....	140
5.5	Acknowledgements	141
Chapter 6: Exploring Variations in Properties of Lead Pipe Scales from Different Drinking Water Systems		142
6.1	Introduction	143
6.2	Material and Methods.....	145
6.2.1	Public Water Systems in the Research.....	145
6.2.2	Scale Analysis Methods.....	146
6.2.3	Layering of Lead Scales.....	146
6.2.4	Chemical Equilibrium Model Predictions of Crystalline Lead Phases Present.... ..	147
6.2.5	Statistical Significance Analysis.....	147
6.3	Results and Discussion.....	147

6.3.1	Lead-carbonate Solids: pH and dissolved organic carbon.....	147
6.3.2	Lead (IV) oxide solids: Disinfectant and Corrosion Control Method.....	151
6.3.3	Lead-phosphate Solids: Phosphate Inhibitors and Water Chemistry.....	152
6.3.4	Amorphous Materials: Elements in Scale Phase and Finished Water... ..	153
6.3.5	Applications of Scale Analysis Techniques and Their Limitations... ..	154
6.4	Environmental Implications.	155
6.5	Acknowledgements	157
Chapter 7: Conclusions and Recommendations for Future Work		158
7.1	Conclusions	158
7.2	Recommendations for Future Work.....	162
References.....		165
Appendix A1: Supporting Information for Chapter 2.....		184
A1.1	Lead Pipes Used in the Pipe Loop Experiments	184
A1.2	Flow Regime and Water Preparation	185
A1.3	Scale Characterization and Water Sample Analysis.. ..	187
A1.4	pH and the Residual Free Chlorine Change during the Experiment.....	189
A1.5	Coefficient of Variation (CV) for Total and Dissolved Lead Concentrations.. ..	188
A1.6	Summary of Lead Concentrations in Different Treatment Stages	196
A1.7	Total Lead Concentrations After First 6-h Stagnation Period of Each Week.....	201
A1.8	Additional Scale Analysis Results and Summary	203
Appendix A2: Supporting Information for Chapter 3.....		209
A2.1	Chemicals for Water Chemistry Preparation.	209
A2.2	Electrochemical polarization.....	209
A2.3	Calculations of PbO ₂ Generation from Electrochemical Polarization and Chemical Conditioning.	210
A2.4	Changes in Residual Free Chlorine and pH during Chemical Conditioning	211
A2.5	Equilibrium Solubility of Lead(IV) Oxide.....	212
A2.6	Calculations of Threshold Free Chlorine	212
Appendix A3: Supporting Information for Chapter 4.....		224
A3.1	Harvesting Procedures for Pipes.. ..	224
A3.2	Set-up of Pipe-loop Reactors.....	224
A3.3	Preparation of Water Chemistry.....	225

A3.4	Scale Analysis	225
A3.5	Calculations of Threshold Free Chlorine	227
A3.6	Calculations of the Proportion of Pb Released from Scales.....	228
Appendix A4: Supporting Information for Chapter 5.....		240
A4.1	Formation of PbO ₂ on Lead Coupons..	240
A4.2	Set up of Pipe-loop Reactors.....	240
A4.3	Preparation of Water Chemistry.....	241
A4.4	Scale Analysis	241
A4.5	Statistical Analysis	242
Appendix A5: Effect of Water Blending on Lead Release from PbO ₂ -coated Lead Pipes		261
A5.1	Introduction.	261
A5.2	Materials and Methods	262
A5.2.1	Set-up of Pipe Loops.....	262
A5.2.2	Water Preparation and Blending	263
A5.2.3	Scale Analysis Methods.....	264
A5.2.4	Conditioning.....	265
A5.2.5	Water Blending Experiments.....	265
A5.2.6	Statistical Analysis Methods.....	265
A5.3	Results and Discussion.....	266
A5.3.1	Lead Release during Conditioning.....	266
A5.3.2	Lead Release during Experimental Phase	267
A5.3.3	Scale Analysis.....	270
A5.3	Conclusions.	274
Appendix A6: Supporting Information for Chapter 6.....		275
A6.1	Lead Pipe Harvesting Protocols	275
A6.2	Scale Analysis Methods	275
A6.3	Model Predication for Crystalline Lead Phase.....	276
A6.4	Lead-phosphate Solids: Phosphate Inhibitors and Water Chemistry	277
A6.5	Amorphous Material: Elements in Scale Phase and Finished Water.....	278
A6.6	Applications of Scale Analysis Techniques and Their Limitations	278

List of Figures

Figure 1.1: Schematic of lead service lines and premise plumbing to household (right) and formation of lead corrosion products in distribution systems (left).....	1
Figure 1.2: Equilibrium lead solubility for a system with 2.2 mM dissolved inorganic carbon (a) with no orthophosphate and (b) with orthophosphate of 1.5 mg/L as PO_4^{3-} (0.0156 mM). This DIC corresponds to that of Buffalo, NY, which distributes water at a pH of 7.5-7.9. Calculations were performed using MINTEQ 3.1.....	4
Figure 1.3: Lead solubility of plattnerite ($\beta\text{-PbO}_2$).....	6
Figure 1.4: pe-pH diagram for Pb in Buffalo water system (DIC equals 2.2mM) (a) with no orthophosphate and (b) with orthophosphate of 1.5 mg/L as PO_4^{3-} (0.0156 mM).....	8
Figure 1.5: (a) Reductive dissolution of lead oxide (PbO_2) due to disinfectant switch, and (b) factors affecting the dissolution rate of lead oxide (PbO_2).....	9
Figure 1.6: Illustrations of the studies presented in Chapters 2-6 of this dissertation.....	12
Figure 1.6: Overview of research objectives and chapters.....	13
Figure 2.1: Initial orthophosphate concentration (C:0.2, P:1.5 mg/L as PO_4) and concentration after one week during (a) treatment stage 1 (16 weeks in total) and (b) treatment stage 2 (11 weeks in total) for both control pipe loops (C1, C2, and C3) and test pipe loops receiving additional orthophosphate (P1, P2, and P3).The horizontal dashed line is the target initial orthophosphate concentration in the control and test experiments.....	26
Figure 2.2: Total lead concentrations presented (a) as the full data series for each pipe loop and (b) as box plots showing the variation and central tendency of each pipe loop. The conditioning stage only includes data starting in Week 18. The vertical red and blue lines indicate the beginning of treatment stages 1 and 2, respectively.....	30
Figure 2.3: (a) Average total lead and (b) dissolved lead concentrations with standard deviations in different test stages for the last seven weeks of each stage.....	31
Figure 2.4: Dissolved lead concentrations presented (a) as the full data series for each pipe loop and (b) as box plots showing the variation and central tendency of each pipe loop. The conditioning stage only includes data starting in Week 18. The vertical red and blue lines indicate the beginning of treatment stage 1 and 2, respectively.....	32
Figure 2.5: Equilibrium lead solubility for artificial Buffalo water with 2.2 mM dissolved inorganic carbon and 3.9 mM ionic strength for (a) control pipes: orthophosphate of 0.2 mg/L as PO_4^{3-} (0.0156 mM) and (b) test pipes: orthophosphate of 1.5 mg/L as PO_4^{3-} (0.0156 mM). Orange dots with error bars (standard deviations) indicate the dissolved lead at pH 8 for control and test pipe loops, respectively. Calculations were performed using Visual MINTEQ and its default	

database (relevant reactions indicated in Table A1.4). This database does not include any reactions for dissolved lead complexation with polyphosphate..... 36

Figure 2.6: The SEM image of the cross-section (top) and elemental mapping of different elements detected by EDS (bottom) for pipes at the end of treatment stage 1 for (a) test pipe P3 and (b) control pipe C3. The yellow line in SEM images corresponds to the line scans in the Appendix A1..... 38

Figure 2.7: SEM image of the cross-section (top) and elemental mapping of different elements detected by EDS (bottom) for pipe segments at the end of treatment stage 2 for (a) test pipe P3 and (b) control pipe C3. The yellow line in the SEM images corresponds to the line scan in the Appendix A1..... 39

Figure 2.8: XRD patterns obtained from scale materials removed from the surface of pipes (a) at the end of treatment stage 1 and (b) at the end of treatment stage 2. The XRD reference patterns are shown for hydrocerussite ($Pb_3(CO_3)_2(OH)_2$), quartz (SiO_2), elemental lead (Pb), cerussite ($PbCO_3$), phosphohedyphane ($Ca_2Pb_3(PO_4)Cl$) and litharge (PbO). Labels used throughout the patterns are peaks corresponding to solid phases abbreviated as H, Si, Pb, C, Ph and L in the same order as just mentioned..... 41

Figure 3.1: Information on the properties of the lead coupons with scales rich in PbO_2 provided by (a) optical images of a lead coupons before scale development, after electrochemical polarization, after chemical conditioning, and after the experiments. (b) XRD patterns of PbO_2 powder and the scale on lead coupons after electrochemical polarization, after chemical conditioning, and after the experiments. (c) Electron micrographs of the scale on lead coupons after electrochemical polarization, after chemical conditioning, and after the experiments. 58

Figure 3.2: Free chlorine decay in water with pure PbO_2 powder, lead coupons with PbO_2 -rich scale, bare lead coupons, and without any solids over 5 days from an initial concentration of 3.0 mg/L as Cl_2 (Solution pH: 8; Alkalinity: 91 mg/L as $CaCO_3$). The lines represent the fitted first-order kinetic model, and the error bars denote standard deviations calculated from the triplicate experiments..... 62

Figure 3.3: Free chlorine decay (top part of each panel) and dissolved lead concentration with and without free chlorine readjustment (bottom part of each panel) at initial concentrations of (a) 3.0 mg/L (b) 2.0 mg/L (c) 1.0 mg/L, and (d) 0.5 mg/L as Cl_2 (Solution pH: 8; Alkalinity: 91 mg/L as $CaCO_3$). The error bars denote standard deviations calculated from the triplicates..... 64

Figure 3.4: Dissolved lead concentrations with free chlorine controlled at constant concentrations of (a) 0.3-0.4 mg/L, (b) 0.2-0.3 mg/L, and (c) 0.1-0.2 mg/L for five days. One longer experiment (20 days) measured (d) dissolved lead concentration with chlorine controlled at threshold residual free chlorine (0.2-0.3 mg/L) (Solution: pH 8 and 91 mg/L as CaCO₃ alkalinity). The error bars denote standard deviations calculated from duplicate experiments..... 69

Figure 3.5: Diagram of processes influencing PbO₂ formation, dissolution, and stability on metal lead surface. From left to right the diagram illustrates (1) the formation and stability of PbO₂ in the presence of sufficient residual free chlorine, (2) free chlorine depletion in the presence of reductants in water, and (3) dissolved and particulate lead and dissolved lead leaching into water when residual free chlorine is not sufficient. Pb(IV) reduction can be from reductants in the water or through electron transfer with the elemental lead..... 71

Figure 4.1: XRD patterns for top and bottom scale layers of (a) control pipe C1 and (b) test pipe T1. Reference patterns are shown in Figure A3.3 for hydrocerussite (Pb₃(CO₃)₂(OH)₂), lead (Pb), plattnerite (β-PbO₂) and litharge (PbO). Labels used throughout the patterns are peaks from corresponding solid phases abbreviated as H for hydrocerussite, Pb for elemental lead, P for plattnerite, and L for litharge..... 86

Figure 4.2: Stagnation experiment for free chlorine decay (top part of each panel) and lead concentrations (bottom part of each panel) at initial free chlorine of (a) 3.0 mg/L (b) 2.0 mg/L (c) 1.0 mg/L (d) 0.5 mg/L as Cl₂. The error bars denote standard deviations calculated from triplicate experiments..... 90

Figure 4.3: (a) Average dissolved lead and (b) average total lead concentrations for pipe loops during stagnation experiments at different initial free chlorine concentrations before (from beginning to D_t) and after the time (from D_t to 72 h) when the free chlorine concentration fell below the detection level (D_t). D_t values are 4 h, 8 h, 16 h and 16 h for initial free chlorine concentration at 0.5 mg/L, 1 mg/L, 2 mg/L and 3 mg/L as Cl₂..... 91

Figure 4.4: Dissolved and total lead concentration with free chlorine controlled at concentrations of (a) 2-3 mg/L (b) 1-2 mg/L (c) 0.6-1 mg/L (d) 0.4-0.6 mg/L (e) 0.2-0.4 mg/L (f) 0-0.2 mg/L. The error bars denote standard deviations calculated from the triplicate pipes..... 92

Figure 4.5: (a) Average dissolved lead and (b) average total lead concentrations for pipe loops at different residual free chlorine concentrations over a ten-day test. The error bars denote standard deviations calculated from the triplicate pipes..... 94

Figure 4.6: Conceptual diagrams for PbO₂ precipitation and dissolution in free-chlorinated water: (a) Oxidation of metal Pb(0) to dissolved Pb (Pb(II)_{diss}); (b) Precipitation of Pb(II) carbonate solids; (c) Oxidation of Pb(II) carbonate solids to PbO₂; (d) Reduction of PbO₂ to Pb(II) by reductants in water; (e) Lead release to water from the detachment of aqueous Pb²⁺ and particulate Pb..... 97

Figure 5.1: Coupon study: stagnation experiments for free chlorine decay (top part of the panel), dissolved and total lead concentrations (middle part and bottom part of the panel) at initial free chlorine concentrations of (a) 3.0 mg/L and (b) 0.5 mg/L as Cl₂. (c) Average dissolved lead and (d) average total lead concentrations for lead coupons at different continuously maintained stable free chlorine concentrations over a five-day test. The error bars denote standard deviations calculated from the triplicate experiments..... 119

Figure 5.2: Scanning electron micrographs (left side) of the cross-section of the with elemental mappings (right side) of different elements detected by EDS for (a) a control coupon before test, (b) a control coupon after test, (c) a test coupon before test, and (d) a test coupon after test.....122

Figure 5.3: Pipe-loop study: stagnation experiments for free chlorine decay (top part of the panel), dissolved and total lead concentrations (middle and bottom part of the panel) at initial free chlorine of (a) 3.0 mg/L and (b) 1.0 mg/L as Cl₂. (c) Average dissolved lead and (d) average total lead concentrations for lead coupons at different residual free chlorine concentrations over a five-day test. The error bars denote standard deviations calculated from the triplicate experiments..... 127

Figure 5.4: Box plots for (a) dissolved lead and (b) total lead concentrations for control and test (1 mg/L PO₄ orthophosphate) pipe loops under continuous flow conditions (ten weeks, free chlorine: 3 mg/L as Cl₂) and periodic flow conditions (five weeks, free chlorine: 1 mg/L as Cl₂)..... 131

Figure 5.5: XRD patterns of corrosion products in the scales of test pipes (T1-T3) before and after test. The pipes were used for real-world water use pattern experiments. Reference patterns were shown in Figure.S7 for H: hydrocerussite (Pb₃(CO₃)₂(OH)₂), Ph: phosphohedyphane Ca₂Pb₃(PO₄)₃Cl, Pb: lead (Pb), Pl: plattnerite (β-PbO₂) and L: litharge (PbO)..... 134

Figure 6.1: (a) pH and (b) DIC of PWSs for which certain Pb-C solids were observed through scale analysis. (c) DIC-pH diagram for predicted cerussite and hydrocerussite formation (lines demarcate regions in which a particular lead species is predicted) and the actual presences of Pb-C solids in PWSs shown with points. (d) Prediction accuracy for cerussite and hydrocerussite by the equilibrium model..... 148

Figure 6.2: (a) Free chlorine concentration in PWSs with and without PbO₂ solids. (b) Presence of PbO₂ solids in PWSs using free chlorine and blended-phosphate (8 PWSs in total). (c) Orthophosphate concentration in PWSs with and without Pb-P solids. (d) Presence of Pb-P solid in PWSs using blended-phosphate (9 PWSs in total)..... 150

Figure 6.3: Correlations between the presence of amorphous material and (a) mass concentrations of different elements (Al, Ca, Cu, Fe, Mg, Mn and P) in lead pipe scales, (b) concentrations of Ca, Mg and P in finished water. “Y” means amorphous material was found on scales, while “N” means amorphous material was not..... 153

Figure A1.1: (a) Pipe loop reactors. (b) Schematic diagram of a pipe loop consisting of a pump, valves, flowmeter and reservoir. The harvested lead pipe assembly consists of one 10-inch

section and three 4-inch segments that are connected with rubber connectors. The 4-inch segments allow scale analysis to be performed at different stages in the experiment while retaining the majority of the lead pipe length in the reactor and without any cutting of lead pipe..... 184

Figure A1.2: pH of the water in the pipe loops shown with (a) weekly measurements and (b) box plots of variability. The conditioning stage only includes the data starting from Week 18..... 193

Figure A1.3: Residual free chlorine concentration in the pipe loops after 24 hours from (a) daily measurements and (b) box plots of variation and (c) coefficient of variation (CV) of measurements. The conditioning stage only includes data starting from Week 18..... 194

Figure A1.4: Coefficient of variation (CV) of (a) total lead and (a) dissolved lead concentrations of the pipe loops. CV was calculated for the weekly data for the preceding 5-week periods. Because the water chemistry of the test loops (P1, P2, and P3) changed when treatment stage 1 (dashed vertical red lines) and treatment stage 2 (dashed vertical blue lines) began, the CV value is not reported until five weeks after the changes in water chemistry for the test loops (P1, P2, and P3)..... 195

Figure A1.5: Box plots showing the variation and central tendency for (a) total lead concentration and (b) dissolved lead concentration of pipe loops..... 196

Figure A1.6: Total lead concentrations after the first 6-h stagnation period of each week shown as (a) full data series for each loop and (b) box plots of variation and (c) coefficient of variation (CV) for 6-h stagnation lead concentrations..... 201

Figure A1.7: Line scans of different elements detected by EDS. (The yellow line in SEM images corresponds to the line scan); (a) for treatment stage 1 (b) for treatment stage 2..... 204

Figure A1.8: XRD patterns obtained from the two layers removed from the surfaces of two pipe assemblies (C2 and P2) at the end of conditioning. The XRD patterns (panel a) are shown together with references patterns (panel b) for hydrocerussite $Pb_3(CO_3)_2(OH)_2$, quartz (SiO_2), elemental lead (Pb), cerussite ($PbCO_3$), phosphohedyphane ($Ca_2Pb_3(PO_4)Cl$) and litharge (PbO). Labels used throughout the patterns are peaks from corresponding solid phases abbreviated as H, Si, Pb, C, Ph and L in the same order as mentioned in the caption..... 205

Figure A2.1: Calcite contact for synthetic water preparation. (b) Syringe pump set-up for threshold free chlorine experiment..... 214

Figure A2.2: Illustration of lead coupon experiment in beakers and (b) formation methods of lead(IV) PbO_2 on coupons..... 214

Figure A2.3: (a) Cyclic voltammetry of the lead coupon in a 0.1 M $NaHCO_3$ solution at pH 8.0 (b) The polarization curve for the lead coupon at a constant voltage of 1.43 V (vs Ag/AgCl in 1 M KCl)..... 215

Figure A2.4: (a) Residual free chlorine concentration during chemical conditioning with an initial dosing at 40 mg/L as Cl₂ and daily readjustment (b) pH change during chemical conditioning with an initial pH of 8..... 215

Figure A2.5: (a) Dissolved lead concentrations for Jar 1-Jar 6 during chemical conditioning at 40 mg/L free chlorine (25 weeks in total) (b) Dissolved lead concentrations and (c) residual free chlorine for Jar 1'-Jar 6' during chemical conditioning at 3 mg/L free chlorine (6 weeks in total). At the end of week 25, the best-conditioned coupon from Jar 1-Jar 6 was selected for subsequent testing, and the corresponding jars were labeled Jar 1'-Jar 6' and underwent conditioning for additional 6 weeks..... 216

Figure A2.6: Edge corrosion on lead coupons and the application of epoxy coating to address it..... 217

Figure A2.7: Equilibrium lead solubility for artificial water used in this study. Calculations were performed using Visual MINTEQ3.1 and its default database (relevant reactions indicated in Table A2.4). Equilibrium solubility of planerite (β -PbO₂) was calculated as the summation of the Pb⁴⁺ and the hydrolysis complexes PbO₃²⁻ and PbO₄⁴⁻ according to Table A2.5..... 217

Figure A2.8: Free chlorine decay with lead coupons with PbO₂-rich scale, bare lead coupons, and without lead coupons over 5 days of stagnation at initial concentrations of (a) 2.0 mg/L (b) 1.0 mg/L and (c) 0.5 mg/L as Cl₂. The lines represent the fitted first-order kinetic model, and the error bars denote standard deviations calculated from the triplicate samples..... 218

Figure A2.9: Dissolved lead concentration changes without the presence of free chlorine for PbO₂-coated lead coupon. The error bars denote standard deviations calculated from the triplicate samples..... 219

Figure A2.10: Dissolved lead concentration changes without free chlorine control at an initial concentration of 3.0 mg/L for metallic lead coupon and PbO₂ powder. The error bars denote standard deviations calculated from the triplicate samples..... 219

Figure A2.11: Dissolved and total lead concentrations with free chlorine controlled at constant concentrations of (a) 2-3 mg/L and (b) 0.1-0.2 mg/L. The error bars denote standard deviations calculated from the duplicate experiments..... 220

Figure A2.12: Eh-pH diagram for lead species in water system (Lead species = 0.015 mg/L, DIC= 14 mg/L as C) constructed using The Geochemist's Workbench 2023..... 220

Figure A3.1: (a) Pipe loop reactors, with C for control pipes and T for test pipes. (b) Schematic diagram of a pipe loop consisting of a pump, valves, flowmeter and reservoir. The harvested lead pipe assembly consists of one 18-inch section and three 4-inch segments that are connected with rubber connectors. The 4-inch segments allow scale analysis to be performed at different stages in the experiment while retaining the majority of the lead pipe length in the reactor..... 229

Figure A3.2: Longitudinal cross-sections of (a) control pipe C1 and (b) test pipe T1 collected before conditioning, after conditioning, and after test..... 230

Figure A3.3: XRD Reference patterns for hydrocerussite ($\text{Pb}_3(\text{CO}_3)_2(\text{OH})_2$), lead (Pb), plattnerite ($\beta\text{-PbO}_2$) and litharge (PbO)..... 230

Figure A3.4: Dissolved lead concentrations during conditioning (Free chlorine: 3 mg/L as Cl_2) for pipe loops to be used as control and test groups. Error bars denote standard deviations calculated from the triplicate pipe loops. Before Week 19, only two pipes were available for conditioning, one for each group, thus no error bars are presented for that period..... 231

Figure A3.5: Equilibrium lead solubility for the artificial water used in this study. Calculations were performed using Visual MINTEQ3.1 and its default database (relevant reactions indicated in Table A3.4). Equilibrium solubility of plattnerite ($\beta\text{-PbO}_2$) was calculated as the summation of the Pb^{4+} and the hydrolysis complexes PbO_3^{2-} and PbO_4^{4-} according to Table A3.5..... 231

Figure A3.6: (a) Dissolved lead concentrations; (b) Total lead concentrations; (c) Residual free chlorine; and (d) pH during the last five weeks of conditioning (Weeks 38 to 42) for pipe loops to be used as control and test groups in the test phase. Free chlorine was adjusted to the initial value every day, and pH was adjusted to the initial value every week. Error bars denote standard deviations calculated from the triplicate pipe loops..... 232

Figure A3.7: Free chlorine decay in lead pipe loops over three days of stagnation at initial concentrations of (a) 3.0 mg/L (b) 2.0 mg/L (c) 1.0 mg/L and (d) 0.5 mg/L as Cl_2 . The lines represent the fitted first-order kinetic model, and the error bars denote standard deviations calculated from the triplicate pipe loops..... 233

Figure A3.8: Stagnation experiment (up to 14 days) for dissolved and total lead concentrations at initial free chlorine of 3.0 mg/L. The error bars denote standard deviations calculated from triplicate experiments..... 233

Figure A3.9: (a) Dissolved lead concentrations; (b) Total lead concentrations; (c) Residual free chlorine; and (d) pH for control pipe loops after conditioning. Free chlorine was adjusted to the initial value every day and the pH was adjusted to the initial value every week. Error bars denote standard deviations calculated from the triplicate pipe loops..... 234

Figure A3.10: SEM images and elemental mapping of lead (Pb), oxygen (O), carbon (C), and aluminum (Al) of the cross-section of the pipes for (a) control pipe C1 after conditioning, (b) control pipe C1 after test, (c) test pipe T1 after conditioning, and (d) test pipe T1 after test..... 235

Figure A4.1: (a) Illustration of lead coupon experiments in beakers. (b) Images for a lead coupon, a jar with lead coupons and a jar covered by aluminum foil. (c) Control and test lead coupons after test..... 243

Figure A4.2: (a) Pipe loop reactors for C1-C3. and T1-T3. The pipes were used for real-world water use pattern experiments. (b) Pipe loop reactors for C1'-C2', and P1-P2. The pipes were used stagnation and free chlorine experiments. (c) Schematic diagram of a pipe loop consisting of a pump, valves, flowmeter and reservoir. The harvested lead pipe assembly consists of one 18-inch section and three 4-inch segments that are connected with rubber connectors. The 4-inch

segments allow scale analysis to be performed at different stages in the experiment while retaining the majority of the lead pipe length in the reactor..... 243

Figure A4.3: Coupon study: (a) Dissolved lead concentrations; (b) Total lead concentrations; (c) Residual free chlorine and (d) orthophosphate concentrations during conditioning (1 mg/L as PO₄ orthophosphate added to test coupons starting from Week 6). Water was refreshed every week, free chlorine was adjusted to initial value every day, orthophosphate and pH was monitored and adjusted to initial value every week. Error bars denote standard deviations calculated from the triplicate experiments..... 244

Figure A4.4: Coupon study: Free chlorine decay for lead coupons over five days of stagnation at initial concentrations of (a) 3.0 mg/L and (b) 0.5 mg/L as Cl₂. The lines represent the fitted first-order kinetic model, and the error bars denote standard deviations calculated from the triplicate experiments..... 244

Figure A4.5: Coupon study: Dissolved lead concentrations with free chlorine controlled at concentrations of (a) 1-1.5 mg/L (b) 0.6-1 mg/L (c) 0.3-0.6 mg/L and (d) 0-0.3 mg/L. The error bars denote standard deviations calculated from the triplicate experiments..... 245

Figure A4.6: Coupon study: Total lead concentrations with free chlorine controlled at concentrations of (a) 1-1.5 mg/L (b) 0.6-1 mg/L (c) 0.3-0.6 mg/L and (d) 0-0.3 mg/L. The error bars denote standard deviations calculated from the triplicate experiments..... 245

Figure A4.7: XRD Reference patterns for hydrocerussite (Pb₃(CO₃)₂(OH)₂), phosphohedyphane Ca₂Pb₃(PO₄)₃Cl, lead (Pb), plattnerite (β-PbO₂) and litharge (PbO)..... 246

Figure A4.8: XRD patterns for corrosion products in scales of control and test coupons before and after test. Reference patterns were shown in Figure A4.7 for H: hydrocerussite (Pb₃(CO₃)₂(OH)₂), Ph: phosphohedyphane Ca₂Pb₃(PO₄)₃Cl, Pb: lead (Pb), Pl: plattnerite (β-PbO₂) and L: litharge (PbO)..... 246

Figure A4.9: Pipe-loop study: (a) Dissolved lead concentrations; (b) Total lead concentrations; (c) Residual free chlorine and (d) orthophosphate concentrations during conditioning (1 mg/L as PO₄ orthophosphate was added to test pipes). Water was refreshed every week, free chlorine was adjusted to initial value every day, orthophosphate and pH was adjusted to initial value every week. Error bars denote standard deviations calculated from the duplicate experiments..... 247

Figure A4.10: Pipe-loop study: Free chlorine decay in lead pipe loops with and without orthophosphate (1 mg/L as PO₄) over five days of stagnation at initial concentrations of 3 mg/L and 1 mg/L as Cl₂. The lines represent the fitted first-order kinetic model, and the error bars denote standard deviations calculated from the duplicate experiments..... 247

Figure A4.11: Pipe-loop study: Dissolved lead concentrations with free chlorine controlled at concentrations of (a) 1-1.5 mg/L (b) 0.6-1 mg/L (c) 0.3-0.6 mg/L and (d) 0-0.3 mg/L. The error bars denote standard deviations calculated from the duplicate experiments..... 248

Figure A4.12: Pipe-loop study: Total lead concentrations with free chlorine controlled at concentrations of (a) 1-1.5 mg/L (b) 0.6-1 mg/L (c) 0.3-0.6 mg/L and (d) 0-0.3 mg/L. The error bars denote standard deviations calculated from the duplicate experiments..... 248

Figure A4.13: Pipe-loop study: (a) Dissolved lead concentrations, (b) total lead concentrations, and (d) orthophosphate concentrations under continuous and periodic flow conditions (1 mg/L as PO₄ orthophosphate added to test pipes). Water was refreshed every week, free chlorine was adjusted to initial value every day, orthophosphate and pH was adjusted to initial value every week. Error bars denote standard deviations calculated from the triplicate experiments.....249

Figure A4.14: Longitudinal cross-sections of control pipes C1', C2', and test pipes P1, P2 after test. The pipes were used for stagnation and free chlorin experiments..... 250

Figure A4.15: XRD patterns for control and test pipes (C' and P pipes) after test. The pipes were used stagnation and free chlorin experiments. Reference patterns were shown in Figure A4.7 for H: hydrocerussite (Pb₃(CO₃)₂(OH)₂), Ph: phosphohedyphane Ca₂Pb₃(PO₄)₃Cl, Pb: lead (Pb), Pl: plattnerite (β-PbO₂) and L: litharge (PbO)..... 251

Figure A4.16: SEM images (left side) of the cross-section of the with elemental mappings (right side) of different elements detected by EDS after test for (a) Control Pipe C2' (b) Control Pipe C3' (c) Test Pipe P1, and (d) Test Pipe P2. The pipes were used for stagnation and free chlorin experiments)..... 252

Figure A4.17: Longitudinal cross-sections of control pipes C1-C3, and test pipes T1-T3 before and after test. The pipes were used for real-world water use pattern experiments..... 253

Figure A4.18: SEM images (left side) of the cross-section of the with elemental mappings (right side) of different elements detected by EDS after test for (a) Control Pipe C1 (b) Control Pipe C3 (c) Test Pipe T2, and (d) Test Pipe T3. The pipes were used for real-world water use pattern experiments..... 254

Figure A4.19: XRD patterns for control pipes C1-C3 before and after test. The pipes were used for real-world water use pattern experiments. Reference patterns were shown in Figure A4.7 for H: hydrocerussite (Pb₃(CO₃)₂(OH)₂), Ph: phosphohedyphane Ca₂Pb₃(PO₄)₃Cl, Pb: lead (Pb), Pl: plattnerite (β-PbO₂) and L: litharge (PbO)..... 255

Figure A5.1: Pipe loop reactors for C1-C3. and B1-B3. The harvested lead pipe assembly consists of one 18-inch section and three 4-inch segments that are connected with rubber connectors. The 4-inch segments allow scale analysis to be performed at different stages in the experiment while retaining the majority of the lead pipe length in the reactor..... 263

Figure A5.2: (a) Dissolved lead concentrations and (b) total lead concentrations during conditioning treated by artificial ECWA water with 3 mg/L as Cl₂. Error bars denote standard deviations calculated from the triplicate experiments..... 266

Figure A5.3: Free chlorine concentrations (top part of the panel), dissolved lead (middle part of the panel) and total lead concentrations (bottom part of the panel) for pipes assigned to control and test groups before water blending. Both the control and test pipes had identical conditions, as

described above the figure, prior to water blending. The results from the final three weeks of the previous stage of conditioning with 3 mg/L Cl₂ and continuous flow (beginning at week 38 in Figure A5.2 and denoted here as days 0-22) are included for comparison with the concentrations once the free chlorine concentration and flow regime were adjusted..... 267

Figure A5.4: Free chlorine, dissolved lead and total lead concentrations during water blending for test pipes. Here day 0 indicates the first day in which blended water was introduced to the test pipes. (b) Box plots for dissolved and total lead concentrations for control and test (water blending) pipe loops..... 268

Figure A5.5: Cross-sections of control pipes C1-C3, and test pipes B1-B3 after test..... 270

Figure A5.6: XRD patterns for control and test pipes (C1-C3 and B1-B3 pipes) after the test stage when blending was done for the test pipes. Reference patterns were shown in Figure A4.3 for H : hydrocerussite (Pb₃(CO₃)₂(OH)₂), Ph: phosphohedyphane Ca₂Pb₃(PO₄)₃Cl, Pb: lead (Pb), Pl: plattnerite (β-PbO₂) and L: litharge (PbO)..... 270

Figure A5.7: SEM images (left side) of the cross-section of the with elemental mappings (right side) of different elements detected by EDS after test for (a) Control Pipe C1, (b) Control Pipe C2, (c) Test Pipe B1, and (d) Test Pipe B2..... 271

Figure A6.1: Locations for PWSs with laboratory pipe scale analysis by this study..... 281

Figure A6.2: Longitudinal cross-sections of LSLs dominated by different phases: (a) Pb-C solids from PWSs J, K, L. (b) PbO₂ solids from PWSs B, C, N. (c) Pb-P solids from PWSs D, E, G. (d) Amorphous layers from PWSs I, H, L..... 281

Figure A6.3: (a) Venn diagram of the presence of different Pb-C solids in pipe scales. (b) Percentage of PWSs with Pb-C solids: cerussite (C), hydrocerussite (Hc), cerussite and hydrocerussite (C+Hc) and no Pb-C solid. (c) Percentage of PWSs with and without plumbonacrite (Pn)..... 282

Figure A6.4: Eh-pH diagram for lead species in water system constructed using the Geochemist's Workbench 2023 using MINTEQA2 database (Table S5). (a) Lead species = 0.01 mg/L, DIC = 12 mg/L as C. (b) Lead species = 0.01 mg/L, DIC = 20 mg/L as C, orthophosphate = 1.0 mg/L as PO₄. (c) Eh-Log DIC diagram for lead species (Lead species = 0.01 mg/L, pH = 8). (d) Eh-Log PO₄ diagram for lead species (Lead species = 0.01 mg/L, pH = 8, DIC = 12 mg/L)..... 283

Figure A6.5: Equilibrium lead solubility for water (a) with free chlorine and without (b) free chlorine. (Lead species = 0.01 mg/L, DIC = 12 mg/L as C. orthophosphate = 1.0 mg/L as PO₄.) Calculations were performed using Visual MINTEQ3.1 and its default database (relevant reactions indicated in Table A5.5). This database does not include any reactions for dissolved lead complexation with polyphosphate. Equilibrium solubility of plattnerite (β-PbO₂) was calculated as the summation of the Pb⁴⁺ and the hydrolysis complexes PbO₃²⁻ and PbO₄⁴⁻ according to Table A6.6 and Table A6.7..... 284

Figure A6.6: Disinfectant types in PWSs included in this research. (b) Percentage of PWSs using free chlorine with and without PbO ₂ solids. (c) pH of PWSs with and without PbO ₂ solids. (d) DIC of PWSs with and without PbO ₂ solids.....	284
Figure A6.7: (a) Corrosion control treatment methods in PWSs included in this research. Presence of Pb-P solids in PWSs using (b) orthophosphate (c) blended-phosphate and (d) zinc phosphate. (e) pH and (f) DIC of PWSs with and without Pb-P solids.....	285
Figure A6.8: Correlations between mass concentrations in pipe segment scales and concentrations in finished water for (a) P, (b) Ca, and (c) Mg.....	286
Figure A6.8: XRD patterns pipe scales from different PWSs. (a) Pb-C solids scale; (b) PbO ₂ solids scale; (c) Pb-P solids scale; (d) Amorphous material. The patterns at the bottom are the reference patterns for H : hydrocerussite (Pb ₃ (CO ₃) ₂ (OH) ₂), C: cerussite (PbCO ₃), P: plumbonacrite (Pb ₁₀ (CO ₃) ₆ (OH) ₆ O), L: litharge (PbO), Pl: plattnerite (β-PbO ₂), S: scrutinyite (α-PbO ₂), Ph: phosphohedyphane (Ca ₂ Pb ₃ (PO ₄) ₃ Cl), Lp: lead phosphate (Pb ₉ (PO ₄) ₆), Ca: calcium lead phosphate hydroxide (Ca ₂ Pb ₈ (PO ₄) ₆ (OH) ₂), and Hyp: hydroxylpyromorphite (Pb ₅ (PO ₄) ₃ (OH)).....	287
Figure A6.10: 10 SEM image of the cross-section of the pipe for (a) PWS-D and (b) PWS-L. Elemental mapping of different elements detected by EDS for (c) PWS-D and (d) PWS-L.....	289

List of Tables

Table 2.1: Summary of lead concentrations (dissolved and total lead), standard deviations in different test stages and the relative percentage of dissolved to total lead concentrations.....	34
Table 2.2: Mass concentrations (mg/g) of elements in the scales determined by acid digestion of solids followed by analysis with ICP-MS for pipes at the end of treatment stage 2.....	43
Table 4.1: Mass concentrations (mg/g) of elements in the scales determined by acid digestion of solids followed by analysis with ICP-MS.....	95
Table 5.1: Dissolved lead and total lead concentrations for lead coupons and pipe loops at different continuously-maintained stable free chlorine concentration ranges.....	128
Table 5.2: Summary of lead concentrations (dissolved and total lead) and p-value (Wilcoxon rank-sum test) for control and test pipes with the real-world water use pattern.....	132
Table A1.1: (a) Pipe loop reactors. (b) Schematic diagram of a pipe loop consisting of a pump, valves, flowmeter and reservoir. The harvested lead pipe assembly consists of one 10-inch section and three 4-inch segments that are connected with rubber connectors. The 4-inch segments allow scale analysis to be performed at different stages in the experiment while retaining the majority of the lead pipe length in the reactor and without any cutting of lead pipe.....	185
Table A1.2: Artificial Buffalo Water composition compared to actual water composition reported by Buffalo Water.....	186
Table A1.3: Water quality parameters measurement and scale analysis.....	189
Table A1.4: Potential dissolution-precipitation and aqueous reactions involving lead in the system.....	198
Table A1.5: Summary of the results from the T test performed on the dissolved and total lead concentrations in the pipe loops.....	199
Table A1.6: Summary of the results from the Shapiro-Wilk Test performed on the dissolved and total lead concentrations in the pipe loops.....	200
Table A1.7: Summary of XRD results for the powdered samples from the lead pipe surfaces.....	206
Table A1.8: Mass concentrations (mg/g) of elements in the scales.....	207
Table A2.1: Synthetic water composition.....	221
Table A2.2: Syringe pump operational parameters.....	221
Table A2.3: Half-reactions associated with lead(IV) oxide interactions with free chlorine.....	222

Table A2.4: Dissolution-precipitation and aqueous reactions involving lead in the system.....	222
Table A2.5: Reactions associated with planerite (β -PbO ₂) dissolution.....	223
Table A2.6: Redox potentials corresponding to different free chlorine concentrations.....	223
Table A3.1: Synthetic water composition compared to actual water.....	236
Table A3.2: Initial concentration and test time points during water stagnation experiments.....	236
Table A3.3: Syringe pump operational parameters.....	237
Table A3.4: Potential dissolution-precipitation and aqueous reactions involving lead in the system.....	237
Table A3.5: Reactions associated with plattnerite (β -PbO ₂) dissolution.....	238
Table A3.6: Reactions associated with plattnerite (β -PbO ₂) dissolution.....	238
Table A3.7: Mass percentage (w%) of the elements in lead solids.....	239
Table A3.8: Kinetic parameters of free chlorine decay.....	239
Table A4.1: Water composition of ECWA water and artificial water.....	256
Table A4.2: Identification for pipe loops assigned to different tests.....	256
Table A4.3: Kinetic parameters of free chlorine decay for lead coupons and lead pipes.....	257
Table A4.4: Summary of XRD results for the powdered samples from the lead coupons and lead pipes.....	258
Table A4.5: Mass concentrations (mg/g) of elements in the scales determined by acid digestion of solids followed by analysis with ICP-MS.....	260
Table A5.1: Water composition of Artificial Buffalo and ECWA Water.....	264
Table A5.2: Summary of average lead concentrations (dissolved and total lead) and p-value for control and test pipes in water blending tests.....	269
Table A5.3: Mass concentrations (mg/g) of elements in the scales after test determined by acid digestion of solids followed by analysis with ICP-MS.....	272
Table A6.1: Finished water chemistry from different PWSs.....	290
Table A6.2: Finished water element concentrations from different PWSs.....	292
Table A6.3: Identification of lead crystalline solids in pipe scales.....	294
Table A6.4: Identification of lead mineral solids in pipe scales based on Tully et al. (2019).....	295
Table A6.5: Dissolution-precipitation and aqueous reactions involving lead in the model calculations.....	296
Table A6.6: Reduction half-reactions associated with lead(IV) oxide interactions with free	

chlorine.....	297
Table A6.7: Reactions associated with planerite (β -PbO ₂) dissolution.....	297
Table A6.8: DIC, pH for PWSs and their calculated values for Pb-C solids formation.....	298
Table A6.9: Free chlorine concentration for PWSs and the required and calculated Eh for PbO ₂ form.....	299
Table A6.10: Phosphate type, dosing concentration for PWSs and the calculated orthophosphate threshold for Pb-P solids formation.....	300

Acknowledgments

I am deeply indebted to my academic advisor, Dr. Daniel Giammar, for his guidance and encouragement. Working with him has been both an enjoyable and profoundly meaningful experience, and this journey will remain a cherished memory throughout my life. He has not only imparted invaluable knowledge in science but also taught me the importance of treating others with kindness and how to become a better individual. I would like to express my heartfelt gratitude for his mentorship, continuous support during my PhD journey, as well as for his expertise, patience, and dedication.

I would like to sincerely acknowledge my thesis committee members, Dr. Jeffrey Catalano, Dr. Young-Shin Jun, Dr. Peng Bai, and Dr. Fangqiong Lin, for their valuable suggestions and feedback throughout the course of this research. Their generous contributions of time and insightful advice have been instrumental in improving my work. I am also deeply grateful to Dr. Daniel Giammar, Dr. Jeffrey Catalano, and Dr. Kimberly Parker for their recommendations and support during my postdoctoral search.

I would also like to express my sincere gratitude to the faculty and staff in the EECE department and McKelvey School of Engineering for their support, both academically and personally, as well as the members during my service in the EECE Graduate Student Council. I am thankful to the laboratory managers in the EECE, IMSE, and the Department of Earth, Environmental, and Planetary Sciences, who provided essential assistance with my experiments.

I would like to acknowledge the financial support from my funding sources, including Hazen and Sawyer, Buffalo Water, and the Erie County Water Authority. I also wish to recognize my collaborators: Mr. Roger Arnold, P.E., Dr. Javier Locsin, Dr. Benjamin Trueman, and Dr.

Graham Gagnon. It has been a great pleasure to collaborate with them on lead corrosion control projects and to learn from their expertise.

I feel privileged to have been part of the Aquatic Chemistry Lab. During my research rotation, I had the guidance of Dr. Anshuman Satpathy, and I have learned a lot from him beyond the research itself. Dr. Anushka Mishra was the mentor in getting me started on my first lead project. She was knowledgeable and always helpful. I am truly thankful for Dr. Weiyi Pan's consistent support and generous assistance, which were timely and critical in helping me overcome the obstacles I encountered during my PhD. I also appreciate the continuous support from Dr. Yeunook Bae, Dr. Neha Sharma, Yihang Yuan, Elmira Ramazanova, and Xicheng He. I extend special thanks to Zehua Wang and Bella Stull, whose exceptional assistance and contributions to the lead projects were instrumental. Without their support, I could not have managed on my own. Moreover, working alongside talented undergraduates and rotation PhD students was a rewarding experience. I would also like to express my heartfelt gratitude to my friends and colleagues:

Dr. Zixuan Wang, Ying Wang, Qiufeng Lin, Dr. Wensi Chen, Dr. Fubin Liu, Dr. Matthew Ferby, Yue Rao, Dr. Zhenwei Gao, John Weir, Jing Xie, Zhenyang Jiang, Dr. Chenggang Xi, Jianshang Li, Haihui Zhu, Ziqi Wang and all those not mentioned.

Most importantly, I am profoundly indebted to my parents, Xiaojun Ma and Hong Gao, for their unconditional, unwavering, and loving support. I could not have completed my PhD without your continuous encouragement and assistance.

Yao Ma

Washington University in St. Louis

December 2024

Dedicated to my parents.

ABSTRACT OF THE DISSERTATION

Impacts of Phosphate and Residual Free Chlorine on the Precipitation, Stability and Dissolution of Lead Corrosion Products

by

Yao Ma

Doctor of Philosophy in Energy, Environmental and Chemical Engineering

Washington University in St. Louis, 2024

Professor Daniel E. Giammar, Chair

Lead release from lead pipes into drinking water is a critical threat to public health. Orthophosphate addition is an established method of controlling lead concentrations in tap water. Many phosphate-based inhibitors currently used by utilities are blends of orthophosphate and polyphosphate. Orthophosphate can limit lead release from pipes by forming low-solubility lead phosphate solids on pipe inner surfaces. In contrast, polyphosphate can accelerate lead release by forming soluble lead-phosphate complexes. Due to the potential conversion from polyphosphate to orthophosphate in the distribution system and to complex dynamics of water chemistry in lead service lines (LSLs), the net impact of a blended phosphate chemical on lead in tap water had been challenging to assess. In addition to lead-phosphate solids, lead(IV) oxide (PbO_2) solids in the scales of LSLs can play an important role in controlling lead concentrations. PbO_2 has an extremely low solubility (below $0.1\mu\text{g/L}$ for most situations) that has the potential to maintain desired low lead concentrations in water. However, PbO_2 is only formed and stable at a high redox potential environment, as Pb(IV) is highly oxidative and can easily undergo reductive dissolution. Free chlorine, as an important tap water infectant, is a strong oxidant that can help form and maintain PbO_2 in LSLs. However, the threshold free chlorine to maintain PbO_2 had been determined for layers of PbO_2 on the surfaces

of elemental lead materials. There were also unresolved questions regarding the impacts of stagnation time and orthophosphate dosing on the stability of PbO_2 in scales of harvested lead pipes.

This dissertation includes five studies aimed at providing a better understanding of the role of phosphate and residual free chlorine on the precipitation, stability and dissolution of lead(IV) oxide and lead-phosphate solids at conditions relevant to LSLs involved in residential drinking water supply. In the first study, the effects of polyphosphate presence as a component of a mixture with orthophosphate on lead release were investigated on harvested lead pipes. This study confirmed that orthophosphate will be a better corrosion control choice for LSLs than a blended phosphate for a system that has a major goal of lead corrosion control and no specific need for metal sequestration. The second study investigated the stability of PbO_2 on the surface of metallic lead coupons and its potential role in corrosion control. This study found that for systems that have PbO_2 already present in lead scales, promoting conditions that maintain PbO_2 stability could be an effective method for limiting lead release to drinking water. A threshold concentration of residual free chlorine was identified to maintain PbO_2 stability. In the third study, the effect of residual free chlorine and water stagnation on lead release associated with PbO_2 dissolution was evaluated with actual LSLs harvested from a public water system. Similarly to in the study with lead coupons, this study with lead pipes identified a threshold free chlorine concentration below which PbO_2 undergoes reductive dissolution. Long water stagnation times (five days) can exacerbate the lead release from pipes into water especially for particulate lead. Scale analysis reveals that plattnerite ($\beta\text{-PbO}_2$) was the primary component in the pipe scales and that most PbO_2 pipe scales maintained their integrity during periods of water stagnation even when stagnation did result in substantial increases in dissolved lead. The fourth

study investigated the effect of orthophosphate on lead release from PbO₂-rich layers on lead pipes and coupons. The study found that the use of orthophosphate in LSLs with rich PbO₂ layers in scales may not provide a substantial benefit for lead corrosion control during the initial phase of its addition. The fifth study explored the variations in lead pipe scales from 43 different drinking water systems based on laboratory scale analysis together with data from previous research. It also evaluated the applications and limitations of chemical equilibrium models for predicting the solid phases present in lead pipe scales. The study found that the compositions of lead pipe scales depend on water chemistry, corrosion control methods, and disinfectant types. While equilibrium predictions are not completely predictive and have certain limitations, they remain valuable for making initial assessments and screening lead solids in pipe scales.

Chapter 1: Introduction

1.1 Background

1.1.1 Lead Service Lines

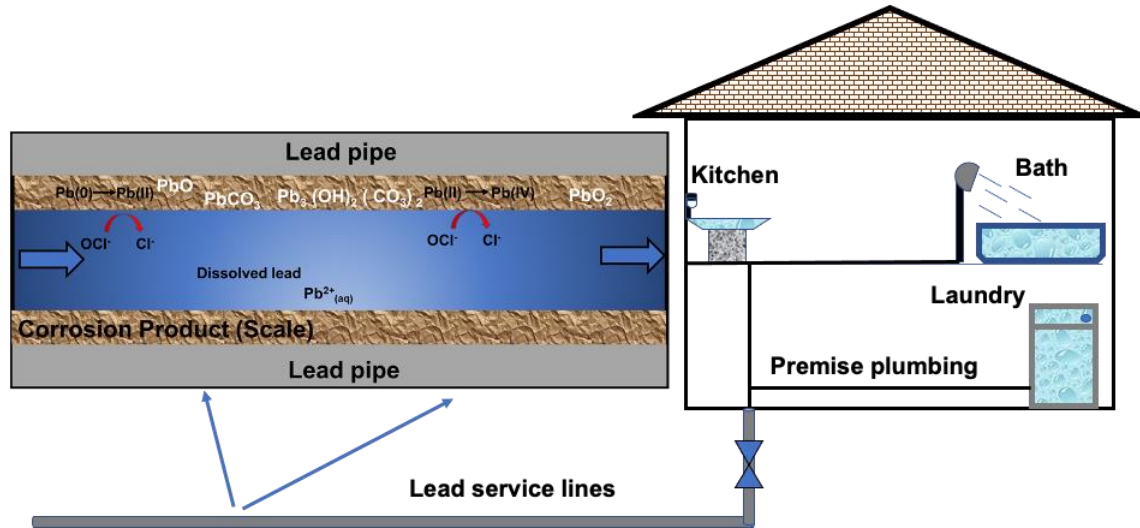


Figure 1.1 Schematic of lead service lines and premise plumbing to household (right) and formation of lead corrosion products in distribution systems (left).

Lead pipes were historically used to deliver water due to their durability and the malleability of lead for pipe manufacture (Dave and Yang, 2022). However, the potential lead release from lead pipes has become a significant concern (Pontius, 1991). Lead is rarely present at concentrations of concern in water sources used for drinking supply. It primarily enters tap water from lead service lines (LSLs) (Doré et al., 2019a), which connect residences to distribution system pipes, and premise plumbing (Figure 1.1). Premise plumbing includes lead-bearing solders and fittings. According to a survey (Cornwell et al., 2016) from the American Water Works Association, about 6.1 million LSLs are still currently in use in US community water

systems, and about 7% households in the US are served by LSLs, which is a population of 15 to 22 million.

Lead released from LSLs and premise plumbing to drinking water is detrimental to human health. Exposure to lead-contaminated drinking water can increase blood lead levels and cause various neurological disorders and physical dysfunctions (Edwards et al., 2009; Swaringen et al., 2022). The high-profile events of elevated lead concentrations in drinking water in Washington, DC (Roy and Edwards, 2019), Newark, New Jersey (Faherty, 2021) and Flint, Michigan (Roy et al., 2019), were major crises involving lead release to drinking water.

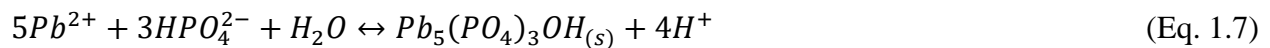
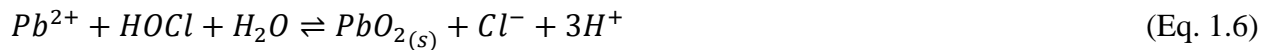
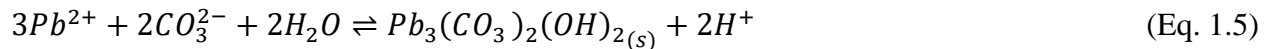
The Lead and Copper Rule (LCR), initially established in 1991 (USEPA, 1991), set a lead action level of 15 $\mu\text{g}/\text{L}$. It requires actions such as public education and lead service line replacement if 10 percent of the household tap water samples measured have lead water concentrations greater than the action level. In the recent Lead and Copper Rule Revisions (LCRR) (USEPA, 2021), although the lead action level has been maintained at 15 $\mu\text{g}/\text{L}$, a trigger level of 10 $\mu\text{g}/\text{L}$ has been added that will trigger additional planning, monitoring, and treatment requirements when the 90th percentile lead concentration exceeds it. Furthermore, the LCRR requires that the volume of water collected for lead sampling should be the 5th liter for households with lead service lines, which will usually have a higher concentration than the 1st liter because it is more likely to have stagnated within a lead service line (Masters et al., 2021; Rome et al., 2022). Consequently, this

change is expected to increase the 90th percentile lead concentrations for many water systems (Mishrra et al., 2021a).

1.1.2 Lead Contamination in Water

Lead corrosion is the major contributor of lead release to water. It consists of a series of chemical or electrochemical interactions between the lead pipe and the water in the pipe (Figure 1.1). The chemical composition of the water strongly influences the nature of those interactions. Pb(0) easily gets oxidized to Pb(II) by oxidants that include oxygen (O₂) and chlorine-based disinfectant species (HOCl, OCl⁻, and NH₂Cl). For lead monitoring in water, dissolved lead and total lead are two critical indicators used to track lead levels. Dissolved lead refers to the soluble form of lead present in water, which in this research is defined as the lead that passes through 0.22-µm filters. Total lead encompasses all forms of lead, dissolved, colloidal, and particulate present in a water sample. In this study, total lead is defined as the lead present in the sample without filtration. Total lead concentrations are determined using unfiltered samples that are acidified to dissolve any lead-containing suspended particles and treated with a reductant to promote the dissolution of any PbO₂ particles. The Pb(II) that is produced can be present as soluble species as well as in a layer of solid corrosion products on the inner surface of lead pipe that can include the lead(II) carbonates hydrocerussite [(Pb₃(CO₃)₂(OH)₂] and cerussite (PbCO₃). When phosphate is added as a corrosion inhibitor, lead phosphate solids can also form, and they have a lower solubility than lead carbonate solids (McNeill and Edwards, 2002). Lead(II) oxide

is primarily found as litharge (α -PbO), and in the presence of free chlorine (HOCl and OCl⁻), Pb(II) can be oxidized to generate lead(IV) oxide that can be present as both plattnerite (β -PbO₂) and scrutinyite (α -PbO₂) (Lytle and Schock, 2005). The reactions leading to the formation of different lead corrosion products are shown in reactions 1.1-1.7.



The release of lead to water is affected by the pH, alkalinity, dissolved inorganic carbon (DIC), hardness and oxidant concentrations (Xie et al., 2010b).

1.1.3 Lead Corrosion Control with Phosphate Inhibitors

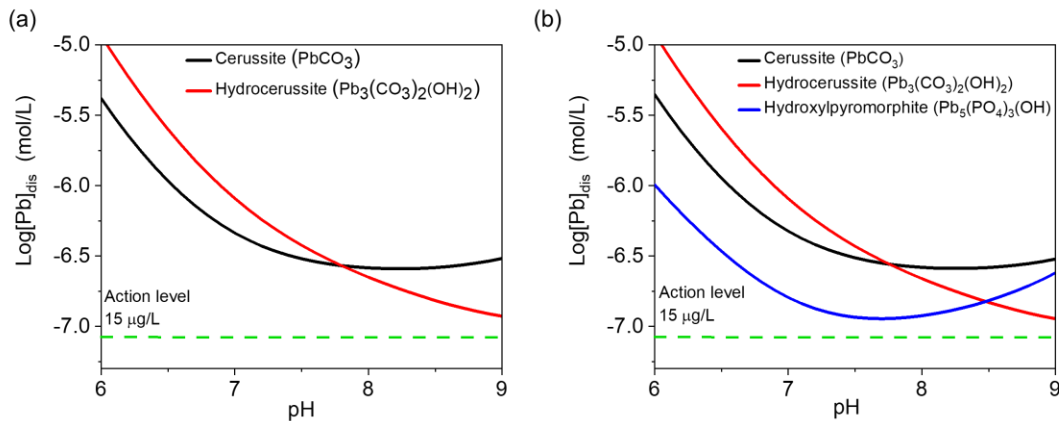


Figure 1.2 Equilibrium lead solubility for a system with 2.2 mM dissolved inorganic carbon (a) with no orthophosphate and (b) with orthophosphate of 1.5 mg/L as PO₄³⁻ (0.0156 mM). This DIC corresponds to that of Buffalo, NY, which distributes water at a pH of 7.5-7.9. Calculations were performed using MINTEQA 3.1.

Orthophosphate is effective in preventing lead release from pipes by forming low solubility lead phosphate solids, including hydroxylpyromorphite ($\text{Pb}_5(\text{PO}_4)_3\text{OH}$) and phosphohedyphane ($\text{Ca}_2\text{Pb}_3(\text{PO}_4)_3\text{Cl}$), that have a lower solubility than lead carbonate solids (Figure 1.2). In the meantime, the precipitation or adsorption of orthophosphate onto the lead pipe surface can limit the contact between oxidants and pipe, which can limit lead dissolution (Nancollas, 1983).

Reaction (1.7) shows the formation of a typical lead phosphate solid hydroxylpyromorphite ($\text{Pb}_5(\text{PO}_4)_3\text{OH}$) in LSLs.

Polyphosphate is an effective sequestering agent for certain metals in water, especially calcium, iron and manganese (Cantor et al., 2000; Lytle and Edwards, 2024). Its interactions with those metals can prevent them from further reaction and precipitation, which in the case of iron and manganese could result in complaints of “colored water” from the presence of iron and manganese oxides in the tap water. Based on the theoretical computations of Holm and Shock, (1991), polyphosphate could significantly increase lead solubility in plumbing systems by forming soluble lead-polyphosphate complexes. An experimental study by McNeill and Edwards (2002) about the effect of phosphate inhibitors on lead release from pipes confirmed that polyphosphate chemicals such as hexametaphosphate can increase release of both particulate and soluble lead in lead pipes compared with the same condition dosed with orthophosphate. That study recommended that polyphosphate not be used for lead corrosion control. Trueman et al., (2018) studied the effects of orthophosphate and polyphosphate on lead speciation (dissolved or

particulate lead) in drinking water from LSLs using size-exclusion chromatography (SEC). They found that lead was mainly present in the form of dissolved species in the presence of polyphosphate, Due to the potential conversion of polyphosphate to orthophosphate in the distribution system and to complex dynamics of water chemistry in LSLs, the net impact of the orthophosphate and polyphosphate in a blended phosphate chemical on lead in tap water has been challenging to assess. There is limited relevant literature and laboratory-scale studies using commercial phosphate-based inhibitors. Furthermore, the composition of the scales from lead pipes that have been dosed with orthophosphate or polyphosphate has received only limited study.

1.1.4 Lead Corrosion Product Lead Oxide (PbO_2)

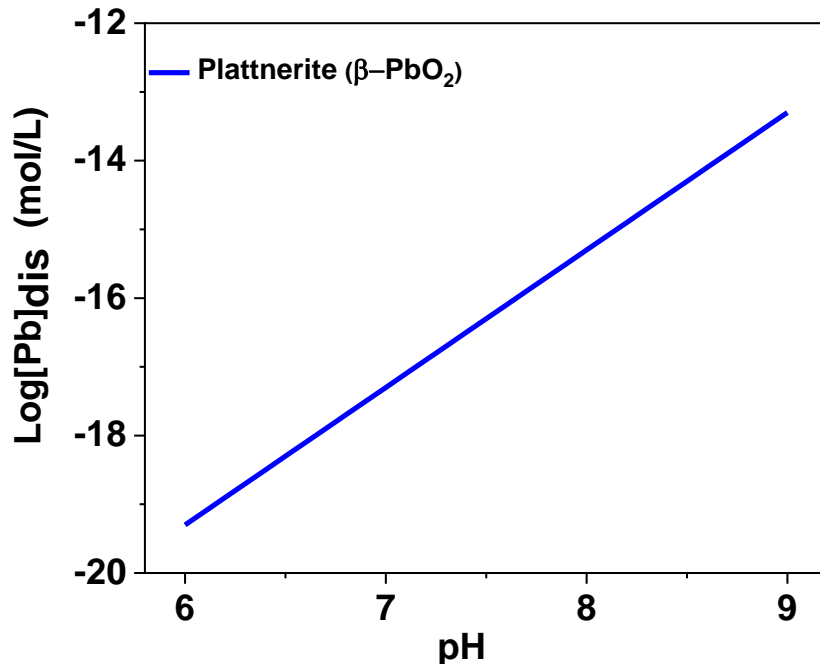
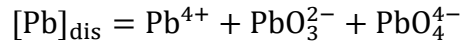


Figure 1.3 Lead solubility of plattnerite ($\beta\text{-PbO}_2$).



Lead oxide (PbO₂) is an important component of lead scales found on LSLs, and it has been observed as the two polymorphs scrutinyite (α-PbO₂) and plattnerite (β-PbO₂). Lead oxide (PbO₂) has an extremely low solubility (Figure 1.3) compared with lead carbonate or lead phosphate solids. The solubility of plattnerite (β-PbO₂) was calculated based on the reactions 1.8-1.10.

The formation of lead oxide (PbO₂) on the surface of lead pipes can potentially provide good protection and a passivating layer for the lead pipe surface that can effectively prevent lead from further corrosion or dissolution (Triantafyllidou et al., 2015). The stability of lead oxide (PbO₂) on the surface of lead pipes can potentially control lead release into water flowing through or stagnating in lead pipes. However, lead is not stable in the +IV oxidation state of lead oxide (PbO₂) in the absence of a strong oxidant like free chlorine (Lin and Valentine, 2009). PbO₂ is a strong oxidant, and it is susceptible to the change of water chemistry factors such as pH, DIC and various reductants. Among them, the presence of species that can act as reductants can be a key factor affecting the maintenance of lead oxide (PbO₂) on pipe loops (Figure 1. 4). From half reactions (Reactions 1.11 and 1.12) and the associated pe-pH diagram, we can see that the stability of PbO₂ requires very oxidizing conditions.



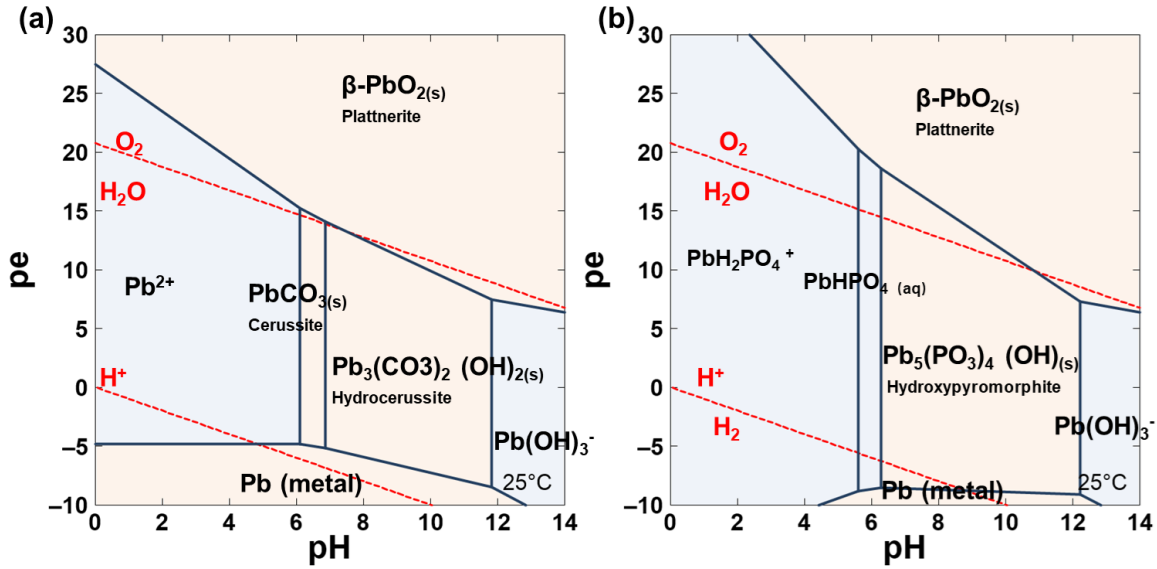


Figure 1.4 pe-pH diagram for Pb in Buffalo water system (DIC equals 2.2mM) (a) with no orthophosphate and (b) with orthophosphate of 1.5 mg/L as PO_4^{3-} (0.0156 mM).

A good example of the crucial impact of the presence or absence of free chlorine as a strong oxidant on the stability of lead oxide (PbO_2) is the lead crisis that happened in Washington DC from late 2000 to 2004. A switch from free chlorine (a strong oxidant) to free chloramine (a less strong oxidant) was the major culprit (shown in half reactions 1.13-1.14). In the presence of chloramine, reductive dissolution of lead oxide (PbO_2) can take place quickly (Edwards and Dudi, 2004; Switzer et al., 2006). Additional species that can act as reductants of PbO_2 include natural organic matter (NOM) and Fe(II) (Dryer and Korshin, 2007; Lin et al., 2008). Therefore, the lead concentration increased quickly after the disinfectant switch (Figure 1. 5a). Several studies have investigated the stability and maintenance of lead oxide (PbO_2) over a range of water chemistry conditions.



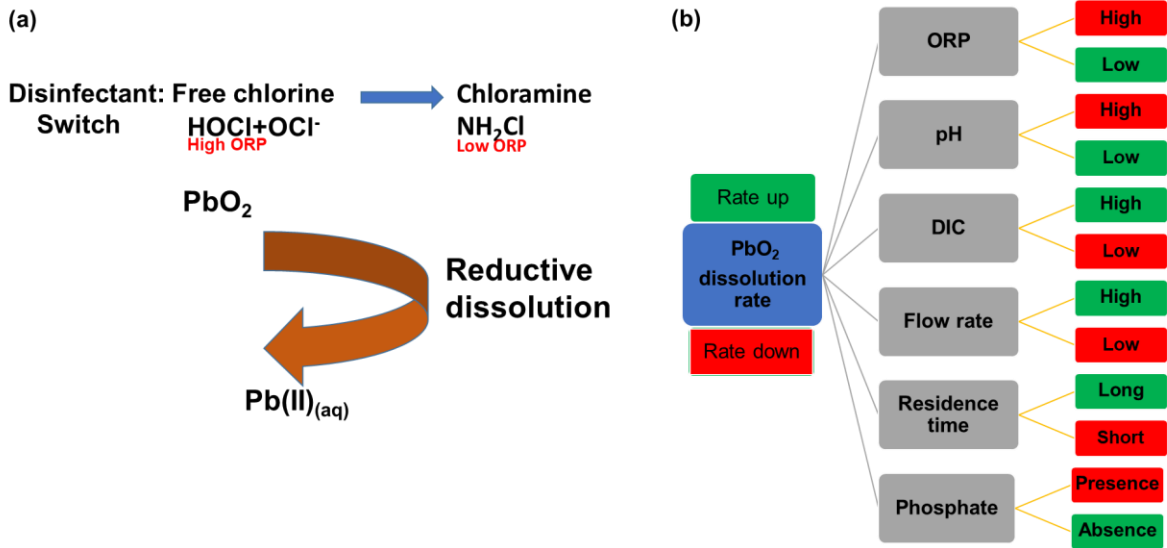


Figure 1.5 (a) Reductive dissolution of lead oxide (PbO_2) due to disinfectant switch, and (b) factors affecting the dissolution rate of lead oxide (PbO_2).

The maintenance of lead oxide (PbO_2) is of great importance for lead corrosion control in LSLs. Many studies have focused on the dissolution, formation and transformation of lead oxide (PbO_2). The water chemistry factors that affect PbO_2 dissolution are shown in Figure 1.5b. A study from Xie et al., (2010) found that decreasing pH will accelerate the dissolution of lead oxide (PbO_2), which is consistent with the formula of reaction 1.9. Higher DIC also accelerates the dissolution rate of lead oxide (PbO_2) by favoring the detachment of reduced $Pb(II)$ from the surface of lead oxide (PbO_2) through the formation of soluble lead-carbonate complexes. Another study (Xie et al., 2010a) on the impacts of disinfectants on lead oxide (PbO_2) found that the dissolution rate of plattnerite (β - PbO_2) decreased in the order of no disinfectant, monochloramine, and free chlorine, which was consistent with the oxidation-reduction potentials that would be set by these species. According to another study of Xie and Giammar, (2011), water flow can increase the dissolution rates of lead oxide (PbO_2) by destabilizing pipe scales physically, and both dissolved and

particulate lead concentrations increased with increasing water flow rate. Residence time and the presence of phosphate are two other important factors affecting the stability of lead oxide (PbO_2). Longer residence time will contribute to more depletion of free chlorine of the pipe loops and aggravate the dissolution of lead oxide (PbO_2) (Arnold and Edwards, 2012). With the presence of phosphate, phosphate-lead solids can form on the surface of lead oxide (PbO_2) particles and enhance its stability against changing conditions (Zhao et al., 2018). According to the study of Bae et al., (2020b), the dosing of orthophosphate and the solid precipitation of lead-phosphate on the surface of lead pipes can effectively alleviate potential reductive dissolution and release of lead into water after a disinfectant switch from free chlorine to chloramine that induces PbO_2 reductive dissolution. However, there is limited literature that has investigated and quantified the impacts of residence time and orthophosphate dosing on the stability of PbO_2 in scales of harvested lead pipes. Furthermore, the stability of lead oxide (PbO_2) in response to changing water chemistry associated with blending of waters with different phosphate corrosion inhibitors has not been studied previously.

1.2 Research Objectives

The overall objective of this thesis is to advance our understanding of corrosion control in lead service lines, including the formation and stability of lead corrosion products, impacts of water chemistry and operational parameters on lead release, and optimization for lead corrosion control strategies. Four specific research objectives were pursued.

Objective 1: Determine the effects of polyphosphate presence as a component of a mixture with orthophosphate on lead release from harvested lead pipes at a particular water composition.

Objective 2: Develop a predictive understanding of the effects of free chlorine concentration and stagnation time on the formation and stability of PbO_2 as a component of pipe scales on lead pipes.

Objective 3: Identify the interactions of orthophosphate with lead oxide (PbO_2) and the impacts of changing influent sources with different polyphosphate and orthophosphate concentrations on the stability of lead oxide (PbO_2).

Objective 4: Explore the influence of key water chemistry parameters and corrosion control methods on lead scale composition, and their implications for corrosion.

1.3 Dissertation Overview

The dissertation consists of five major studies. It aims at providing a better understanding of the role of phosphate and residual free chlorine on the precipitation, stability and dissolution of lead(IV) oxide and lead-phosphate solids at conditions relevant to LSLs involved in residential drinking water supply.

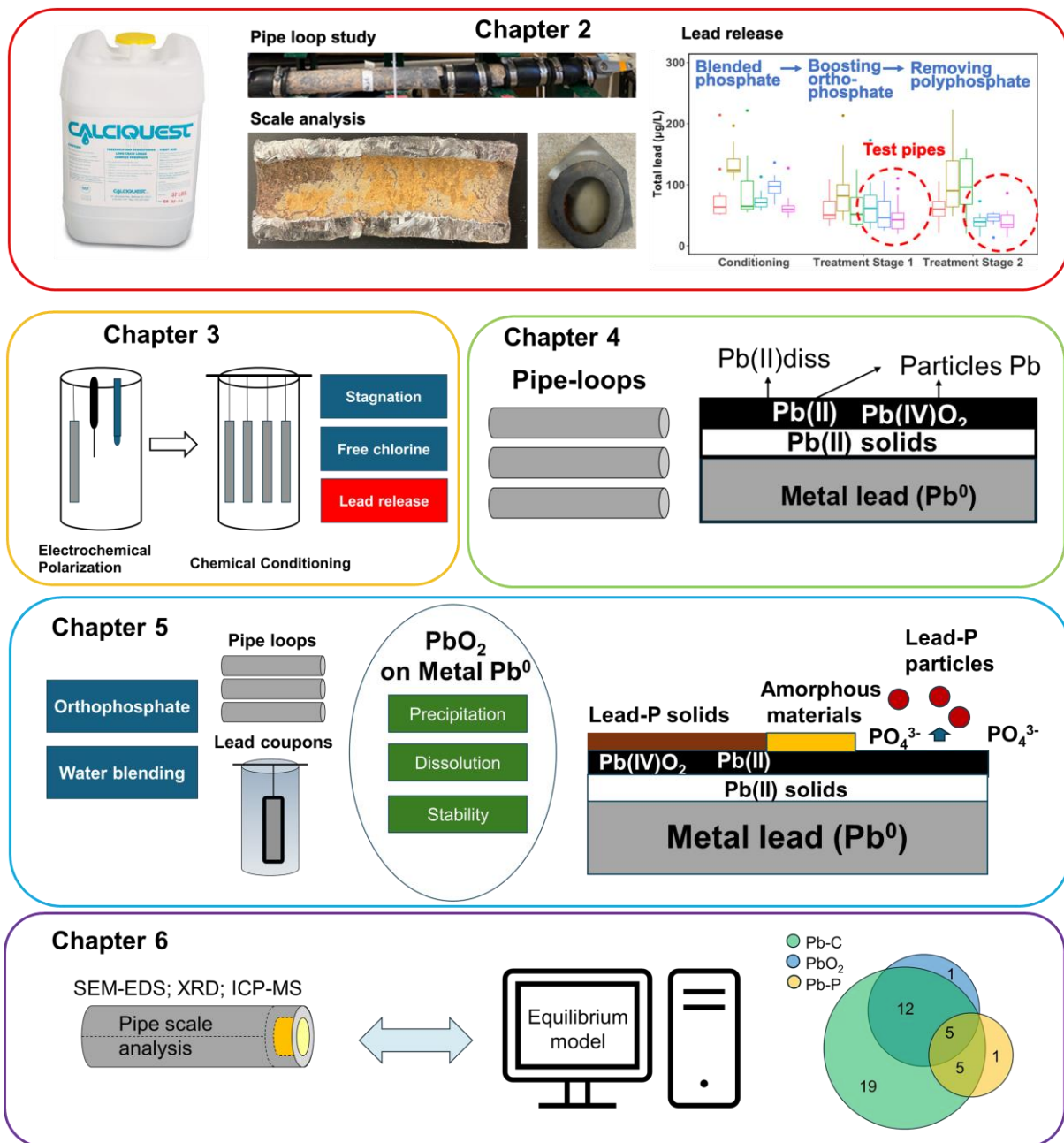


Figure 1.6 Illustrations of the studies presented in Chapters 2-6 of this dissertation.

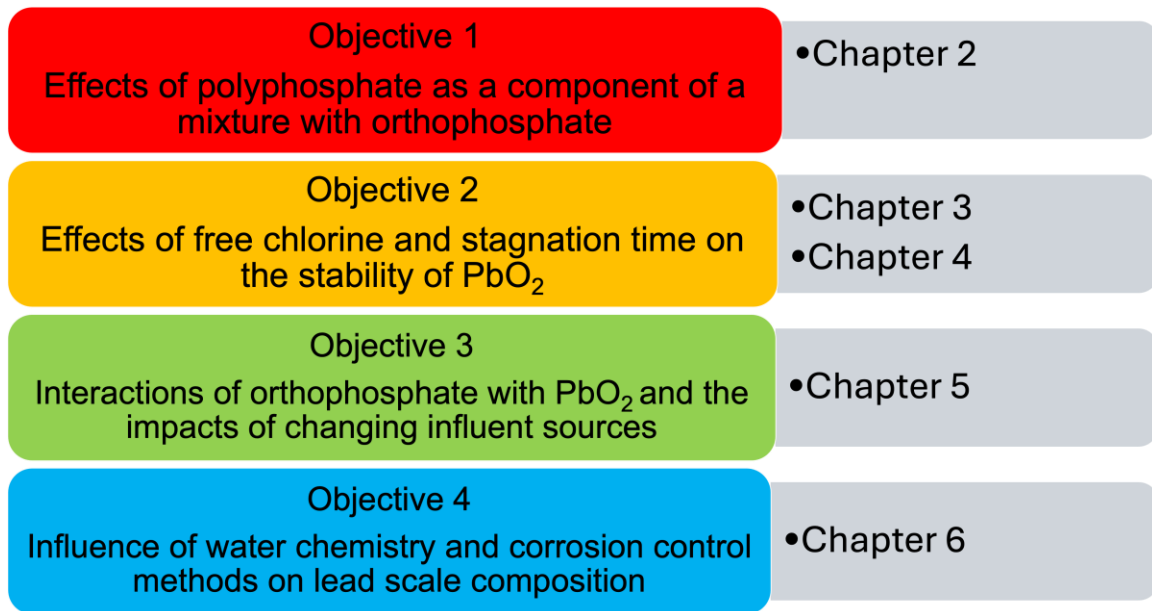


Figure 1.7 Overview of research objectives and chapters.

The first study used pipe-loop experiments with harvested pipes from Buffalo, New York (Figure 1.6a) to investigate the effects of boosting orthophosphate concentrations on lead concentrations in pipes previously exposed to a blended phosphate and removing the polyphosphate from the inhibitor. It corresponds to Objective 1 and the results are presented in **Chapter 2** (Figure 1.7).

The second study used bench-scale lead coupon experiments (Figure 1.6b) to investigate stagnation times and identify a threshold free chlorine value necessary to maintain PbO₂ stability. An electrochemical deposition method and water chemistry conditioning were used to form PbO₂ on the surface of lead coupons. These PbO₂-coated lead coupons were then exposed to artificial tap water. It corresponds to Objective 2 and the results are presented in **Chapter 3** (Figure 1.7).

The third study used pipe loops with harvested LSLs that contained PbO₂ scale from Erie County, New York to quantitatively investigate the impacts of residual free chlorine concentration and stagnation time on the stability of PbO₂. As with the second study, this third study corresponds to Objective 2 and the results are presented in **Chapter 4** (Figure 1.7).

The fourth study used both pipe-loop experiments and bench-scale batch experiments to investigate the potential ability of orthophosphate to maintain PbO₂ as a stable component of lead scale on LSLs. Its results are presented in **Chapter 5** (Figure 1.7). The results for water blending effects on PbO₂ are presented in **Appendix 5**. Those were for Objective 3.

The fifth study combined the results of scale analysis of 70 harvested pipes from 16 different systems across the U.S., together with the data from previously published research to identify key factors impacting lead pipe scale composition. This study also evaluated the applications and limitations of chemical equilibrium models for predicting the solid phases present in lead pipe scales. This study addressed Objective 4 and the results are presented in **Chapter 6** (Figure 1.7).

Chapter 1 is the introduction of the dissertation. **Chapter 7** summarizes the results of the dissertation and provide insights and recommendations for future work.

Chapter 2: Improved Control of Lead Release from Boosting Orthophosphate and Removing Polyphosphate from a Blended Phosphate Corrosion Inhibitor

This chapter has been published in *ACS ES&T Engineering*, 2023, 3(11), 1826-1836.

Abstract

Orthophosphate addition can be an effective lead corrosion control method. Commercial phosphate-based inhibitors used in water treatment are often a blend of orthophosphate and polyphosphate. Orthophosphate (PO_4) can limit lead release from pipes by forming low-solubility lead phosphate compounds on the pipe inner surfaces. In contrast, polyphosphate can increase lead release by forming soluble lead phosphate complexes. In a controlled laboratory study using recirculating pipe loops, the effects of boosting the orthophosphate concentration and removing polyphosphate on lead release were investigated. The study began with conditioning of six harvested lead service lines (LSLs) from locations in the service area of Buffalo Water with artificial Buffalo water that received a 70%/30% poly/ortho blended phosphate chemical (orthophosphate concentration: 0.2 mg/L as PO_4). Three of the pipes were tested in two treatment stages, while the other three remained as controls. During treatment stage 1, the orthophosphate concentration in the test pipes was boosted to 1.5 mg/L as PO_4 while maintaining the original blended phosphate concentration. Both the total and dissolved lead concentrations decreased and

became more stable during this treatment stage. During treatment stage 2, blended phosphate was no longer added to the test pipes, and they received only orthophosphate (1.5 mg/L as PO₄). During treatment stage 2 the total and dissolved lead concentrations continued to decrease from their values at the end of treatment stage 1. Scale analysis revealed that the phosphorus content of the scales on the test pipes increased during treatment. A crystalline lead/calcium phosphate was observed that was phosphohedyphane (Ca₂Pb₃(PO₄)₃Cl) or a similar solid. The lead phosphate increased in abundance in moving from treatment stage 1 to treatment stage 2.

2.1 Introduction

More than 6 million lead service lines (LSLs) are still currently in use in the United States and serve a population of 15 to 22 million (Cornwell et al., 2016). Potential lead release from LSLs to drinking water is a critical concern for public health (Bradham et al., 2022; Doré et al., 2019b; Gould, 2009; Johnson et al., 2022; Levallois et al., 2018; Obasi and Akudinobi, 2020; Swaringen et al., 2022) as exemplified by the lead crises in the United States in Washington DC (Roy and Edwards, 2019), Flint (Roy et al., 2019), Michigan (Pieper et al., 2018), and Newark, New Jersey (Faherty, 2021). The Lead and Copper Rule Revisions (LCRR) in the United States include protocols that are likely to necessitate improved corrosion control for many public water systems (Kurajica et al., 2022; Latham and Jennings, 2022). These new aspects of the LCRR include the collection of 5th liter samples for residences with a LSL and a “Lead Trigger Level” of 10 µg/L (USEPA, 2021) that will require re-optimization of corrosion control treatment if it is exceeded.

Recent studies have suggested that the inclusion of the 5th liter sample will increase the number of systems exceeding the current 15 µg/L action level and the new trigger level (Lytle et al., 2021; Masters et al., 2021; Mishra et al., 2021a).

Corrosion inhibitor addition is one water treatment method for controlling lead release to tap water. According to a survey about corrosion inhibitor use in the United States, more than half of U.S. public water systems are using corrosion inhibitors, and phosphate-based inhibitors are the ones most commonly used (Arnold et al., 2020). Phosphate-based inhibitors include orthophosphate and blended phosphate inhibitors, and around 30% of water utilities use blended phosphate as their major corrosion inhibitor. Blended phosphate is a mixture of orthophosphate and polyphosphates, and the ratio between the two as well as the specific form of polyphosphate varies among different commercially available products (Wasserstrom et al., 2017).

Orthophosphate can limit lead release by forming low solubility lead phosphate solids (Bae et al., 2020a; Doré et al., 2019a; Kim and Herrera, 2010; Masters et al., 2022), such as hydroxylpyromorphite ($\text{Pb}_5(\text{PO}_4)_3\text{OH}$) and phosphohedyphane ($\text{Ca}_2\text{Pb}_3(\text{PO}_4)_3\text{Cl}$) that limit lead dissolution. Polyphosphates are a class of polymeric compounds containing PO_4 structural units that can have linear or cyclic structures. Polyphosphates are effective sequestering agents for certain metals in water, especially calcium, iron and manganese (Locsin et al., 2022; Lytle and Edwards, 2023). Polyphosphate interactions with those metals can prevent them from further reaction and precipitation, which in the case of iron and manganese could result in complaints of

“colored water” from the presence of iron and manganese oxides in the tap water (Rashchi and Finch, 2002), and in the case of calcium, excessive scaling could occur in LSLs (Cantor et al., 2000; Ketrane et al., 2009). The use of blended phosphate as a corrosion inhibitor seeks to benefit from both its corrosion control property (orthophosphate) and its sequestering ability (polyphosphate).

Polyphosphate can exacerbate dissolved lead release from LSLs to tap water. Polyphosphate substantially increased dissolved lead concentrations in plumbing systems by forming soluble lead phosphate complexes (Holm and Shock, 1991). (McNeill and Edwards, (2002) investigated the effect of phosphate inhibitors on lead release from pipes, and they found that polyphosphate chemicals such as hexametaphosphate increased release of both particulate and soluble lead from lead pipes compared with the same condition dosed with orthophosphate. Therefore, they and others recommended that polyphosphate not be used for lead corrosion control. Using size-exclusion chromatography (SEC) Trueman et al., (2018) studied the effects of orthophosphate and polyphosphate on lead speciation (dissolved and particulate lead) in drinking water that had been in contact with LSLs. They found that lead was mainly present in the form of dissolved species in the presence of polyphosphate.

Previous investigations of phosphate-based corrosion control treatment have primarily focused on orthophosphate, and only limited information is available for the use of blended phosphate. Most previous studies have focused on the effectiveness of orthophosphate (Aghasadeghi et al.,

2021; Lytle et al., 2020a, 2009a; Miller, 2014), and only a few have holistically investigated the scale deposits for phosphate-based corrosion control (Harmon et al., 2022; Nadagouda et al., 2011). Wasserstrom et al., (2017) investigated scale formation in the presence of blended phosphate. Despite the water having sufficient orthophosphate to make formation of lead phosphate solids thermodynamically favorable, they did not identify any lead orthophosphate solids in the scale. Instead, an amorphous material containing aluminum (Al), calcium (Ca) and phosphorus (P) was found in the outer scale layer that might limit lead release by acting as a physical barrier to mass transfer. In their study of lead pipe scales, Tully et al., (2019) analyzed pipes from ten systems that added orthophosphate, either on its own or as part of a phosphate blend for corrosion control. They only observed lead phosphates in the pipe scales for four systems, and lead phosphates scales were the dominant solid for only one system. Moreover, due to the potential conversion of polyphosphate to orthophosphate in the distribution system (De Jager and Heyns, 1998; Holm and Edwards, 2003; Holm and Schock, 1991; Shekhar, 2007), the net impacts of the polyphosphate in blended phosphate corrosion inhibitor in LSLs have been challenging to assess.

The objectives of this study were to determine the effects of (a) boosting orthophosphate concentrations on lead concentrations in pipes previously exposed to a blended phosphate and (b) removing the polyphosphate from the inhibitor. These objectives were pursued in a laboratory-based study with harvested lead pipe segments that integrated measurements of

dissolved and total lead in water with characterization of the pipe scales. The pipes were conditioned for 6 months with artificial water that received a 70%/30% poly/ortho blended phosphate. Three pipes were tested in two treatment stages while the others remained as controls. During treatment stage 1, test pipes received additional orthophosphate (1.5 mg/L as PO₄) while still receiving the blended phosphate. During treatment stage 2, the blended phosphate was no longer added to the test pipes while the orthophosphate concentration was maintained at 1.5 mg/L as PO₄.

2.2 Materials and Methods

2.2.1 Set-up of Pipe Loops

Six recirculating pipe loops were utilized in the experiment, incorporating materials from six different harvested lead pipes sourced from various locations in Buffalo, New York (Figure A1a). The harvesting procedures were followed to ensure minimal disruption to both the pipes and the scales on their inner surfaces (Appendix A1). Four of the pipes had inner diameters of 2.54 cm (1 inch), and one had an inner diameter of 2.22 cm (P1) and another 2.97 cm (C3). The pipe assemblies for each loop consisted of one 38.1-cm (15 inch) segment and three 10.2-cm (4 inch) segments. The harvesting procedures were followed to ensure minimal disruption to both the pipes and the scales on their inner surfaces (Appendix A1). Each pipe had an inner diameter around 2.54 cm (1 inch) and consisted of one 38.1-cm (15 inch) segment and three 10.2-cm (4 inch) segments. These segments were cut from the same pipe and reassembled in the same order

with rubber connectors, PVC pipes and plastic tubing. The cut surfaces were fully coated with epoxy (J-B Weld 8281 Professional) to prevent contact with water. Each pipe loop used a magnetic drive pump and a 10-L reservoir for water recirculation (Figure A1b). Valves and flowmeters enabled control and monitoring of the flow rate. Three of the pipe loops were controls (C1, C2, and C3), which received baseline artificial Buffalo water throughout the entire experiment. Control experiments at the baseline water composition are helpful for accounting for any changes over time that are not associated with the corrosion control treatment. The other three pipe loops (P1, P2, P3) served as the test experiments that received additional orthophosphate. The pipe assemblies used in this study had previously been conditioned and used as control pipes in a previous study (Mishra et al., 2021) for 66 weeks. Due to a lab shutdown in early 2020 caused by the COVID-19 pandemic, the conditioning period did have a 2-month period in which the water in the pipes was stagnant. There was no movement or physical disturbance of the pipes during shutdown. After the laboratory reopened, we flushed the pipes for approximately two weeks before collecting the data for the conditioning period. Conditioning following the period of stagnation due to the COVID-19 shutdown lasted for 33 weeks before corrosion control treatment stages began, resulting in a total conditioning time of 99 weeks. Because the pipes had been the control pipes in that previous study, they had been receiving the baseline Artificial Buffalo water over the entire conditioning period.

2.2.2 Preparation of Water Chemistry

Artificial Buffalo water was used for each pipe, and a fresh volume of this water was introduced to each pipe loop once per week. Artificial Buffalo water was prepared to match the key water chemistry parameters (pH, hardness, alkalinity, free chlorine, and blended phosphate concentration) of actual Buffalo water as indicated in the 2019 – 2020 Buffalo Water Quality Report (Table A1.1). The reagents used to create the Artificial Buffalo water are listed in the Appendix A1. In actual Buffalo water, poly-aluminum chloride is added as a coagulant. Fe and Mn in finished water are low, and the water was not highly supersaturated with calcium.

2.2.3 Experiment Stages

The experiment consisted of three stages: conditioning (Weeks 0 to 32), treatment stage 1 (Weeks 33 to 49) and treatment stage 2 (Weeks 50 to 60). Conditioning of pipes was performed before the testing phase to acclimate and stabilize lead release after any disturbances associated with the harvesting and shipping of the pipes. During conditioning, all pipes were treated with the baseline artificial Buffalo water with the same blended phosphate inhibitor (Calciquest, Carus Corporation with a 70%/30% blend of poly/ortho phosphate) and same dose that the pipes had received when in use in Buffalo. This dose provided 0.2 mg/L as PO₄ orthophosphate. At the end of the conditioning process, three pipes were chosen as control pipes, while the remaining three were designated as test pipes. The selection was such that of the pipes with the highest lead concentrations during conditioning, one was assigned to the control set (C2) and one

to the test set (P2). The other four pipes have similar concentrations to one another during conditioning and were randomly assigned to the test and control sets. During treatment stage 1, three test pipes were treated with additional orthophosphate (total of 1.5 mg/L as PO₄) while maintaining the presence of the blended phosphate. During treatment stage 2, blended phosphate was no longer dosed to the water in the test pipe loops, and they received only orthophosphate (1.5 mg/L as PO₄).

During the first phase (Week 0 to 17) of the conditioning stage, all pipe loops received continuously recirculating water because this was expected to be most efficient for conditioning pipes. When a stable lead concentration was achieved, the flow regime was adjusted to a pattern of three periods of stagnation (6.5 h) and three periods of flow (1.5 h) per day at a flow rate of 4-5 L/min. This provided a daily total volume of flow of about 1100 L (280 gallons) per pipe, which simulated typical household use. Stagnation and flow periods were controlled by an automatic timer switch. The details of the phosphate dosing and water flow are listed in Table A1.2.

2.2.4 Analytical Methods

Samples for free chlorine, pH and orthophosphate were collected from a sampling port downstream of the lead pipe assembly and located between the flow meter and reservoir (sampling port 2 in Figure A1.1). Free chlorine samples were collected and measured in the morning of every weekday by the DPD (N, N-diethyl-p-phenylenediamine) method (4500-Cl G,

Standard Method), and the free chlorine concentration was re-adjusted to the target value (1.1 mg/L) after measurement. The pH was measured every weekday morning and re-adjusted to a target of 7.7 every Wednesday and Friday. Orthophosphate concentrations were measured according to the modified molybdate colorimetric method (Method 365.3, EPA) at the beginning and at the end of each week of water circulation.

Inductively coupled plasma mass spectrometry (ICP-MS, NexION 2000) was used to measure lead concentrations (Method 200.8, EPA, 1996)⁴⁷. The dissolved and total lead concentrations were measured at the end of each week (168-hours) prior to the exchange of the water in the reservoirs. Samples for measurement of dissolved lead were collected from the reservoir, filtered with 0.22 μm polyethersulfone (PES) filters (Environmental Express, Inc.), and then acidified to 1% (w/w) nitric acid. For the total lead samples, the water remaining in the 10-L reservoirs at the end of the week was treated with reductant and acid to dissolve any lead-containing particles in the reservoir. First 9 mL of hydroxylamine hydrochloride (0.2 g/L) was added to each 10-L reservoir and allowed to react for 24 h to reductively dissolve any Pb(IV) solids that might be present. The water in each reservoir was then acidified with nitric acid (ACS, 68-70%) to provide a final nitric acid concentration of 1% (w/w); the reservoirs were held for at least 24 hours prior to sample collection. To assess lead release to initially lead-free water, the total lead concentration in the water after the first 6-h stagnation period of each week was measured on samples collected from a sampling port immediately downstream of the pipe

assembly (sampling port 1 in Figure A1.1). We conducted a statistical analysis on both the dissolved and total lead concentrations averaged over seven-week intervals at the end of each stage, using a two-tailed t-test and a Wilcoxon rank-sum test with a significance level of 0.05. The coefficient of variation (CV) was used as an indicator for the stability, which is calculated by the ratio between the standard deviation and the mean of samples for a specific time range of interest.

Scale analysis examined the morphology, mineralogy, and elemental composition of the scales of solids present on the inner surface of the pipes. Scale analysis was conducted at the end of the conditioning stage, treatment stage 1, and treatment stage 2 on both control and test pipes. The scale was collected from a large area of the inner pipe surface of a 10.2-cm long lead segment that was in the pipe loop. Samples from multiple pipe loops were collected and analyzed for each stage of the study: segments from C2 and P2 at the end of the conditioning stage, segments from C1, C3, P2, and P3 at the end of treatment stage 1, and segments from all six pipes at the end of treatment stage 2. Two different layers of scale were scraped off the inner pipe surface. A top layer was in contact with the water, and the bottom layer was between that top layer and the unaltered lead pipe. The morphology of the scale was characterized by scanning electron microscopy (SEM, Thermo Fisher Quattro S E-SEM). The element distribution within the scales was characterized by energy dispersive X-ray spectroscopy (EDS, Oxford AzTec). X-ray powder diffraction (XRD, Bruker d8 Advance X-ray) was conducted for crystalline phase identification.

ICP-MS of acid-digested scale was conducted for quantification of element mass concentration.

Additional information on scale analysis is provided in the Appendix A1.

2.3 Results and Discussions

2.3.1 Phosphate, pH and Residual Free Chlorine in Lead Pipe Assemblies

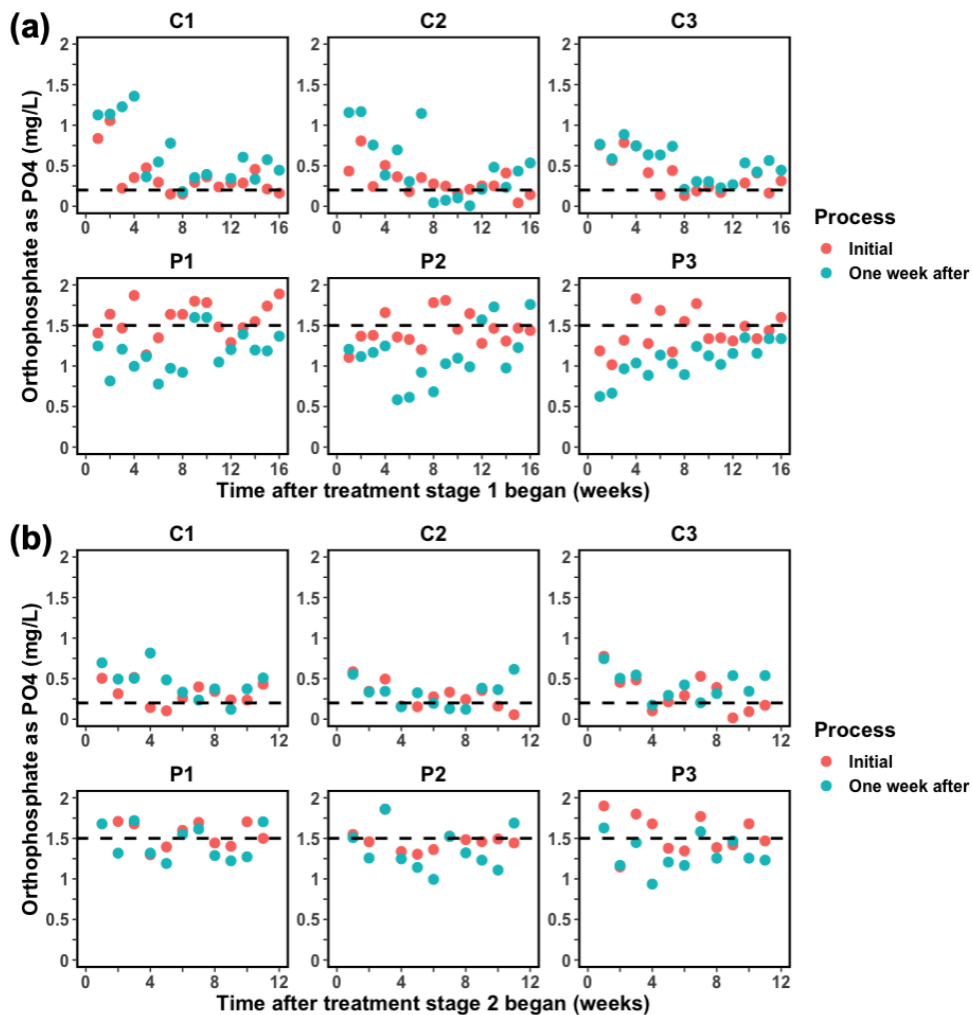


Figure 2.1 Initial orthophosphate concentration (C:0.2, P:1.5 mg/L as PO₄) and concentration after one week during (a) treatment stage 1 (16 weeks in total) and (b) treatment stage 2 (11 weeks in total) for both control pipe loops (C1, C2, and C3) and test pipe loops receiving additional orthophosphate (P1, P2, and P3). The horizontal dashed line is the target initial orthophosphate concentration in the control and test experiments.

During treatment stage 1, substantial consumption of orthophosphate occurred during a week of recirculation in the test pipes as seen by the lower concentrations at the end of the week than at the start (Figure 2.1a). The consumption of orthophosphate declined as treatment progressed. By the end of treatment stage 2, the orthophosphate concentration after one week was around 1.1 mg/L as PO₄ (Figure 2.1b) for an average consumption of orthophosphate by the pipes of about 0.4 mg/L as PO₄ per week. The loss of orthophosphate from the water was an early indication that lead phosphate solids were growing in the pipe scales, which will be discussed later in the context of scale analysis.

In contrast, no significant change in the orthophosphate concentration occurred for the control pipes. Notably, some control pipes exhibited a slight increase in the orthophosphate concentration for certain weeks. The increase ranges from 0.01 to 0.5 mg/L as PO₄, and the median increase was 0.12 mg/L. The increase of phosphate concentration noticed in the control pipes is probably from the conversion of some of the polyphosphate to orthophosphate during the week of recirculation. A previous study has also suggested that amorphous layers of scale can be physically unstable. Hence, the detachment of orthophosphate from the scale could also contribute to its elevation. For the first 4-6 weeks of treatment stage 1, the initial orthophosphate was above the target due to an issue with the blended phosphate stock solution that was then resolved.

The pH and free chlorine concentration are important water chemistry parameters that can affect lead release. The pH and free chlorine were measured every weekday morning. The pH was adjusted to a target of 7.7 every Wednesday, and free chlorine was re-adjusted to the target value (1.1 mg/L) in the morning every weekday. In this study, pH always increased from the target (pH 7.7) as water flowed through the loops, but the extent of the increase in pH declined and stabilized as the experiment progressed (Figure A1.2a). By the end of treatment stage 2, the pH after one week was 7.8-8.1 for most pipe loops (Figure A1.2b). Notably, the test pipes had a more stable and lower pH than did the control pipes. The residual free chlorine after one day gradually increased as the experiment progressed, going from about 0.1 mg/L at the beginning of conditioning to about 0.7 mg/L by the end of treatment stage 2. No significant difference was noticed between control and test pipes regarding residual free chlorine concentrations. The stabilization of pH and residual free chlorine both suggest that the pipe loops had become more stable with time. Additional information about pH and free chlorine can be found in Section 4 of the Appendix A1.

2.3.2 Lead release in the Presence of Blended and Orthophosphate Corrosion Inhibitors

Total lead

The total lead concentration decreased and stabilized compared to the early stage of conditioning (150-200 µg/L, CV above 1.0) as conditioning continued, and it dropped below 100 µg/L and

became stable (CV below 0.7) for all the pipes before treatment stage 1 (Figure A1.2a). Control pipe C2 began with an initially higher lead concentration (130 µg/L) than in the other pipes, which progressively decreased to 90 µg/L over the initial five-week period of treatment stage 1. The total lead concentration gradually declined from 100 to 60 µg/L as treatment stage 1 progressed, and it became increasingly stable (CV below 0.5). By the end of treatment stage 1, the average total lead concentration for the test pipes had decreased to 43.1±34.1 µg/L (Table 2.1) and the average CV had dropped to 0.35. In contrast, the average total lead concentration for control pipes was 58.3±26.5 µg/L with an average CV of 0.5. During treatment stage 2, blended phosphate was no longer present in the water supplied to the test pipe loops, and they received only orthophosphate (1.5 mg/L as PO₄). The total lead concentrations of test pipe loops decreased to 40.0±17.0 µg/L by the end of treatment stage 2 (Table 2.1), while the total lead concentrations for the control pipe loops remained higher and more variable (91.9±38.2 µg/L, CV of 0.6) (Figure 2.3). The lead concentrations for the test pipes became more stable from conditioning to treatment stage 1 and then to treatment stage 2 as seen in the box plots (Figure 2.2b and Figure A1.5a) and in the decrease in CV for the final portions of each stage (Figure A1.4a)

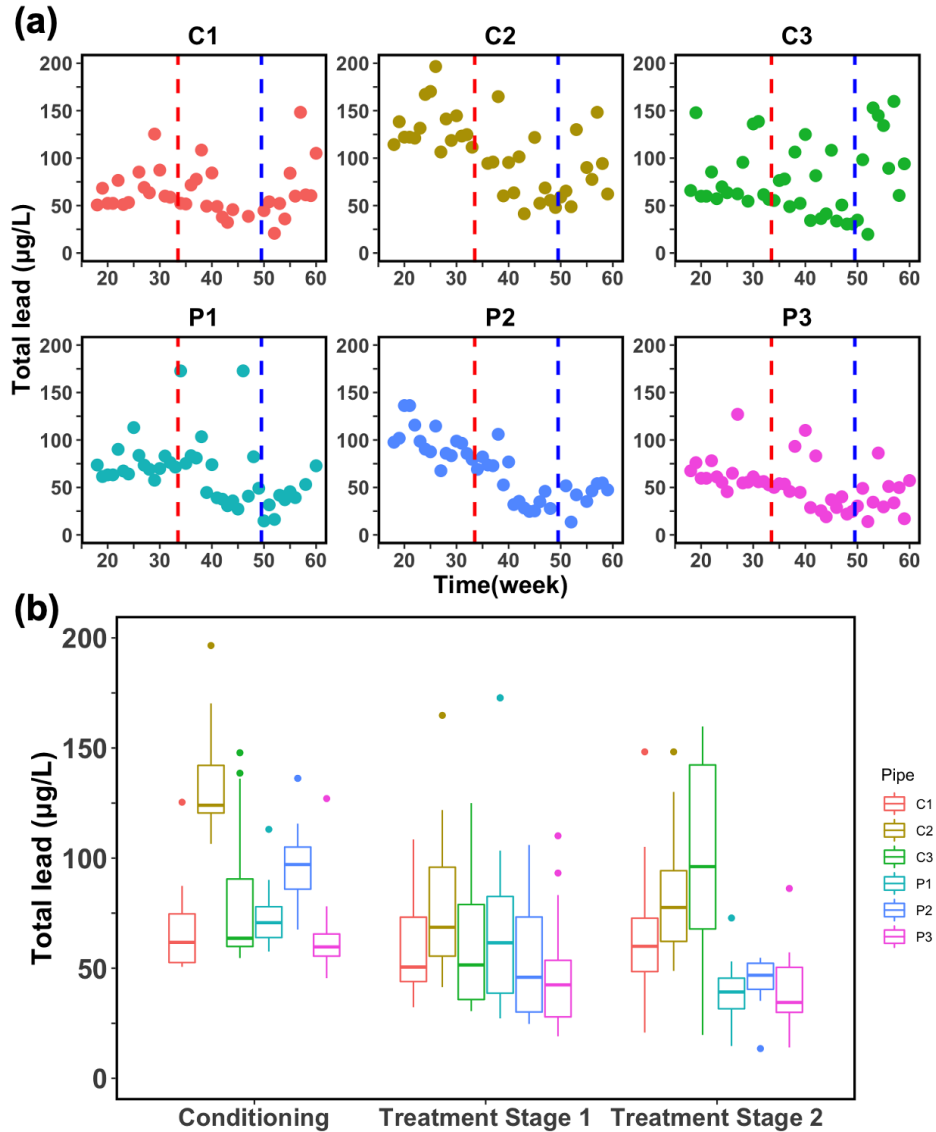


Figure 2.2 Total lead concentrations presented (a) as the full data series for each pipe loop and (b) as box plots showing the variation and central tendency of each pipe loop. The conditioning stage only includes data starting in Week 18. The vertical red and blue lines indicate the beginning of treatment stages 1 and 2, respectively.

The total lead concentrations after the first 6-h stagnation period have similar trends to those for total lead after one week of recirculation for both control and test pipes (Figure A1.6). For the test pipes, the 6-h-stagnation concentrations achieved 38.4 ± 26.4 µg/L and 36.6 ± 30.7 µg/L by the end of treatment stages 1 and 2, respectively. In contrast, the control pipes still showed high 6-h-

stagnation concentrations with great variability: $52.8 \pm 26.4 \mu\text{g/L}$, $61.8 \pm 33.3 \mu\text{g/L}$ for treatment stages 1 and 2, respectively. For test pipes, during treatment stage 1 the lead concentration after the first 6-h stagnation period had reached about 89% of the value that it would achieve at the end of one week of recirculation, and by the end of treatment stage 2 the lead concentration was reaching 92% of the value at the end of one week of recirculation in the first 6-h stagnation period. For control pipes, the ratio between the first 6-h stagnation total lead and the value at the end of one week of recirculation is around 80% by the end of treatment stage 1 and 70% at the end of treatment stage 2.

Dissolved lead

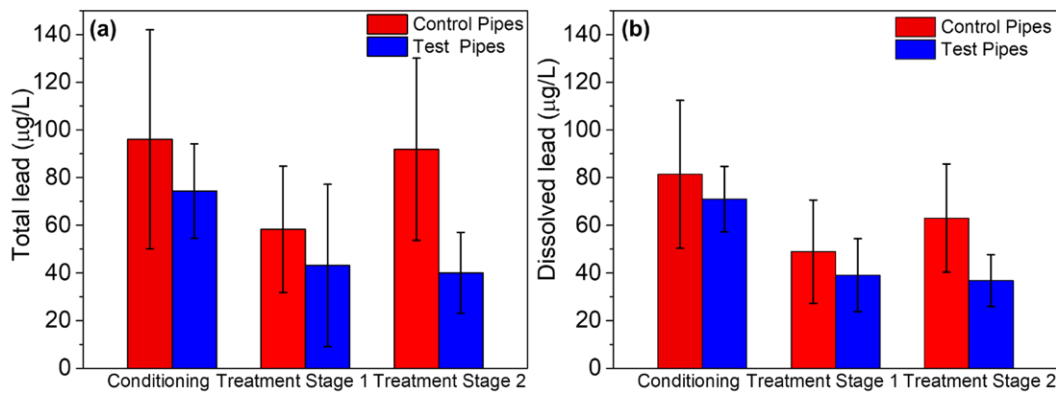


Figure 2.3 (a) Average total lead and (b) dissolved lead concentrations with standard deviations in different test stages for the last seven weeks of each stage.

As treatment stage 1 progressed, the dissolved lead concentrations for the test pipes declined from about $70 \mu\text{g/L}$ to about $40 \mu\text{g/L}$ (Figure 2.4a). The dissolved lead concentration of the control pipe loops also decreased during treatment stage 1 but to a lesser extent (from about 80 to about $60 \mu\text{g/L}$) and with greater variability compared to the test pipes (CV of 0.5 vs 0.3). The

dissolved lead concentration in the test pipes decreased further in treatment stage 2, reaching an average of $36.8 \pm 10.9 \mu\text{g/L}$ (Table 2.1) at the end of treatment stage 2. Furthermore, the dissolved lead concentrations of test pipes were more stable than during treatment stage 1 (Figure 2.3) with the CV decreasing from 0.3 to 0.2.

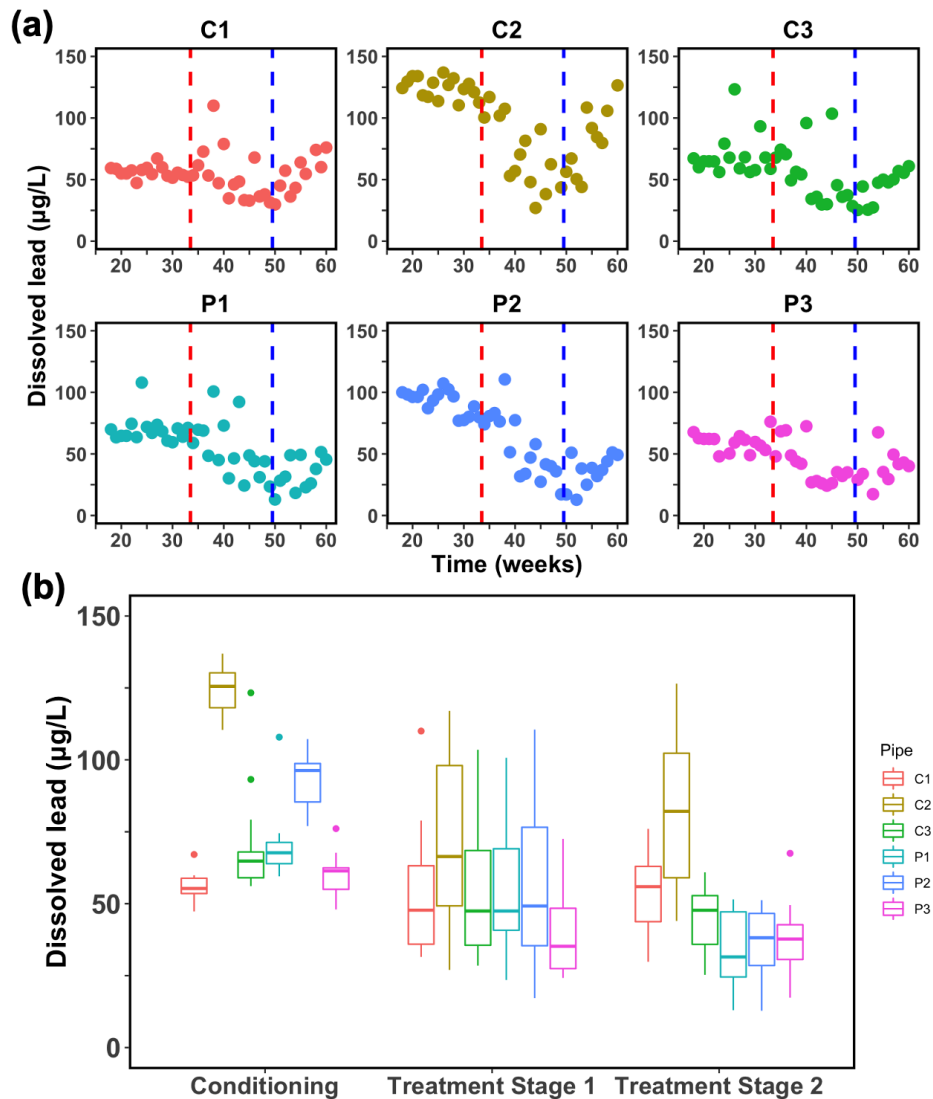


Figure 2.4 Dissolved lead concentrations presented (a) as the full data series for each pipe loop and (b) as box plots showing the variation and central tendency of each pipe loop. The conditioning stage only includes data starting in Week 18. The vertical red and blue lines indicate the beginning of treatment stage 1 and 2, respectively.

The dissolved lead in the control pipes had also decreased but to a lesser extent and with a greater variability compared to the test pipes, and the concentrations were still above 50 µg/L for most control pipes at the end the treatment stage 1 (Figure 2.4b and Figure A1.5b). During treatment stage 2 for the control pipes, we observed an elevated average concentration of lead for which we lack a clear explanation. Taking a comprehensive view of the lead concentrations in the control pipes throughout the entire experiment duration, they maintained higher lead concentrations than the test pipes during the test stages of the experiment. Further the lead concentrations in the control pipes were more variable than in the test pipes during treatment stage 2. Thus, the occurrence of elevated lead concentrations during treatment stage 2 might be understood within the context of this broader trend. The CV (Figure A1.4b) for most pipes (except C2) were around or below 0.2 by the end of treatment stage 2, indicating stable dissolved lead concentrations for each pipe loop. Overall, dissolved lead concentrations were more stable than the total lead for pipe loops indicated by their smaller CV values and standard deviations (Table 2.1), which has also been overserved in other studies (Bae et al., 2020b; Mishrra et al., 2021b). For the test pipes, the dissolved lead concentration accounted for 90-95% of the total lead concentration by the end of treatment stages 1 and stayed in that range for treatment stages 1 and 2. For the control pipes, the dissolved lead concentration accounted for 80-85% of the total lead concentration by the end of treatment stage 1, and it declined to 70% by the end of treatment stage 2. The percentage of total lead that is dissolved indicates that the treatment in the test pipes

helped lower both total and dissolved lead while the control pipes still had considerable release of lead-containing particles.

2.3.3 Comparison of Measured and Predicted Equilibrium Dissolved Lead

Concentrations

Table 2.1 Summary of lead concentrations (dissolved and total lead), standard deviations in different test stages and the relative percentage of dissolved to total lead concentrations.

Test Stage	Dissolved ¹ Lead Concentration (µg/L)		Total Lead Concentration (µg/L)		Dissolved lead / Total lead %	
	Control ²	Test Condition ²	Control ²	Test Condition ²	Control ²	Test Condition ²
Conditioning	81 ± 31 ³	71 ± 13	96 ± 45	74 ± 19	84.6%	95.4%
Treatment Stage 1	48 ± 21	39 ± 15	58 ± 26	43 ± 34	83.9%	90.7%
Treatment Stage 2	63 ± 22	36 ± 10	91 ± 38	40 ± 17	68.6%	92.0%

Note:

1. Dissolved lead defined as the lead concentration passing a 0.22 µm filter.
2. This table presents an average of three distinct pipe replicates for the control and test conditions for the final seven weeks of each stage. Refer to detailed graphs for individual pipe replicate trends.
3. $X \pm Y$ with X as the mean and Y as the standard deviation.

With the recirculation of 10 L of water through the pipe loop over the course of one week, the dissolved lead probably had enough time to achieve equilibrium in the pipe loops, which had been corroborated by previous dissolution kinetic studies (Al-Jasser, 2007; Vasconcelos et al., 1997). Consequently, those experimental measurements can be compared with the predicted lead

solubility as determined by the dominant lead corrosion product in the scale. Equilibrium lead solubility was calculated by Visual MINTEQ 3.1, and the main reactions and associated equilibrium constants are listed in Table A1.4.

Phosphohedyphane ($\text{Ca}_2\text{Pb}_3(\text{PO}_4)\text{Cl}$) or a similar solid was identified as the lead phosphate solid in pipe loops, which will be discussed later in the context of scale analysis. Due to the unavailability of an equilibrium constant for phosphohedyphane ($\text{Ca}_2\text{Pb}_3(\text{PO}_4)\text{Cl}$), the structurally similar solid hydroxypyromorphite ($\text{Pb}_5(\text{PO}_4)_3(\text{OH})$) was selected as a model lead phosphate solid for solubility calculations instead. A previous study found that predictions based on hydroxypyromorphite yielded reasonable approximations (within 20%) of the dissolved lead concentrations in water equilibrated with phosphohedyphante.

According to the predicted equilibrium dissolved lead concentrations (Figure 2.5a), for control pipe loops the equilibrium dissolved lead concentration is expected to be 42-56 $\mu\text{g/L}$ from pH 7.8 to 8.1 with hydrocerussite ($\text{Pb}_3(\text{CO}_3)_2(\text{OH})_2$) as the dominant lead-containing solid in the scale. This range of values is similar to the results of the dissolved lead concentrations for most control pipes at the end of treatment stage 2 which were around 60 $\mu\text{g/L}$ (Table 2.1). For the test pipes which had lead phosphate solids predicted as the solubility-controlling solids, the predicted equilibrium dissolved lead concentration is 26-28 $\mu\text{g/L}$ (Figure 2.5b) from pH 7.8 to 8.1, which also matched well for the experimental data of approximately 30 $\mu\text{g/L}$ (Table A1.4) in the pipe loops. The dissolved lead in the test pipes was consistent with the solubility of a lead phosphate

solid in test pipes with some substantial amount of lead phosphate formed (discussed later in scale analysis section). Lead phosphate might not be the dominant lead-containing solid with respect to the mass fraction of the overall scale, but it was abundant enough to exert solubility control for lead.

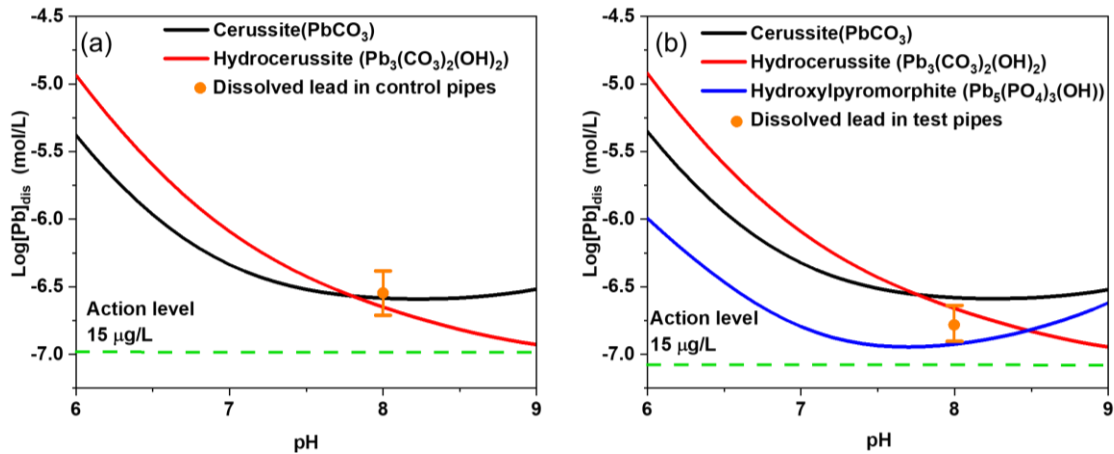


Figure 2.5 Equilibrium lead solubility for artificial Buffalo water with 2.2 mM dissolved inorganic carbon and 3.9 mM ionic strength for (a) control pipes: orthophosphate of 0.2 mg/L as PO_4^{3-} (0.0156 mM) and (b) test pipes: orthophosphate of 1.5 mg/L as PO_4^{3-} (0.0156 mM). Orange dots with error bars (standard deviations) indicate the dissolved lead at pH 8 for control and test pipe loops, respectively. Calculations were performed using Visual MINTEQ and its default database (relevant reactions indicated in Table A1.4). This database does not include any reactions for dissolved lead complexation with polyphosphate.

Solubility calculations as well as the scale analysis discussed below indicate that some lead phosphate solids might also have formed in the control pipes that received 0.2 mg/L as PO_4 .

Based on the solubility calculation, when the orthophosphate concentration is higher than 0.15 mg/L as PO_4 (1.6 mM), hydroxypyromorphite should start to precipitate (DIC:2.2 mM, pH:8).

XRD analysis (discussed below) did identify small amounts of phosphohedyphane in some of the control pipes. However, considering the dissolved lead concentrations and phosphorus

concentration in the scales of control pipes, the amount of phosphohedyphane was not enough in the control pipes to function as an effective solid for limiting lead release.

2.3.4 Statistical Significance Analysis on Dissolved and Total Lead

Concentrations

Statistical significance analysis was performed using a t-test and a Wilcoxon rank-sum test on dissolved and total lead concentrations (Table A1.5 and Table A1.6). Additional details on the approach are provided in the Appendix A1. Any differences of the dissolved and total lead concentrations between the control and test pipes at the end of the conditioning stage were not statistically significant. This lack of significant differences at the end of conditioning allowed us to evaluate any differences that could result from changes in corrosion control treatment. In contrast to the insignificant differences in concentrations between the test and control pipes at the end of the conditioning period, the observed difference in both the total and dissolved concentrations between the test and control pipes at the end of treatment stage 2 were statistically significant. While the average total and dissolved lead concentrations at the end of treatment stage 1 were lower in the test pipes than in the control pipes, those differences were not statistically significant. Either the removal of polyphosphate from the blend in treatment stage 2 or the additional time of treatment provided by treatment stage 2 did result in significantly lower lead concentrations. When the analysis was applied to the test pipes at different stages, the decreases in lead concentrations when comparing conditioning with treatment stage 2 were

statistically significant, but the differences between the concentrations at the end of treatment stage 1 and the end of treatment stage 2 were not.

2.3.5 Characterization of Scale Morphology and Element Distribution

Aluminum was present in the top scale layer for both test and control pipes based on SEM-EDS images (Figure 2.6 and Figure 2.7). Mishrra et al., (2021b) also observed similar high concentrations of Al in top scale layer of pipes from this same system.

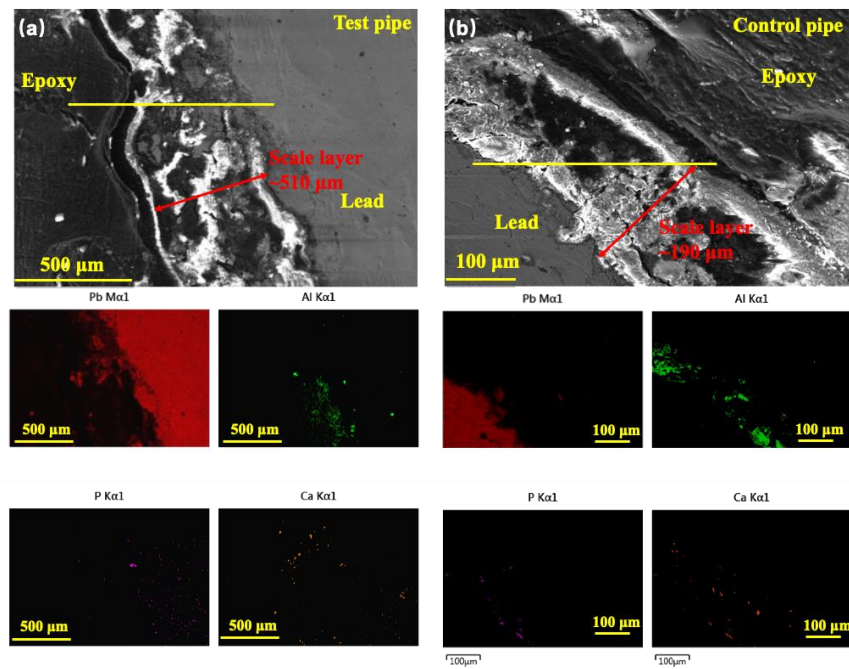


Figure 2.6 The SEM image of the cross-section (top) and elemental mapping of different elements detected by EDS (bottom) for pipes at the end of treatment stage 1 for (a) test pipe P3 and (b) control pipe C3. The yellow line in SEM images corresponds to the line scans in the Appendix A1.

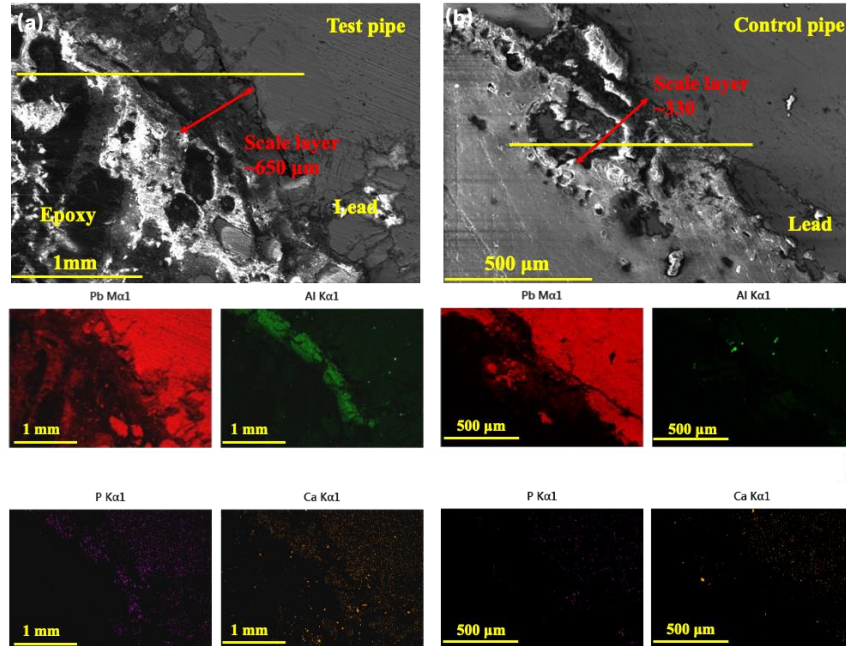


Figure 2.7 SEM image of the cross-section (top) and elemental mapping of different elements detected by EDS (bottom) for pipe segments at the end of treatment stage 2 for (a) test pipe P3 and (b) control pipe C3. The yellow line in the SEM images corresponds to the line scan in the Appendix A1.

The spatial distributions of calcium and phosphorus had some overlap but were not completely identical, indicating that phosphorus and calcium could also be present in other phases besides phosphohedyphane such as an amorphous material that makes up much of the top layer. EDS line scans (Figure A1.7) also showed that the line segment corresponding to scale layers have higher weight percentages of Al, Ca and P. The thickness of scales was 200-650 μm (Figure 2.6 and Figure 2.7). The determination of scale thickness and the precise division between the top and bottom scale layers are not possible using the current SEM images because the images were taken for only one cross section.

2.3.6 Characterization of Scale Crystalline Phases

Hydrocerussite ($\text{Pb}_3(\text{CO}_3)_2(\text{OH})_2$) was the dominant lead-containing solid for both pipes (Figure A1.8) before treatment, and small amounts of litharge (PbO) and phosphohedyphane ($\text{Ca}_2\text{Pb}_3(\text{PO}_4)_3\text{Cl}$) were detected in the bottom scale layer of pipe C2. The XRD results of scales are summarized in Table A1.7. At the end of treatment stage 1, phosphohedyphane ($\text{Ca}_2\text{Pb}_3(\text{PO}_4)_3\text{Cl}$) was found in the bottom layer of both the test and control pipes (Figure 2.8). By the end of treatment stage 1 the test and control pipe bottom scale layers had similar mass concentrations of phosphorus (both around 10 mg/g). Hydrocerussite ($\text{Pb}_3(\text{CO}_3)_2(\text{OH})_2$), cerussite (PbCO_3) and litharge (PbO) were also found in the bottom layer of both the test and control pipes in addition to phosphohedyphane ($\text{Ca}_2\text{Pb}_3(\text{PO}_4)_3\text{Cl}$). Hydrocerussite ($\text{Pb}_3(\text{CO}_3)_2(\text{OH})_2$) was the only lead-containing solid found in the top layer of both the test and control pipes.

During treatment stage 2, more phosphohedyphane ($\text{Ca}_2\text{Pb}_3(\text{PO}_4)_3\text{Cl}$) formed on the test pipes as indicated by more prominent XRD peaks and a substantial increase of the phosphorus mass concentration in the bottom scale layers. Longer reaction times with orthophosphate can generate more phosphohedyphane in pipes, and the removal of polyphosphate may have also contributed to the increased amount of phosphohedyphane. Based on previous work, polyphosphate can complex with lead which limits the driving force for Pb solid formation and thereby reduce the precipitation rate of lead solids and promote their dissolution. The presence of polyphosphate

could have impeded the formation of phosphohedyphane. By removing the polyphosphate from the water in treatment stage 2, more rapid formation of phosphohedyphane may have been facilitated.

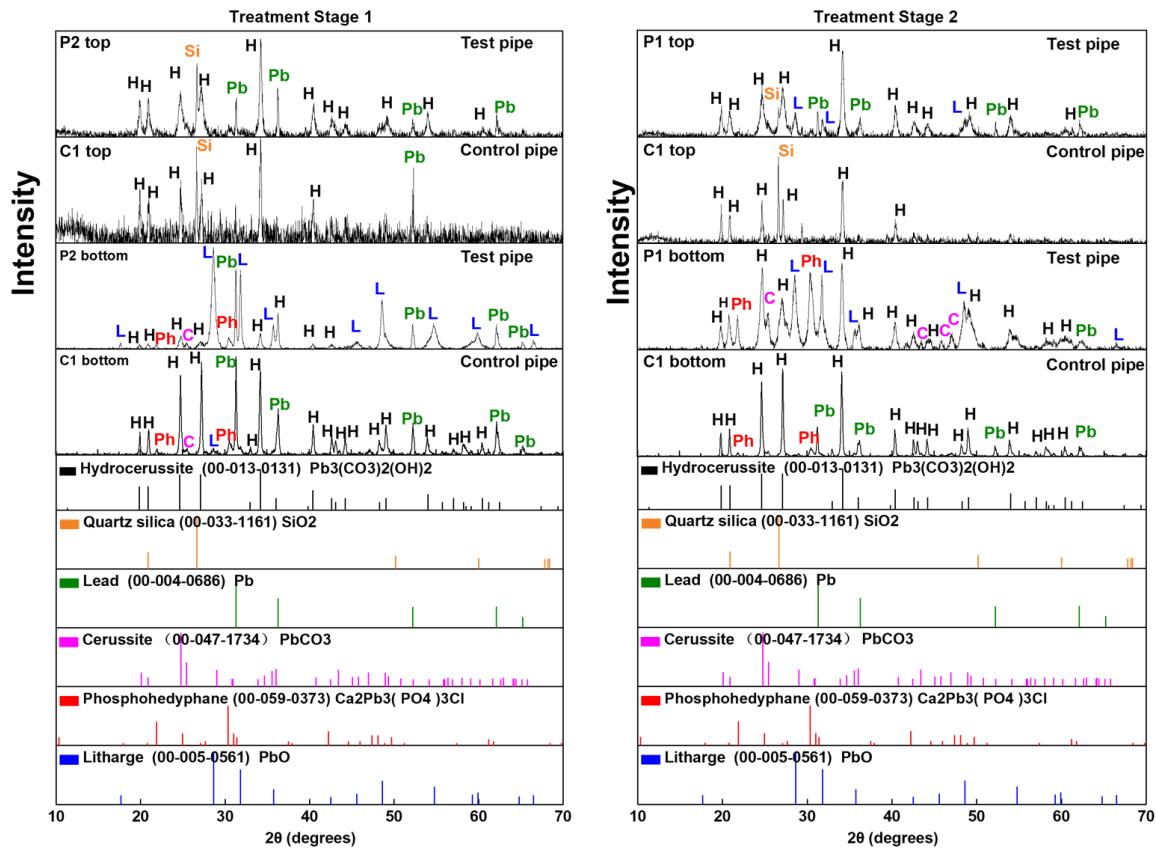


Figure 2.8 XRD patterns obtained from scale materials removed from the surface of pipes (a) at the end of treatment stage 1 and (b) at the end of treatment stage 2. The XRD reference patterns are shown for hydrocerussite ($\text{Pb}_3(\text{CO}_3)_2(\text{OH})_2$), quartz (SiO_2), elemental lead (Pb), cerussite (PbCO_3), phosphohedyphane ($\text{Ca}_2\text{Pb}_3(\text{PO}_4)_3\text{Cl}$) and litharge (PbO). Labels used throughout the patterns are peaks corresponding to solid phases abbreviated as H, Si, Pb, C, Ph and L in the same order as just mentioned.

2.3.7 Element Concentrations of Scales on the Pipes of the Pipe Loops during Different Stages

The pipes analyzed at the end of the conditioning stage all contained measurable Pb, Al and P, but P was only found in a very small amount (3 mg/g) (Table A1.8). At the end of treatment stage 1, pipes treated with additional orthophosphate had greater increases in the P concentration (up to 35 mg/g) of their scales than did the control pipes (Table A1.8). At the end of treatment stage 2, substantial P was present in the bottom layer of the scales of the test pipes with values up to 69 mg/g, while the P concentration for the bottom layers of the control pipes only had 6.6-9.6 mg/g (Table 2.2). Mass concentrations of key elements in the scales at the end of treatment stage 2 are summarized in Table 2.2, and full results for all scales analyzed are provided in Table A1.7. Some lead metal is inevitably scraped during scale preparation, which resulted in higher Pb concentrations and relatively decreases in concentrations for the bottom scale layer.

Al was abundant in the top layer for all the experimental stages. Al-based coagulants added for drinking water treatment can be its original source (Zhang et al., 2016). The residual Al is mainly present in the amorphous phase in pipe scales together with elements that include Si and P.

Similar Al-rich amorphous phase have been reported in scale analysis of other LSLs from other systems (Gerke et al., 2016; Knowles et al., 2015; Trueman et al., 2022). An amorphous phase was found in both the test and control pipes in the top scale layer as indicated by the broad diffraction peak around 2θ of 15° (Figure 2.7). The amorphous phase can function as a sink for

Al and phosphate through adsorption or precipitation. The Al-rich amorphous layer can function as a protective layer to limit lead corrosion and release (Snoeyink et al., 2003; Tully et al., 2019), while some work also reported that the lead contained in this Al-rich amorphous layer could be more easily detached and exacerbate lead release (Kvech and Edwards, 2001; Li et al., 2020, 2018).

Table 2.2 Mass concentrations (mg/g) of elements in the scales determined by acid digestion of solids followed by analysis with ICP-MS for pipes at the end of treatment stage 2.

Sample ID		Pb	P	Al
P1	Top	330.6	1.5	38.6
	Bottom	333.3	21.7	29.0
P2	Top	113.5	0.7	69.6
	Bottom	521.2	69.1	24.8
P3	Top	91.0	1.9	103.0
	Bottom	302.0	10.3	47.5
C1	Top	76.0	0.6	77.0
	Bottom	781.9	6.6	2.5
C2	Top	251.9	0.6	54.0
	Bottom	435.5	7.7	51.2
C3	Top	88.1	1.1	80.4
	Bottom	454.0	9.6	9.7

Note: 'Top' indicates top scale layer and 'Bottom' indicates bottom scale layer.

2.3.8 Corrosion Control Implications

The presence of polyphosphate in a blended phosphate can effectively increase the time for orthophosphate as a corrosion inhibitor to lower and stabilize dissolved lead release. In our study, by boosting orthophosphate from 0.2 to 1.5 mg/L and keeping the polyphosphate, both dissolved and total lead began to decline within 2 weeks. However, it took more than three months for the total lead concentration to stabilize, and the dissolved lead concentration was still higher than the predicted solubility. By removing the polyphosphate, further drops and more stability were noticed in dissolved lead. Based on previous studies (Colling et al., 1992; Ng and Lin, 2016), by adding orthophosphate to lead pipes, dissolved lead could substantially decline within 2 months while the total lead concentration stayed high and even increased in some scenarios. The formed particulate lead-orthophosphate could increase the total lead before lead-orthophosphate precipitation becomes a stable part of the scale layer (Lytle et al., 2020b).

The speciation of lead phosphate solids is diverse, and it varies for different LSLs. For example, hydroxypyromorphite ($\text{Pb}_5(\text{PO}_4)_3(\text{OH})$), chloropyromorphite ($\text{Pb}_5(\text{PO}_4)_3\text{Cl}$) and phosphohedyphane ($\text{Ca}_2\text{Pb}_3(\text{PO}_4)_3\text{Cl}$) have been reported as the potential lead phosphate solids. The composition of the phosphate-based inhibitors as well as the water chemistry can be the main factors determining the speciation of the lead phosphate solids. The lead phosphate scale formed in this experiment was identified as phosphohedyphane ($\text{Ca}_2\text{Pb}_3(\text{PO}_4)_3\text{Cl}$) or a structurally similar phase, which has been reported in other LSLs (King, 2020; Olds et al., 2021).

By removing the polyphosphate during treatment stage 2, more lead phosphate solids formed in the bottom layer of the scale. Our study revealed that 0.2 mg/L PO₄ orthophosphate as part of a blend phosphate could thermodynamically promote lead phosphate solid, but the small amount of lead phosphate solid exerted limited influence on lead release. Also, the presence of polyphosphate could impede the formation of lead-phosphate solids. Once enough lead phosphate had formed, it could then effectively control lead concentrations. The results of the combined measurements of lead concentrations and scale properties indicate that it is not necessary to convert all of the lead solids to lead phosphate solids before orthophosphate addition can effectively lower lead concentrations.

2.4 Conclusions

Boosting the orthophosphate concentration from 0.2 to 1.5 mg/L as PO₄ can have a major benefit on lead corrosion control in LSLs, and the benefit improves over time and likely also with the removal of polyphosphate in blended phosphate. Continuing boosted orthophosphate and removing polyphosphate led to more stable and consistently low total and dissolved lead and larger amounts of phosphohedyphane (Ca₂Pb₃(PO₄)₃Cl). The lead phosphate solid formed can be beneficial in limiting lead release. Generally, boosting orthophosphate and removing polyphosphate can be beneficial to lead corrosion control in terms of limiting lead release and forming lead phosphate solids. Orthophosphate will be a better corrosion control choice for LSLs

than using a blended phosphate for a system that has a major goal for lead corrosion control and no specific need for metal sequestration.

2.5 Acknowledgements

We are grateful to Buffalo Water for their contributions to this work, including providing the harvested lead service lines, funding of the study, and valuable insights on the study's technical objectives. We appreciate the technical and administrative support of Hazen and Sawyer for the completion of the work.

Chapter 3: Stability of Lead(IV) Oxide in a Lead Pipe Scale and its Potential Role in Corrosion Control

This chapter is under revision for resubmission to *Environmental Science & Technology*.

Abstract

Lead(IV) oxide (PbO_2) is an important component of the scale in many lead pipes used for water supply. When PbO_2 is stable, it has an extremely low solubility, but it can undergo reductive dissolution to release soluble Pb(II) in the absence of free chlorine. For systems that have PbO_2 already present in pipe scales, promoting conditions that maintain their stability could be an effective method for limiting lead release to drinking water. In this study, we applied a feasible and effective method, combining electrochemical and free chlorine conditioning to form and maintain PbO_2 scales on coupons. Lead coupons with a surface scale rich in PbO_2 were then used to investigate the impacts of water stagnation time and residual free chlorine on the stability of PbO_2 . Free chlorine depletion and associated lead release were investigated from 30 min to 5 days for different initial free chlorine concentrations (0.5, 1.0, 2.0, and 3.0 mg/L as Cl_2). While lead concentrations eventually increased after free chlorine depletion, there was a lag time of up to 24 h between free chlorine depletion and observed lead increases. With daily readjustment of free chlorine to target levels of 0.2 mg/L as Cl_2 or higher, the stability of the PbO_2 scale on the lead coupon was maintained and dissolved lead remained consistently below 10 $\mu\text{g/L}$. This study

provides information on key factors affecting reductive dissolution of PbO_2 present in lead scales, proposes and identifies a threshold concentration of residual free chlorine that can maintain the stability of PbO_2 lead scale. It also compares the computational and experimental results of free chlorine concentrations and redox potentials in water and provides implications for actual water quality monitoring and household drinking water use.

3.1 Introduction

The presence of lead in drinking water is a significant threat to human health (Gould, 2009; Levallois et al., 2018; Obasi and Akudinobi, 2020; Swaringen et al., 2022). Among the sources of lead to drinking water, lead service lines (LSLs) are major contributors (Bae et al., 2020b, 2020a; Doré et al., 2019a; Mishra et al., 2021b). Lead service lines have been extensively used for water supply, and more than six million remain in use in the United States (U.S.) (Cornwell et al., 2016). The Lead and Copper Rule Revisions (LCRR) introduced by the USEPA has elements that will require many water systems to re-optimize corrosion control treatment (Bradham et al., 2022). The LCRR mandates more stringent water sampling protocols with fifth liter sampling and puts forth a lead trigger level of $10 \mu\text{g/L}$ (Masters et al., 2021; Mishra et al., 2021a; Rome et al., 2022).

Lead concentrations in drinking water can be controlled by the solubility of the dominant lead-containing solids that are present in pipe scales (Kim and Herrera, 2010; Korshin and Liu, 2019; Nadagouda et al., 2011; Snoeyink et al., 2003; Tully et al., 2019; Wasserstrom et al., 2017).

Corrosion control treatment (CCT) methods currently employed involve the addition of corrosion inhibitors and adjustment of pH and alkalinity (Churchill et al., 2000; Edwards et al., 2002; Edwards and McNeill, 2002; Kogo et al., 2017; Lytle and Edwards, 2023; Ma et al., n.d.; Ng et al., 2012). These treatments are focused on the behavior of lead(II)-containing solids with the goals of either minimizing the solubility of lead(II) carbonate solids (hydrocerussite and cerussite) (Noel et al., 2014; Xie et al., 2010b) or promoting the formation of low solubility lead(II) phosphate solids (Tully et al., 2019; Wang et al., 2010; Zhang and Lin, 2011). Lead(IV) oxide (PbO_2) is another important solid found in the scales of many lead pipes (Lytle et al., 2009b; Pan et al., 2019). PbO_2 has two polymorphs, scrutinyite ($\alpha\text{-PbO}_2$) and plattnerite ($\beta\text{-PbO}_2$), and both have extremely low solubility. The development of a passivating layer of PbO_2 on the interior surface of a lead pipe could substantially decrease the release of lead into the water. Triantafyllidou et al., (2015) found that water supplied by PbO_2 -coated LSLs exhibited much lower and more stable lead levels compared to those with solubility controlled by lead(II) solids, and they suggested that PbO_2 formation in LSLs could potentially serve as a lead corrosion control strategy. However, the stability of PbO_2 is susceptible to changes in water chemistry such as pH, disinfectant type and concentration, and the presence of chemical reductants like Fe(II) or natural organic matter make it unstable (Edwards and Dudi, 2004; Lin and Valentine, 2008a, 2009, 2010).

Disinfectants play a crucial role in lead scale stability, particularly in the formation and maintenance of PbO_2 (Edwards and Dudi, 2004; Guo et al., 2014; Liu et al., 2009; Lytle et al., 2009b; Xie et al., 2010a). Due to PbO_2 's highly oxidative nature, it readily undergoes reductive dissolution, so maintaining a high oxidation-reduction potential (ORP) is crucial for its stability (Pan et al., 2022; Wang et al., 2010). Free chlorine provides a sufficient ORP to prevent PbO_2 dissolution (Bergendahl and Stevens, 2005; Kim et al., 2006). Chloramine, another disinfectant, is not sufficiently oxidizing to induce the formation of PbO_2 and can actually contribute to PbO_2 reduction (Bae et al., 2020a; Edwards and Dudi, 2004). In the absence of free chlorine, PbO_2 becomes unstable and releases lead to the water (Roy and Edwards, 2019; Xie et al., 2010a). Thus, maintaining a residual free chlorine concentration is crucial to preventing reductive dissolution of PbO_2 (Roy and Edwards, 2019; Xie et al., 2010a). It is imperative to investigate the relationship between lead release and residual free chlorine for PbO_2 -coated lead materials and to determine the minimum concentration of residual free chlorine required to maintain PbO_2 stability.

Most previous research on PbO_2 has focused on the dissolution of pure PbO_2 solids. Pan et al., (2021) found that Cu(II) and Zn(II) initially slowed PbO_2 dissolution in water by decreasing protonated sites on PbO_2 , but then enhanced dissolution after 48 hours due to competitive adsorption with Pb(II) onto PbO_2 . Xie et al., (2010b) revealed that plattnerite ($\beta\text{-PbO}_2$) dissolution rates are highest with no disinfectant, lower with monochloramine, and lowest in the

presence of chlorine, consistent with the trend in redox potential. Lin and Valentine, (2008b) found that NH_2Cl can reduce PbO_2 to Pb(II) in water, and the resulting Pb(II) generation was directly proportional to the concentration of NH_2Cl . In contrast to these studies with pure PbO_2 solids, only limited research has delved into the stability and dissolution of PbO_2 present as a scale on metallic lead materials, which can be representative of PbO_2 present in scales found on LSLs. The stability and dissolution properties of PbO_2 can differ when it coexists with other corrosion products and lead metal. The elemental lead (i.e., in the 0 oxidation state) is a potential reductant for the Pb(IV) present in the PbO_2 , so the pipe itself could act as a reductant that reductively dissolves PbO_2 in the pipe scale if free chlorine is not present. Impacts of free chlorine depletion have been studied in water systems using copper and PVC pipes. Nguyen et al., (2011) revealed a rapid decay of free chlorine in new copper pipe systems due to catalyzed reactions of Cu(OH)_2 to CuO . Al-Jasser, (2007) found that service age impacted the decay of free chlorine in iron and PVC pipes with decay constants ranging from -92% to +431%. However, limited studies have systematically investigated the influence of free chlorine depletion on PbO_2 -coated water pipes nor proposed a concept of threshold of free chlorine to maintain the stability for PbO_2 pipe scales. Triantafyllidou et al., (2015) revealed increased lead concentrations in actual homes after stagnation when free chlorine was depleted, but there was no information regarding the rate at which this occurred or whether or not there would be a lag time between free chlorine depletion and observable dissolved lead increases. The Pb coupon study is an important corrosion control assessment tool, known for its low cost, quick results, and ease of

scale analysis(Arnold et al., 2021). Previous Pb coupon studies rarely examined PbO₂ scales, likely because PbO₂ is difficult to form and maintain on coupons.

We developed a feasible and effective method, combining electrochemical and free chlorine conditioning, to form and maintain PbO₂ scales on coupons. Experiments with lead coupons explored the range of processes that can occur inside of LSLs. These PbO₂-coated lead coupons were then exposed to artificial tap water to investigate the impact of stagnation time on residual free chlorine decay and associated lead release. Further experiments using the continuous maintenance of constant residual free chlorine concentrations determined the threshold level of free chlorine required to maintain PbO₂ stability. Scanning electron microscopy (SEM) and X-ray powder diffraction (XRD) provided information about the corrosion scales on the surface of the coupons. This study examines the dissolution behavior of PbO₂ scales when free chlorine is insufficient and identifies the time lag between free chlorine depletion and lead increase.

Expanding from previous studies that had established that PbO₂ is not stable in the absence of free chlorine, the current study sought to identify if there would be a threshold free chlorine concentration that could maintain the stability of PbO₂ scales. This research also compares computational predictions of free chlorine concentration and redox potential with experimental results and discusses their impacts on the stability of the PbO₂ scale. Additionally, it provides implications for water quality monitoring and offers suggestions for household drinking water use.

The objectives of this study were to (1) assess the effectiveness of maintaining PbO₂ on lead pipes in limiting lead leaching into water, (2) determine the impacts of stagnation time and the associated residual free chlorine concentration on the stability of PbO₂ on the surface of elemental lead, and (3) identify the threshold free chlorine concentration needed to maintain the stability of PbO₂ on the surface of elemental lead.

3.2 Materials and Methods

3.2.1 Materials

Lead coupons (McMaster Carr, 5×1×0.12 cm) were first polished using sandpaper (3M, 800 and 2000 grit). They were then immersed in pH 2.0 nitric acid (HNO₃, TraceMetal™ Grade, Fisher) for two days, followed by a thorough rinse with deionized water. PbO₂ powder used in this study was purchased from Acros Organics and cleaned with 10% nitric acid (HNO₃, TraceMetal™ Grade, Fisher) to remove trace impurities. PbO₂ powder was identified as plattnerite (β-PbO₂) by XRD diffraction (Figure 3.1c). Synthetic tap water was prepared to be representative of treated water from the U.S. Great Lakes by adding specific inorganic chemicals to ultrapure water (Table A2.1). To represent the alkalinity and hardness levels, the calcium and inorganic carbon were provided to the synthetic water from a solution of water that had been equilibrated with calcite (CaCO₃) (Figure A2.1a).

3.2.2 Formation of PbO₂ on Lead Coupons

The USEPA has recommended lead coupon studies as tools for assessing corrosion control options. Such studies can either use flat strips or sheets or segments of pipe (Masters et al., 2022). As a complement to desktop analyses and pipe loop studies, coupon studies can be cost-effective, relatively fast, and they can provide valuable insights into corrosion mechanisms (Arnold et al., 2021; Li et al., 2020).

A two-step method, combining electrochemical polarization and chemical conditioning (Figure 3.1a), was employed to develop a layer of PbO₂ on metallic lead coupons (Figure A2.2b) (Lobo et al., 2022; Lobo and Gadgil, 2021; Peng et al., 2022). To determine the corrosion voltage at which metallic lead oxidizes to lead(IV), cyclic voltammetry analysis with a potentiostat (Gamry reference 600, Cathode: Pt, Reference electrode: Ag/AgCl in 1 M KCl) was performed on coupons in a 0.1 M NaHCO₃ solution at pH 8.0. Two distinctive peaks became evident at steady state corresponding to potentials of -0.52 and 1.43 V (vs Ag/AgCl in 1 M KCl) (Figure A2.3a). These peaks were ascribed to the corrosion potentials associated with Pb(II) and Pb(IV) species, respectively (Lobo and Gadgil, 2021). Notably, the corrosion potentials for Pb(II) and Pb(IV) shifted toward higher potentials as scanning progressed. These shifts are attributed to the formation of scale and the passivation of the metal surface (Refaey, 1996; Wessling, 1994). Ultimately, the potential of 1.43 V at steady state was selected for the two-hour electrochemical

polarization treatment of the coupons. The current density of the lead coupon remained consistently around 1 mA/cm² (Figure A2.3b).

Following electrochemical polarization, the coupons were rinsed with DI water and then conditioned with 40 mg/L as Cl₂ of free chlorine for one week to establish a thicker PbO₂ scale (Peng et al., 2022). The pH of the solutions increased over the course of the week, accompanied by a substantial consumption of free chlorine (Figure A2.4). The detailed changes in residual free chlorine and pH during conditioning can be found in the Supporting Information. Glass jars (240 mL, Qorpak Bottle Beakers®) were used for lead coupon immersion during conditioning and experimental testing. Within each jar, the coupons were positioned vertically and has with fishing line into 200 mL aqueous solutions (Figure A2.2b). A magnetic stir bar mixed the solution (diameter 3mm; length: 10 mm, Fisher) at 200 rpm throughout all experiments to ensure that free chlorine was evenly distributed throughout the solutions in the jars. Each jar was covered with aluminum foil to prevent any photochemical reactions.

Following the one week of conditioning with 40 mg/L as Cl₂ free chlorine, the lead coupons were conditioned with 3 mg/L of free chlorine as Cl₂ for 25 weeks in six jars as illustrated in Figure A2.5. Between weeks 12 and 13, epoxy was applied to the outside edges of each coupon to mitigate corrosion where the metal surface was not totally covered by PbO₂ coating. We applied a protective coating of J-B Weld 8281 professional epoxy to the edges of each coupon while leaving the faces exposed (Figure A2.6). As conditioning advanced, lead concentrations

gradually decreased from 300 µg/L to 100 µg/L (Figure A2.5a). At the end of week 25, one of the best-conditioned coupons from each jar was chosen for the subsequent testing phase. The coupons were screened through a one-day stagnation experiment, during which dissolved lead concentrations were measured under an initial free chlorine concentration of 3 mg/L. The best-conditioned coupons were identified as those demonstrating the lowest dissolved lead levels after the one-day stagnation period. Conditioning of the remaining coupons continued for the purpose of scale analysis. After an additional six weeks of conditioning, the dissolved lead concentrations for all jars consistently measured below 10 µg/L (Figure A2.5b). Additionally, the residual free chlorine concentration in each jar reached a stable level of approximately 2.2 mg/L after a 24-hour period (Figure A2.5c). These findings collectively indicated that the lead coupons had attained a state of stability and were ready for the testing phase.

3.2.3 Analytical Methods

Free chlorine samples were measured by the DPD (N, N-diethyl-p-phenylenediamine) method (4500-Cl G, Standard Method) on a spectrophotometer (Thermo Scientific™ GENESYS™ 140) (W et al., 2012). Inductively coupled plasma mass spectrometry (ICP-MS, NexION 2000) was used to measure lead concentrations (Method 200.8, EPA). Samples for measurement of dissolved lead were collected with syringes, filtered with 0.22 µm polyethersulfone (PES) filters (Environmental Express, Inc.), and then acidified to 1% (w/w) nitric acid. Total lead samples were initially treated with hydroxylamine hydrochloride (0.2 g/L) as a reductant to dissolve any

Pb(IV) solids. They were then acidified to pH 1 using trace metal grade nitric acid to dissolve any remaining lead-containing particles. A pH meter and associated electrodes (Fisherbrand accumet AB15) were used to measure the pH and ORP of the solution.

Scale analysis was performed on the lead coupons that underwent the same conditioning process as the coupons that had been used in the test phases. A scanning electron microscope (SEM, Thermo Fisher Quattro S E-SEM) was used to characterize the morphology of the scale. X-ray powder diffraction (XRD, Bruker d8 Advance X-ray) was conducted for crystalline phase identification.

3.2.4 Characterization of PbO₂ on Lead Coupons

Through electrochemical polarization, the color of the lead coupon transitioned from silver to black, indicating the formation of scrutinyite (α -PbO₂) or plattnerite (β -PbO₂) on the coupon surfaces.⁶¹ By the end of conditioning with 3 mg/L of free chlorine (Week 31) and at the end of the test, the surfaces were dark brown (Figure 3.1a). This color is consistent with that of lead scales found in LSLs containing lead(IV) oxide and lead carbonate solids. The scale had a thickness around 50 μ m after electrochemical polarization (Figure 3.1b). At the conclusion of the chemical conditioning, the scale had become more uniform and increased to a thickness of around 200 μ m. The scale thickness further increased to 220 μ m at the end of the test, potentially due to the extended contact with free chlorine. Based on the XRD patterns (Figure 3.1c), plattnerite (β -PbO₂) and litharge (PbO) comprised the lead scale following electrochemical

polarization. After chemical conditioning, hydrocerussite ($\text{Pb}_3(\text{CO}_3)_2(\text{OH})_2$) was also identified. After the experiments, plattnerite ($\beta\text{-PbO}_2$) was the only detectable crystalline component in the scale. The crystalline phases present in the coupon scale matched well with those commonly found in LSLs (Tully et al., 2019), suggesting that the lead coupons provide a good representation of scales on actual LSLs used for water supply. Based on mass and electron balance calculations (see Supporting Information), PbO_2 generated from electrochemical polarization accounted for only about 2.2% of the total PbO_2 scale at the end of the test.

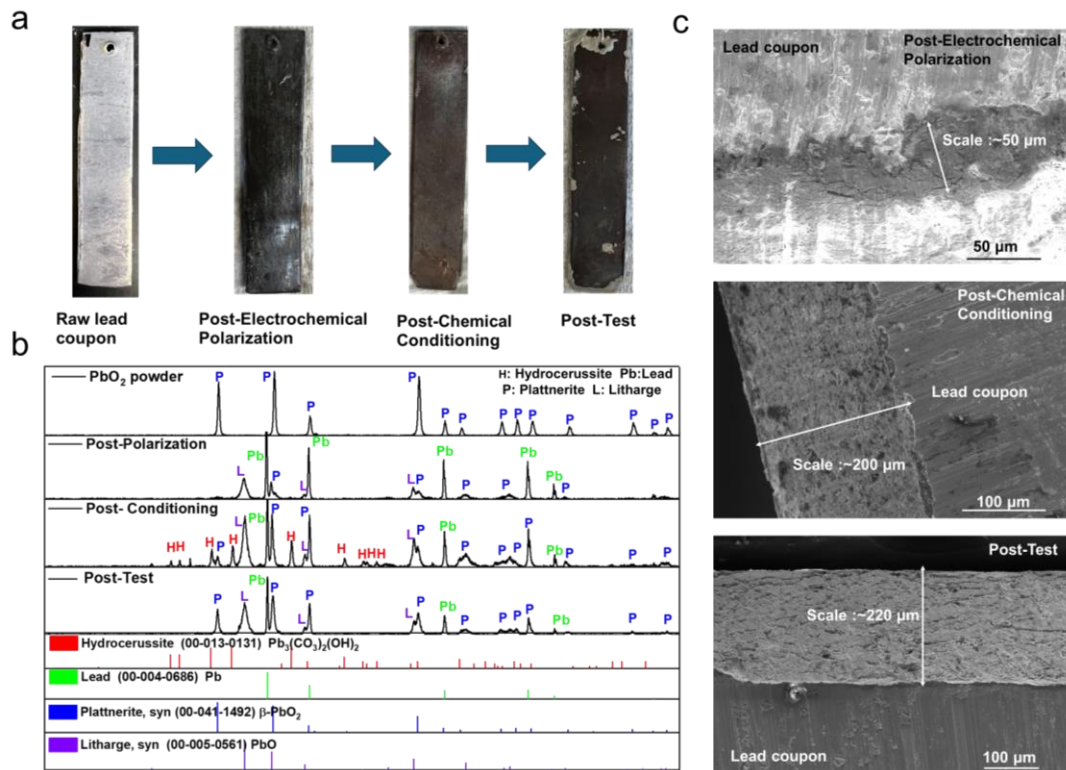


Figure 3.1 Information on the properties of the lead coupons with scales rich in PbO_2 provided by (a) optical images of a lead coupons before scale development, after electrochemical polarization, after chemical conditioning, and after the experiments. (b) XRD patterns of PbO_2 powder and the scale on lead coupons after electrochemical polarization, after chemical conditioning, and after the experiments. (c) Electron micrographs of the scale on lead coupons after electrochemical polarization, after chemical conditioning, and after the experiments.

The majority of the scale was formed through reactions with free chlorine. However, without PbO₂ formation on lead coupons via electrochemical polarization, solutions had high concentrations of lead, and free chlorine conditioning resulted in dark red precipitation in solutions instead of forming PbO₂ on the coupon surface. Therefore, electrochemical polarization played an important role in ensuring that free chlorine reacted favorably on the coupon surface to form PbO₂.

3.2.5 Impact of Stagnation Time on the Free Chlorine Depletion and Lead Release

During the stagnation study, the coupons with scales rich in PbO₂ were exposed to different initial free chlorine concentrations with no subsequent readjustments. We conducted the test with four different initial free chlorine concentrations of 0.5, 1.0, 2.0, and 3.0 mg/L as Cl₂. The stagnation times were studied in sequential order, ranging from the shortest to the longest durations from 30 min to 5 d. Throughout the stagnation study, water was not refilled or refreshed for each jar. The pH of the solution was measured at the conclusion of each experiment. The variation in pH was minimal, generally within ± 0.2 , likely due to the high alkalinity of the water. For comparison, we investigated the free chlorine depletion and lead release using both bare metallic lead coupons with no lead scale and with pure PbO₂ powder (3 g/L) at the same initial free chlorine concentrations. Each test was conducted in triplicate experiments. This experiment was designed to simulate free chlorine decay and lead release that

can occur in LSLs during water stagnation. Although stir bars were employed to ensure the uniform distribution of free chlorine, there were no inputs of free chlorine during the experiments and chlorine decayed with time as it would during stagnation of water in an LSL.

3.2.6 Identification of the Threshold Residual Free Chlorine to Maintain the Stability of PbO₂ in Scale

We maintained stable free chlorine concentrations at different values (0.2- 3.0 mg/L as Cl₂) to determine if there is a threshold free chlorine concentration needed to preserve the stability of PbO₂ in a lead pipe scale. To maintain stable free chlorine concentrations, periodic redosing (for values above 0.5 mg/L as Cl₂) and a constant slow addition method with a syringe pump (for the remaining lower values) were used. The water used in this study was sourced from a reverse osmosis (RO) system, resulting in negligible levels of dissolved organic carbon (DOC) and consequently minimal generation of DBPs that could influence the study. The increase in chloride ion had a negligible effect on the ionic strength (less than 1% increase in ionic strength). For the higher free chlorine concentrations, readjustments were conducted twice a day. For the lower values, a syringe pump introduced a continuous flow of 20 mg/L of free chlorine into the test jar (Operational parameters shown in Table A2.2).

We monitored the residual free chlorine present in the test jars twice a day and assessed the dissolved lead concentration daily. For each free chlorine level, we conducted a five-day testing period in duplicate jars. We considered the PbO₂ in the scale to be unstable if the dissolved lead

concentration exceeded 10 µg/L (i.e., the trigger level in the LCRR) for at least two consecutive sampling points.

Once a threshold free chlorine concentration had been identified, a twenty-day test was conducted with coupons exposed to that free chlorine concentration. We monitored the residual free chlorine daily and tracked the dissolved lead concentration every five days. The solution in the jars was replaced with fresh synthetic water every five days. The pH was monitored and maintained daily throughout the threshold free chlorine experiments at a target of 8.0 ± 0.1 using nitric acid and sodium hydroxide. Tests were performed in duplicate experiments.

3.3 Results and Discussion

3.3.1 Residual Free Chlorine Decay during Water Stagnation

The decay of residual free chlorine, coupled with extended contact time between water and lead pipes, can elevate the risk of increased lead concentrations in lead pipes. We investigated the decay of free chlorine at initial concentrations of 0.5, 1.0, 2.0, and 3.0 mg/L as Cl₂ under three conditions: no solid present, with PbO₂ powder in suspension, and with PbO₂-coated lead coupons. For all initial concentrations, the rate of free chlorine depletion was in the order of PbO₂-coated lead > with PbO₂ powder > no solid present (Figure 3.2 and Figure A2.7). The study also investigated the decay of free chlorine for water in contact with a metallic lead coupon for the 3 mg/L Cl₂ initial concentration, revealing a higher decay rate (as shown in Figure 3.2) compared to other conditions.

Free chlorine can oxidize metallic lead to Pb(II) and subsequently to Pb(VI). Consequently, free chlorine exhibited the highest decay rate in the presence of metallic lead. A coupon with a PbO₂ scale retained some Pb(II) solids as well as metallic lead Pb(0), which could undergo further oxidation and consume a moderate amount of free chlorine. Although pure PbO₂ consumed less free chlorine, it still required some to maintain the redox equilibrium between Pb(II) and Pb(VI) and showed higher decay rate than free chlorine alone.

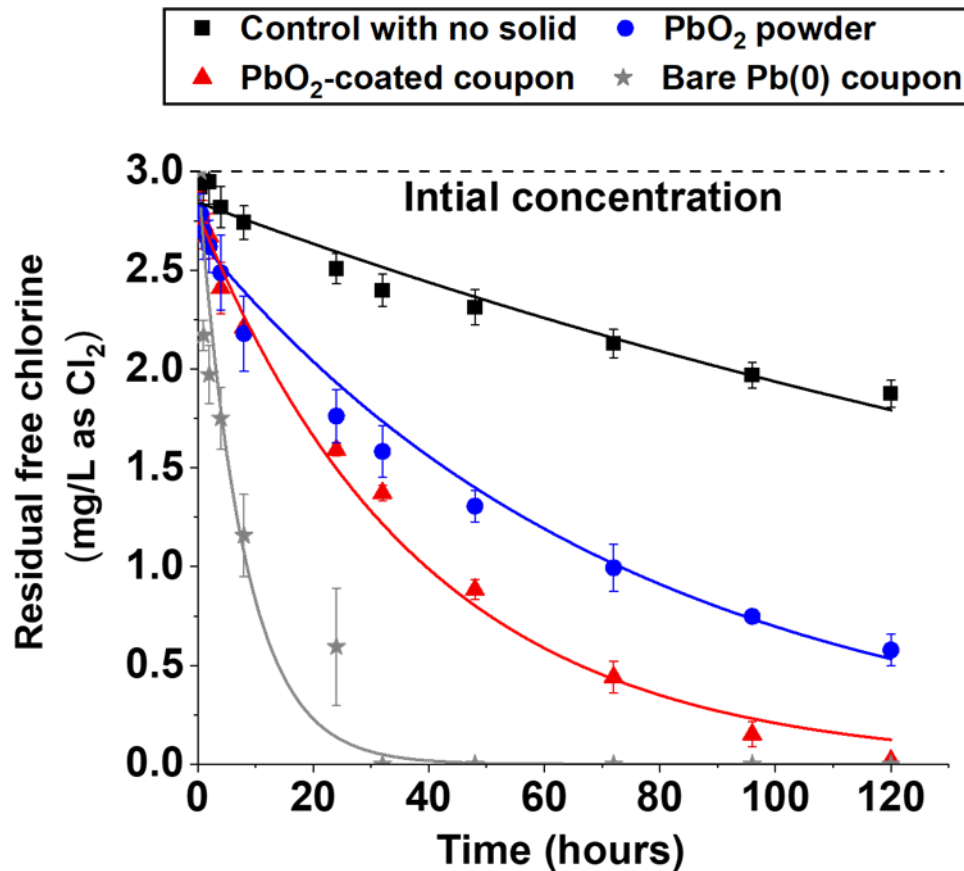


Figure 3.2 Free chlorine decay in water with pure PbO₂ powder, lead coupons with PbO₂-rich scale, bare lead coupons, and without any solids over 5 days from an initial concentration of 3.0 mg/L as Cl₂ (Solution pH: 8; Alkalinity: 91 mg/L as CaCO₃). The lines represent the fitted first-order kinetic model, and the error bars denote standard deviations calculated from the triplicate experiments.

Free chlorine decay followed first-order kinetics well for PbO₂-coated lead coupons over different initial free chlorine concentrations (Figure 3.2 and Figure A2.7). These findings regarding first-order kinetics for free chlorine depletion were consistent with previous research (Kastl et al., 1999; Zhang and Andrews, 2012). Achieving complete depletion of 3.0 mg/L of initial free chlorine necessitated a substantial amount of time, taking up to five days in our study.

3.3.2 Effect of Residual Free Chlorine and Stagnation Time on Lead Release

The decay of residual free chlorine, coupled with extended contact time between water and lead pipes, can elevate the risk of increased lead concentrations in lead pipes. We investigated the decay of free chlorine at initial concentrations of 0.5, 1.0, 2.0, and 3.0 mg/L as Cl₂ under three conditions: no solid present, with PbO₂ powder in suspension, and with PbO₂-coated lead coupons. For all initial concentrations, the rate of free chlorine depletion was in the order of PbO₂-coated lead > with PbO₂ powder > no solid present (Figure 3.2 and Figure A2.7). The study also investigated the decay of free chlorine for water in contact with a metallic lead coupon for the 3 mg/L Cl₂ initial concentration, revealing a higher decay rate (as shown in Figure 3.2) compared to other conditions.

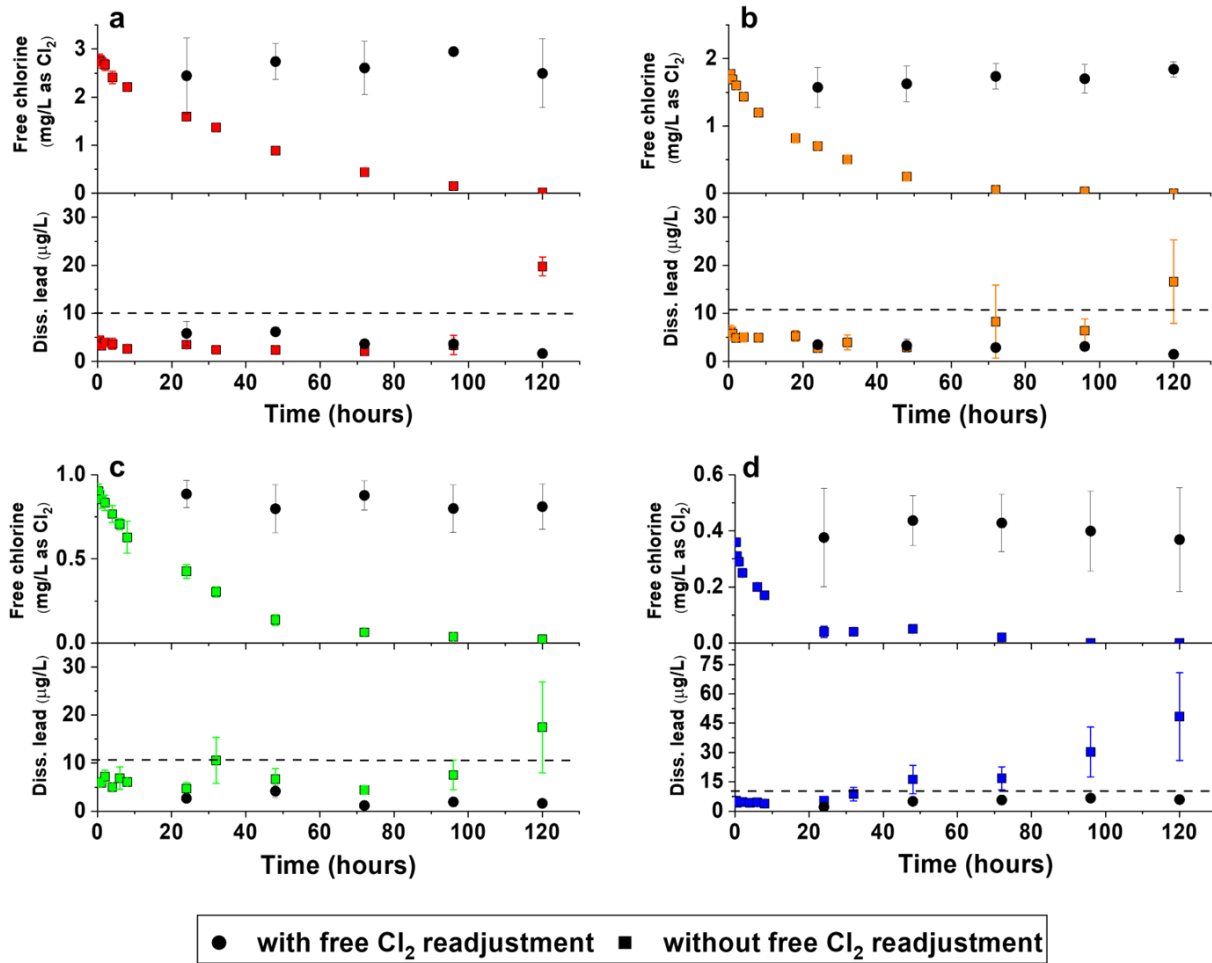


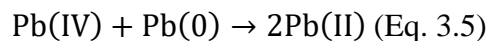
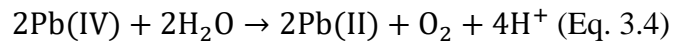
Figure 3.3 Free chlorine decay (top part of each panel) and dissolved lead concentration with and without free chlorine readjustment (bottom part of each panel) at initial concentrations of (a) 3.0 mg/L (b) 2.0 mg/L (c) 1.0 mg/L, and (d) 0.5 mg/L as Cl₂ (Solution pH: 8; Alkalinity: 91 mg/L as CaCO₃). The error bars denote standard deviations calculated from the triplicates.

An additional experiment was conducted for PbO₂-coated lead coupons with no initial free chlorine. In this experiment, the concentration of dissolved lead remained below 10 µg/L during the first 8 hours (Figure A2.9), consistent with the delayed lead increase observed in experiments with free chlorine. Additionally, the increased dissolved lead showed a wide range of concentrations among the replicates when stagnation time exceeded 15 hours, indicating that the delay before the lead concentration increases can differ among coupons. This variability may be

due to slight differences in the properties of the layer of PbO_2 on each coupon. Some PbO_2 -coated coupons began destabilizing sooner, while those with more robust PbO_2 scales destabilized later. Xie et al. (2011) studied dissolved lead release for PbO_2 -coated lead pipes during stagnation experiments with free chlorine. Their findings also revealed a plateau in lead increase as free chlorine levels decreased, followed by an increase in lead concentration after 24 hours.

We also conducted experiments with metallic lead coupons and with PbO_2 powder, both starting with an initial free chlorine concentration of 3.0 mg/L and without adjustments. For metallic lead coupons, the dissolved lead concentration exceeded 10 $\mu\text{g/L}$ within the first hour, reaching around 100 $\mu\text{g/L}$ and 300 $\mu\text{g/L}$ after eight hours and five days of stagnation, respectively (Figure A2.10). Elemental Pb metal can be oxidized to form Pb(II) species by oxygen (Eq. 3.1) or free chlorine (Eq. 3.2), which generates dissolved Pb(II) and enables the formation of Pb(II)-containing solids. Pb(II) is further oxidized to PbO_2 by free chlorine (Eq. 3.3). For pure PbO_2 , the reductants can be those present in the water including H_2O itself (Eq. 3.4), which is a thermodynamically favorable reductant for Pb(IV). In contrast, for PbO_2 on the surface of an elemental lead coupon, the reductants can be from the water and also through electron transfer between the Pb(0) of the Pb metal and the Pb(IV) of the PbO_2 to yield Pb(II) species (Eq. 3.5). The increase in dissolved lead in the water in contact with the metallic lead coupons was much higher than that in water with the PbO_2 -coated coupons after five days of stagnation. The

observed lead release from PbO₂-coated lead coupons amounted to less than 0.002 wt% of the total PbO₂ scale. The majority of the PbO₂ layer on the coupons remained intact when free chlorine levels were insufficient, and most of the PbO₂ stayed in the solid phase. The increase in dissolved lead for PbO₂-coated coupon was primarily due to the reductive dissolution of a small portion of the PbO₂ scale rather than the oxidation of the lead metal. PbO₂ powder maintained a residual free chlorine concentration above 0.5 mg/L after five days in our study, with dissolved lead consistently below 10 µg/L throughout the five-day study (Figure A2.10). The faster depletion of free chlorine and greater increase in lead release for PbO₂ present as a scale on a metallic lead coupon than for pure PbO₂ indicates that the elemental lead of the lead coupon is acting as a reductant that destabilizes Pb(IV) in PbO₂ once free chlorine is depleted.



The delay in the rise of dissolved lead concentrations noted for PbO₂-coated coupons could be attributed to the series of steps involved in the reductive dissolution of PbO₂. The first step in this process is reduction of a surface Pb(IV) atom in the PbO₂ to yield a surface-associated Pb(II)

atom. The observable dissolution then occurs when the surface-associated Pb(II) detaches and goes into solution. It may take time for the Pb(II) on the surface to accumulate to levels that drive release to solution. Xie et al. (2010) proposed a conceptual model for the dissolution of PbO₂, emphasizing the detachment of Pb(II) from the surface of solid PbO₂ as a crucial rate-limiting step. Their investigation revealed that increased carbonate concentrations in the solution facilitated the detachment of Pb(II), consequently expediting the release of lead. The lag time identified in the present study may vary across systems with different water chemistry.

While measurable lead release to water was observed from the scale after the free chlorine had been depleted, most of the PbO₂ in the scale did not dissolve and remained in the solid phase.

The observed lead release in this study was minimal of the total PbO₂ scale. The lead scales on coupons in our study consist of PbO₂ and hydrocerussite (Figure 3.1b). PbO₂ has a theoretical solubility of 2×10^{-8} µg/L for the water conditions in our study, and hydrocerussite has a theoretical solubility of 44 µg/L (Figure A2.8). When free chlorine is sufficient, the dissolved lead concentration is low (1-5 µg/L). Although it is higher than theoretical PbO₂ solubility, it is still much lower than that of hydrocerussite. As the PbO₂ dissolves when free chlorine is no longer sufficient to maintain Pb(IV) stability, the dissolved lead increases toward the solubility of hydrocerussite; however, over the timescales of these experiments dissolved lead increased toward but did not reach hydrocerussite solubility.

While the lead release has important implications for water quality, only a negligible quantity of PbO_2 underwent reduction when residual free chlorine was absent. The majority of PbO_2 remains present and can control lead at low levels once water with sufficient free chlorine is supplied. This suggests the necessity of a minimum residual free chlorine concentration to maintain the stability of the PbO_2 scale on the surface of a lead coupon, referred to as the threshold residual free chlorine. Therefore, further experiments at lower free concentrations that were maintained at stable experiments then sought to identify a threshold residual free chlorine needed to maintain PbO_2 stability on elemental lead.

3.3.3 Threshold Residual Free Chlorine that Maintains the Stability of Lead(IV) PbO_2 Scale.

From the control experiments in the stagnation study that maintained stable free chlorine concentrations, we had already established that a concentration of 0.5 mg/L as Cl_2 is sufficient to maintain the stability of the PbO_2 scale on lead coupons. The investigation into threshold free chlorine initiation commenced at an initial concentration range of 0.4-0.5 mg/L as Cl_2 . For concentrations in this range, PbO_2 -coated lead coupons successfully maintained low lead concentrations below 10 $\mu\text{g/L}$ (Figure 3.3).

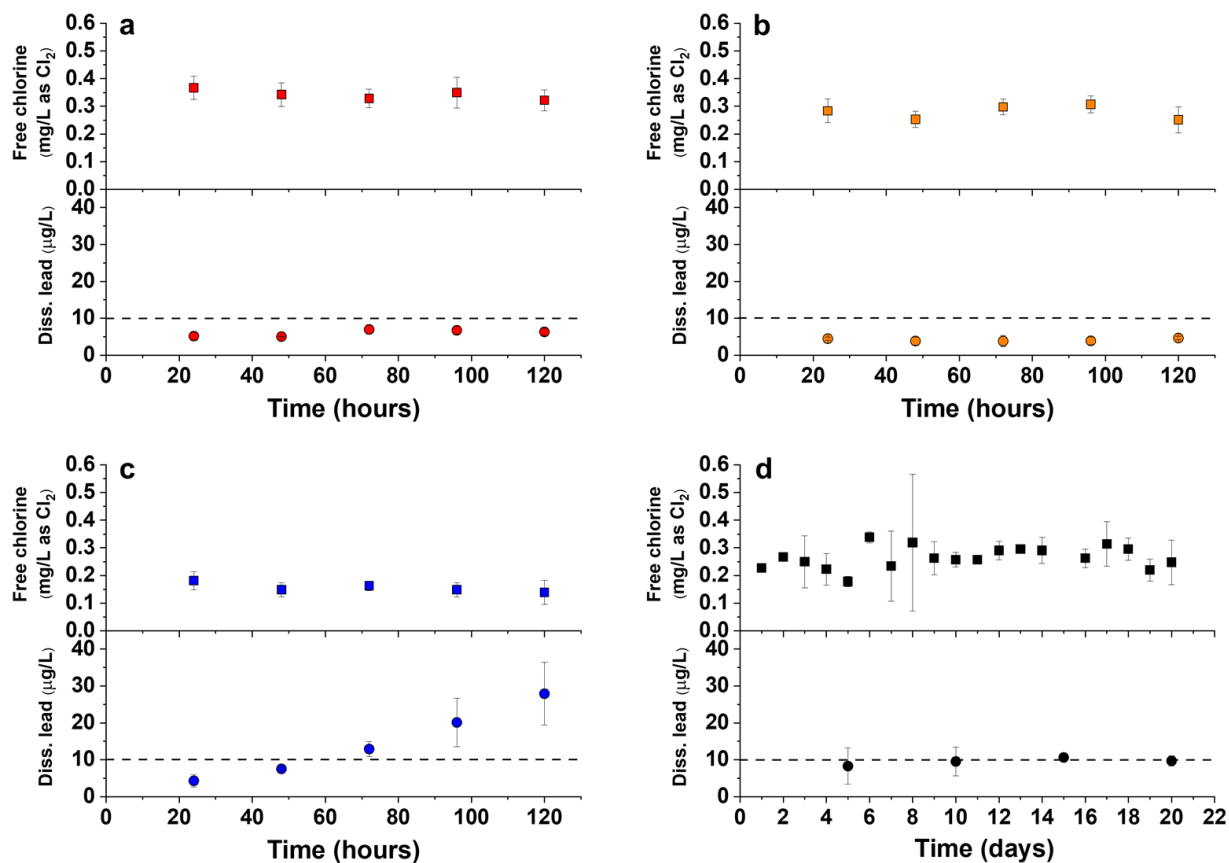


Figure 3.4. Dissolved lead concentrations with free chlorine controlled at constant concentrations of (a) 0.3-0.4 mg/L, (b) 0.2-0.3 mg/L, and (c) 0.1-0.2 mg/L for five days. One longer experiment (20 days) measured (d) dissolved lead concentration with chlorine controlled at threshold residual free chlorine (0.2-0.3 mg/L) (Solution: pH 8 and 91 mg/L as CaCO₃ alkalinity). The error bars denote standard deviations calculated from duplicate experiments.

The dissolved lead level was also stable and lower than 10 µg/L for residual free chlorine above 0.2 mg/L (Figure 3.4). However, when the residual free chlorine was maintained at concentrations of 0.2 mg/L or lower, the dissolved lead exceeded 10 µg/L after three days and further rose to 30 µg/L after five days (Figure 3.4c). Consequently, we propose a threshold free chlorine concentration of 0.2-0.3 mg/L as Cl₂ to maintain PbO₂ stability and control lead. To evaluate this range in a long-term study, we conducted a twenty-day experiment with lead

coupons, maintaining free chlorine levels at 0.2-0.3 mg/L as Cl₂. The PbO₂ scale on lead coupons remained stable, with consistent low dissolved lead concentrations (Figure 3.4d). This long-term experiment further established that there is a threshold range for residual free chlorine between 0.2 and 0.3 mg/L as Cl₂ for maintaining the stability of PbO₂. Total lead concentrations for PbO₂-coated coupons exhibited coherent release patterns with dissolved lead at residual free chlorine concentrations of 2-3 mg/L and 0.1-0.2 mg/L as Cl₂. Under conditions of adequate free chlorine, both total and dissolved lead levels remained low and stable. Conversely, in the absence of sufficient free chlorine, the concentrations of total and dissolved lead surpassed action levels. In previous research by Arnold and Edwards, (2012), total lead showed significant release after water stagnation for four weeks. In our study, the longest water stagnation time was five days. The limitation of our study's conclusions is being only up to five days and that lead concentrations would continue to increase and that particulate lead may become much more than dissolved lead over longer time.

Our experiments were conducted in well-stirred systems that provided a flow of water across the surface of the coupons. In actual LSLs, while particulate lead release is an issue in many systems, for the reductive dissolution of a PbO₂-rich scale, the released of dissolved lead from this dissolution reaction was expected to be dominant. These scales are stable and do not detach easily even free chlorine is not sufficient for some time. However, the presence of reductants such as biofilms and natural organic matter (NOM) can increase the rate of free chlorine

depletion, and then they can also act as reductants that accelerate the reductive dissolution of PbO_2 . There will be a considerable risk to drinking water quality from the leaching of dissolved and particulate lead (Figure. 3.5), which can be exacerbated by high flow rate and the deterioration of pipe scale integrity when residual free chlorine is insufficient.⁶⁸ The dissolution of PbO_2 pipe scale can also be affected by pH, dissolved inorganic carbon (DIC) and temperature in water. The threshold range for residual free chlorine identified in this study provides a valuable reference for systems with similar water chemistry, yet the specific threshold value for a given system may vary.

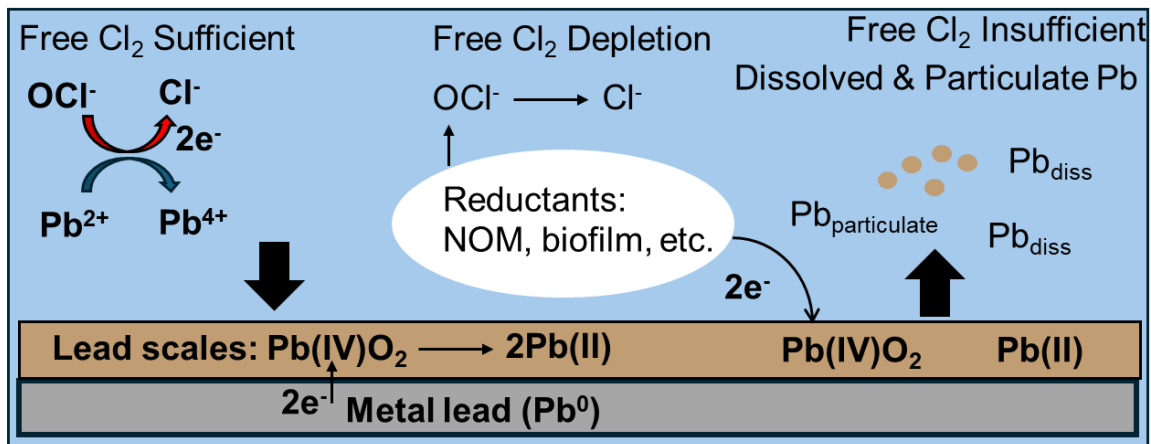


Figure 3.5 Diagram of processes influencing PbO_2 formation, dissolution, and stability on metal lead surface. From left to right the diagram illustrates (1) the formation and stability of PbO_2 in the presence of sufficient residual free chlorine, (2) free chlorine depletion in the presence of reductants in water, and (3) dissolved and particulate lead and dissolved lead leaching into water when residual free chlorine is not sufficient. Pb(IV) reduction can be from reductants in the water or through electron transfer with the elemental lead.

3.3.4 The Corresponding ORP to Threshold Residual Free Chlorine

The stability of PbO₂ is responding to free chlorine present in the solution, and free chlorine measurements has similarity to electrode-based measurements of ORP. The ORP is an indirect indication of the concentration of free chlorine in the system. The measurement of ORP using an electrode can provide a real-time measure of the adequacy of free chlorine levels for sustaining PbO₂ stability. Assessing ORP, particularly in remote and real-time scenarios, may offer a more convenient alternative to directly measuring free chlorine concentrations.

The predominant redox reactions occurring within the system are catalogued in Table A2.3. An Eh-pH (Figure A2.11) diagram was constructed with inputs for water chemistry derived from Table A2.1. The array of reactions governing the aqueous system are enumerated in Table A2.4. Based on calculations in the Supporting Information, a minimum redox potential of around 870 mV (vs SHE) is expected to stabilize plattnerite (β -PbO₂) at pH 8.0 with a corresponding free chlorine concentration of 3.59×10^{-11} mg/L as Cl₂. The environmental redox potentials at various residual free chlorine concentrations in the aqueous solution were measured with an ORP electrode. The ORP values were measured against the Ag/AgCl (saturated KCl) electrode and then readjusted to be versus SHE (Table A2.5). Notably, all experimental redox potentials were consistently lower than their corresponding theoretical values. In the established free chlorine threshold range (0.2-0.3 mg/L as Cl₂), the theoretical redox potential falls within the range of 1157-1162 mV (vs SHE), whereas its experimental counterpart ranges from 630-690 mV (vs

SHE) (Table A2.5). The ability of PbO_2 scale to maintain its stability despite a lower experimental redox potential may be attributed to several potential factors. The redox potential measured for the bulk solution phase could be different from at the solid-water interface near PbO_2 -coated lead coupons (Li et al., 2019). The thermodynamic model developed for calculating Eh to maintain PbO_2 stability may not be valid at the water chemistry of this study, potentially due to differences in the activity of PbO_2 on the surface of metallic lead ($\text{Pb}(0)$) compared to its presence as an isolated solid phase. Furthermore, in a complex and heterogeneous aqueous environment, the reactivity of free chlorine can vary significantly, and the transfer of electrons between the ORP electrode and specific chemical substances may be hindered by a slow rate of electron exchange, resulting in a discrepancy between the experimental and environmental redox potentials (Copeland and Lytle, 2014; Silvester et al., 2005).

3.4 Environmental Implications

PbO_2 is an important lead phase that is widely present in LSLs that deliver water containing free chlorine. Due to its low solubility, PbO_2 in the scales of LSLs can maintain low and stable lead concentrations when a sufficient free chlorine residual is present. This study's findings suggest that promoting the formation and stability of PbO_2 scale might be an effective lead corrosion control method. The crucial factor in preserving the stability of pre-existing PbO_2 is the water system's residual free chlorine concentration. This research identified a threshold free chlorine concentration of 0.2-0.3 mg/L as Cl_2 to sustain this stability. While measurable lead release to

water was observed from the scale when free chlorine dropped below this threshold, the vast majority of PbO_2 remained in the solid phase. Consequently, after stagnation periods that resulted in increased lead concentrations, the return to conditions with sufficient free chlorine are likely to restore the stability of the PbO_2 .

Water stagnation time is a significant factor in managing lead levels, particularly when the free chlorine concentration within the system is insufficient to maintain the stability of PbO_2 scale.

When the free chlorine falls below the threshold level, there is a delay between reaching that level and observable lead release, which offers a valuable time window for preventing lead release. However, for stagnation times beyond that time lag, lead levels will increase as stagnation time extends. The measurement of ORP serves as both a direct and secondary indicator of PbO_2 scale stability maintenance. The disparity between experimental and theoretical redox potentials necessitates thorough scrutiny in practical applications across varying water systems.

The findings of this research are grounded in laboratory-scale batch experiments with lead coupons. These experiments aimed to emulate PbO_2 -coated LSLs and offer insights into PbO_2 scale formation and stability. In the case of actual LSLs with scales containing PbO_2 , prolonged water stagnation poses a risk of the residual free chlorine dropping below the threshold, triggering the destabilization of PbO_2 . Therefore, regular water use to resupply each LSL with water from the distribution system that has free chlorine will be an important component of this

corrosion control strategy. One approach would be to have an automatic flushing valve that allows a short period of flow from the distribution system through the LSL each day with diversion of that water directly to the drain. This approach would draw the volume of water from the distribution system into LSLs and effectively replace stagnant water.

3.5 Acknowledgments

The experimental costs and support of Yao Ma for this project were provided in part by a sub-award from Hazen and Sawyer as part of a grant from Erie County Water Authority. Additional support was provided by discretionary funds available to Daniel Giammar from the Provost Office of Washington University in St. Louis.

Chapter 4: Dynamics of Lead Release from Pipes Containing PbO₂ in response to Free Chlorine Depletion during Water Stagnation

Abstract

Lead(IV) oxide (PbO₂) is an important lead corrosion product found on many lead service lines (LSLs). Because PbO₂ has a very low solubility, its formation on the surface of lead pipes can potentially minimize the release of lead to water. However, PbO₂ is only stable in the presence of free chlorine, and it undergoes reductive dissolution in the absence of free chlorine. There was a need to determine how the PbO₂-rich layer on the lead pipe would respond to free chlorine depletion and how long after depletion had occurred effects would be observed. In this study, a laboratory-scale pipe loop test was conducted with six harvested LSLs. These LSLs contained pipe scales rich in PbO₂ and came from a utility with free chlorine as the residual disinfectant. The impacts of residual free chlorine concentration and stagnation time on the stability of PbO₂ were quantitatively investigated. Depletion of free chlorine led to substantial increases in both dissolved and total lead concentrations, but increases were not observed until lag times up to 48 hours after free chlorine depletion. Total lead concentrations generally increased earlier and were higher than dissolved lead. A free chlorine concentration of 0.4 mg/L as Cl₂ was able to maintain the stability of PbO₂ in for the full duration of a 10-day experiment. Although the reductive dissolution of PbO₂ after free chlorine decay resulted in substantial increases in lead

concentrations in the water, the vast majority (greater than 99.93%) of the PbO₂ remained in the scale. This research provides insights into the effects of key factors on the reductive dissolution of PbO₂ present in the scales of LSLs, and it offers insights into how PbO₂ formation and stability might effectively limit lead release into water from pipes.

4.1 Introduction

Lead pipes have been used to deliver drinking water since the Roman Empire due to their malleability and durability (Delile et al., 2014). However, the health risks associated with lead leaching from these pipes have raised significant concerns (Edwards et al., 2009; Obasi and Akudinobi, 2020; Shrivatsa et al., 2023; Triantafyllidou and Edwards, 2012). They have prompted the needs for corrosion control treatment and lead pipe replacement (Arnold et al., 2020; Dodrill and Edwards, 1995; Kogo et al., 2017; Schock, 1989; Triantafyllidou and Edwards, 2011). With the implementation of the Lead and Copper Rule Revisions (LCRR) by USEPA, which mandates more stringent water sampling protocols, including fifth liter sampling, and establishes a lead trigger level of 10 µg/L (USEPA, 2021), the development of optimized lead corrosion control strategies is imperative (Betanzo et al., 2021; Masters et al., 2021; Mishra et al., 2021a; Rome et al., 2022).

Traditional corrosion control methods include pH and alkalinity adjustment (Kuh et al., 2006; Tam and Elefsiniotis, 2009) and the addition of orthophosphate as a corrosion inhibitor (Duranceau et al., 2010; Formal et al., 2024; Ma et al., n.d.; Ng et al., 2012). These approaches

aim to decrease the solubility of lead(II) carbonate solids or to precipitate low solubility lead(II) phosphate solids on pipe walls. While not considered by the U.S. EPA to be an corrosion control treatment method, maintaining the existing PbO₂ in pipe scales is effective in limiting lead leaching into drinking water and helpful to optimize corrosion control. Triantafyllidou et al., (2015) found that pipes with lead(IV) oxide (PbO₂) as a dominant component in pipe scales had significantly lower and more stable lead concentrations than pipes dominated by lead(II) solids. Therefore, they proposed that promotion of PbO₂ formation and stability equals or exceeds the effectiveness of Pb(II)-based corrosion control treatments.

PbO₂ is often found in lead service lines that use free chlorine as a disinfectant (Liu et al., 2016; Tully et al., 2019). PbO₂ has two polymorphs, scrutinyite (α -PbO₂) and plattnerite (β -PbO₂) (Lytle et al., 2009b; Wang et al., 2010), both of which have extremely low calculated equilibrium solubility at the pH of drinking water supply (<1 ng/L). Pb(IV) requires a high redox potential to be generated by Pb(II) to produce PbO₂ in LSLs (Copeland and Lytle, 2014; Lytle and Schock, 2005). This high redox potential cannot be provided by dissolved oxygen, but it can be provided by free chlorine. PbO₂ is readily reduced by reductants in water, including natural organic matter (Dryer and Korshin, 2007; Lin and Valentine, 2009, 2008a), biofilm (Learbuch et al., 2021; Yan et al., 2022), and iodide (Lin et al., 2008; Wang et al., 2012). The reductive dissolution of PbO₂ with water itself as the reductant is even thermodynamically favorable (Pan et al., 2022). The reductive dissolution of PbO₂ in lead pipe scales has been identified as the

primary cause of the period of elevated lead levels in Washington, DC from 2000-2004. This crisis occurred due to the switch from of the disinfectant from free chlorine to chloramine (Roy and Edwards, 2019). Chloramine does not provide an adequate redox potential to maintain the stability of PbO_2 (Bae et al., 2020a; Lin and Valentine, 2008b; Switzer et al., 2006).

Several prior studies have investigated the stability and dissolution of PbO_2 as an isolated solid Chloramine (Lin and Valentine, 2008b; Switzer et al., 2006; Xie et al., 2010a), natural organic matter (NOM) (Dryer and Korshin, 2007; Lin and Valentine, 2008a), iodide (Lin et al., 2008; Wang et al., 2012) and bromide (Lin and Valentine, 2010) accelerated the dissolution of PbO_2 in water through reductive dissolution. When no reductants are present and residual free chlorine is sufficient, the stability of PbO_2 can be maintained and lead dissolution is very low (Avasarala et al., 2021; Guo et al., 2014; Triantafyllidou et al., 2015). Xie et al., (2010b) showed that the PbO_2 dissolution rate increases at lower pH and when dissolved inorganic carbon (DIC) is higher. Pan et al., (2019) revealed that the adsorption of Cu(II) and Zn(II) on the PbO_2 solid surface can decrease its reductive dissolution in the absence of free chlorine. However, these studies were conducted with pure PbO_2 solids and not with PbO_2 that is part of a scale on lead pipe. For situations of PbO_2 in the scale of a lead pipe, a metastable situation exists with a Pb(IV) solid persisting while in contact with the Pb(0) of the lead pipe or with just a few 10s of micrometers of a Pb(II) solid between them. For these situations, the Pb(0) can also serve as a reductant to destabilize the PbO_2 . Additionally, the effects of residual free chlorine concentration and water

stagnation have not been systematically investigated for PbO_2 as an isolated solid or as part of a scale. There has been limited analysis of scales in PbO_2 -dominated lead pipes (DeSantis et al., 2020; Tully et al., 2019), which is valuable for understanding the stability of PbO_2 and its reductive dissolution in pipe scales.

The objectives of this study were to (a) explore the impacts of stagnation time and residual free chlorine concentration on dissolved and total lead concentrations for PbO_2 -dominated lead pipes; (b) investigate the formation, stability and dissolution of PbO_2 pipe scales; and (c) evaluate the effectiveness of maintaining PbO_2 scales to limit lead leaching into water. To achieve these objectives, a laboratory-based study was conducted using harvested lead pipe segments with scales rich in PbO_2 and with free chlorine as the residual disinfectant. The study included both measurements of dissolved and total lead in the water and an analysis of the pipe scales.

4.2 Material and Methods

4.2.1 Set-up of Pipe Loop Reactors

Six recirculating pipe loops were used in the experiment, utilizing materials from six different lead pipes harvested from various locations of the service area of Erie County Water Authority (ECWA) in New York State (Figure A3.1a). The harvesting procedures were carefully followed to ensure minimal disruption to both the pipes and the scales on their inner surfaces (Supplementary Material). Each pipe had an inner diameter of approximately 1.9 cm (0.75 inch). Pipe assemblies used in the loops were composed of one 45.7-cm (18-inch) segment and three

10.2-cm (4-inch) segments. These segments were cut from the same pipe and reassembled in the original order using rubber connectors, PVC pipes, and plastic tubing. The cut surfaces were fully coated with epoxy (J-B Weld 8281 Professional) to prevent contact with water. Each pipe loop utilized a magnetic drive pump and a 10-liter reservoir for water recirculation (Figure A3.1b). The water in the reservoirs was replaced with lead-free water once per week. Valves and flowmeters enabled control and monitoring of the flow rate. Three of the pipe loops (C1, C2, and C3) served as controls, receiving continuous baseline artificial ECWA water throughout the entire experiment with 3 mg/L of Cl₂ free chlorine. These control experiments with baseline water composition help account for any changes over time that are not related to the test studies. The remaining three pipe loops (T1, T2, T3) were used for the tests.

4.2.2 Preparation of Water Chemistry

Artificial ECWA water was prepared to match the key water chemistry parameters of actual ECWA water according to a 2022-2023 water quality report and actual measurements of local tap water chemistry (Table A3.1). The reagents used to create the artificial ECWA water are listed in the Supplementary Material.

4.2.3 Experiment Design

Conditioning

Conditioning of pipes was performed before the testing phase to acclimate and stabilize lead release after any disturbances associated with the harvesting and shipping of the pipes. During

conditioning, all pipes were treated with the baseline ECWA water and with 3 mg/L as Cl₂ free chlorine to establish PbO₂-rich scales on inner pipe walls. This concentration is higher than the 1.5 mg/L as Cl₂ value leaving the ECWA treatment plant. The pipes were conditioned immediately upon arrival in the lab. Their total conditioning time varied depending on their arrival dates. Pipe T1 commenced conditioning in Week 1 and was followed by Pipe C1 in Week 7. The remaining pipes started conditioning in Week 19. All pipes were conditioned for 6 to 10 months before testing began. At the end of the conditioning process, three pipes were selected as control pipes, while the remaining three were designated as test pipes. This selection was made to ensure that control and test groups were comparable in terms of the lead concentrations, free chlorine consumption, pH, and total conditioning time.

Water Stagnation

In the water stagnation experiment, the test pipes were tested at initial free chlorine concentrations of 0.5 mg/L, 1 mg/L, 2 mg/L, and 3 mg/L as Cl₂ for each trial. No readjustments of free chlorine were made during the stagnation study. The stagnation times were studied sequentially, starting from the shortest to the longest duration (from 1 hour to 72 hours), as outlined in Table A3.2. A relatively long-time stagnation experiment was also conducted for initial free chlorine concentrations of 3 mg/L as Cl₂ up to 14 days. Prior to each stagnation time point, the test pipe underwent a flush with freshly prepared lead-free water. The flushed water was discarded and not returned to the carboy. Following the flush, the pipe received lead-free

water to begin the stagnation tests. Before each stagnation time point, the pH and residual free chlorine concentration in each carboy were checked and readjusted to ensure they met the target values.

Throughout the stagnation time study, residual free chlorine, pH, and dissolved and total lead concentrations were monitored at each time point. Water samples were collected from a sampling port. The full system design is shown in Figure A3.1. Sampling was facilitated by pump and valve controls, with a total volume of approximately 100 mL collected for each time point. Before each sample was collected, the initial 20 mL of solution was discarded. After each sampling event, the remaining stagnant solution in the pipe loop was flushed and discarded.

After any stagnation time in the series for which the free chlorine concentration fell below the detection limit, the test pipes underwent a two-day reconditioning with 3 mg/L as Cl₂ of free chlorine. This reconditioning step was also performed between experiments with different initial free chlorine concentrations. This reconditioning was conducted before starting the next test to ensure no influence from the previous one.

Threshold Free chlorine

Residual free chlorine concentrations at different constant values (0-3.0 mg/L as Cl₂) were maintained to determine if there is a threshold free chlorine concentration that can preserve the stability of PbO₂ in pipe scales. To maintain stable free chlorine concentrations, different methods were employed: periodic redosing for free chlorine values above 0.6 mg/L as Cl₂ and a

constant slow addition of a free chlorine stock solution using a syringe pump for lower values. For the higher concentrations, adjustments were made manually each day. For the lower concentrations, a syringe pump continuously introduced free chlorine into the carboys of the test pipes (operational parameters included in Table A3.3).

The water in the pipes was constantly recirculating during the threshold free chlorine experiments, which helped maintain the same free chlorine concentration everywhere in the system. Residual free chlorine in pipe loops was monitored once a day, and the dissolved and total lead concentrations were tracked daily. For each free chlorine concentration, we conducted a ten-day testing period in duplicate pipe loops. We considered the PbO_2 in the scale to be unstable if the lead concentrations exceeded $15 \mu\text{g/L}$ (i.e., the action level in the LCR) for at least two consecutive sampling points.

4.2.3 Analytical Methods

Samples were collected from a sampling port downstream of the lead pipe assembly and located between the flow meter and reservoir (Sampling port A in Figure A3.1). Free chlorine samples were collected and measured by the DPD (N, N-diethyl-p-phenylenediamine) method (4500-Cl G, Standard Method) on a spectrophotometer (Thermo Scientific™ GENESYS™ 140). A pH meter (Fisherbrand accumet AB15) was used to measure the pH. Inductively coupled plasma mass spectrometry (ICP-MS, NexION 2000) was used to measure lead concentrations. Samples for measurement of dissolved lead were filtered with $0.22\text{-}\mu\text{m}$ polyethersulfone (PES) filters

(Environmental Express, Inc.) and then acidified to 1% (w/w) nitric acid. Total lead samples were first treated with hydroxylamine hydrochloride (0.2 g/L) to reductively dissolve any Pb(IV) solids and then acidified to pH 1 by trace metal grade nitric acid (Fisher scientific.) to dissolve any lead-containing particles.

Scale analysis examined the morphology, mineralogy, and elemental composition of the scales present on the inner surface of the pipes. The scale analysis was performed with removable 4-inch segments at a midpoint of the overall experiment while still maintaining the majority of the lead in the loop. The analysis was conducted before conditioning, at the end of the conditioning stage, and at the conclusion of the tests. Scale samples were collected from a large area of the inner pipe surface, comprising two different layers: a top layer in contact with the water and a bottom layer situated between the top layer and the unaltered lead pipe. The morphology of the scale was characterized using scanning electron microscopy (SEM, Thermo Fisher Quattro S E-SEM). The elemental distribution within the scales was analyzed by energy dispersive X-ray spectroscopy (EDS, Oxford AzTec). Crystalline phase identification was performed using X-ray powder diffraction (XRD, Bruker d8 Advance). ICP-MS was conducted to quantify element mass concentration of acid-digested scale. Additional information on scale analysis is provided in the Supplementary Material.

4.3 Results and Discussion

4.3.1 Establishment of PbO_2 as a Dominant Component in Pipe Scales

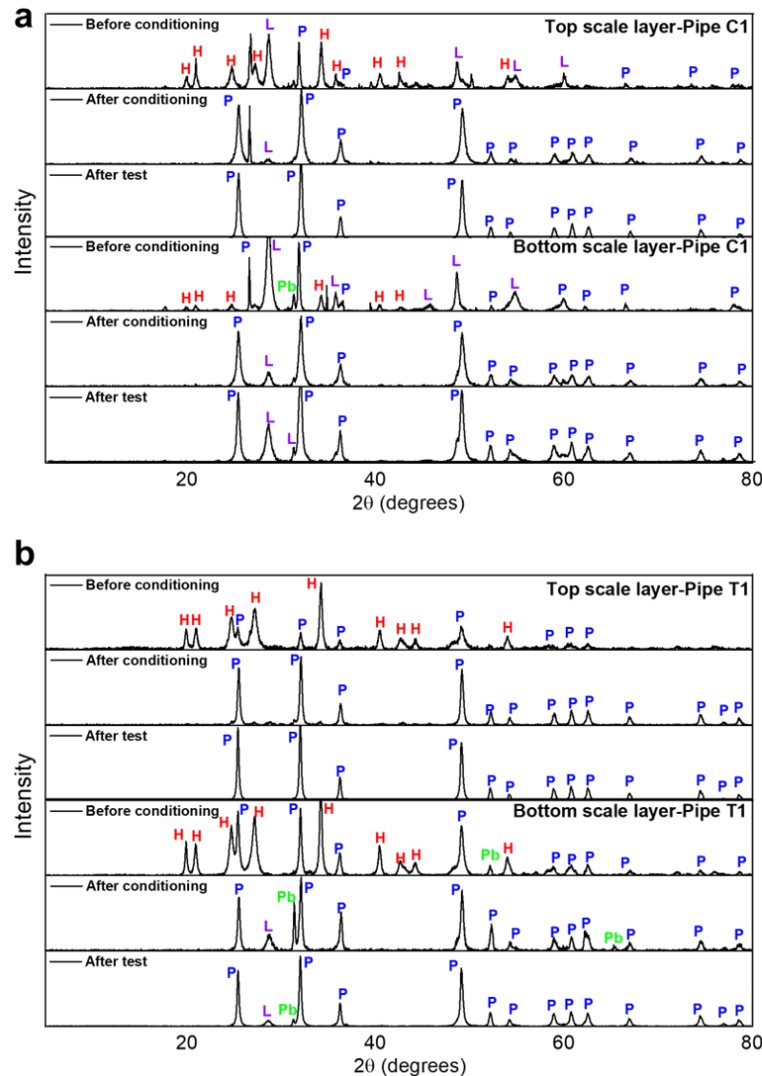


Figure 4.1 XRD patterns for top and bottom scale layers of (a) control pipe C1 and (b) test pipe T1. Reference patterns are shown in Figure A3.3 for hydrocerussite ($\text{Pb}_3(\text{CO}_3)_2(\text{OH})_2$), lead (Pb), plattnerite ($\beta\text{-PbO}_2$) and litharge (PbO). Labels used throughout the patterns are peaks from corresponding solid phases abbreviated as H for hydrocerussite, Pb for elemental lead, P for plattnerite, and L for litharge.

The pipes were first conditioned to establish PbO_2 as a dominant component in pipe scales before testing. Scale analyses were conducted on pipes right upon their arrival in the laboratory. Pipe scales were brownish (Figure A3.2), with plattnerite ($\beta\text{-PbO}_2$), hydrocerussite ($\text{Pb}_3(\text{CO}_3)_2(\text{OH})_2$) and litharge (PbO) identified as the major lead solids present (Figure 4.1). A continuous flow of synthetic water with 3 mg/L as Cl_2 of free chlorine was used to condition all pipes with the goal of increasing the amount of PbO_2 in the scales. As conditioning progressed, the average dissolved lead concentrations for pipes dropped from above 100 $\mu\text{g/L}$ to below 15 $\mu\text{g/L}$ (Figure A3.4), suggesting that the pipe scales had become increasingly rich in PbO_2 , which has a much lower theoretical solubility (2×10^{-8} $\mu\text{g/L}$) than hydrocerussite (44 $\mu\text{g/L}$) at the water chemistry conditions of the experiments (Figure A3.5). By the end of the conditioning period (Week 42), the pipes assigned to the control and test groups had similar low and stable dissolved and total lead concentrations. Dissolved lead concentrations were below 5 $\mu\text{g/L}$, and total lead concentrations were below 15 $\mu\text{g/L}$ in the final weeks before testing (Figure A3.3). Additionally, the residual free chlorine levels and pH were comparable between the pipes in the control and test groups (Table A3.6).

Scale analyses were conducted on Pipes C1 and T1 at the end of conditioning (Week 42). XRD patterns revealed that hydrocerussite ($\text{Pb}_3(\text{CO}_3)_2(\text{OH})_2$) was no longer a major scale component and that plattnerite ($\beta\text{-PbO}_2$) had become the only dominant component (Figure 4.1). The scale had become dark red (Figure A3.2), which is typical for PbO_2 -dominated pipe scales

(DeSantis et al., 2020; Lytle et al., 2009a; Triantafyllidou et al., 2015). The thicknesses of the scale for the control and test pipes were approximately 65 μm and 70 μm , respectively (Figures 4.2a and 4.2b). Appreciable aluminum was also found in the scale, consistent with previous research (Kvech and Edwards, 2001; Li et al., 2020; Snoeyink et al., 2003). The mass concentration of lead in the bottom scale layer increased from 483 ± 132 mg/g to 556 ± 132 mg/g (Table A3.1), consistent with the transition from hydrocerussite to plattnerite that has a higher lead percentage by mass (hydrocerussite: 80% Pb, plattnerite: 87% Pb, Table. A3.7). These results suggest the successful establishment of PbO_2 as the dominant component in the pipe scales.

4.3.2 Stability of PbO_2 Lead Scale during Water Stagnation

Water stagnates in pipes when they are not in use, leading to a decrease in residual free chlorine concentration. When the residual free chlorine concentration is insufficient, reductive dissolution of PbO_2 can occur, leading to an increase in lead concentrations in the drinking water. We investigated the depletion of free chlorine during water stagnation over periods ranging from 1 hour to 72 hours in test pipes, using different initial concentrations (0.5, 1, 2, and 3 mg/L as Cl_2). Residual free chlorine concentrations decreased during stagnation, and they fell below the detection level (0.1 mg/L as Cl_2) after 4, 8, 16 and 24 hours for initial concentrations of 0.5, 1, 2, 3 mg/L as Cl_2 , respectively (Figure A3.7). Consistent with previous research (Al-Jasser, 2007; Kastl et al., 1999; Rossman et al., 1994), first-order kinetics can fit the depletion of free chlorine

during water stagnation ($R^2=0.86\sim 0.99$), with similar rate constants ($0.34\sim 0.56\text{ h}^{-1}$) across different initial free chlorine concentrations (Table A3.2).

When detectable residual free chlorine was present, dissolved lead concentrations in all pipes remained consistently low ($<15\text{ }\mu\text{g/L}$) and stable. After residual free chlorine was below detection, the dissolved lead concentrations began to increase (Figure 4.2). Concentrations exceeded the action level ($15\text{ }\mu\text{g/L}$) and continued to increase with longer stagnation times until the end of the 72-hour stagnation test. Total lead concentrations exceeded the action level ($15\text{ }\mu\text{g/L}$) at some points even in the presence of detectable free chlorine, and total lead concentrations were more variable than those of dissolved lead (Figure 4.2).

When the residual free chlorine fell below the detection limit, the total lead concentrations kept increasing with stagnation time and exhibited greater variability with concentrations up to $27\pm 21\text{ }\mu\text{g/L}$. Average lead concentrations in pipes before and after free chlorine depletion are summarized in Figure 4.3. Dissolved lead concentrations increased 30~70% after chlorine depletion and showed greater variability with concentrations increasing from $8\pm 2\text{ }\mu\text{g/L}$ to $15\pm 7\text{ }\mu\text{g/L}$. Total lead concentrations increased after chlorine depletion but with increased variability, with concentrations increasing from $15\pm 8\text{ }\mu\text{g/L}$ to $27\pm 21\text{ }\mu\text{g/L}$.

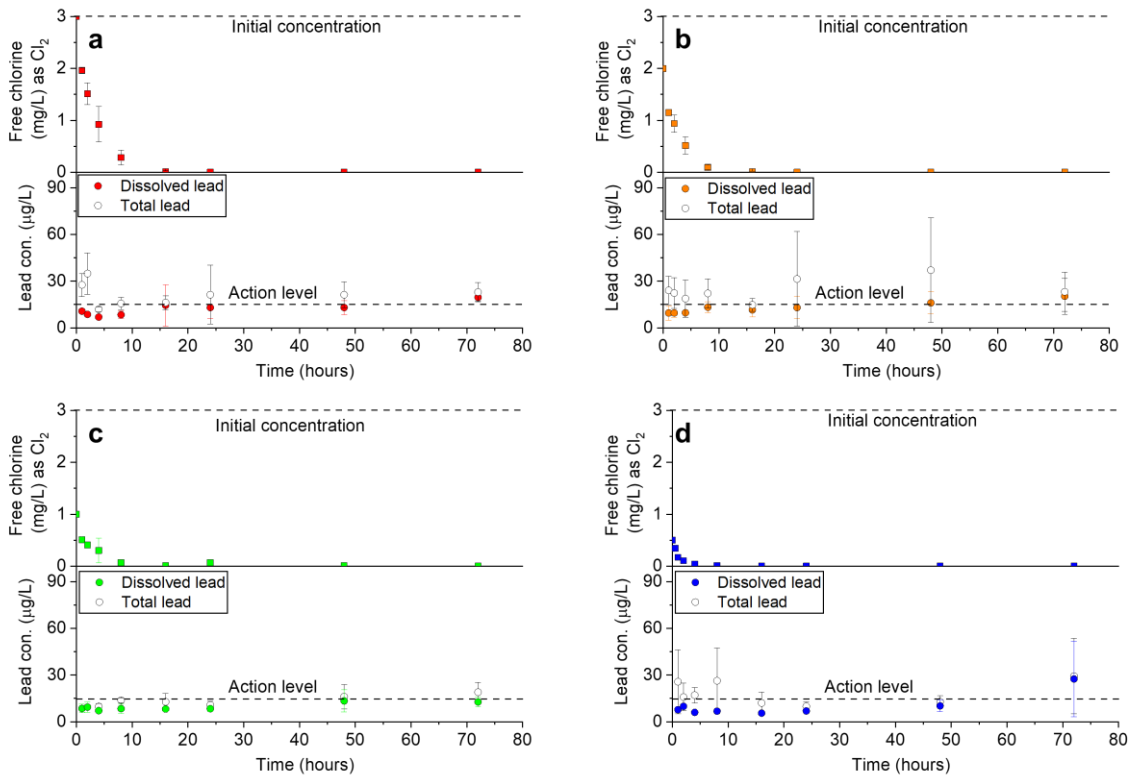


Figure 4.2 Stagnation experiment for free chlorine decay (top part of each panel) and lead concentrations (bottom part of each panel) at initial free chlorine of (a) 3.0 mg/L (b) 2.0 mg/L (c) 1.0 mg/L (d) 0.5 mg/L as Cl_2 . The error bars denote standard deviations calculated from triplicate experiments.

Despite the rise and variations in lead concentrations when free chlorine levels were insufficient, the increases in lead concentrations were not immediate. Instead, there was a delay of up to 48 hours before lead concentrations increased notably and exceeded the action level (Figure 4.3).

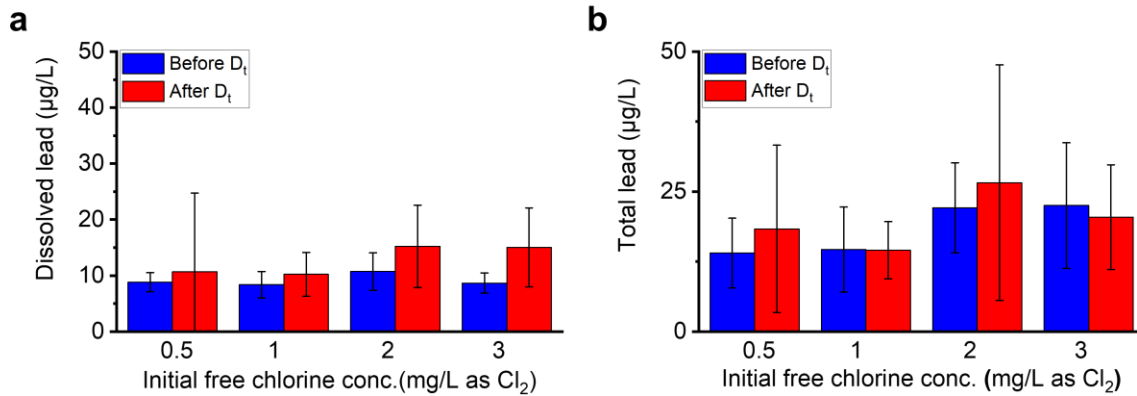


Figure 4.3 (a) Average dissolved lead and (b) average total lead concentrations for pipe loops during stagnation experiments at different initial free chlorine concentrations before (from beginning to D_t) and after the time (from D_t to 72 h) when the free chlorine concentration fell below the detection level (D_t). D_t values are 4 h, 8 h, 16 h and 16 h for initial free chlorine concentration at 0.5 mg/L, 1 mg/L, 2 mg/L and 3 mg/L as Cl_2 .

This time lag could be attributable to the generation and accumulation of Pb(II) on the solid surface from the reduction of Pb(IV). Once the Pb(II) has accumulated beyond the capacity of the solid to bind it to the surface, the Pb(II) could be substantially released from the surface to the water. The detachment of Pb(II) from PbO_2 in pipe scales may be the rate-limiting step for PbO_2 dissolution. Previous research also revealed that the dissolution of PbO_2 can be faster under DIC and pH conditions for which complexation of Pb(II) with carbonate or hydroxide can accelerate detachment of Pb(II) from the surface (Wang et al., 2013; Xie et al., 2010b). The total lead levels increased before those of dissolved lead, which may indicate that the structural integrity of PbO_2 -dominated pipe scale was compromised prior to the observable dissolution of PbO_2 . A longer stagnation experiment (up to 14 days) found that both dissolved lead and total

lead concentrations remained below the action level (15 $\mu\text{g/L}$) until water stagnation reached 14 days and 7 days, respectively (Figure A3.8).

4.3.3 Threshold Residual Free Chlorine to Maintain the Stability of PbO_2

Lead Scales

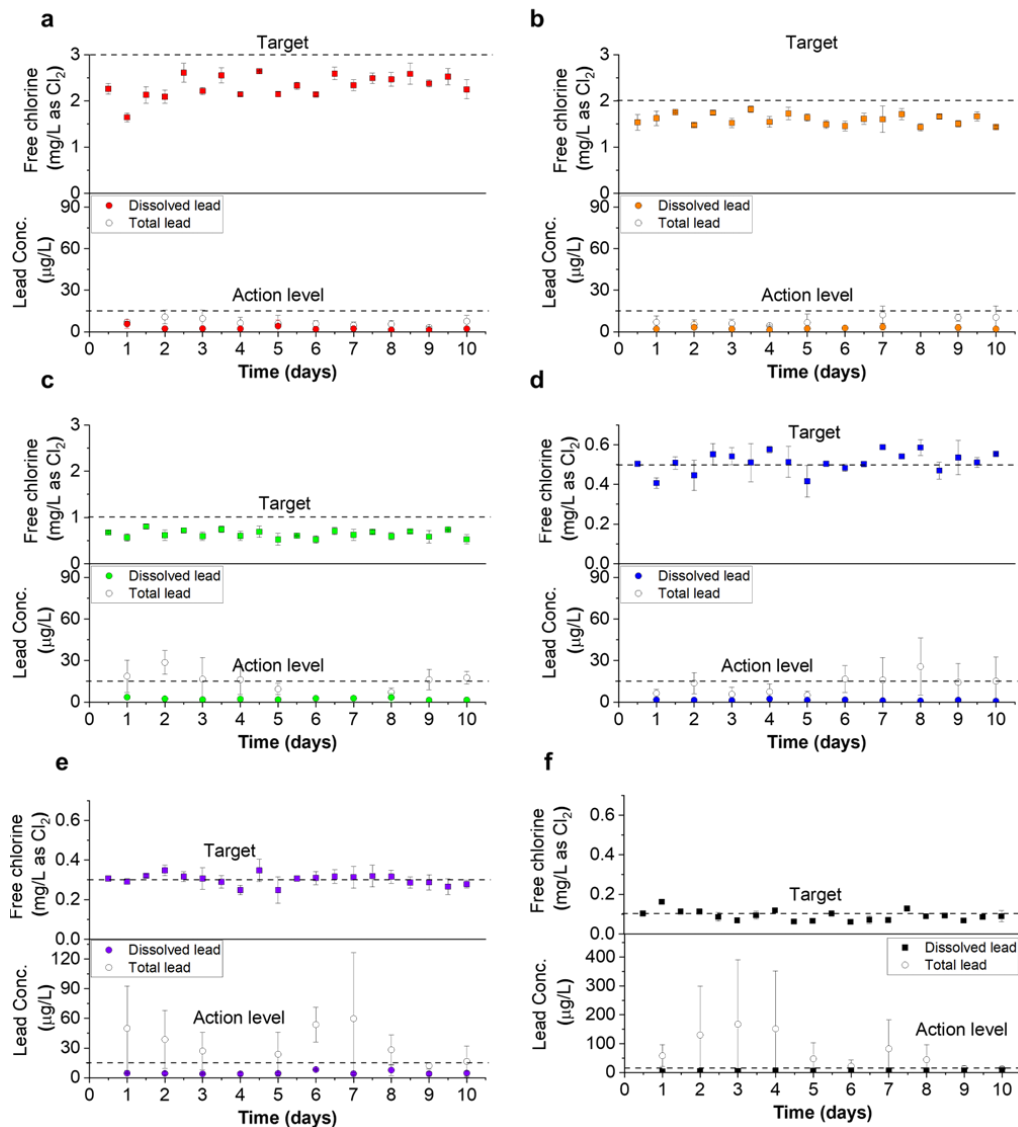


Figure 4.4 Dissolved and total lead concentration with free chlorine controlled at concentrations of (a) 2-3 mg/L (b) 1-2 mg/L (c) 0.6-1 mg/L (d) 0.4-0.6 mg/L (e) 0.2-0.4 mg/L (f) 0-0.2 mg/L.

The error bars denote standard deviations calculated from the triplicate pipes.

Dissolution of PbO₂-dominated pipe scale can be influenced by the redox conditions of the water, which are controlled by the residual free chlorine concentration. To explore whether there is a threshold free chlorine concentration that could maintain the stability of PbO₂, experiments were conducted in which the residual free chlorine concentrations in water were maintained at stable values that were incrementally stepped down from 3 mg/L to 0.1 mg/L as Cl₂.

When the residual free chlorine concentration was maintained at 0.4 mg/L as Cl₂ and above dissolved and total lead concentrations remained below the action level of 15 µg/L and stayed stable throughout the ten-day experimental period (Figures 4.4a and 4.4b). A higher residual free chlorine concentration of 2-3 mg/L did not have additional benefits in limiting dissolved lead concentrations compared to lower concentrations of 0.4-0.6 mg/L. When the residual free chlorine concentrations were below 0.4 mg/L, dissolved lead concentrations remained below 10 µg/L but increased from 2 ± 1 µg/L for concentrations at 0.4 mg/L as Cl₂ free chlorine to 6 ± 4 µg/L below that threshold. Total lead concentrations largely remained below the action level (15 µg/L) when the residual free chlorine concentration was above 1 mg/L. When the residual free chlorine concentration decreased to 0.4-1.0 mg/L, total lead concentration exceeded the action level and increased to 20 µg/L. When the free chlorine concentration were 0.2-0.4 mg/L, the total lead concentrations were much higher and also more variable, reaching to 45 ± 53 µg/L. The total lead concentrations higher still (73 ± 129 µg/L) when the residual free chlorine was 0-0.2 mg/L.

The total lead release from PbO₂-dominated pipe scale was more strongly influenced than was dissolved lead by the decrease of free chlorine concentrations being lowered from 3 to 0.2 mg/L as Cl₂ (Figure 4.5). Threshold levels of 0.4 mg/L and 1.0 mg/L as Cl₂ were identified for dissolved and total lead, respectively. Below these levels, higher lead concentrations can be observed. The increase in total lead for residual free chlorine concentrations below the threshold can primarily be attributed to the release of particulate and colloidal lead. When residual free chlorine is insufficient, the Pb(IV)O₂ component in pipe scales can undergo reductive dissolution, partially compromising the integrity of the scale phase and potentially enabling the release of PbO₂ particles into the water.

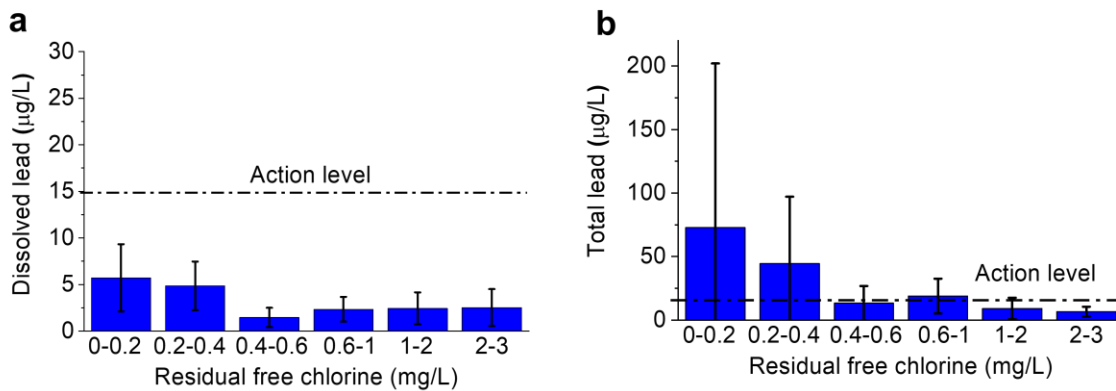


Figure 4.5 (a) Average dissolved lead and (b) average total lead concentrations for pipe loops at different residual free chlorine concentrations over a ten-day test. The error bars denote standard deviations calculated from the triplicate pipes.

The Pb(II) may remain attached to pipe scales through adsorption and in-situ precipitation as lead-carbonate solids (Wang et al., 2013). Consequently, while a notable increase in total lead concentrations was observed when residual free chlorine levels were set to be below 1.0 mg/L,

an increase in dissolved lead was not detected until the free chlorine level was set at a stable value below 0.4 mg/L. Our hypothesis is that at the lower stable free chlorine concentrations studied, the reductive dissolution of PbO₂ was more intense, resulting in an increased conversion of Pb(IV) to Pb(II) within the pipe scales. This process could lead to a greater accumulation of Pb(II) in the scales, followed by its subsequent leaching into the water.

Table 4.1 Mass concentrations (mg/g) of elements in the scales determined by acid digestion of solids followed by analysis with ICP-MS.

Sample ID		Pb	Al	Fe	Mg
C1-BC	Top	485	43	BDL	BDL
	Bottom	576	14	BDL	BDL
C1-AC	Top	104	20	20	BDL
	Bottom	607	BDL	BDL	BDL
C1-AT	Top	557	9	BDL	8
	Bottom	645	11	BDL	8
T1-BC	Top	338	108	BDL	BDL
	Bottom	390	59	BDL	BDL
T1-AC	Top	137	40	9	16
	Bottom	504	BDL	BDL	BDL
T1-AT	Top	503	7	17	5
	Bottom	513	40	14	7
Detection limit		10	5	5	5

C1: Control pipe 1; T1: Test pipe 1; BC: Before conditioning; AC: After conditioning; AT: After tests. "BDL" represents below the detection limit.

After all experiments were completed, scale analysis was performed on both the control and test pipes. Plattnerite (β - PbO_2) was still the dominant crystalline phase for both control and test pipes, and litharge (PbO) was only detectable in the bottom layer. The scale thickness remained relatively unchanged for both control and test pipes at approximately 45 μm and 50 μm , respectively (Figure A3.10), indicating that the dissolution of the pipe scales on the test pipes was minimal. Lead (Pb) was the primary element in the pipe scales, with concentrations ranging from 500 to 650 mg/g. Other elements, such as aluminum (Al), iron (Fe), and magnesium (Mg), were also detectable in the pipe scales at concentrations of less than 50, 20, and 10 mg/g, respectively (Table 4.1).

4.4 Implications for Corrosion Control in PbO_2 -dominated Lead Pipes

4.4.1 Develop and Preserve PbO_2 in Pipe Scales

PbO_2 is only present in water systems that use free chlorine as the disinfectant. In this study, a continuous flow of 3 mg/L as Cl_2 free chlorine at pH 8 was applied to condition pipes over 40 weeks. This approach effectively established PbO_2 as a dominant component in the pipe scales and successfully maintained consistently low lead concentrations in the water ($< 5 \mu\text{g/L}$). Other studies also successfully developed or preserved PbO_2 as a dominant pipe scale component using free chlorine. Xie and Giammar, (2011) successfully developed PbO_2 pipe scales on new lead pipes using stagnant water containing 3.5 mg/L as Cl_2 free chlorine at pH 10 (refreshed once per

day) after eight months of conditioning. Peng et al., (2022) utilized stagnant solution containing 40 mg/L as Cl₂ free chlorine (Initial pH 10.6, replenished daily) to establish PbO₂ pipe scales on new lead pipes, and the process took 10 days.

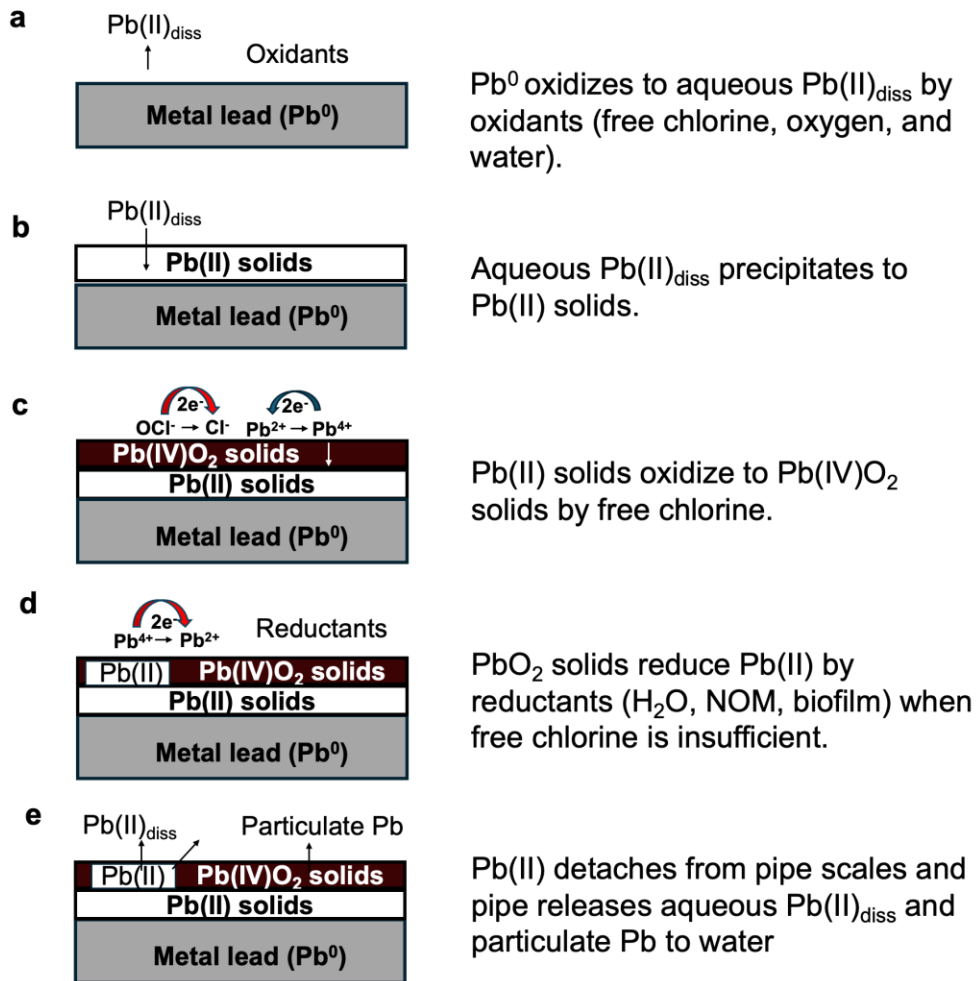


Figure 4.6 Conceptual diagrams for PbO₂ precipitation and dissolution in free-chlorinated water: (a) Oxidation of metal Pb(0) to dissolved Pb ($\text{Pb(II)}_{\text{diss}}$); (b) Precipitation of Pb(II) carbonate solids; (c) Oxidation of Pb(II) carbonate solids to PbO₂; (d) Reduction of PbO₂ to Pb(II) by reductants in water; (e) Lead release to water from the detachment of aqueous Pb^{2+} and particulate Pb.

Some studies also revealed that the formation of PbO_2 in pipe scales might be influenced by other factors besides free chlorine. Wang et al., (2010a) found that DIC accelerated PbO_2 formation. Ma et al., (2023) used a periodic flow of 1.1 mg/L as Cl_2 free chlorine at pH 7.7 to condition harvested pipes that had no PbO_2 in the presence of blended-phosphate for 30 weeks and did not find detectable PbO_2 in pipe scales after conditioning. Lytle et al., (2009) also found the PbO_2 formation was inhibited in the presence of orthophosphate. In general, free chlorine water is effective to help develop PbO_2 on new pipes or preserve the pre-existing PbO_2 using continuous or periodic flow at different pH (7.5~11). The presence of DIC, higher concentrations of residual free chlorine and pre-existing PbO_2 on pipe walls might facilitate the process to develop PbO_2 as a dominant pipe scale component (Figure 4.6), whereas the presence of phosphate might impede the process. The impediment could be due to the competitive reactions with Pb between inhibitors and free chlorine, which decrease the chance for Pb(II) to be oxidized to Pb(IV) needed to precipitate PbO_2 .

4.4.2 Threshold Free Chlorine Concentration

Residual free chlorine concentrations influence the redox potential in LSLs, which determines whether Pb(IV) can remain stable or undergo reductive dissolution. Adequate residual free chlorine is necessary to preserve PbO_2 pipe scales. However, excessively high concentrations of free chlorine may increase the formation of disinfectant byproducts (DBPs) (Roth and Cornwell, 2018; Wang et al., 2015) and cause unnecessary use of free chlorine. In our study, we propose a

threshold concentration for residual free chlorine, which represents the minimum level necessary to maintain the stability of PbO₂. Our results indicate that both total lead and dissolved lead concentrations increase substantially when the residual free chlorine is below 0.4 mg/L. Consequently, we suggest a threshold residual free chlorine concentration of approximately 0.4 mg/L to effectively preserve PbO₂ stability for the LSLs. This proposed threshold is notably higher than the theoretical free chlorine concentration of 3.59×10^{-11} mg/L calculated to be needed to have PbO₂ present based on thermodynamic calculations (see the Supplementary Material). The threshold free chlorine concentrations determined in our study were established using a continuously recirculating flow system, which operated for five days prior to water replenishment. This process allowed additional particulate lead to be flushed out and accumulate in the reservoir. Regardless, the findings remain valuable for understanding how PbO₂ scales respond to different concentrations of free chlorine and the subsequent reduction of Pb(IV) and detachment of Pb(II) into the water (Figure 4.6).

In actual lead service lines (LSLs), the threshold concentration of residual free chlorine can vary significantly across different water systems. Factors influencing this threshold may include water chemistry (Xie et al., 2010b), flow dynamics (Xie and Giammar, 2011), pipe aging (Al-Jasser, 2007), and the presence of additional reductants such as natural organic matter and biofilms (Arnold and Edwards, 2012; Masters et al., 2016; Nguyen et al., 2011).

4.4.3 Release of Dissolved Lead and Particulate Lead

PbO₂ in pipe scales becomes destabilized and undergoes reductive dissolution when the redox potential is insufficient to maintain its stability, leading to the release of lead into drinking water. In the presence of other reductants, such as natural organic matter (NOM) (Lin and Valentine, 2008a) and iodide (Wang et al., 2012), the reductive dissolution process can be further accelerated. The reductive dissolution of Pb(IV) and the subsequent rise in lead concentrations in water occur rapidly when exposed to reductants or during the transition from free chlorine to chloramine. In contrast, our experimental results suggest that dissolved lead concentrations may remain low and stable for up to two days following the depletion of residual free chlorine. The observed time lag may be attributed to the detachment of reduced lead and the adsorption of Pb(II) onto pipe scales (Wang et al., 2013). Conversely, a significant increase in total lead concentrations was observed when residual free chlorine levels were insufficient, likely due to the release of particulate lead. The release of particulate lead may be associated with the structural compromise of the scale layer resulting from the reductive dissolution of PbO₂. Masters et al., (2016) also suggested that particulate lead poses a greater concern than dissolved lead, with significantly higher concentrations of lead observed during reductive dissolution in PbO₂-dominated pipes. In this study, recirculating flow experiments revealed that total lead release was substantially higher when free chlorine concentrations were below 0.4 mg/L, reaching levels as high as 400 µg/L, compared to in stagnation experiments where concentrations remained below 30 µg/L. This finding suggests that high flow rates in pipes can exacerbate the

release of particulate lead from pipe scales, aligning with the results reported by Clark et al. (2014) and Xie and Giammar (2011).

In actual LSLs, lead release is likely to occur during prolonged periods of water stagnation when residual free chlorine is depleted and Pb(IV) undergoes reductive dissolution. High lead concentrations are expected in the initial liters of water that flow through the pipes following stagnation (Mishra et al., 2021a). Particulate lead is typically released at higher concentrations and at an earlier stage, with its release being further exacerbated by extended stagnation times and increased flow rates. Our experiments indicate that the proportion of lead released during water stagnation accounts for less than 0.07 wt% of the total lead in the PbO₂ scales (Calculated in Supplementary Material), suggesting that the majority of PbO₂ pipe scales maintain their integrity during periods of stagnation. Additionally, as fresh water from the distribution system flows through the pipes, free chlorine is replenished. With re-contact with free chlorine, lead concentrations in the water can quickly decrease below action levels and stabilize. This indicates that flushing the pipes before using water after prolonged stagnation can effectively prevent lead contamination and help preserve the integrity of PbO₂ pipe scales

4.5 Conclusions

Preserving Pb(IV) is crucial to preventing lead release to drinking water from LSLs containing PbO₂ as a major component in pipe scales. The presence of residual free chlorine in water plays a significant role in determining whether Pb(IV) will undergo reductive dissolution. During

stagnation once the residual free chlorine fell below the detection limit (0.1 mg/L as Cl₂), dissolved lead and total lead concentrations increased from 8 ± 2 µg/L to 15 ± 7 µg/L, and from 15 ± 8 µg/L to 27 ± 21 µg/L, respectively. Total lead increased earlier and with greater variability compared to dissolved lead. In this study, a threshold level of residual free chlorine that could maintain the stability of PbO₂ was identified as 0.4 mg/L as Cl₂. However, this specific threshold may vary across different water systems. Our scale analysis revealed that plattnerite (β-PbO₂) was the primary constituent of the pipe scales, with thicknesses ranging from 40 to 80 µm. While reductive dissolution of Pb(IV) when free chlorine was insufficient can generate lead concentrations in water that are concerns, most of the PbO₂ in the scale (greater than 99.93%) remains as PbO₂. In summary, PbO₂-dominated LSLs can maintain low and stable lead concentrations in water when sufficient free chlorine is present. However, during periods of water stagnation, the depletion of free chlorine could lead to a potential risk of lead release, with the release of particulate lead being a greater concern than dissolved lead. Flushing the pipes with fresh tap water can help both remove lead-contaminated water that has stagnated in the pipes and provide an influx of free chlorine to restore and maintain the stability of the PbO₂ scales on the pipe walls.

4.6 Acknowledgments

We are grateful to Erie County Water Authority for their contributions to this work, including providing the harvested lead service lines, funding of the study, and valuable insights on the

study's technical objectives. We appreciate the technical and administrative support of Hazen and Sawyer for the completion of the work. We also would like to thank Isabella N. Stull who was an undergraduate student at WUSTL and who helped set up and condition the pipe-loop reactors.

Chapter 5: Effect of Orthophosphate on Lead Release from PbO₂-rich Layers on Elemental Lead

Abstract

Lead(IV) oxide (PbO₂) is an important lead corrosion product that can be found on LSLs that convey water with free chlorine as the residual disinfectant. PbO₂ has an extremely low solubility, and the formation and preservation of PbO₂ on the surface of lead pipes could effectively limit the release of lead into water. However, during water stagnation, Pb(IV) may undergo reductive dissolution when residual free chlorine concentration is insufficient.

Orthophosphate is an important corrosion control inhibitor that can help precipitate lead(II) phosphate solids on pipe walls and limit lead release. This study was based on laboratory-scale pipe loops and a set of bench-scale batch experiments with lead coupons. The harvested lead pipes and the lead coupons both had scales that were rich in PbO₂-rich. The effect of orthophosphate on lead release from these materials was investigated during water stagnation in which free chlorine decayed completely and reductive dissolution of PbO₂ occurred. For the coupons the presence of 1.0 mg/L as PO₄ of orthophosphate resulted in higher lead release during water stagnation. At the end of the five-day stagnation, total lead concentrations reached up to 350 µg/L for coupons in water with orthophosphate, compared to 20 µg/L in control experiments without orthophosphate. For the lead pipes, in contrast to the behavior of the

coupons, there was and there was no significant difference in lead release between pipes with and without orthophosphate. A lead-phosphate solid, phosphohedyphane ($\text{Ca}_2\text{Pb}_3(\text{PO}_4)_3\text{Cl}$), was detected in pipes treated with 1 mg/L as PO_4 of orthophosphate as PO_4 after four months; however, it was absent in the scales on coupons and on pipes subjected to shorter durations of exposure to orthophosphate. For the pipes and water compositions of this particular system, the use of orthophosphate may not provide a substantial benefit for lead corrosion control during the initial phase of orthophosphate addition for PbO_2 -domianted LSLs.

5.1 Introduction

Lead contamination in drinking water poses risks to public health, as highlighted by the lead crises in Washington D.C., Newark, New Jersey, and Flint, Michigan (Faherty, 2021; Pieper et al., 2018; Roy et al., 2019; Roy and Edwards, 2019). The primary source of lead in water is lead service lines (Doré et al., 2019b), millions of which are still in use across the United States (Cornwell et al., 2016). The Lead and Copper Rule Revisions in the United States that become effective in October 2024 will impose more stringent requirements for water sampling and establish a lead trigger level of 10 $\mu\text{g}/\text{L}$ that will necessitate improvements in lead corrosion control strategies for many water utilities (Masters et al., 2021; Mishrra et al., 2021a; Rome et al., 2022).

The two most widely used lead corrosion control strategies are pH and alkalinity adjustment (Tam and Elefsiniotis, 2009) and the addition of corrosion inhibitors (Edwards and McNeill, 2002; Kogo et al., 2017; Mishra et al., 2021b). Phosphate-based inhibitors constitute about half of the corrosion control methods, with orthophosphate being the most widely used (Arnold et al., 2020; Ma et al., n.d.; McNeill and Edwards, 2002). The introduction of orthophosphate aids in the precipitation of lead-phosphate solids (Bae et al., 2020b; Davidson et al., 2004; Hopwood et al., 2016; Locsin et al., 2022; Lytle and Edwards, 2023), which have low solubility and effectively limit lead release into the water. In addressing the lead crisis in Washington D.C., orthophosphate addition successfully lowered lead concentrations in the water (The Cadmus Group, 2007). Apart from traditional lead corrosion control strategies, in systems that use free chlorine as a disinfectant and that have lead(IV) oxide (PbO_2) in pipe scales, maintaining the stability of existing PbO_2 also has been reported to be effective in limiting lead release from pipes (Triantafyllidou et al., 2015).

Lead(IV) oxide (PbO_2) has two polymorphs, scrutinyite ($\alpha\text{-PbO}_2$) and plattnerite ($\beta\text{-PbO}_2$), both of which have extremely low solubility (Lytle et al., 2009b; Lytle and Schock, 2005). PbO_2 can help to develop a protective layer on the surfaces of pipes that are in contact water, which effectively limits lead release to the water. Pb(IV) requires a high redox potential to maintain its stability (Pan et al., 2022). In the presence of reductants in drinking water systems such as natural organic matter (NOM) (Dryer and Korshin, 2007; Lin and Valentine, 2009) and biofilms

(Masters et al., 2016; Yan et al., 2022), PbO_2 can undergo reductive dissolution, quickly leading to high lead concentrations in the water (Pan et al., 2019). The lead crisis in Washington D.C. was attributed to the switch from free chlorine to chloramine as the disinfectant (Edwards et al., 2009). Unlike free chlorine, chloramine is not a sufficiently strong oxidant to provide the necessary redox potential to preserve the stability of PbO_2 (Lin and Valentine, 2008b; Switzer et al., 2006; Xie et al., 2010a).

Some previous studies have focused on the effect of orthophosphate on PbO_2 pipe scales. One study found that the presence of orthophosphate effectively limited lead release following a switch from free chlorine to chloramine disinfectant in PbO_2 -dominated pipes; the control of lead release was due to the precipitation of Pb(II) released from PbO_2 in low-solubility lead(II) phosphate solids (Bae et al., 2020). Xie and Giammar, (2011) also found that orthophosphate can help limit lead release from pipes primarily consisting of hydrocerussite ($\text{Pb}_3(\text{CO}_3)_2(\text{OH})_2$) and minor amounts PbO_2 in the presence of chloramine. Another study based on batch experiments reported that orthophosphate limited lead release when PbO_2 solids undergo reductive dissolution in the presence of monochloramine (Ng et al., 2012). However, in these studies the process that induced PbO_2 dissolution was the introduction of chloramine, which can serve as a reductant to accelerate PbO_2 dissolution, and not the depletion of the free chlorine. Several previous studies also focused on particulate lead release in the presence of orthophosphate in PbO_2 -dominated pipes. Xie and Giammar, (2011) noted that the addition of orthophosphate may

increase particulate lead release, a finding consistent with that of Lytle et al., (2020). Lytle et al. reported increased total lead in water after the addition of orthophosphate in the Newark, NJ water system, a system that has free chlorine as the disinfectant and pipes with PbO₂-rich pipe scales. This increase was attributed to the formation of phosphate-lead nanoparticles that did not become a physically stable adhered component of the pipe scale. However, those studies did not examine whether stable lead-phosphate solids can form in water pipes containing PbO₂, and if the formed lead-phosphate solids can help limit lead release when free chlorine is not sufficient.

Other studies have focused on the effect of orthophosphate regarding PbO₂ formation and their interactions but not targeted at water pipes in use. Lytle et al., (2009) found that the presence of orthophosphate can inhibit the formation of PbO₂ in chlorinated water systems. This study was based on batch experiments using a solution of lead(II) chloride as the lead(II)-containing material that could potentially be oxidized to yield PbO₂, and the study did not investigate the effect of orthophosphate on existing PbO₂ pipe scales. DeSantis et al., (2020) investigated the interactions of orthophosphate with destabilized PbO₂ after a disinfectant switch from free chlorine to chloramine. Their study was based on scale analysis and lead concentrations from sampling. It revealed that phosphorus permeated through destabilized PbO₂ and that a calcium-substituted hydroxylpyromorphite solid formed in pipe scales.

In addition to pipe-loop tests, lead coupon studies are recommended as a valuable tool for assessing lead corrosion control. Several previous studies have investigated the effects of

orthophosphate on lead corrosion control using coupons. These studies have involved measurement of lead release and surface characterization of the coupons. Li et al., (2020) demonstrated that the presence of aluminum can adversely affect lead corrosion control in water systems that use orthophosphate inhibitors, with free chlorine as a disinfectant, according to findings from lead coupons containing PbO₂. Masters et al., (2022) compared the results of coupon and pipe experiments examining the effect of orthophosphate on lead release. They found that lead concentrations decreased in both coupons and pipes after the addition of orthophosphate, and the coupon experiments exhibited greater variability in the results.

Water pipes dominated by PbO₂ pipe scales were reported to have lower and more stable lead concentrations in water compared to those dominated by Pb(II) solids (Triantafyllidou et al., 2015). However, longer water stagnation time can lead to increased lead levels due to the depletion of free chlorine and reductive dissolution of Pb(IV) (Arnold and Edwards, 2012; Clark et al., 2014). Many free-chlorine water systems that have PbO₂ in pipe scales have implemented orthophosphate as a corrosion inhibitor to optimize lead control and to comply with the Lead and Copper Rule Revisions (LCRR) requirements (Arnold et al., 2020; Tully et al., 2019). However, to date, no study has systematically examined the effectiveness of orthophosphate on existing PbO₂ pipe scales or its impact on free chlorine decay and scale composition in those pipes.

In this study, the effect of orthophosphate on the chemical and physical stability of PbO₂ corrosion products on elemental lead materials was investigated for both harvested lead pipes

and for lead coupons. The objectives of this study were to 1) examine the effects of orthophosphate on lead release from PbO₂-dominated lead materials and 2) investigate the composition, stability, and dissolution of pipe scales with existing PbO₂ in the presence of orthophosphate. The pipe-loop study utilized ten harvested lead service lines from a free chlorine system operated by the Erie County Water Authority (ECWA) in New York, USA, which had pre-existing PbO₂ pipe scales. These pipes had been conditioned for over six months with 3 mg/L of free chlorine (as Cl₂) to promote the development of a PbO₂-rich layer on the pipe scales before tests on the effects of orthophosphate. Lead coupons were conditioned for five weeks prior to tests to develop PbO₂-rich surface layers on top of the elemental lead. Using both the conditioned pipes and coupons with PbO₂-rich scales, the study investigated the effect of orthophosphate (1 mg/L as PO₄) on PbO₂ dissolved and total lead concentrations upon depletion of free chlorine that initiated the onset of PbO₂ dissolution. These measurements of lead in the water were complemented by analysis of the scale at different points in the experiments.

5.2 Materials and Methods

5.2.1 Materials

Ten lead coupons (McMaster-Carr, 5 × 1 × 0.12 cm, Figure A4.1) with pre-existing PbO₂-rich layers were used in the batch experiments. A two-step method, combining electrochemical polarization and chemical conditioning, was employed to develop a PbO₂ layer on metallic lead

coupons (Details are in Supplementary Material). The PbO_2 in the scales was identified as plattnerite ($\beta\text{-PbO}_2$) by XRD before experiments.

Ten harvested pipes from Erie County Water Authority were used in the pipe loop experiments of this study (Figure A4.2). These pipes were conditioned for more than six months. Four of them were used to examine the effect of orthophosphate during water stagnation and at different residual free chlorine concentrations. The other six pipes were used to investigate the impact of orthophosphate under different water flow patterns (continuous and periodic flows). The details of the set-up for pipe loops are included in Supplementary Material. Artificial ECWA water was prepared in the laboratory (Table A4.1) and used for both coupon and pipe-loop studies with additional details provided in the Supplementary Material.

5.2.2 Lead Coupon Experiments

Glass jars (240 mL, Qorpak Bottle Beakers®) were used to immerse the lead coupons during both conditioning and experimental tests (Figure A4.1a). In each jar, one coupon was positioned vertically and suspended with fishing line into 200 mL of aqueous solution. A magnetic stir bar (3 mm in diameter, 10 mm in length; Fisher) was used to mix the solution at 200 rpm throughout all experiments to ensure even distribution of free chlorine and to provide a flow of water across the surface of the coupons. The jars were covered with aluminum foil to prevent photochemical reactions (Figure A4.1b).

Ten coupons were conditioned in artificial ECWA water containing 3 mg/L of free chlorine as Cl_2 for five weeks, after which the test coupons (five coupons) were treated with 1 mg/L of orthophosphate as PO_4 for nine weeks. Water was replenished for each jar every week. Before testing, two control coupons and two test coupons were used for scale analysis.

For the stagnation study, the coupons were investigated at two different initial free chlorine concentrations (0.5 and 3.0 mg/L as Cl_2). The test coupons had received 1 mg/L of orthophosphate for nine weeks of conditioning, and they continued to receive the orthophosphate during the stagnation tests. No subsequent readjustments were made to free chlorine or orthophosphate during stagnation experiments. The stagnation times were studied sequentially, ranging from the shortest to the longest durations from 30 min to 5 d. For a given stagnation time being studied, the water in each jar was neither refilled nor refreshed. The pH of the solution was measured at the conclusion of each experiment, with minimal variation observed (generally within ± 0.2), likely due to the high alkalinity of the water. For comparison, we also investigated free chlorine depletion without lead coupons, both with and without orthophosphate. All tests were conducted in triplicate experiments.

We investigated the effect of orthophosphate on lead release for coupons at four different free chlorine concentrations (0-0.3, 0.3-0.6, 0.6-1, 1-1.5 mg/L as Cl_2) that were continuously maintained within these ranges for five days. To maintain stable free chlorine concentrations, a constant slow addition method with a syringe pump were used. The syringe pump introduced a

continuous slow flow of 20 mg/L of free chlorine into the test jars at rates that had been determined to then provide a stable free chlorine concentration in the water with the addition of free chlorine from the stock solution exactly balancing the consumption of free chlorine in the mixed jars. Water in each jar was replenished every week. The test coupons received 1 mg/L of orthophosphate, and no readjustments were made before water replenishment. The pH was monitored and maintained daily throughout the threshold free chlorine experiments at a target of 8.0 ± 0.1 using nitric acid and sodium hydroxide. Tests were performed in triplicate experiments.

5.2.3 Pipe-loop Experiments

Four pipes (Figure A4.2b) were used to investigate the orthophosphate effect during water stagnation and at different residual free chlorine concentrations. All pipes had preexisting PbO_2 in scales, and they were conditioned for three weeks using a continuously recirculating flow of ECWA water with 3.0 mg/L as Cl_2 free chlorine before moving to the test phase of the study. Two of them were designated as test pipes (Table A4.2) that were treated with 1 mg/L of orthophosphate (Labeled as T1 and T2). The remaining two served as control pipes (Labeled C1' and C2') and continued to receive ECWA water with 3.0 mg/L as Cl_2 of free chlorine without orthophosphate.

In the water stagnation experiment, the pipes were evaluated at initial free chlorine concentrations of 1 mg/L, and 3 mg/L as Cl_2 . Test pipes received 1 mg/L as PO_4 of

orthophosphate, and water in pipes was replenished at the beginning of each stagnation time point. The stagnation times were studied sequentially, starting from the 1 hour to 5 days. Before each stagnation time point, the pH and residual free chlorine concentration in each carboy were checked and readjusted to target values. Throughout the stagnation time study, the residual free chlorine, pH, and dissolved and total lead concentrations were monitored at each time point. The details of sampling procedures are included in the Supplementary Material. After each selected time point, when the free chlorine concentration fell below the detection limit (0.1 mg/L as Cl₂), and between each initial free chlorine concentration, the pipes underwent a two-day reconditioning with 3 mg/L of free chlorine. This reconditioning was performed prior to initiating the next time point test to mitigate any influence from the previous experiment.

The effect of phosphate on lead release was also investigated in experiments at which the free chlorine was maintained at different stable concentrations (0-0.3, 0.3-0.6, 0.6-1, 1-1.5 mg/L as Cl₂) using continuously recirculating flow. Similarly to how stable free chlorine concentrations were maintained in the experiments with the lead in the jars, the syringe pump introduced a continuous flow of a 1000 mg/L of free chlorine stock solution into the carboys used for water recirculation through the pipe loops. The flow rate was set to a value that introduced free chlorine to the recirculating system at the same rate at which it was consumed by reactions within the system. Water in each pipe-loop was replenished every week. The test pipes received 1 mg/L of orthophosphate, and no readjustments were made before water replenishment. The pH

was monitored and maintained daily at a target of 8.0 ± 0.1 using nitric acid and sodium hydroxide. Tests were performed in duplicate experiments.

The other six pipes (Figure A4.2a) were used to investigate the effect of orthophosphate on PbO_2 stability under real-world water use patterns in which a realistic free chlorine concentration was used and the free chlorine concentration in the pipes would vary based on typical periods of flow and stagnation. The pipes were conditioned using a continuously recirculating flow of ECWA water with 3.0 mg/L as Cl_2 of free chlorine for twenty weeks before adding orthophosphate to the test pipes. After conditioning, three test pipes (T1, T2, T3, Table A4.2) were treated with 1 mg/L as PO_4 of orthophosphate and the remaining three served as control pipes. This test phase lasted for ten weeks (Week 21 to Week 30), during which all pipes maintained continuously recirculating flow. Beginning in Week 31, the flow regime of all pipes was adjusted to a pattern of three periods of stagnation (6.5 h) and three periods of flow (1.5 h) per day at a flow rate of 4-5 L/min. This provided a daily total volume of flow of about 1100 L (280 gallons) per pipe, which simulated typical household use. Additionally, the residual free chlorine concentration was adjusted to 1.0 mg/L as Cl_2 which is more commonly found in drinking water systems compared to the 3.0 mg/L. Free chlorine samples were collected and measured in the morning of every weekday, and the free chlorine concentration was re-adjusted to the target value (1 mg/L) after measurement. The pH was measured and readjusted to a target of 8.0 every Wednesday and Friday. Orthophosphate concentrations were measured according to the modified molybdate

colorimetric method (Method 365.3, EPA) at the beginning and at the end of each week of water circulation. The dissolved and total lead concentrations were measured at the end of each week prior to the exchange of the water in the reservoirs.

5.2.4 Analytical Methods

Free chlorine concentrations were measured using the DPD (N, N-diethyl-p-phenylenediamine) method (4500-Cl G, Standard Methods), and orthophosphate concentrations were determined following EPA Method 365.3, both using a spectrophotometer (Thermo Scientific™ GENESYS™ 140). The pH was measured with a pH meter (Fisherbrand Accumet AB15). Lead concentrations were analyzed using inductively coupled plasma mass spectrometry (ICP-MS, NexION 2000). For dissolved lead measurements, samples were filtered through 0.22 µm polyethersulfone (PES) filters (Environmental Express, Inc.) and acidified to 1% (w/w) nitric acid. Total lead samples were pre-treated with hydroxylamine hydrochloride (0.2 g/L) to reductively dissolve any Pb(IV) solids and then acidified to pH 1 with trace metal grade nitric acid (Fisher Scientific) to dissolve any remaining lead-containing particles prior to measurements.

5.2.5 Scale Analysis

The morphology, crystalline phase, and elemental compositions were evaluated by scale analysis for lead coupons and pipes. For lead coupons, scale analysis was conducted at the end of

reconditioning (Week 14) and after the completion of all experiments. For pipe loops C1'-C2' and P1-P2 (Table A4.2), the scale analysis was conducted at the conclusion of all experiments. For pipe loops C1-C3 and T1-T3 (Table A4.2), scale analysis was performed before conditioning, at the end of the conditioning, and at the end of all experiments. Cross-section segment samples from each pipe loop were acquired for analysis. Scales in harvested segments were separated into top and bottom layers for solids and elemental composition analysis. Scanning electron microscopy (SEM, Thermo Fisher Quattro S E-SEM) was used to examine the morphology of scales and energy dispersive X-ray spectroscopy (EDS, Oxford AzTec) was utilized to acquire information on the spatial distribution of different elements in scales. Crystalline solid compositions were characterized by X-ray powder diffraction (XRD, Bruker d8 Advance X-ray). Acid-digested top and bottom scale materials were analyzed for elemental compositions by inductively coupled plasma mass spectrometry (ICP-MS). More details for scale analysis are included in the Supplementary Material.

5.3 Results and Discussion

5.3.1 Lead Coupon Study: Effects of Orthophosphate on Lead Release and Scale Composition

Conditioning of lead coupons

The lead coupons used in this study were initially conditioned for five weeks with 3 mg/L of free chlorine as Cl_2 , followed by the addition of 1 mg/L of orthophosphate as PO_4 . They were then further conditioned for an additional ten weeks. During the first five weeks, both dissolved and total lead concentrations remained stable and below 5 $\mu\text{g/L}$ (Figures A4.3a and A4.3b), with dissolved lead constituting the majority of the total lead in the water. After the addition of orthophosphate, lead concentrations in the jars with orthophosphate rose to 25 $\mu\text{g/L}$, largely due to an increase in dissolved lead (Figures A4.3a and A4.3b). In addition, the coupons in the jars with orthophosphate consumed 0.3 mg/L as Cl_2 more free chlorine daily than the control coupons (Figure A4.3c). Following six weeks of orthophosphate treatment, starting in week 7, lead concentrations in the jars with orthophosphate stabilized and dropped below 5 $\mu\text{g/L}$. These concentrations then remained low and stable for the remaining three weeks before experiment. The consumption of orthophosphate for test coupons ranged from 0.1-0.4 mg/L as PO_4 per week (Figure A4.3d), indicating that orthophosphate was being taken up by the lead coupons. The jars with control coupons (i.e. no orthophosphate addition) consistently maintained low lead concentrations and stable free chlorine consumption throughout the conditioning period.

Water stagnation and residual free chlorine

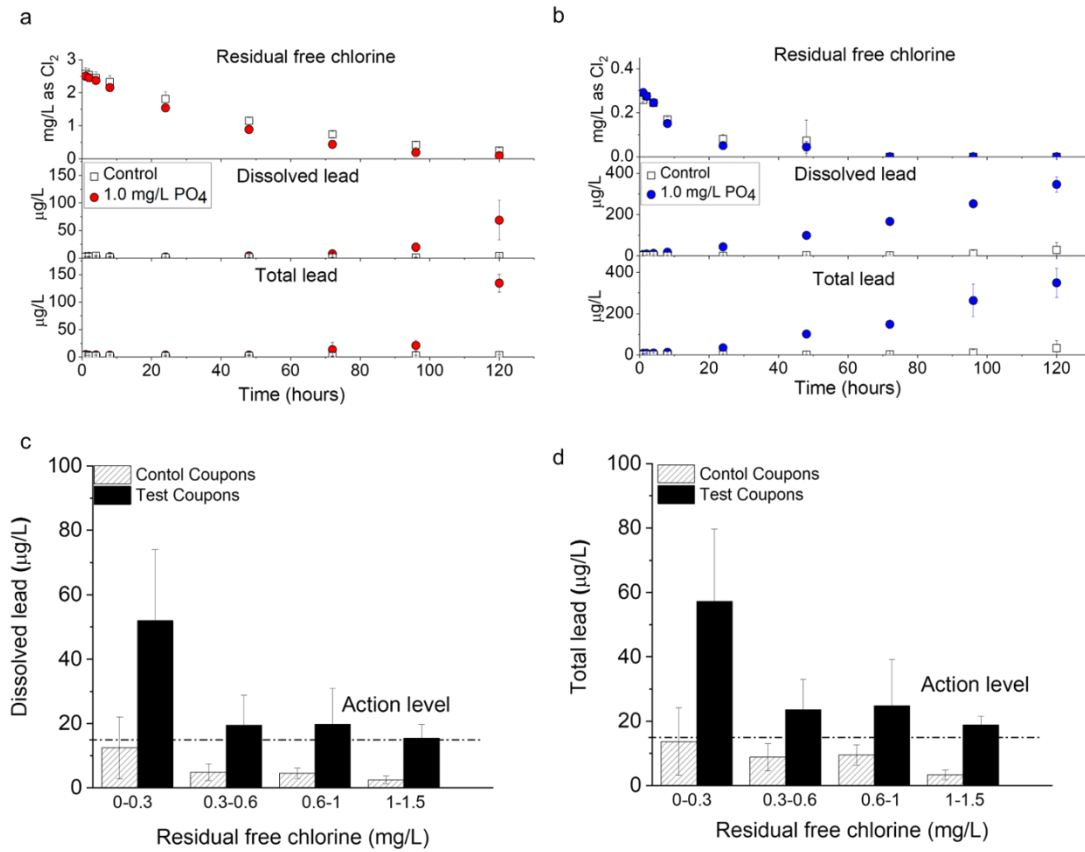


Figure 5.1 Coupon study: stagnation experiments for free chlorine decay (top part of the panel), dissolved and total lead concentrations (middle part and bottom part of the panel) at initial free chlorine concentrations of (a) 3.0 mg/L and (b) 0.5 mg/L as Cl₂. (c) Average dissolved lead and (d) average total lead concentrations for lead coupons at different continuously maintained stable free chlorine concentrations over a five-day test. The error bars denote standard deviations calculated from the triplicate experiments.

Free chlorine decay in jars was faster when lead coupons were present, but the addition of orthophosphate did not have any discernible effect on its kinetics (Figure A4.4). The depletion of free chlorine followed first-order kinetics with a good fit ($R^2 = 0.86\text{--}0.99$, Table A4.3), with the first-order rate constants being higher for jars with lead coupons than the jars without lead

coupons. Residual free chlorine dropped below the detection limit (0.1 mg/L as Cl₂) after 72 and 120 hours of water stagnation (Figure A4.4) for initial free chlorine doses of 0.5 and 3 mg/L as Cl₂, respectively.

When free chlorine concentrations remained above 0.3 mg/L as Cl₂, lead release showed minimal differences between control and test coupons (Figures 5.1a and 5.1b), with total lead concentrations being stable and below 15 µg/L. After free chlorine had become depleted, lead concentrations in both control and test pipes began to rise. Jars with the test coupons had significantly higher lead concentrations than those with the control coupons, with dissolved and total lead reaching up to 134 µg/L and 350 µg/L (Figures 5.1a and 5.1b), respectively, at the end of day five of water stagnation. In contrast, the jars with control coupons had dissolved and total lead concentrations of only 3 µg/L and 32 µg/L, respectively, after the five-day stagnation period. The high lead concentrations in the jars with the test coupons after long-time water stagnation were due to both dissolved and particulate lead. In contrast, the rise in lead concentrations in control coupons was primarily attributed to particulate lead.

The effect of orthophosphate on lead release when the free chlorine was maintained at stable values of 0-0.3, 0.3-0.6, 0.6-1 and 1-1.5 mg/L as Cl₂ was investigated. When the free chlorine concentration was above 0.3 mg/L, dissolved lead concentrations ranged from 2 to 6 µg/L for control coupons and 12 to 20 µg/L for test coupons (Figures A4.5 and A4.6). When residual free chlorine was above 0.3 mg/L, a gradual decrease from 3 mg/L to 0.3 mg/L did not significantly

affect dissolved lead concentrations for either control or test coupons. However, the test coupons consistently had higher lead concentrations than control coupons (Figures 5.1c and 5.1d). When the free chlorine concentration was below 0.3 mg/L, dissolved lead concentrations increased to $12 \pm 10 \mu\text{g/L}$ for control coupons and $52 \pm 22 \mu\text{g/L}$ for test coupons (Table 5.1). The increase in lead concentrations for test coupons was more pronounced and had greater variability than control coupons. Total lead for both control and test coupons exhibited similar release patterns and was mainly comprised of dissolved lead. When free chlorine concentration was below a threshold but was still present above the detection limit, the dissolved lead was the main contributor for lead release, and the total lead concentration increased to 100 $\mu\text{g/L}$. In contrast, when residual free chlorine was fully depleted, as seen in stagnation experiments, particulate lead release was dominant, and the total lead concentration increased substantially to 400 $\mu\text{g/L}$ for test coupons. These observations suggest that a minimal amount of residual free chlorine present in water could still play an essential role in maintaining the structural integrity of PbO_2 scales, which helps prevent the release of particulate lead.

Scale analysis

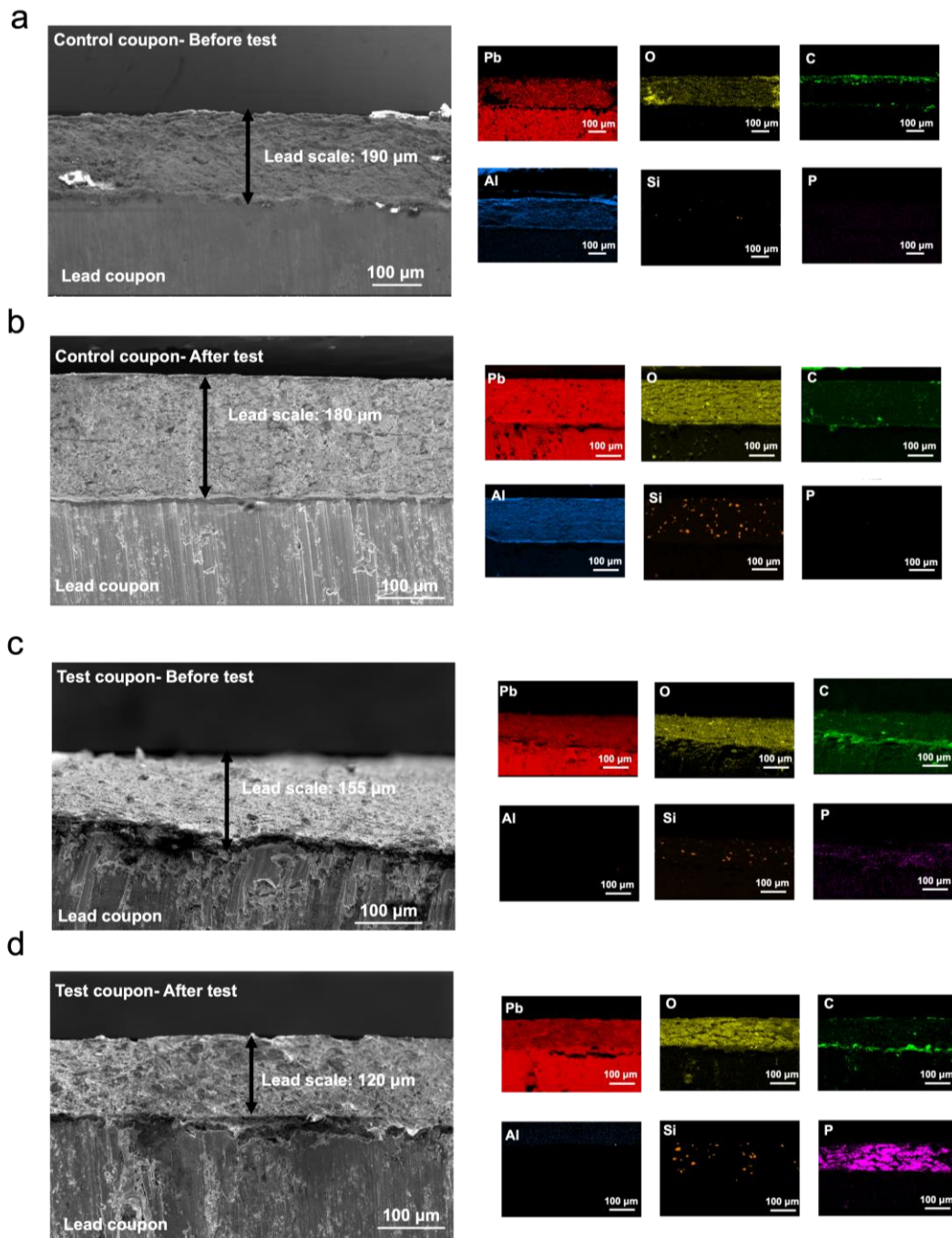


Figure 5.2 Scanning electron micrographs (left side) of the cross-section of the with elemental mappings (right side) of different elements detected by EDS for (a) a control coupon before test, (b) a control coupon after test, (c) a test coupon before test, and (d) a test coupon after test.

At the conclusions of the conditioning period scale analysis was conducted on four coupons, two that were then used in control experiments and two that were used in tests with orthophosphate.

At this stage of the experiment the four coupons had all experienced the same treatment conditions. The color of all coupons was dark red (Figure A4.1c), and the crystalline phases in all coupons was dominated by plattnerite (β -PbO₂) with minor amounts of litharge (PbO) also being detectable (Figure A4.8). No lead-phosphate solids were identified in the scales. The thicknesses of lead coupons were in the range of 150-200 μ m (Figure 5.2).

After the experiments on the effects of free chlorine concentrations and decay in the presence and absence of orthophosphate, additional coupon scales analysis was conducted. The thicknesses of lead coupon were approximately 180 μ m and 120 μ m for control and test coupons, respectively (Figure 5.2). The crystalline phase of coupons scales did not differ from the results before test, with β -PbO₂ being the dominant phase and PbO detectable (Table A4.4). Neither XRD nor ICP-MS results identified lead-phosphate solids or phosphorus in the scales of the test coupons. This indicates that either lead phosphate solids were not present or that the amounts present were below the detection limit of the techniques (<1 mg/g for ICP-MS analysis of acid-digested solids, Table A4.5).

Potential mechanisms

The presence of orthophosphate (1 mg/L as PO_4) increased lead release for PbO_2 -coated lead coupons. One explanation for this observation could be that orthophosphate promoted the detachment of Pb(II) from the coupon surface through precipitation with orthophosphate, which led to the release of lead-phosphate nanoparticles. The release of Pb(II) exposes more Pb(IV) on the remaining surface of the coupons to reductants, which would accelerate Pb(IV) reduction and increased lead release. The formation of nanoparticles is consistent with our observed increases in total lead concentrations for long stagnation times. Such nanoparticle formation upon reaction of Pb(II) with orthophosphate has been observed in other studies (Zhao et al., 2018). Notably, lead phosphate nanoparticles can be smaller than the 0.22 μm -filters used in our study (Lytle et al., 2020b), indicating that it is possible that the observed increase in dissolved lead could result from both dissolved Pb(II) and the release of lead phosphate nanoparticles into the water. The presence of nanoparticles could be probed in future research using light scattering and ultrafiltration techniques. After treatment with orthophosphate for about three months, phosphorus could have permeated into the coupon scale and coexisted with $\beta\text{-PbO}_2$ without forming detectable lead-phosphate solids. The permeation of phosphorus was confirmed by its concentrated presence in the element mapping (Figure 5.2), while lead-phosphate solids were below the detectable limit in the XRD patterns of our study (Figure A4.8). The penetration of phosphate into scale layers was also reported in previous research (DeSantis et al., 2020), and

this could damage the lead scale structure and lead to an increase in particulate lead in the water (Clark et al., 2014). A previous study reported that orthophosphate just in water had minimal impact on free chlorine decay (Zhang and Andrews, 2012), a result corroborated by our findings in jars without lead coupons. In the presence of PbO₂-coated lead coupons, our study also showed little or no difference in free chlorine depletion when orthophosphate was added.

5.3.2 Pipe-loop Study: Effects of Orthophosphate on Lead Release and Scale Composition

Conditioning of pipe loops

Pipe loops used in this study had pre-existing PbO₂- rich scales. They were conditioned for three weeks in the presence and absence of orthophosphate. Throughout the conditioning, dissolved lead concentrations were similar between the control and total pipes and were usually below 5 µg/L (Figure A4.9a). Total lead concentrations were slightly higher in the test pipes in the first two weeks, averaging around 5 µg/L, compared to 1–2 µg/L in the control pipes (Figure A4.9b). Total lead concentrations in the test pipes began to decrease and stabilize starting at week 3. The differences observed in the first two weeks were not statistically significant. Residual free chlorine concentrations in the pipe loops after one day gradually increased to 2 mg/L and stabilized around 2.5 mg/L by the end of the three-week reconditioning, suggesting that the pipes had stabilized and were ready for further tests. Orthophosphate consumption in the test pipes remained stable, which was about 0.4-0.5 mg/L as PO₄ every five days per pipe (Figure A4.9d).

Water stagnation and residual free chlorine

Free chlorine decayed in pipes during water stagnation, and there was no significant difference between control and test pipes (Figure A4.10). The depletion of free chlorine fit well to first-order kinetics, with R^2 values exceeding 0.9. The first-order rate constants for both control and test pipes were consistently similar, varying from 0.09 to 0.11 h^{-1} (Table A4.3), and at initial free chlorine concentrations of 0.5 mg/L and 3 mg/L as Cl_2 . Unlike for the lead coupons, orthophosphate had minimal impact on the free chlorine decay in the pipes. Free chlorine fell below the detection limit (<0.1 mg/L) after 48 hours for initial concentrations of both 0.5 mg/L and 3 mg/L as Cl_2 (Figure A4.10).

Total lead concentrations decreased and stabilized below 15 $\mu\text{g/L}$ after eight hours, and they maintained this low concentration until an increase was observed when residual free chlorine concentrations continued to decrease. As residual free chlorine decreased in the pipes, dissolved lead concentrations remained relatively unchanged though the five-day stagnation period at values below 10 $\mu\text{g/L}$ (Figure A4.3a). In contrast, total lead concentrations increased above the action level of 15 $\mu\text{g/L}$, reaching 14 ± 11 $\mu\text{g/L}$ in control pipes and 20 ± 31 $\mu\text{g/L}$ in test pipes for stagnation times for which the residual free chlorine had fallen below the detection limit. The variability among pipes was substantial, and there was no statistically significant difference

between the control and test pipes. This suggests that the impact of orthophosphate on lead release during water stagnation was minimal compared to its effect observed in coupon tests. The concentrations of total lead had great variability during the initial hours, especially within the first eight hours for the initial free chlorine concentration of 3 mg/L as Cl₂ (Figures A4.3a and 4.3b).

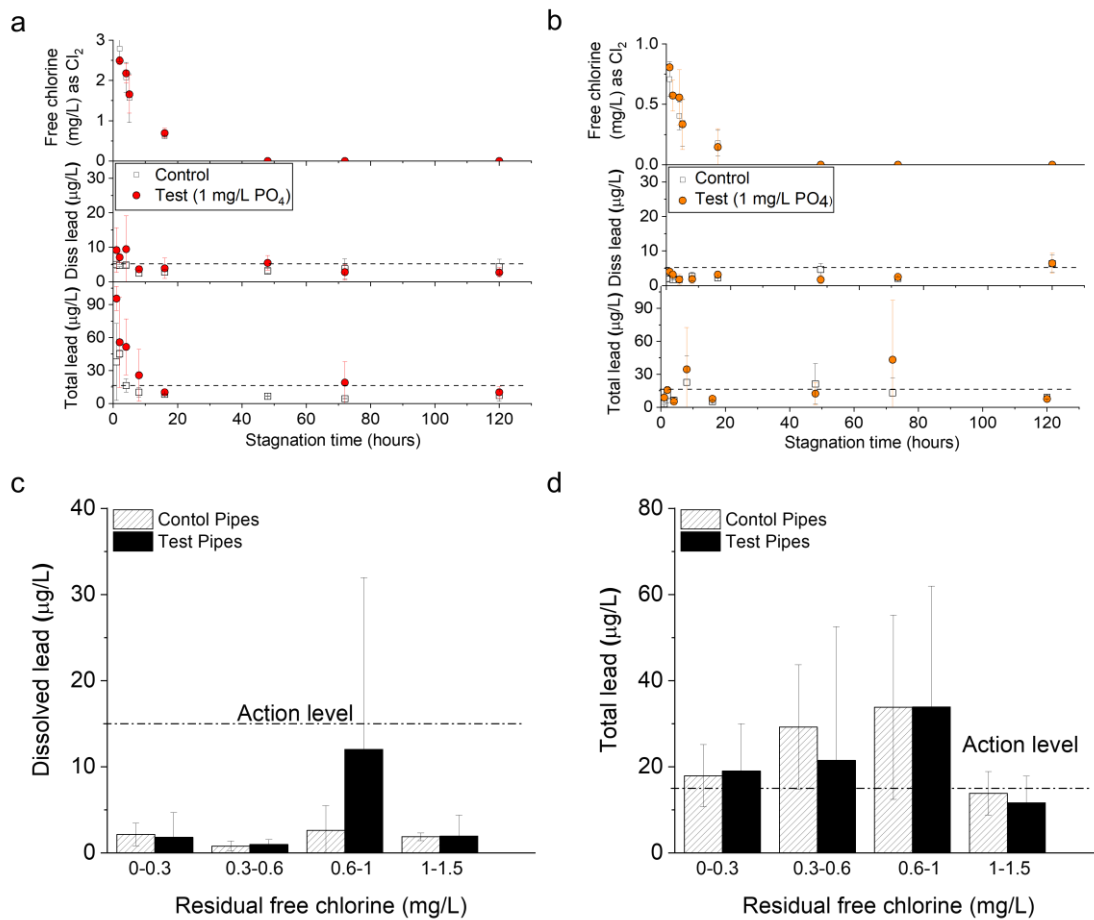


Figure 5.3 Pipe-loop study: stagnation experiments for free chlorine decay (top part of the panel), dissolved and total lead concentrations (middle and bottom part of the panel) at initial free chlorine of (a) 3.0 mg/L and (b) 1.0 mg/L as Cl₂. (c) Average dissolved lead and (d) average total lead concentrations for lead coupons at different residual free chlorine concentrations over a five-day test. The error bars denote standard deviations calculated from the triplicate experiments.

This variability may be attributed to the fact that immediately following reconditioning with continuously recirculating flow, the pipes had not yet been stagnated, and some of them might contain particulate lead in pipe scale or at the outlets despite water flushing, and the stagnation experiment had released those particulate lead. Therefore, the discussions were not based on the total results during the first eight hours. During the first eight hours, total lead concentrations ranged from 20 to 95 µg/L in the test pipes and from 10 to 60 µg/L in the control pipes (Figure 5.3b).

Table 5.1 Dissolved lead and total lead concentrations for lead coupons and pipe loops at different continuously-maintained stable free chlorine concentration ranges.

ID	Residual free Cl ₂ con. (mg/L)	Dissolved lead (µg/L)	Total lead (µg/L)
Control Coupons	1-1.5	2±1	3±1
Control Coupons	0.6-1	5±3	9±3
Control Coupons	0.3-0.6	6±4	9±4
Control Coupons	0-0.3	12±10	14±10
Test Coupons	1-1.5	15±4	19±3
Test Coupons	0.6-1	20±11	25±14
Test Coupons	0.3-0.6	19±9	24±9
Test Coupons	0-0.3	52±22	57±22
Control Pipes	1-1.5	2±1	3±2
Control Pipes	0.6-1	3±3	9±3
Control Pipes	0.3-0.6	1±1	9±4
Control Pipes	0-0.3	2±1	13±10
Test Pipes	1-1.5	2±2	18±3
Test Pipes	0.6-1	3±3	25±14
Test Pipes	0.3-0.6	12±20	24±9
Test Pipes	0-0.3	1±1	57±22

Note: The lead concentrations were averages calculated from the daily values of a five-day test with standard deviations from triplicate experiments for coupons and duplicate experiments for pipe loops.

Lead release was investigated at different constant free chlorine concentrations (0-0.3, 0.3-0.6, 0.6-1, and 1-1.5 mg/L as Cl₂) shown in Figures A4.11 and A4.12. Dissolved lead for both control and test pipes were below the 15 µg/L action level for most conditions with exception of one test with a high dissolved lead concentration for 0.6-1 mg/L residual free chlorine (Figure 5.3c). Total lead concentrations were below 15 µg/L when the free chlorine was stable above 1 mg/L as Cl₂ for both control and test pipes. When the residual free chlorine was maintained at concentrations below 1.0 mg/L, the total lead concentrations exceeded 15 µg/L for control pipes and for test pipes (Figure 5.3d). Similar as in the water stagnation experiments, no significant difference in lead release was observed between pipes receiving and not receiving 1 mg/L as PO₄ of orthophosphate (Table 5.1). The effect of orthophosphate on lead release corresponding to different stable free chlorine levels is minimal.

Orthophosphate impact for lead pipes with the real-world water use pattern

The impact of orthophosphate on PbO₂-coated lead pipes was investigated under conditions of lower free chlorine concentrations and periodic water stagnation that can emulate conditions of actual real-world water use. Six pipes with pre-existing PbO₂ scales were studied under different free chlorine concentrations and flow patterns (continuous and periodic flow). The pipe loops were first conditioned by continuously recirculating flow with 3 mg/L as Cl₂ of free chlorine for twenty weeks. Dissolved lead concentrations decreased from 150 µg/L to below 10 µg/L across all pipes by the end of the conditioning phase (Figure A4.13a). Total lead concentrations were

monitored from week 15, stabilizing around 40 $\mu\text{g/L}$ prior to the introduction of orthophosphate in the test pipes (Figure A4.13b). The pipes designated as control and test groups exhibited similar lead concentrations with no statistically significant differences, indicating they were prepared and comparable for subsequent test.

Test pipes were treated with 1 mg/L as PO_4 of orthophosphate starting from week 21 to week 30 and used continuously recirculating flow with 3 mg/L as Cl_2 of free chlorine. Dissolved lead concentrations remained consistently low and stable, at $4 \pm 3 \mu\text{g/L}$ for the control pipes and $7 \pm 7 \mu\text{g/L}$ for the test pipes. Total lead concentrations were $8 \pm 7 \mu\text{g/L}$ and $9 \pm 6 \mu\text{g/L}$ for the control and test pipes, respectively. Lead release was primarily composed of dissolved lead, and no statistically significant differences were observed between the control and test pipes. Residual orthophosphate levels were low during the first week of treatment, dropping from 1 mg/L to 0.2 mg/L after five days, but they gradually increased and stabilized at 0.6-0.8 mg/L by week 30 (Figure A4.13c). Lead release was primarily the result of release of dissolved lead, and no statistically significant differences were found between control and test pipes. Residual orthophosphate concentrations were low during the first week of treatment, dropping from 1 mg/L to 0.2 mg/L after five days, but gradually increasing and stabilizing at 0.6-0.8 mg/L by week 30. This change in residual orthophosphate suggests that the pipes had consumed orthophosphate most likely by adsorption to or precipitation of phosphate in the pipe scales.

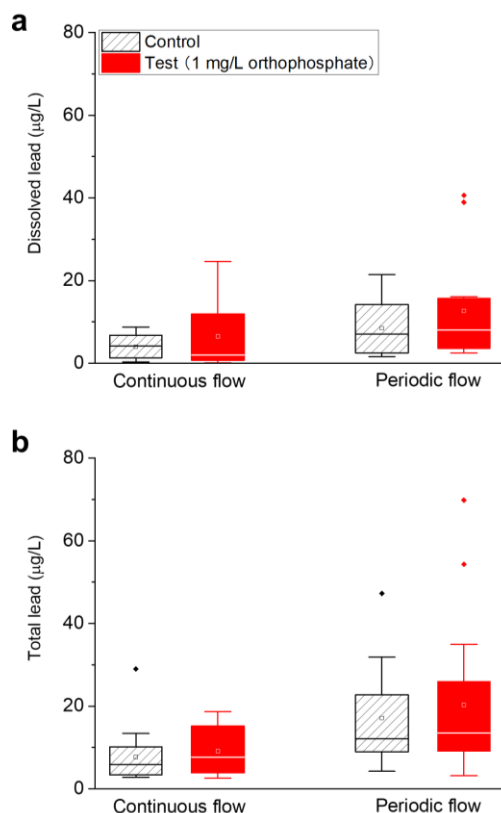


Figure 5.4 Box plots for (a) dissolved lead and (b) total lead concentrations for control and test (1 mg/L PO₄ orthophosphate) pipe loops under continuous flow conditions (ten weeks, free chlorine: 3 mg/L as Cl₂) and periodic flow conditions (five weeks, free chlorine: 1 mg/L as Cl₂).

From week 31 to week 35, the flow pattern was changed from continuous to periodic, and free chlorine concentrations were adjusted to 1 mg/L as Cl₂ for pipes to simulate real-world household conditions with more realistic free chlorine concentrations and water use for short periods followed by prolonged stagnation. Following the switch in free chlorine concentration and flow pattern, lead concentrations rose, with dissolved lead increasing to 8 ± 6 µg/L in the control pipes and 13 ± 12 µg/L in the test pipes (Table 5.2). Total lead concentrations also increased to 17 ± 11 µg/L and 20 ± 19 µg/L for the control and test pipes (Table 5.2), respectively. The change of flow patterns and drop of free chlorine addition increased the lead

release in both control and total pipes which showed statistical significance compared to the conditions of continuously recirculating flow and with 3 mg/L as Cl₂ of free chlorine (Figure 5.4).

Table 5.2 Summary of lead concentrations (dissolved and total lead) and p-value (Wilcoxon rank-sum test) for control and test pipes with the real-world water use pattern.

ID	Flow pattern	Dissolved lead (µg/L)	Total lead (µg/L)
Control pipes C	Continuous	4±3	8±7
Control pipes C	Periodic	8±6	17±11
p-value		0.06	0.001
Test pipes T	Continuous	7±7	9±6
Test pipes T	Periodic	13±12	20±19
p-value		0.2	0.1
Control pipes C	Continuous	4±3	8±7
Test pipes T	Continuous	7±7	9±6
p-value		0.3	0.4
Control pipes C	Periodic	8±6	17±11
Test pipes T	Periodic	13±12	20±19
p-value		0.6	0.7

Note: Dissolved lead defined as the lead concentration passing a 0.22 µm filter. This table presents an average of three distinct pipe replicates for the control and test pipes. For the continuous flow periods for Control pipes C and Test pipes T, the final five weeks of lead concentrations were averaged. $X \pm Y$ with X as the mean and Y as the standard deviation.

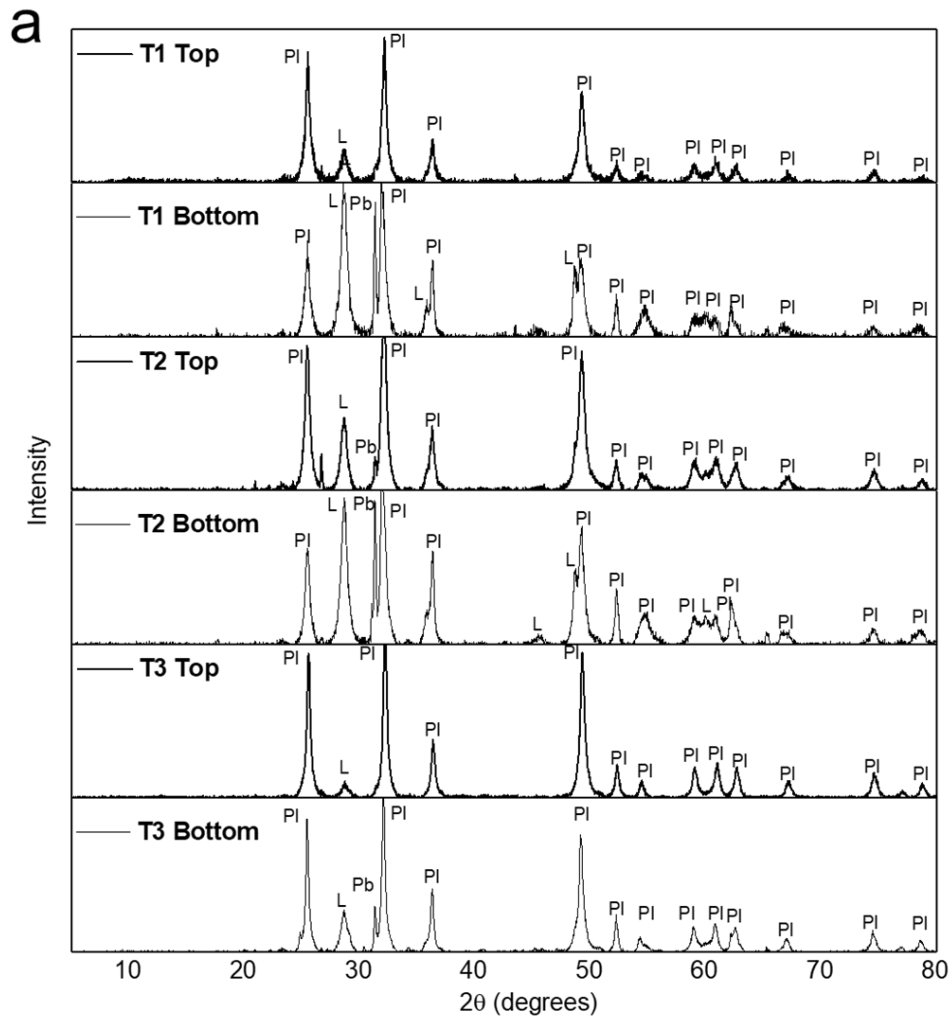
Notably, particulate lead constituted a great portion of the total lead increase alongside dissolved lead. The rise in particulate lead can be attributable to the water stagnation that allows lead to detach. The increase of dissolved lead might also result from water stagnation, as it led to low residual free chlorine concentrations that promote the reductive dissolution of Pb(IV) to Pb(II). Lead concentrations in the test pipes were slightly higher than in the control pipes, particularly

for dissolved lead; however, no statistically significant difference was observed between them. The residual orthophosphate concentration increased to 0.8–1.2 mg/L by the end of the five-day treatment each week (Figure A4.13c), indicating minimal consumption of orthophosphate after the change in conditions.

Scale analysis

At the conclusion of all tests with lead pipes, pipe segments (C1', C2', P1, P2) from experiments on orthophosphate effect for lead release during water stagnation and different residual free chlorine concentrations were collected for scale analysis. All of them were red (Figure A4.14), and all of them had plattnerite (β -PbO₂) as the dominant phase with minor amounts of litharge (PbO) also detectable (Figure A4.15a). No lead-phosphate solid was identified in test pipes that had been treated with 1 mg/L as PO₄ of orthophosphate for two months (Figure A4.15b). The thickness of the pipe scale showed minimal difference between control and test pipes, ranging from 40 to 100 μ m (Figure A4.16). Notably, aluminum was detectable in the by both element mapping with SEM-EDS and ICP-MS of acid-digested scale materials (Table A4.5). Phosphorus was detectable in the ICP-MS analysis in test pipes, with concentrations ranging from 9 to 24 mg/g; however lead phosphate solids were not observed by XRD. The lack of detectable lead phosphate solids by XRD could mean that such solids are completely absent, but for this study it is more likely that it indicates that the amounts of lead(II) phosphate solids formed on pipes scales after just two months were not sufficiently abundant to be detectable by XRD.

Scale analysis was also performed on segments of the pipes (C1-C3, T1-T3) that were used for experiments on the effect orthophosphate at real-world free chlorine concentrations and water use patterns. The analysis was conducted before conditioning (Week 1), at the end of conditioning (Week 20) and at the end of all experiments (Week 35).



b

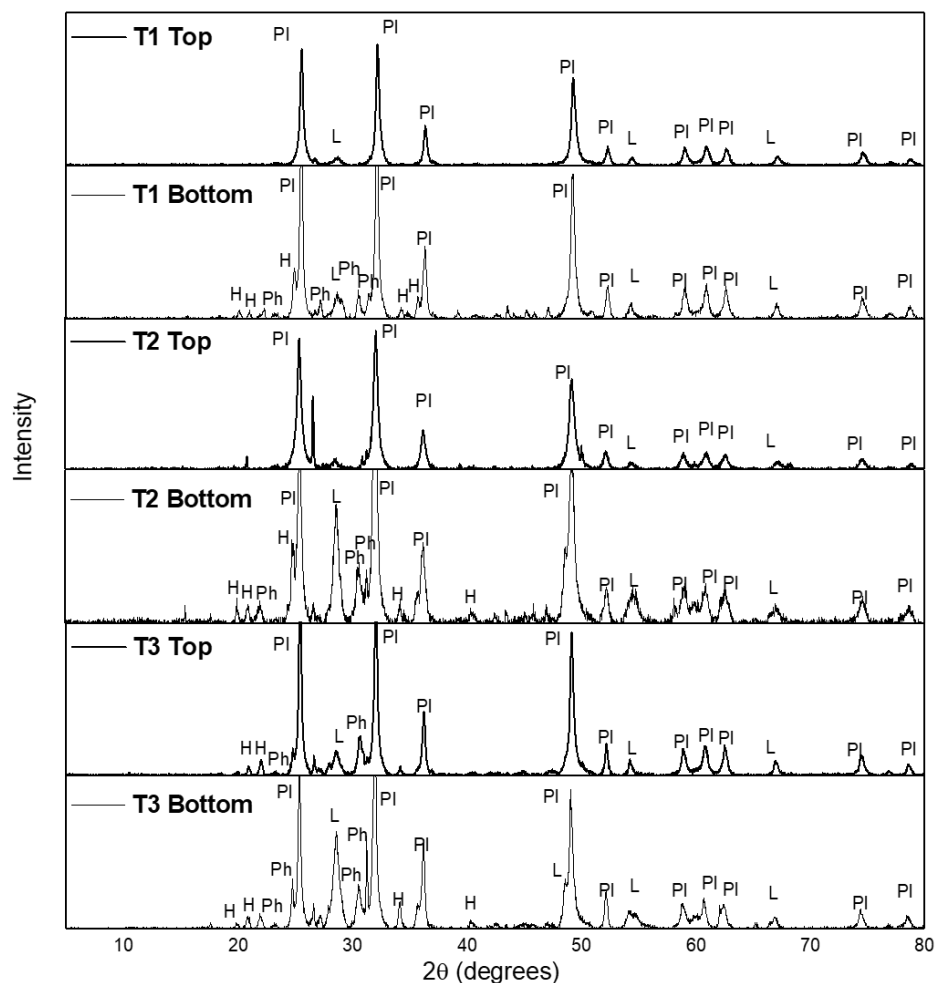


Figure 5.5 XRD patterns of corrosion products in the scales of test pipes (T1-T3) before and after test. The pipes were used for real-world water use pattern experiments. Reference patterns were shown in Figure.A4.7 for H: hydrocerussite ($\text{Pb}_3(\text{CO}_3)_2(\text{OH})_2$), Ph: phosphohedyphane $\text{Ca}_2\text{Pb}_3(\text{PO}_4)_3\text{Cl}$, Pb: lead (Pb), Pl: plattnerite ($\beta\text{-PbO}_2$) and L: litharge (PbO).

Before conditioning, the pipe scales were yellowish and crystalline phases were hydrocerussite ($\text{Pb}_3(\text{CO}_3)_2(\text{OH})_2$), plattnerite ($\beta\text{-PbO}_2$), and litharge (PbO) (Table A4.4). After twenty weeks of conditioning, the scales had turned dark red (Figure A4.17) with plattnerite ($\beta\text{-PbO}_2$) being the only dominant crystalline phase in scales (Table A4.4). After four months of treatment with 1

mg/L of orthophosphate as PO_4 , there was no significant difference in thickness between the control and test pipes, with both ranging from 50 to 150 μm (Figure A4.18) and pipe scales remained dark red (Figure A4.18). In the test pipes, a lead-phosphate solid, phosphohedyphane ($\text{Ca}_2\text{Pb}_3(\text{PO}_4)_3\text{Cl}$) was identified in pipes scales (Figure 5.5), alongside the presence of hydrocerussite ($\text{Pb}_3(\text{CO}_3)_2(\text{OH})_2$) and plattnerite ($\beta\text{-PbO}_2$). This was further corroborated by the concentrated phosphorus shown in element mapping in scale layer (Figure A4.18). ICP-MS results also indicated phosphorus was detectable in all test pipes, and its mass concentrations ranged from 3 to 28 mg/g (Table A4.5). In contrast, the control pipes showed little change in scale composition compared to the end of conditioning, with plattnerite ($\beta\text{-PbO}_2$) remaining the sole dominant crystalline phase (Figure A4.19). The scale analysis of test pipes treated with 1 mg/L of orthophosphate as PO_4 revealed that lead-phosphate solids can form on pipes with pre-existing $\beta\text{-PbO}_2$ scales. Their formation can be dependent on the time of treatment. In this study, lead-phosphate solids were detectable after more than four months of treatment, but not after two months.

5.3.3 Pipe-loop and Coupon Study

Pipe-loop and coupon studies are both valuable tools to evaluate lead corrosion control methods, each with its own advantages and limitations. Coupon studies are relatively easy to set up, cost-effective, and capable of forming lead scales in a shorter time. Furthermore, coupon studies are better suited for examining changes in lead dissolution and its underlying mechanisms, as their

smaller systems allow for easier manipulation of experimental conditions and quicker observation of corresponding changes. Additionally, scale analysis can be conducted more easily on coupons. However, a coupon study has limitations in replicating the dynamic water flow conditions in pipes, and the composition of lead scales may differ from those formed in actual water pipes. Pipe-loop studies can overcome these limitations and provide a more accurate representation of lead corrosion conditions in water pipes; however, they take more time and are more costly

In our study, PbO_2 rapidly formed on the lead coupon surfaces within a few weeks, whereas conditioning of pipe loops required several months before making PbO_2 a rich component in pipe scales. The effects of orthophosphate differed between the coupon and pipe-loop studies. In the coupon study, the presence of orthophosphate accelerated the depletion of free chlorine and enhanced lead dissolution, particularly in terms of dissolved lead. Additionally, no lead-phosphate solids were observed on the lead surfaces in the coupon study. In contrast, the effect of orthophosphate on free chlorine decay was minimal in the pipe-loop studies, and its impact on lead release was not significant. Although there were instances where test pipes exhibited higher lead release than control pipes, no significant adverse effects comparable to those observed in the coupon studies were noted. Furthermore, lead-phosphate solids were detectable in pipe loops after four months orthophosphate treatment, whereas such solids were not observed in coupon studies.

The differences in behavior of coupons and pipes that are both rich in PbO_2 may be attributed to several factors. First, coupon studies are conducted in smaller systems, which can exhibit changes in lead dissolution more rapidly and to a greater extent. For example, the total water volume in our coupon study was 200 ml, compared to 10 liters used in the pipe-loop tests. Consequently, even minor changes in lead dissolution in the presence of orthophosphate may be amplified in the coupon study, making them appear more pronounced. Conversely, similar adverse effects might also occur in pipe-loop studies, but these effects may not be as evident due to the larger system size. Second the composition of pipe scales varied between the coupon and pipe-loop studies. Although PbO_2 was a dominant component in the lead coupon scales, it differed from the scales formed in pipes over years of use. A notable difference was the presence of aluminum-containing amorphous materials in the pipe scales, as evidenced by our ICP-MS analysis. These materials may act as sinks for both lead and phosphorus, thereby limiting observable increases in lead concentration in the water while simultaneously facilitating the precipitation of lead-phosphate solids. Masters et al. (2022) also identified differences in lead release between strip lead coupon and pipe-loop studies, despite both employing the same orthophosphate treatment. They found that coupon studies exhibited greater variability and uncertainty. Consequently, they suggested that a pipe-loop study would be a more accurate representation of the conditions in water pipes in real systems. In general, results from pipe-loop studies are more representative and useful for assessing lead corrosion in actual pipes. However, results from lead coupon studies, such as the increased lead release in the presence of

orthophosphate observed in our study, can offer valuable insights into potential reactions and highlight risks that may also be pertinent to lead pipes.

5.3.4 Implications for Lead Corrosion Control

Lead concentrations for LSLs with pre-existing PbO_2 pipe scales are typically low and more stable compared to LSLs with Pb(II) solids as the dominant component in pipe scales (Clark et al., 2014; Triantafyllidou et al., 2015). However, lead release from PbO_2 -coated pipes becomes a more pronounced issue during water stagnation. This occurs when residual free chlorine is insufficient to maintain the stability of PbO_2 , leading to the reductive dissolution of Pb(IV) and the subsequent release of dissolved lead into the water. The addition of orthophosphate has been reported to be beneficial for limiting lead release when the disinfectant is switched from free chlorine to chloramine, or when other reductants are present. This effect is primarily due to the formation of lead-phosphate solids (Shock and Clement, 1998; Xie and Giammar, 2007), which become the dominant phase in pipe scales and are not susceptible to changes in the redox conditions in water. In our study, following more than four months of orthophosphate treatment (1 mg/L as PO_4), lead-phosphate solids were detectable in the test pipes, and PbO_2 remained present within the pipe scales. During stagnation tests, the pipes containing lead-phosphate solids did not exhibit any advantages in limiting lead release. As PbO_2 remains within the pipe scales, lead release may increase when residual free chlorine concentrations drop below the threshold to maintain its stability. Scale analysis of actual LSLs revealed that for some free-chlorine water

systems using orthophosphate for corrosion control, PbO_2 can be absent from pipe scales, with lead-phosphate being the dominant component (Tully et al., 2019).

Another finding from our study is that the addition of orthophosphate may initially increase lead release before the formation of stable lead-phosphate solids in the pipe scales. This finding, although primarily observed in lead coupon studies, aligns with previous research indicating that the use of orthophosphate in pipes with pre-existing PbO_2 can lead to the release of lead-phosphate particles into the water. This highlights a potential risk for water systems considering the use of orthophosphate in systems with PbO_2 . Overall, our study indicates that the use of orthophosphate in pipes dominated by PbO_2 does not provide a significant benefit for lead corrosion control over the 4-month time scales examined in this study. While the application of orthophosphate leads to changes in pipe scale composition, resulting in the presence of lead-phosphate alongside PbO_2 , the effectiveness of these changes in corrosion control remains unclear.

5.4 Conclusions

The effect of orthophosphate on lead release from PbO_2 -rich layers was investigated for both lead pipes and coupons. In the presence of orthophosphate, increased lead release was observed in lead coupon studies, while there were no statistically significant effects of orthophosphate on lead release in pipe-loop studies. A lead-phosphate solid, phosphohedyphane ($\text{Ca}_2\text{Pb}_3(\text{PO}_4)_3\text{Cl}$),

became detectable in pipes treated with 1 mg/L as PO_4 of orthophosphate for more than four months but was absent in coupons or in the pipes with shorter orthophosphate treatment time.

Our findings suggests that the use of orthophosphate in LSLs with rich PbO_2 layers in scales may not provide a substantial benefit for lead corrosion control during the initial phase of its addition.

The differences between the coupon and pipe-loop studies indicate that while pipe-loop experiments can be more representative of real-world conditions, coupon studies can reveal potential risks and underlying mechanisms. Future research should focus on long-term orthophosphate treatment to examine whether the crystalline phase can transition to be more phosphohedyphane-dominated and whether this scale phase transition can help limit lead release, particularly during extended water stagnation when residual free chlorine is insufficient.

5.5 Acknowledgments

We are grateful to Erie County Water for their contributions to this work, including providing the harvested lead service lines, funding of the study, and valuable insights on the study's technical objectives. We appreciate the technical and administrative support of Hazen and Sawyer for the completion of the work. We also would like to thank Andy Kim and Priya Gupta, undergraduate students in WUSStL and helped to condition the pipe-loop reactors.

Chapter 6: Exploring Variations in Properties of Lead Pipe Scales from Different Drinking Water Systems

Abstract

The scales of corrosion products that form on the inside of lead pipes used for drinking water supply exert a strong control on lead concentrations in tap water. Compositions of lead pipe scales from different drinking water distribution systems vary in appearance, crystalline phases present, and element concentrations. This study is based on analysis of the scales of 70 harvested pipes from 16 different systems across the U.S. together with the data from previously published research. Key factors impacting lead pipe scale composition are identified. The characterization data are integrated with statistical analysis and chemical equilibrium predictions. The specific crystalline lead carbonate solid present depends on the pH and dissolved inorganic carbon (DIC) concentration. Systems with only hydrocerussite ($\text{Pb}_3(\text{CO}_3)_2(\text{OH})_2$) tend to have a higher pH (8.5 ± 0.8) and lower DIC (1.3 ± 0.6 mM) than systems with only cerussite (PbCO_3) (pH: 7.5 ± 0.2 , DIC: 5.5 ± 1.3). While lead(IV) oxide solids are predicted in all systems using free chlorine as a disinfectant, they were only actually observed in 44% of them. The formation of lead(IV) oxide solids may be adversely affected by blended-phosphate corrosion inhibitors. Formation of lead-phosphate solids depends on the type and concentrations of phosphate inhibitors. Lead-phosphate solids are more commonly found in systems using the highest concentrations of orthophosphate

and using orthophosphate as opposed to a blended phosphate. Amorphous materials are present as components of many pipe scales, and these amorphous materials are often rich in aluminum. Equilibrium predictions for lead carbonate, lead(IV) oxide solids, and lead phosphate correspond to observed cases with accuracies of 95%, 44%, and 71%, respectively.

6.1 Introduction

Despite ongoing efforts in the U.S. to replace lead service lines (LSLs), millions of LSLs continue to supply water for daily household use (Cornwell et al., 2016). Lead leaching from LSLs into drinking water poses risks to human health (Gould, 2009; Swarngen et al., 2022). Various lead crises, notably the cases in Washington DC, Flint, Michigan, and Newark, NJ highlight the importance of controlling lead in drinking water (Edwards et al., 2009; Jarvis and Fawell, 2021; Lytle et al., 2020b; Roy and Edwards, 2019).

The Lead and Copper Rule Revisions have stricter protocols aimed at lowering lead concentrations in tap water. These protocols include setting a trigger lead level at 10 $\mu\text{g/L}$ and requiring that the 5th liter rather than the 1st liter of water be tested for lead in homes with lead pipes (USEPA, 2021; Via, 2024). These changes have necessitated improved lead corrosion control strategies for many public water systems (PWSs) (Arnold et al., 2020; Masters et al., 2021). Current corrosion control treatment (CCT) methods include pH and alkalinity adjustment and the addition of corrosion inhibitors (Kogo et al., 2017; Tam and Elefsiniotis, 2009). Corrosion control treatment aims to promote the formation low solubility lead-containing

corrosion products on the pipe walls and to adjust the pH to regions of particularly low solubility of those solids. Pipe scales can form a protective layer on the surface of pipes and effectively inhibit further oxidation of the metal. Because they are in direct contact with water, these scales usually control the lead levels in drinking water (Kim and Herrera, 2010; Triantafyllidou et al., 2015; Xie and Giammar, 2011).

Given the pivotal role of lead pipe scales in determining lead levels in drinking water, scale analysis is a valuable tool for corrosion control assessment (Bae et al., 2020b; Harmon et al., 2022). Scale analysis encompasses analytical techniques to identify the crystalline solid phases, elemental composition, and morphology of a pipe scale. Some previous studies for lead corrosion control have concentrated on the use of corrosion inhibitors or the effects of full and partial replacement of LSLs (Bae et al., 2020a; Doré et al., 2019a; Mishra et al., 2021b). While some studies have incorporated scale analysis, it has not been systematically investigated nor received sufficient emphasis. Tully et al. (2019) investigated the relationship between lead pipe deposits and water quality in the Midwestern U.S (Tully et al., 2019). They found that the theoretical predictions of lead mineral phases based on water quality calculations only partially matched the actual scales observed in LSLs. Wasserstrom et al. (2017) investigated scale formation in lead pipes treated with blended phosphate (Wasserstrom et al., 2017). Their research revealed that an outer amorphous barrier layer, rather than the anticipated lead-phosphate solid, played a key role in inhibiting lead release to water.

Lead pipe scales vary significantly across PWSs due to differences in water chemistry and corrosion control strategies (DeSantis et al., 2020; Li et al., 2016; Mishra et al., 2021a). No prior study has systematically evaluated key factors influencing lead pipe scale properties at a national level. Furthermore, limited research has investigated the applications and limitations of desktop tools such as solid prediction models in scale analysis,(Edwards et al., 1999) an area of significant importance.

This study is founded on scale analysis of lead pipes from PWSs across the U.S, and it also includes results from a prior study focused on lead scale compositions in the Midwestern U.S (Tully et al., 2019). The objectives of this study were to a) explore the influence of water chemistry and corrosion control methods on lead scale composition and b) evaluate the applications and limitations of solid prediction models for scale analysis.

6.2 Material and Methods

6.2.1 Public Water Systems in the Research

This research includes scale analysis of 70 harvested lead pipes from 16 PWSs across the U.S. (Figure A6.1). These scale analyses were evaluated together with the results from the paper of Tully et al. (2019), which include results from 22 PWSs, to provide a holistic view of scale compositions across the U.S (Tully et al., 2019). The water chemistry of the different PWSs is included in Tables A6.1 and A6.2.

6.2.2 Scale Analysis Methods

Scale analysis encompasses the characterization of crystalline minerals present, elemental composition, and morphology. The crystalline phases in the scale were identified using X-ray diffraction (XRD, Bruker d8 Advance). The results of the lead solid phase of each PWS are summarized in Tables A6.3 and A6.4. The elemental composition of each scale was characterized by inductively coupled plasma mass spectrometry (ICP-MS, NexION 2000) after acid digestion. The morphology of the scale was characterized by scanning electron microscopy of pipe cross sections (SEM, Thermo Fisher Quattro S E-SEM). The element distribution within the scales was characterized by energy dispersive X-ray spectroscopy (EDS, Oxford AzTec). The detailed scale analysis procedures and protocols are included in the Supporting Information.

6.2.3 Layering of Lead Scales

In this study, the scale layers from lead pipes were differentiated based on variations in morphology and crystalline phase observed during analysis. These layers were subsequently categorized into top and bottom layers for further examination. The top layer represents the portion of materials in direct contact with finished water. In this study, for certain crystalline phases, we focused primarily on their presence and did not distinguish between layers in Tables A6.3 and A6.4. The mass concentration of elements in the scale layers was presented separately for different layers.

6.2.4 Chemical Equilibrium Model Predictions of Crystalline Lead Phases

Present

The chemical equilibrium program MINTEQA2 3.1 was employed to predict the formation of specific crystalline lead phases. These predictions were based on the thermodynamic constants outlined in Table A6.5 with calculations performed by inputting water chemistry parameters from Tables A6.1 and A6.2 for specific water systems. More details are included in the Supporting Information.

6.2.5 Statistical Significance Analysis

Statistical significance was evaluated in RStudio using a two-tailed t-test for independent samples (function: *t.test()*) with a significance level of 0.05. Normality and variance assumptions were verified by Shapiro-Wilk Test and Levene's Test. Pearson correlations between different elements mass concentrations from scale analysis were calculated in RStudio using the function *cor.test()*.

6.3 Results and Discussion

6.3.1 Lead-carbonate Solids: pH and dissolved organic carbon

Lead-carbonate (Pb-C) solids are white or gray crystalline phases (Figure A6.2a) that are widely found in LSL scales. Pb-C solids were found in 95% of the PWSs (41 out of 43) included in this study, with cerussite (PbCO_3) and hydrocerussite ($\text{Pb}_3(\text{CO}_3)_2(\text{OH})_2$) as the major phases (Tables A5.3 and A5.4). Cerussite and hydrocerussite were also occasionally observed together in a pipe

scale (Figure A6.3a). Cerussite is observed as the sole Pb-C solid in only 8% of the examined PWSs, hydrocerussite is the sole Pb-C solid for 41%, of systems, a combination of cerussite and hydrocerussite is observed in 46% of systems, and 5% of systems had no observable Pb-C solids (Figure A6.3b).

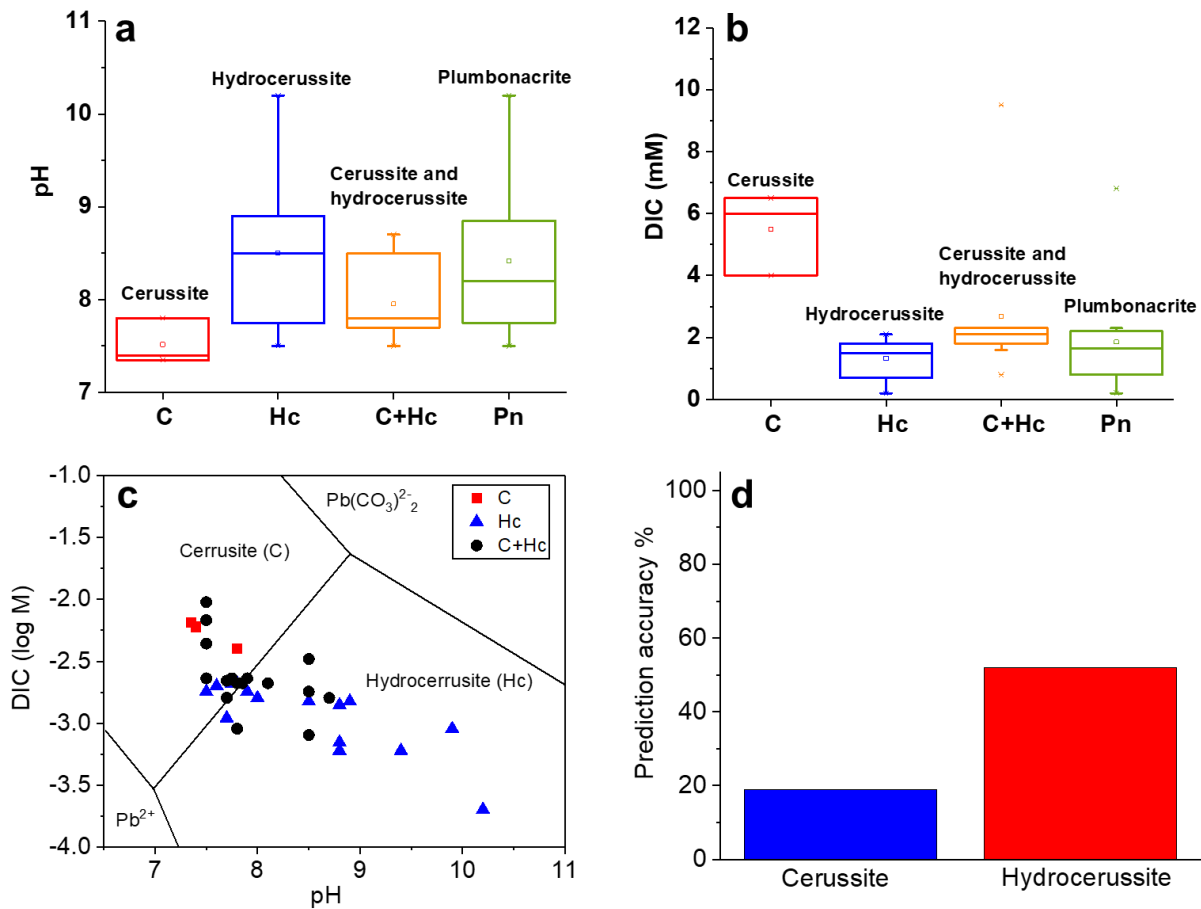


Figure 6.1 (a) pH and (b) DIC of PWSs for which certain Pb-C solids were observed through scale analysis. (c) DIC-pH diagram for predicted cerussite and hydrocerussite formation (lines demarcate regions in which a particular lead species is predicted) and the actual presences of Pb-C solids in PWSs shown with points. (d) Prediction accuracy for cerussite and hydrocerussite by the equilibrium model.

DIC and pH play key roles in determining the speciation of lead-carbonate solids within LSLs, and they also impact the solubility of lead-carbonate solids. High pH promotes the formation of hydrocerussite (Figure A6.4a), whereas high DIC favors cerussite formation (Figure A6.4c). Our analysis of PWSs containing lead-carbonate solids is qualitatively consistent with this expected trend: PWSs with cerussite alone and hydrocerussite alone have average pH values of 7.5 ± 0.2 and 8.5 ± 0.8 (p-value=0.003), respectively, and DIC concentrations of 5.5 ± 1.3 and 1.3 ± 0.6 mM (p-value=0.03), respectively (Figure 6.1a). PWSs containing both cerussite and hydrocerussite have average values for pH and DIC of 7.9 ± 0.4 and 2.6 ± 2.2 mM, respectively (Figure 6.1b). Those values closely align with the transition threshold between the two (Figure 6.1c).

The presence of a Pb-C solid was predicted with an accuracy of 95 % (41 out of 43). The pH and DIC conditions required for the formation of cerussite versus hydrocerussite were calculated using thermodynamic models by MINTEQA2 3.1 (Table A6.8). Only 37% (16 out of 43) of PWSs had the specific Pb-C that was predicted present as the only observable Pb-C solid. Prediction accuracies for cerussite and hydrocerussite were 19% and 52%, respectively (Figure 6.1d). The major mispredictions occur near the transition threshold between cerussite and hydrocerussite (Figure 6.1c). Chemical equilibrium predictions will only predict the presence of one solid, the lower solubility one for a given water chemistry, but for actual water systems both cerussite and hydrocerussite can be present due to temporally varying pH and DIC. Further the predicted solids present are only as accurate as the equilibrium constants used in the predictions, and there

is uncertainty in some of the constants (Noel et al., 2014). Plumbonacrite ($\text{Pb}_{10}(\text{CO}_3)_6\text{O}(\text{OH})_6$) is found in 28% of the PWSs (13 out of 43, Figure A6.2c). It is found at an overall higher pH (average pH of 8.6), and it is usually co-present with hydrocerussite.

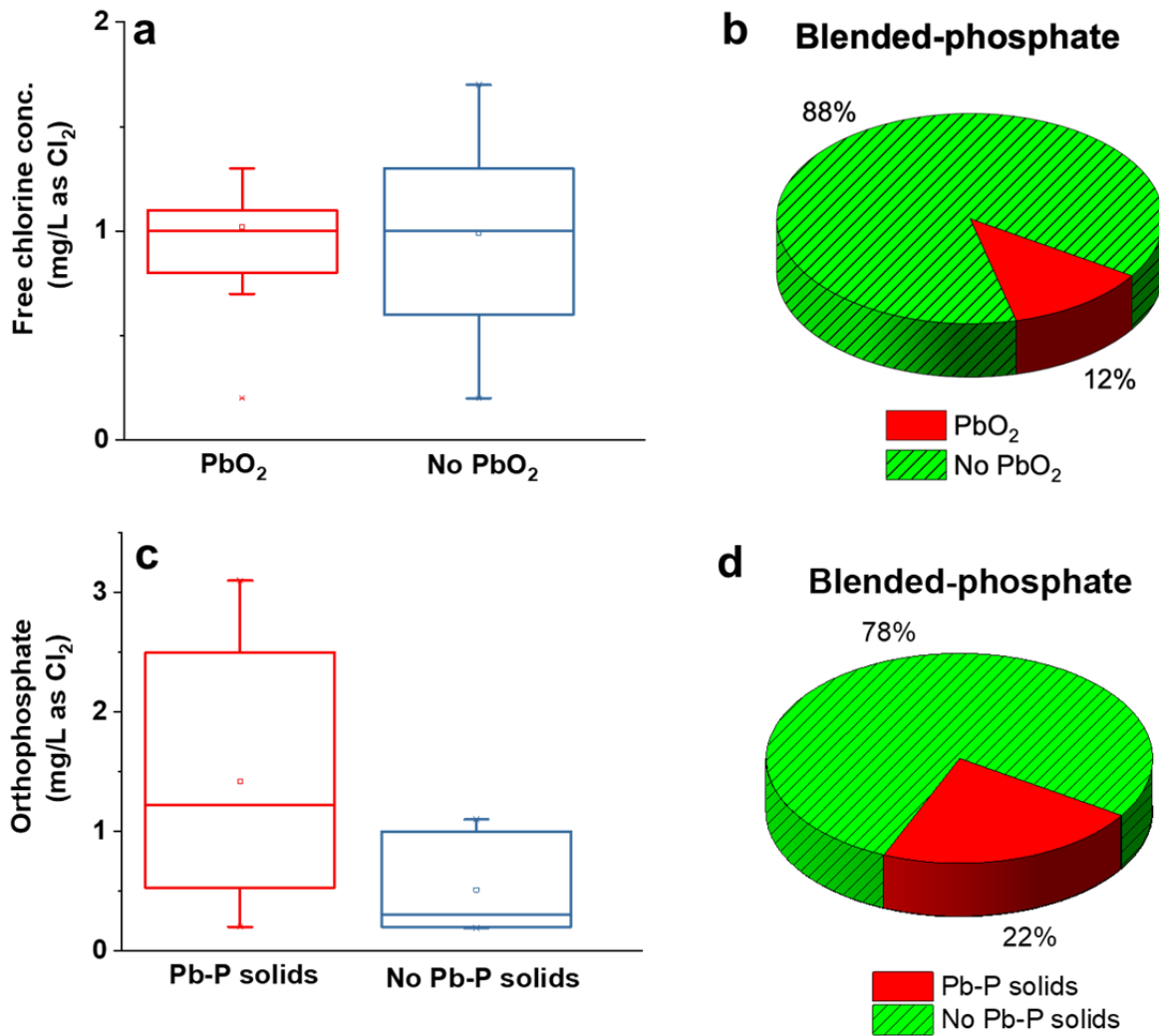


Figure 6.2 (a) Free chlorine concentration in PWSs with and without PbO_2 solids. (b) Presence of PbO_2 solids in PWSs using free chlorine and blended-phosphate (8 PWSs in total). (c) Orthophosphate concentration in PWSs with and without Pb-P solids. (d) Presence of Pb-P solid in PWSs using blended-phosphate (9 PWSs in total).

6.3.2 Lead (IV) oxide solids: Disinfectant and Corrosion Control Method

PbO₂ solids are dark red (Figure A6.2b) and have extremely low solubility. Their theoretical solubility is below 1 ng/L in most PWSs, compared to other lead solids, which range from 10 to 100 µg/L. (Figure A6.5a). Lead(IV) is only s at the high redox potential (Figure A6.4) provided by free chlorine and not that of chloramine.

Thermodynamic calculations predict that the presence of even a small amount of free chlorine (< 0.1 mg/L) is adequate to form and sustain PbO₂ solids (S9). However, in actual conditions, PbO₂ solids are not detectable in all PWSs using free chlorine. Of the PWSs included in this study, 79% (34 out of 43) employ free chlorine (Figure A6.6a), but only 44% (15 out of 34) of those have detected PbO₂ solids (Figure A6.6b). There was no statistically significant difference between the free chlorine concentrations of the PWSs with and without PbO₂ solids (Figure 6.2a, p-value=0.86). Additionally, there were no significant differences in pH (Figure A6.6c, p-value=0.77) and DIC (Figure A6.6d, p-value=0.63) between the PWSs with and without PbO₂ solids.

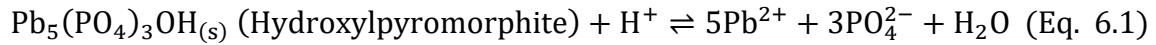
The addition of a phosphate chemical for corrosion control affected the presence of PbO₂ in PWSs. Among free chlorine systems employing blended-phosphate inhibitors for corrosion control, 88% (7 out of 8) have no detectable PbO₂ (Figure 6.2b). The influence of phosphate inhibitors on corrosion control in PbO₂-coated LSLs can be complex.(Holm and Shock, 1991; Holm and Smothers, 1990; Lytle and Edwards, 2023; Ma et al., n.d.) Lytle et al., (2009) reported

an inhibitory effect of orthophosphate on PbO₂ formation (Lytle et al., 2009a). Lytle and Schock, (2005) stated that polyphosphate may solubilize Pb(IV) (Lytle and Schock, 2005). Our analysis of the compiled scale analysis dataset suggests that blended-phosphate could have negative impacts on the formation or preservation of PbO₂ in LSLs compared to other corrosion control methods.

6.3.3 Lead-phosphate Solids: Phosphate Inhibitors and Water Chemistry

Lead-phosphate (Pb-P) solids in scales are generally yellow (Figure A6.2c) and can be present in PWSs treated with phosphate-based corrosion inhibitors. Pb-P solids have lower solubility compared to Pb-C solids within the pH range of 6-8.5 (Figure A6.5b). Forty-nine percent of PWSs (21 out of 43) use phosphate-based inhibitors as their corrosion control method (Figure A6.7a), and 62% of those (13 out of 21) have detected Pb-P solids. As discussed in the next paragraph, equilibrium calculations do not predict that Pb-P solids will form in all systems with added phosphate. PWSs using blended-phosphate inhibitors (Figure 6.2d) are less likely to have Pb-P solids compared to those using orthophosphate or zinc phosphate (Figure A6.7). Research by Wasserstrom et al. (2017) also showed that a water system utilizing blended-phosphate inhibitor formed an amorphous layer containing phosphorus rather than crystalline Pb-P solids (Wasserstrom et al., 2017).

A higher concentration of orthophosphate can facilitate the formation of a Pb-P solid (hydroxylpyromorphite) based on Eq. 6.1.



Our findings confirm that PWSs containing Pb-P solids tend to have a higher orthophosphate concentration (1.5 ± 1.1 mg/L as PO_4 , Figure 6.2c) compared to those without Pb-P solids (0.5 ± 0.4 mg/L as PO_4) (p-value = 0.01). The calculated threshold orthophosphate concentration required for hydroxylpyromorphite formation demonstrated a strong agreement with the observed presence of Pb-P solids. Seventy-one percent (15 out of 21) of the PWSs matched the predictions (Figure 6.1d), with 11 out of 16 matching the prediction of Pb-P solids being present and 4 out of 5 matching the prediction of them not being present (Table A6.10).

6.3.4 Amorphous Materials: Elements in Scale Phase and Finished Water

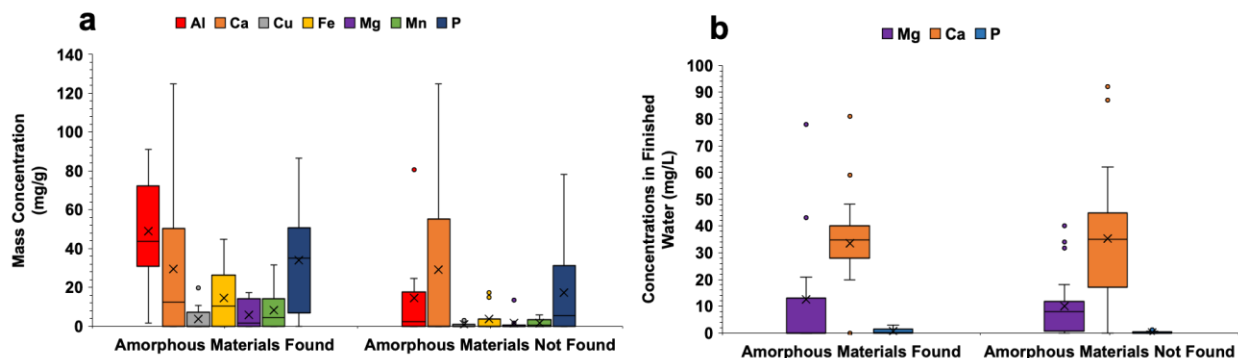


Figure 6.3 Correlations between the presence of amorphous material and (a) mass concentrations of different elements (Al, Ca, Cu, Fe, Mg, Mn and P) in lead pipe scales, (b) concentrations of Ca, Mg and P in finished water. “Y” means amorphous material was found on scales, while “N” means amorphous material was not.

Amorphous materials can form on the inner surfaces of pipe walls containing multiple elements. They often have a rough surface morphology (Figure. A6.2d), and they have broad peaks in XRD patterns around 2θ of $10\text{-}20^\circ$ (Figure A6.9d). In this study, amorphous materials were

found in 47% of PWSs (20 out of 43) applying various disinfectants and corrosion control methods. No significant statistical difference was found between PWSs with and without amorphous materials in terms of pH (p-value = 0.45) and DIC (p-value = 0.98).

Elemental analysis of scales reveals that lead is indeed the major element in pipe scales (Table A6.11). Aluminum (Al), calcium (Ca), copper (Cu), iron (Fe), magnesium (Mg), manganese (Mn), and phosphorus (P) were detectable in scales, and these were more abundant when amorphous materials are present in top scale layer (Figure 6.3a). Specifically, aluminum is statistically much more abundant in scales with amorphous materials (p-value = 0.02). This agrees with previous research (Kvech and Edwards, 2001; Snoeyink et al., 2003; Zhang et al., 2016) that amorphous materials in pipe scale can be comprised of substantial aluminum. The concentrations of Mg, Ca and P in finished water did not show significant difference between PWSs with and without amorphous materials (Figure 6.3b, p-values>0.05). Although Al was not reported in an enough number of systems to draw a robust conclusion, it is reasonable to infer that water systems containing amorphous materials tend to have significant concentrations of Al in the finished water given its abundance in the scale.

6.3.5 Applications of Scale Analysis Techniques and Their Limitations

With the development of characterization techniques, the analysis of lead scale has become more feasible. However, there are limitations from both the overall analysis process and specific techniques. The disturbance of scale materials during excavation, transportation, and sample

preparation could introduce loss of materials and uncertainties to scale analysis. Scale analysis techniques used in this study included XRD, ICP-MS, and SEM-EDS. XRD can readily identify crystalline solids but not amorphous materials. In addition, several common lead solids found in drinking water have similar or even overlapping XRD patterns (Figure A6.9). ICP-MS can provide quantitative information on mass concentrations of elements, but its detection limits are not ideal for certain elements. SEM-EDS can help identify the thickness of scale and element distribution (Figure A6.10), but it is semi-quantitative unless performed with standards for calibration. More detailed discussions of XRD, ICP-MS and SEM-EDS can be found in the Supporting Information. Other techniques that have been used include optical microscopy (Hopwood et al., 2023) for visual inspection of scales, Raman spectroscopy (Pasteris et al., 2021) for mineral identification, and X-ray fluorescence for elemental compositions.

6.4 Environmental Implications

Lead pipe scale from different PWSs varies in appearance (color, structure and roughness), crystalline phase, and element composition. A systematic analysis of pipe scales and the investigation of key factors influencing them are important for corrosion control. For example, identifying the dominance of a specific lead solid, such as lead-phosphate, in pipe scales can indicate the effectiveness of corrosion control treatments (e.g., orthophosphate inhibitors); tracking changes in pipe scales regarding lead solid speciation and elemental composition can help assess the risk of lead leaching. Various factors can compromise the accuracy and reliability

of scale analysis, including alterations in scale composition during harvesting and shipment. Optimizing these aspects is essential for achieving precise and timely analyses in the future, potentially through the implementation of standardized protocols and advanced analytical techniques.

Equilibrium models for predicting solids present and their solubility can be useful. Lead-carbonate, lead-phosphate, and lead(IV) oxide solids are the major lead solids present in pipe scales and can coexist. In this study, the solid prediction achieved accuracies of 95%, 44%, and 71% for the presence of lead-carbonate, lead(IV) oxide solids, and lead-phosphate respectively. Most mismatches for lead-carbonate solids were due to the co-occurrence of both cerussite and hydrocerussite, which the model cannot predict. Although distinguishing between a specific lead-carbonate speciation can have some implications for management of lead concentrations in a water systems service area, identifying the dominant lead solids in pipes, e.g. lead phosphate or lead carbonate, plays a more crucial role in helping predict lead levels in water. Lead(IV) oxide solids were predicted to be present in all free-chlorine systems, but they were only detectable in some of those. The causes for the PbO_2 mispredictions remain unclear, possibly due to factors such as the contact time of free chlorine with the pipes and the presence of reductants (e.g., natural organic matter) that can more rapidly consume free chlorine and that can also reductively dissolve PbO_2 . To improve the accuracy of predictions for lead-phosphate solids, additional research into polyphosphate reaction constants and their effects may be required.

Equilibrium models are based on thermodynamic principles and use single values of inputs, so they do not consider temporal variations in water chemistry, residual free chlorine and the treatment time of orthophosphate that occur in real systems. Other factors in lead pipes, such as flow dynamics, reaction kinetics, are also not accounted for. Furthermore, the equilibrium constants involved in these predictions have uncertainty. The prediction model is valuable for screening scale formation. Integrating the results from model predictions with scale analyses is essential.

6.5 Acknowledgments

We are grateful to the numerous people at environmental engineering consulting companies and public water systems who arranged the harvesting and shipment of the lead pipes analyzed in this study. During the period for which this work was performed, Yao Ma was partially supported by funding from the McKelvey School of Engineering at Washington University in St. Louis. We would like to thank the help from undergraduate students at WUSTL, Bella Stull, Andy Kim and Priya Gupta for preparing the samples.

Chapter 7: Conclusions and Recommendations for Future Work

7.1 Conclusions

This dissertation aimed to provide insights into the precipitation, stability and dissolution of lead corrosion products on lead service lines that can help predict lead release to tap water and that can be used to optimize the lead corrosion control. It focused on the use of phosphate-based corrosion inhibitors, the promotion of the formation and stability of Pb(IV)O_2 corrosion products on pipe walls, and the analysis of pipe scale composition across the United States. The research is grounded in multiple experimental methods, including pipe-loop studies, coupon tests, scale analysis, and the application of chemical equilibrium models to predict crystalline phases and solid solubilities.

The findings in Chapter 2 indicate that increasing the orthophosphate concentration from 0.2 to 1.5 mg/L as PO_4 can efficiently limit lead release in lead service lines (LSLs). This benefit improves over time and is further enhanced by the removal of polyphosphate from blended phosphate treatments. The removal of polyphosphate from a blended phosphate corrosion inhibitor facilitated more stable and consistently low levels of total and dissolved lead and promoted the formation of phosphohedyphane ($\text{Ca}_2\text{Pb}_3(\text{PO}_4)_3\text{Cl}$). The formation of phosphohedyphane can be advantageous in limiting lead release. For systems primarily focused

on lead corrosion control without the need for metal sequestration, orthophosphate would be a better choice than blended phosphate.

Chapter 3 showed how a combination of electrochemical and free chlorine conditioning methods was successfully applied to form and maintain PbO₂ scales on lead coupons. These lead coupons, with surface scales rich in PbO₂, were then used to investigate the effects of residence time and residual free chlorine concentrations. The results showed that lead concentrations eventually increased to above 15 µg/L after the depletion of free chlorine, but there was a lag of up to 24 hours between chlorine depletion and the observed rise in lead. With daily adjustment of free chlorine to a threshold level (identified as 0.2 mg/L as Cl₂ in this study) or higher, the stability of the PbO₂ scale on the lead coupons was maintained, and dissolved lead remained consistently below 10 µg/L. The experimental threshold free chlorine concentration was higher than the computational predictions for thermodynamic stability of PbO₂.

Chapter 4 presented the results of pipe-loop studies using harvested pipes from the Erie County Water Authority, which contained preexisting PbO₂ in pipe scales. The study found that when residual free chlorine fell below the detection level (0.1 mg/L as Cl₂) during water stagnation, dissolved lead concentrations increased from 8 ± 2 µg/L to 15 ± 7 µg/L, and total lead concentrations rose from 15 ± 8 µg/L to 27 ± 21 µg/L. A threshold concentration of residual free chlorine required to maintain PbO₂ stability, and this threshold may vary across different water systems in actual lead service lines (LSLs). The study also revealed that while the reductive

dissolution of Pb(IV) in the absence of sufficient free chlorine could generate dissolved lead concentrations that are a concern, the vast majority (more than 99.93%) of the initial PbO₂ solid remained in the scale. These findings suggest that PbO₂-dominated LSLs can maintain low and stable lead concentrations in water when adequate free chlorine is present. However, during periods of water stagnation, the depletion of free chlorine could lead to a potential risk of lead release, with the release of particulate lead posing a greater concern than dissolved lead.

Chapter 5 found that orthophosphate can accelerate lead release for PbO₂-coated lead coupons but not for pipe loops. A lead-phosphate solid, phosphohedyphane (Ca₂Pb₃(PO₄)₃Cl) formed in pipes treated with 1 mg/L as PO₄ of orthophosphate for more than four months but was absent in coupons or in the pipes with shorter orthophosphate treatment time. Our findings suggest that the use of orthophosphate in LSLs with rich PbO₂ layers in scales may not provide a substantial benefit for lead corrosion control during the initial phase of its addition. The differences between the coupon and pipe-loop studies indicate that while pipe-loop experiments might be more representative, coupon studies can reveal detailed potential risks and underlying mechanisms.

Chapter 6 was based on scale analysis of 70 harvested pipes from 16 different systems across the U.S., together with the data from previously published research. The examination of this large composite dataset of scale analysis found that the crystalline phase of lead-carbonate solids depends on pH and dissolved inorganic carbon (DIC) levels of the water. For systems with a lead-carbonate solid present, those with only of hydrocerussite (Pb₃(CO₃)₂(OH)₂) tend to have a

higher pH (8.5 ± 0.8) and lower DIC (1.3 ± 0.6 mM), than those with only cerussite (PbCO_3) (pH: 7.5 ± 0.2 , DIC: 5.5 ± 1.3). Lead(IV) oxide solids are predicted in all systems using free chlorine as a disinfectant but are only seen in some of them. The formation of lead(IV) oxide solids may be adversely affected by blended-phosphate corrosion inhibitors. Formation of lead-phosphate solids depends on the type and concentrations of phosphate inhibitors. Lead-phosphate solids are more commonly found in systems using high-concentration orthophosphate inhibitors compared to those using low-concentration or blended-phosphate inhibitors. Amorphous materials are widely present in lead scales rich in aluminum. Equilibrium predictions for lead carbonate, lead(IV) oxide solids, and lead phosphate correspond to observed cases with accuracies of 95%, 44%, and 71%, respectively. Regardless of their limitations, equilibrium predictions of expected solids remain valuable to predict and screening lead solids in pipe scales.

Additional experiments on the effects of blending water from the Erie County Water Authority (ECWA) and Buffalo Water (50%:50%) were included in Appendix 6. Compared to ECWA water, Buffalo water has a lower pH of 7.7 and uses blended phosphate as a corrosion inhibitor. The results indicated that this water blending had minimal impact on lead release from the test pipes. PbO_2 remained the dominant component of the pipe scale, and no lead-phosphate solids were detectable in the test pipes.

7.2 Recommendations for Future Work

For experiments involving pipe-loops, we used artificial water and employed a continuously recirculating flow. While this approach offers the benefits of efficient water usage and greater feasibility for laboratory studies, it may not accurately reflect real-world conditions. Therefore, it is recommended that future tests be conducted using on-site pipe loops at water utilities, using actual tap water and without recirculation. The advantage of an onsite pipe loop is that the water contains the actual natural organic matter and microorganisms in the local environment.

Additionally, flow patterns should be simulated to better mimic typical household usage, and more frequent scale analyses should be performed to monitor changes in scale composition.

In experiments with lead coupons, we employed lead sheets and applied a combination of electrochemical polarization and chemical conditioning to promote the formation of target scale layers. These studies were conducted in batch experiments using jars. For future research, it is recommended that lead coupons be collected from sections of actual lead service lines, and that flow-through experiments be performed to better simulate the water dynamics found in real pipe systems. Additionally, the methods used to form the target scale layers could be further developed or optimized, particularly with regard to experimental parameters such as the selection of polarization potential, duration, and the use of chemical dosing, in order to achieve more precise control over the scale formation process.

In Chapter 2, the experiments focused on polyphosphate removal were relatively short, which was about two months. However, it typically takes more than six months to assess the long-term impacts of corrosion control inhibitors. Additionally, the role of polyphosphate itself in pipe loops has not been thoroughly explored. As a result, future research could include longer-term studies and also investigate the direct effects of polyphosphate on pipe systems.

In Chapters 3 and 4, a threshold concentration of free chlorine was identified that was below 0.5 mg/L as Cl₂. For future studies and practical implications for water utilities utilizing free chlorine as a disinfectant, it is essential to investigate the effects of different free chlorine concentrations on pipe scale properties, including composition and thickness. Developing an optimized free chlorine dosing strategy for water utilities given water chemistry and pipe conditions is important. It may be a more practical priority to implement a flushing strategy in homes to ensure that the pipes are regularly supplied with water from the distribution system containing adequate free chlorine. The combination of these approaches can help minimize the formation of disinfection byproducts (DBPs) and maintain the stability of PbO₂.

Chapter 5 explored the impact of orthophosphate on lead release and the scale composition of PbO₂-dominated lead materials. The results varied between lead coupons and pipe loops. While some initial discussion and assumptions were made based on the findings and previous research, there was limited evidence to clarify the underlying mechanisms. Future studies should focus on the interactions between orthophosphate and PbO₂, utilizing more advanced analytical

techniques such as Dynamic Light Scattering (DLS) to determine the size of lead particles in water, and X-ray absorption spectroscopy to investigate the oxidation states of the lead released and their interactions with orthophosphate.

Chapter 6 investigated the variations in lead pipe scales from different drinking water systems and also evaluated the applications and limitations of chemical equilibrium models in predicting the solid phases found in lead pipe scales. In future studies, incorporating data from a wider range of water utilities worldwide would provide a more comprehensive analysis. The study revealed that reaction constants from different databases can vary greatly, and some failed to accurately predict real-world conditions. Therefore, future work should focus on refining and optimizing these reaction constants to improve prediction accuracy. Additionally, the equilibrium models should be developed to account for dynamic factors present in actual water systems, such as flow rate, pipe aging, and variations in water chemistry.

References

- Aghasadeghi, K., Peldszus, S., Trueman, B.F., Mishra, A., Cooke, M.G., Slawson, R.M., Giammar, D.E., Gagnon, G.A., Huck, P.M., 2021. Pilot-scale comparison of sodium silicates, orthophosphate and pH adjustment to reduce lead release from lead service lines. *Water Research* 195, 116955. <https://doi.org/10.1016/j.watres.2021.116955>
- Al-Jasser, A.O., 2007. Chlorine decay in drinking-water transmission and distribution systems: Pipe service age effect. *Water Research* 41, 387–396. <https://doi.org/10.1016/j.watres.2006.08.032>
- Arnold, R.B., Edwards, M., 2012. Potential Reversal and the Effects of Flow Pattern on Galvanic Corrosion of Lead. *Environ. Sci. Technol.* 46, 10941–10947. <https://doi.org/10.1021/es3017396>
- Arnold, R.B., Rhoades, J., Criswell, M., Ingels, T., Becker, W., 2021. Colorado's Bench-Scale Lead and Copper Corrosion Testing Protocol. *J Am Water Works Assoc* 113, 30–40. <https://doi.org/10.1002/awwa.1725>
- Arnold, R.B., Rosenfeldt, B., Rhoades, J., Owen, C., Becker, W., 2020. Evolving Utility Practices and Experiences With Corrosion Control. *J Am Water Works Assoc* 112, 26–40. <https://doi.org/10.1002/awwa.1534>
- Avasarala, S., Orta, J., Schaefer, M., Abernathy, M., Ying, S., Liu, H., 2021. Effects of residual disinfectants on the redox speciation of lead(II)/(IV) minerals in drinking water distribution systems. *Environ. Sci.: Water Res. Technol.* 7, 357–366. <https://doi.org/10.1039/D0EW00706D>
- Bae, Y., Pasteris, J.D., Giammar, D.E., 2020a. The Ability of Phosphate To Prevent Lead Release from Pipe Scale When Switching from Free Chlorine to Monochloramine. *Environ. Sci. Technol.* 54, 879–888. <https://doi.org/10.1021/acs.est.9b06019>
- Bae, Y., Pasteris, J.D., Giammar, D.E., 2020b. Impact of orthophosphate on lead release from pipe scale in high pH, low alkalinity water. *Water Research* 177, 115764. <https://doi.org/10.1016/j.watres.2020.115764>

- Bergendahl, J.A., Stevens, L., 2005. Oxidation reduction potential as a measure of disinfection effectiveness for chlorination of wastewater. *Environmental Progress* 24, 214–222. <https://doi.org/10.1002/ep.10074>
- Betanzo, E., Rhyan, C., Hanna-Attisha, M., 2021. Lessons from the first year of compliance sampling under Michigan’s revised Lead and Copper Rule and national Lead and Copper Rule implications. *AWWA Water Science* 3, e1261. <https://doi.org/10.1002/aws2.1261>
- Bradham, K.D., Nelson, C.M., Sowers, T.D., Lytle, D.A., Tully, J., Schock, M.R., Li, K., Blackmon, M.D., Kovalcik, K., Cox, D., Dewalt, G., Friedman, W., Pinzer, E.A., Ashley, P.J., 2022. A national survey of lead and other metal(loids) in residential drinking water in the United States. *J Expo Sci Environ Epidemiol* 1–8. <https://doi.org/10.1038/s41370-022-00461-6>
- Cantor, A.F., Denig-Chakroff, D., Vela, R.R., Oleinik, M.G., Lynch, D.L., 2000. Use of polyphosphate in corrosion control. *Journal AWWA* 92, 95–102. <https://doi.org/10.1002/j.1551-8833.2000.tb08820.x>
- Churchill, D.M., Mavinic, D.S., Neden, D.G., MacQuarrie, D.M., 2000. The effect of zinc orthophosphate and pH-alkalinity adjustment on metal levels leached into drinking water. *Can. J. Civ. Eng.* 27, 33–43. <https://doi.org/10.1139/199-047>
- Clark, B., Masters, S., Edwards, M., 2014b. Profile Sampling To Characterize Particulate Lead Risks in Potable Water. *Environ. Sci. Technol.* 48, 6836–6843. <https://doi.org/10.1021/es501342j>
- Colling, J.H., Croll, B.T., Whincup, P.A.E., Harward, C., 1992. Plumbosolvency Effects and Control in Hard Waters. *Water and Environment Journal* 6, 259–268. <https://doi.org/10.1111/j.1747-6593.1992.tb00750.x>
- Copeland, A., Lytle, D.A., 2014. Measuring the oxidation–reduction potential of important oxidants in drinking water. *Journal AWWA* 106. <https://doi.org/10.5942/jawwa.2014.106.0002>

- Cornwell, D.A., Brown, R.A., Via, S.H., 2016. National Survey of Lead Service Line Occurrence. *JAWWA* 108, E182–E191. <https://doi.org/10.5942/jawwa.2016.108.0086>
- Dave, D.M., Yang, M., 2022. Lead in drinking water and birth outcomes: A tale of two water treatment plants. *Journal of Health Economics* 84, 102644. <https://doi.org/10.1016/j.jhealeco.2022.102644>
- Davidson, C.M., Peters, N.J., Britton, A., Brady, L., Gardiner, P.H.E., Lewis, B.D., 2004. Surface analysis and depth profiling of corrosion products formed in lead pipes used to supply low alkalinity drinking water. *Water Science and Technology* 49, 49–54. <https://doi.org/10.2166/wst.2004.0086>
- De Jager, H.-J., Heyns, A.M., 1998. Kinetics of Acid-Catalyzed Hydrolysis of a Polyphosphate in Water. *J. Phys. Chem. A* 102, 2838–2841. <https://doi.org/10.1021/jp9730252>
- Delile, H., Blichert-Toft, J., Goiran, J.-P., Keay, S., Albarède, F., 2014. Lead in ancient Rome's city waters. *Proc. Natl. Acad. Sci. U.S.A.* 111, 6594–6599. <https://doi.org/10.1073/pnas.1400097111>
- DeSantis, M.K., Schock, M.R., Tully, J., Bennett-Stamper, C., 2020. Orthophosphate Interactions with Destabilized PbO₂ Scales. *Environ. Sci. Technol.* 54, 14302–14311. <https://doi.org/10.1021/acs.est.0c03027>
- Dodrill, D.M., Edwards, M., 1995. Corrosion control on the basis of utility experience. *Journal - American Water Works Association* 87, 74–85. <https://doi.org/10.1002/j.1551-8833.1995.tb06395.x>
- Doré, E., Deshommes, E., Laroche, L., Nour, S., Prévost, M., 2019a. Study of the long-term impacts of treatments on lead release from full and partially replaced harvested lead service lines. *Water Research* 149, 566–577. <https://doi.org/10.1016/j.watres.2018.11.037>
- Doré, E., Deshommes, E., Laroche, L., Nour, S., Prévost, M., 2019b. Lead and copper release from full and partially replaced harvested lead service lines: Impact of stagnation time

- prior to sampling and water quality. *Water Research* 150, 380–391.
<https://doi.org/10.1016/j.watres.2018.11.076>
- Dryer, D.J., Korshin, G.V., 2007. Investigation of the Reduction of Lead Dioxide by Natural Organic Matter. *Environ. Sci. Technol.* 41, 5510–5514.
<https://doi.org/10.1021/es070596r>
- Duranceau, S.J., Lintereur, P.A., Taylor, J.S., 2010. Effects of orthophosphate corrosion inhibitor on lead in blended water quality environments. *Desalination and Water Treatment* 13, 348–355. <https://doi.org/10.5004/dwt.2010.1231>
- Edwards, M., Dudi, A., 2004. role of chlorine and chloramine in corrosion of lead-bearing plumbing materials. *Journal - American Water Works Association* 96, 69–81.
<https://doi.org/10.1002/j.1551-8833.2004.tb10724.x>
- Edwards, M., Hidmi, L., Gladwell, D., 2002. Phosphate inhibition of soluble copper corrosion by-product release. *Corrosion Science* 44, 1057–1071. [https://doi.org/10.1016/S0010-938X\(01\)00112-3](https://doi.org/10.1016/S0010-938X(01)00112-3)
- Edwards, M., Jacobs, S., Dodrill, D., 1999. Desktop guidance for mitigating Pb and Cu corrosion by-products. *Journal - American Water Works Association* 91, 66–77.
<https://doi.org/10.1002/j.1551-8833.1999.tb08635.x>
- Edwards, M., McNeill, L.S., 2002. Effect of PHOSPHATE inhibitors on lead release from pipes. *Journal - American Water Works Association* 94, 79–90. <https://doi.org/10.1002/j.1551-8833.2002.tb09383.x>
- Edwards, M., Triantafyllidou, S., Best, D., 2009. Elevated Blood Lead in Young Children Due to Lead-Contaminated Drinking Water: Washington, DC, 2001–2004. *Environ. Sci. Technol.* 43, 1618–1623. <https://doi.org/10.1021/es802789w>
- Faherty, A., 2021. Tapped Out: How Newark, New Jersey’s Lead Drinking Water Crisis Illuminates the Inadequacy of the Federal Drinking Water Regulatory Scheme and Fuels

- Environmental Injustice throughout the Nation. *Environmental Claims Journal* 33, 304–327. <https://doi.org/10.1080/10406026.2020.1848078>
- Formal, C.L., Lytle, D.A., Harmon, S., Wahman, D.G., DeSantis, M.K., Tang, M., 2024. Impact of orthophosphate on the solubility and properties of lead orthophosphate nanoparticles. *Environ. Sci.: Water Res. Technol.* 10, 1623–1636. <https://doi.org/10.1039/D4EW00152D>
- Gerke, T.L., Little, B.J., Barry Maynard, J., 2016. Manganese deposition in drinking water distribution systems. *Science of The Total Environment* 541, 184–193. <https://doi.org/10.1016/j.scitotenv.2015.09.054>
- Gould, E., 2009. Childhood Lead Poisoning: Conservative Estimates of the Social and Economic Benefits of Lead Hazard Control. *Environ Health Perspect* 117, 1162–1167. <https://doi.org/10.1289/ehp.0800408>
- Guo, D., Robinson, C., Herrera, J.E., 2014. Role of Pb(II) Defects in the Mechanism of Dissolution of Plattnerite (β -PbO₂) in Water under Depleting Chlorine Conditions. *Environ. Sci. Technol.* 48, 12525–12532. <https://doi.org/10.1021/es502133k>
- Harmon, S.M., Tully, J., DeSantis, M.K., Schock, M.R., Triantafyllidou, S., Lytle, D.A., 2022. A holistic approach to lead pipe scale analysis: Importance, methodology, and limitations. *AWWA Water Science* 4. <https://doi.org/10.1002/aws2.1278>
- Holm, T.R., Edwards, M., 2003. Metaphosphate reversion in Laboratory and Pipe-Rig Experiments. *Journal - American Water Works Association* 95, 172–178. <https://doi.org/10.1002/j.1551-8833.2003.tb10343.x>
- Holm, T.R., Schock, M.R., 1991. Polyphosphate Debate. *Journal - American Water Works Association* 83, 10–12. <https://doi.org/10.1002/j.1551-8833.1991.tb07254.x>

Holm, T.R., Shock, M.R., 1991. Potential Effects of Polyphosphate Products on Lead Solubility in Plumbing Systems. *Journal - American Water Works Association* 83, 76–82. <https://doi.org/10.1002/j.1551-8833.1991.tb07182.x>

Holm, T.R., Smothers, S.H., 1990. Characterizing the Lead-Complexing Properties of Polyphosphate Water Treatment Products by Competing-Ligand Spectrophotometry Using 4-(2-Pyridylazo)Resorcinol. *International Journal of Environmental Analytical Chemistry* 41, 71–82. <https://doi.org/10.1080/03067319008030531>

Hopwood, J.D., Casey, H., Cussons, M., Knott, P., Humphreys, P.N., Andrews, H., Banks, J., Coleman, S., Haley, J., 2023. Spherulitic Lead Calcium Apatite Minerals in Lead Water Pipes Exposed to Phosphate-Dosed Tap Water. *Environ. Sci. Technol.* 57, 4796–4805. <https://doi.org/10.1021/acs.est.2c04538>

Hopwood, J.D., Derrick, G.R., Brown, D.R., Newman, C.D., Haley, J., Kershaw, R., Collinge, M., 2016. The Identification and Synthesis of Lead Apatite Minerals Formed in Lead Water Pipes. *Journal of Chemistry* 2016, 1–11. <https://doi.org/10.1155/2016/9074062>

Jarvis, P., Fawell, J., 2021. Lead in drinking water – An ongoing public health concern? *Current Opinion in Environmental Science & Health* 20, 100239. <https://doi.org/10.1016/j.coesh.2021.100239>

Johnson, E.R., Pan, W., Giammar, D.E., 2022. Capture and Extraction of Particulate Lead from Point-of-Use Filters. *ACS ES&T Engineering*. <https://doi.org/10.1021/acsestengg.2c00150>

Kastl, G.J., Fisher, I.H., Jegatheesan, V., 1999. Evaluation of chlorine decay kinetics expressions for drinking water distribution systems modelling. *Journal of Water Supply: Research and Technology—AQUA* 48, 219–226. <https://doi.org/10.2166/aqua.1999.0024>

Ketrane, R., Saidani, B., Gil, O., Leleyter, L., Baraud, F., 2009. Efficiency of five scale inhibitors on calcium carbonate precipitation from hard water: Effect of temperature and concentration. *Desalination* 249, 1397–1404. <https://doi.org/10.1016/j.desal.2009.06.013>

Kim, E.J., Herrera, J.E., 2010. Characteristics of Lead Corrosion Scales Formed during Drinking Water Distribution and Their Potential Influence on the Release of Lead and Other Contaminants. *Environ. Sci. Technol.* 44, 6054–6061. <https://doi.org/10.1021/es101328u>

Kim, H., Kwon, S., Han, S., Yu, M., Kim, J., Gong, S., Colosimo, M.F., 2006. New ORP/pH based control strategy for chlorination and dechlorination of wastewater: pilot scale application. *Water Science and Technology* 53, 145–151. <https://doi.org/10.2166/wst.2006.188>

King, P., 2020. Investigating the Role of Water Quality on the Galvanic Corrosion of Lead in Hard Drinking Water with a Focus on NOM (Master of Applied Science in Civil Engineering (Water)). University of Waterloo.

Knowles, A.D., Nguyen, C.K., Edwards, M.A., Stoddart, A., McIlwain, B., Gagnon, G.A., 2015. Role of iron and aluminum coagulant metal residuals and lead release from drinking water pipe materials. *Journal of Environmental Science and Health, Part A* 50, 414–423. <https://doi.org/10.1080/10934529.2015.987550>

Kogo, A., Payne, S.J., Andrews, R.C., 2017. Comparison of three corrosion inhibitors in simulated partial lead service line replacements. *Journal of Hazardous Materials* 329, 211–221. <https://doi.org/10.1016/j.jhazmat.2017.01.039>

Korshin, G., Liu, H., 2019. Preventing the colloidal dispersion of Pb(IV) corrosion scales and lead release in drinking water distribution systems. *Environ. Sci.: Water Res. Technol.* 5, 1262–1269. <https://doi.org/10.1039/C9EW00231F>

Kuh, S., Woo, D., Lee, D., Kim, J., Ahn, H., Moon, K., 2006. Internal Corrosion Control of Drinking Water Pipes by pH and Alkalinity Control and Corrosion Inhibitor. *Journal of Korean Society of Water and Wastewater* 20, 215–223.

Kurajica, L., Bošnjak, M.U., Kinsela, A.S., Štiglić, J., Waite, T.D., 2022. Heavy metal, organic matter, and disinfection byproduct release from drinking water pipe scales under stagnant conditions. *Environ. Sci.: Water Res. Technol.* 9, 235–248. <https://doi.org/10.1039/D2EW00537A>

- Kvech, S., Edwards, M., 2001. Role of Aluminosilicate deposits in Lead and Copper Corrosion. *Journal - American Water Works Association* 93, 104–112.
<https://doi.org/10.1002/j.1551-8833.2001.tb09339.x>
- Latham, S., Jennings, J.L., 2022. Reducing lead exposure in school water: Evidence from remediation efforts in New York City public schools. *Environmental Research* 203, 111735. <https://doi.org/10.1016/j.envres.2021.111735>
- Learbuch, K.L.G., Smidt, H., Van Der Wielen, P.W.J.J., 2021. Influence of pipe materials on the microbial community in unchlorinated drinking water and biofilm. *Water Research* 194, 116922. <https://doi.org/10.1016/j.watres.2021.116922>
- Levallois, P., Barn, P., Valcke, M., Gauvin, D., Kosatsky, T., 2018. Public Health Consequences of Lead in Drinking Water. *Curr Envir Health Rpt* 5, 255–262.
<https://doi.org/10.1007/s40572-018-0193-0>
- Li, G., Bae, Y., Mishra, A., Shi, B., Giammar, D.E., 2020. Effect of Aluminum on Lead Release to Drinking Water from Scales of Corrosion Products. *Environ. Sci. Technol.* 54, 6142–6151. <https://doi.org/10.1021/acs.est.0c00738>
- Li, G., Ding, Y., Xu, H., Jin, J., Shi, B., 2018. Characterization and release profile of (Mn, Al)-bearing deposits in drinking water distribution systems. *Chemosphere* 197, 73–80.
<https://doi.org/10.1016/j.chemosphere.2018.01.027>
- Li, M., Liu, Z., Chen, Y., Hai, Y., 2016. Characteristics of iron corrosion scales and water quality variations in drinking water distribution systems of different pipe materials. *Water Research* 106, 593–603. <https://doi.org/10.1016/j.watres.2016.10.044>
- Li, X., Liu, L., Wu, Y., Liu, T., 2019. Determination of the Redox Potentials of Solution and Solid Surface of Fe(II) Associated with Iron Oxyhydroxides. *ACS Earth Space Chem.* 3, 711–717. <https://doi.org/10.1021/acsearthspacechem.9b00001>

- Lin, Y.-P., Valentine, R.L., 2010. Reductive Dissolution of Lead Dioxide (PbO₂) in Acidic Bromide Solution. *Environ. Sci. Technol.* 44, 3895–3900.
<https://doi.org/10.1021/es100133n>
- Lin, Y.-P., Valentine, R.L., 2009. Reduction of Lead Oxide (PbO₂) and Release of Pb(II) in Mixtures of Natural Organic Matter, Free Chlorine and Monochloramine. *Environ. Sci. Technol.* 43, 3872–3877. <https://doi.org/10.1021/es900375a>
- Lin, Y.-P., Valentine, R.L., 2008a. The Release of Lead from the Reduction of Lead Oxide (PbO₂) by Natural Organic Matter. *Environ. Sci. Technol.* 42, 760–765.
<https://doi.org/10.1021/es071984w>
- Lin, Y.-P., Valentine, R.L., 2008b. Release of Pb(II) from Monochloramine-Mediated Reduction of Lead Oxide (PbO₂). *Environ. Sci. Technol.* 42, 9137–9143.
<https://doi.org/10.1021/es801037n>
- Lin, Y.-P., Washburn, M.P., Valentine, R.L., 2008. Reduction of Lead Oxide (PbO₂) by Iodide and Formation of Iodoform in the PbO₂/I⁻/NOM System. *Environ. Sci. Technol.* 42, 2919–2924. <https://doi.org/10.1021/es702797b>
- Liu, H., Korshin, G.V., Ferguson, J.F., 2009. Interactions of Pb(II)/Pb(IV) Solid Phases with Chlorine and Their Effects on Lead Release. *Environ. Sci. Technol.* 43, 3278–3284.
<https://doi.org/10.1021/es803179b>
- Liu, J., Chen, H., Huang, Q., Lou, L., Hu, B., Endalkachew, S.-D., Mallikarjuna, N., Shan, Y., Zhou, X., 2016. Characteristics of pipe-scale in the pipes of an urban drinking water distribution system in eastern China. *Water Supply* 16, 715–726.
<https://doi.org/10.2166/ws.2015.183>
- Lobo, G.P., Gadgil, A.J., 2021. Preventing leaching from lead water pipes with electrochemistry: an exploratory study. *Environ. Sci.: Water Res. Technol.* 7, 1267–1278.
<https://doi.org/10.1039/D1EW00160D>

- Lobo, G.P., Kalyan, B., Gadgil, A.J., 2022. Electrochemical deposition of amorphous aluminum oxides on lead pipes to prevent lead leaching into the drinking water. *Journal of Hazardous Materials* 423, 127195. <https://doi.org/10.1016/j.jhazmat.2021.127195>
- Locsin, J., Trueman, B.F., Doré, E., Bleasdale-Pollowy, A., Gagnon, G.A., 2022. Impacts of orthophosphate-polyphosphate blends on the dissolution and transformation of lead (II) carbonate. <https://doi.org/10.26434/chemrxiv-2022-2g0j3-v2>
- Lytle, C.J., Edwards, M.A., 2024. Simultaneous Use of Polyphosphate for Sequestration and Antiscaling. *ACS EST Water* 4, 227–236. <https://doi.org/10.1021/acsestwater.3c00553>
- Lytle, C.J., Edwards, M.A., 2023. Phosphate Chemical Use for Sequestration, Scale Inhibition, and Corrosion Control. *ACS EST Water* 3, 893–907. <https://doi.org/10.1021/acsestwater.2c00570>
- Lytle, D.A., Formal, C., Cahalan, K., Muhlen, C., Triantafyllidou, S., 2021. The impact of sampling approach and daily water usage on lead levels measured at the tap. *Water Research* 197, 117071. <https://doi.org/10.1016/j.watres.2021.117071>
- Lytle, D.A., Formal, C., Doré, E., Muhlen, C., Harmon, S., Williams, D., Triantafyllidou, S., Pham, M., 2020a. Synthesis and characterization of stable lead(II) orthophosphate nanoparticle suspensions. *Journal of Environmental Science and Health, Part A* 55, 1504–1512. <https://doi.org/10.1080/10934529.2020.1810498>
- Lytle, D.A., Schock, M.R., 2005. Formation of Pb(IV) oxides in chlorinated water. *Journal - American Water Works Association* 97, 102–114. <https://doi.org/10.1002/j.1551-8833.2005.tb07523.x>
- Lytle, D.A., Schock, M.R., Formal, C., Bennett-Stamper, C., Harmon, S., Nadagouda, M.N., Williams, D., DeSantis, M.K., Tully, J., Pham, M., 2020b. Lead Particle Size Fractionation and Identification in Newark, New Jersey's Drinking Water. *Environ. Sci. Technol.* 54, 13672–13679. <https://doi.org/10.1021/acs.est.0c03797>

- Lytle, D.A., Schock, M.R., Sheckel, K., 2009a. The Inhibition of Pb(IV) Oxide Formation in Chlorinated Water by Orthophosphate. *Environ. Sci. Technol.* 43, 6624–6631. <https://doi.org/10.1021/es900399m>
- Lytle, D.A., White, C., Nadagouda, M.N., Worrall, A., 2009b. Crystal and morphological phase transformation of Pb(II) to Pb(IV) in chlorinated water. *Journal of Hazardous Materials* 165, 1234–1238. <https://doi.org/10.1016/j.jhazmat.2008.10.058>
- Ma, Y., Mishra, A., Giammar, D.E., Arnold, R.B., 2023. Improved Control of Lead Release from Boosting Orthophosphate and Removing Polyphosphate from a Blended Phosphate Corrosion Inhibitor. *ACS EST Eng.* 3, 1826–1836. <https://doi.org/10.1021/acsestengg.3c00243>
- Masters, S., Welter, G.J., Edwards, M., 2016. Seasonal Variations in Lead Release to Potable Water. *Environ. Sci. Technol.* 50, 5269–5277. <https://doi.org/10.1021/acs.est.5b05060>
- Masters, S.V., Bradley, T.C., Burlingame, G.A., Seidel, C.J., Schmelling, M., Bartrand, T.A., 2021. What Can Utilities Expect from New Lead Fifth-Liter Sampling Based on Historic First-Draw Data? *Environ. Sci. Technol.* 55, 11491–11500. <https://doi.org/10.1021/acs.est.1c00421>
- Masters, S.V., Poncelet-Johnson, N., Walsh, R., Seidel, C.J., Corwin, C.J., 2022. Comparison of coupon and pipe rack studies for selecting corrosion control treatment. *AWWA Water Science* 4. <https://doi.org/10.1002/aws2.1293>
- McNeill, L.S., Edwards, M., 2002. Phosphate inhibitor use at US utilities. *Journal - American Water Works Association* 94, 57–63. <https://doi.org/10.1002/j.1551-8833.2002.tb09506.x>
- Method 200.8, EPA, 1996. DETERMINATION OF TRACE ELEMENTS IN WATERS AND WASTES BY INDUCTIVELY COUPLED PLASMA - MASS SPECTROMETRY, in: *Methods for the Determination of Metals in Environmental Samples.*

- Miller, S.A., 2014. Investigation of Lead Solubility and Orthophosphate Addition in High pH Low DIC Water (M.S.). University of Cincinnati, United States -- Ohio.
- Mishra, A., Johnson, E., Giammar, D.E., 2021a. Estimating Lead Concentrations in Drinking Water after Stagnation in Lead Service Lines Using Water Quality Data from across the United States. *Environ. Sci. Technol. Lett.* 8, 878–883.
<https://doi.org/10.1021/acs.estlett.1c00580>
- Mishra, A., Wang, Z., Sidorkiewicz, V., Giammar, D.E., 2021b. Effect of sodium silicate on lead release from lead service lines. *Water Research* 188, 116485.
<https://doi.org/10.1016/j.watres.2020.116485>
- Nadagouda, M.N., White, C., Lytle, D., 2011. Lead Pipe Scale Analysis Using Broad-Beam Argon Ion Milling to Elucidate Drinking Water Corrosion. *Microsc Microanal* 17, 284–291. <https://doi.org/10.1017/S1431927610094353>
- Nancollas, G. H., 1983. Phosphate precipitation in corrosion protection: Reaction mechanisms. *Corrosion*, 39(3), 77-82. <https://doi.org/10.5006/1.3580822>
- Ng, D.-Q., Lin, Y.-P., 2016. Evaluation of Lead Release in a Simulated Lead-Free Premise Plumbing System Using a Sequential Sampling Approach. *IJERPH* 13, 266.
<https://doi.org/10.3390/ijerph13030266>
- Ng, D.-Q., Strathmann, T.J., Lin, Y.-P., 2012. Role of Orthophosphate As a Corrosion Inhibitor in Chloraminated Solutions Containing Tetravalent Lead Corrosion Product PbO₂. *Environ. Sci. Technol.* 46, 11062–11069. <https://doi.org/10.1021/es302220t>
- Nguyen, C.K., Powers, K.A., Raetz, M.A., Parks, J.L., Edwards, M.A., 2011. Rapid free chlorine decay in the presence of Cu(OH)₂: Chemistry and practical implications. *Water Research* 45, 5302–5312. <https://doi.org/10.1016/j.watres.2011.07.039>
- Noel, J.D., Wang, Y., Giammar, D.E., 2014. Effect of water chemistry on the dissolution rate of the lead corrosion product hydrocerussite. *Water Research* 54, 237–246.
<https://doi.org/10.1016/j.watres.2014.02.004>

- Obasi, P.N., Akudinobi, B.B., 2020. Potential health risk and levels of heavy metals in water resources of lead–zinc mining communities of Abakaliki, southeast Nigeria. *Appl Water Sci* 10, 184. <https://doi.org/10.1007/s13201-020-01233-z>
- Olds, T.A., Kampf, A.R., Rakovan, J.F., Burns, P.C., Mills, O.P., Laughlin-Yurs, C., 2021. Hydroxylpyromorphite, a mineral important to lead remediation: Modern description and characterization. *American Mineralogist* 106, 922–929. <https://doi.org/10.2138/am-2021-7516>
- Pan, W., Catalano, J.G., Giammar, D.E., 2022. Redox-Driven Recrystallization of PbO₂. *Environ. Sci. Technol.* 56, 7864–7872. <https://doi.org/10.1021/acs.est.1c08767>
- Pan, W., Ledingham, G.J., Catalano, J.G., Giammar, D.E., 2021. Effects of Cu(II) and Zn(II) on PbO₂ Reductive Dissolution under Drinking Water Conditions: Short-term Inhibition and Long-term Enhancement. *Environ. Sci. Technol.* 55, 14397–14406. <https://doi.org/10.1021/acs.est.1c04887>
- Pan, W., Schattner, L., Guilak, J., Giammar, D., 2019. Impact of Cu(II) and Zn(II) on the Reductive Dissolution of Pb(IV) Oxide. *Environ. Sci. Technol. Lett.* 6, 745–751. <https://doi.org/10.1021/acs.estlett.9b00612>
- Pasteris, J.D., Bae, Y., Giammar, D.E., Dybing, S.N., Yoder, C.H., Zhao, J., Hu, Y., 2021. Worth a Closer Look: Raman Spectra of Lead-Pipe Scale. *Minerals* 11, 1047. <https://doi.org/10.3390/min11101047>
- Peng, Y.-C., Lu, Y.-F., Lin, Y.-P., 2022. Release of Particulate Lead from Four Lead Corrosion Products in Drinking Water: A Laboratory Study Coupled with Microscopic Observations and Computational Fluid Dynamics. *Environ. Sci. Technol.* 56, 12218–12227. <https://doi.org/10.1021/acs.est.2c02461>
- Pieper, K.J., Martin, R., Tang, M., Walters, L., Parks, J., Roy, S., Devine, C., Edwards, M.A., 2018. Evaluating Water Lead Levels During the Flint Water Crisis. *Environ. Sci. Technol.* 52, 8124–8132. <https://doi.org/10.1021/acs.est.8b00791>

- Pontius, F.W., 1991. The New Lead and Copper Rule. *Journal AWWA* 83, 12–109.
<https://doi.org/10.1002/j.1551-8833.1991.tb07172.x>
- Pourbaix, M., 1996. Atlas of electrochemical equilibria in aqueous solutions. NACE.
- Rashchi, F., Finch, J.A., 2002. Lead-Polyphosphate Complexes. *Water Research* 41, 1–6.
<https://doi.org/10.1179/cmq.2002.41.1.1>
- Refaey, S.A.M., 1996. The corrosion and passivation of tin in borate solutions and the effect of halide ions. *Electrochimica Acta* 41, 2545–2549. [https://doi.org/10.1016/0013-4686\(96\)00068-0](https://doi.org/10.1016/0013-4686(96)00068-0)
- Rome, M., Estes-Smargiassi, S., Masters, S.V., Roberson, A., Tobiason, J.E., Beighley, R.E., Pieper, K.J., 2022. Using the Lead and Copper Rule Revisions Five-Sample Approach to Identify Schools with Increased Lead in Drinking Water Risks. *Environ. Sci. Technol. Lett.* 9, 84–89. <https://doi.org/10.1021/acs.estlett.1c00845>
- Rossman, L.A., Clark, R.M., Grayman, W.M., 1994. Modeling Chlorine Residuals in Drinking-Water Distribution Systems. *J. Environ. Eng.* 120, 803–820.
[https://doi.org/10.1061/\(ASCE\)0733-9372\(1994\)120:4\(803\)](https://doi.org/10.1061/(ASCE)0733-9372(1994)120:4(803))
- Roth, D.K., Cornwell, D.A., 2018. DBP Impacts From Increased Chlorine Residual Requirements: DBP Impacts From Increased Chlorine Residual Requirements. *Journal - American Water Works Association* 110, 13–28.
<https://doi.org/10.5942/jawwa.2018.110.0004>
- Roy, S., Edwards, M.A., 2019. Preventing another lead (Pb) in drinking water crisis: Lessons from the Washington D.C. and Flint MI contamination events. *Current Opinion in Environmental Science & Health* 7, 34–44. <https://doi.org/10.1016/j.coesh.2018.10.002>
- Roy, S., Tang, M., Edwards, M.A., 2019. Lead release to potable water during the Flint, Michigan water crisis as revealed by routine biosolids monitoring data. *Water Research* 160, 475–483. <https://doi.org/10.1016/j.watres.2019.05.091>

- Schock, M.R., 1989. Understanding Corrosion Control Strategies for Lead. *Journal AWWA* 81, 88–100. <https://doi.org/10.1002/j.1551-8833.1989.tb03244.x>
- Shekhar, A., 2007. Reversion Of Poly-phosphates To Ortho-phosphates In Water Distribution Systems (Electronic Theses and Dissertations, 2004-2019. 3346.). University of Central Florida.
- Shock, M.R., Clement, J., 1998. Lead and copper control with non-zinc orthophosphate. *Journal of the New England Water Works Association*.
- Shrivatsa, S., Lobo, G., Gadgil, A., 2023. Data-Sparse Prediction of High-Risk Schools for Lead Contamination in Drinking Water: Examples from Four U.S. States. *IJERPH* 20, 6895. <https://doi.org/10.3390/ijerph20196895>
- Silvester, E., Charlet, L., Tournassat, C., Géhin, A., Grenèche, J.-M., Liger, E., 2005. Redox potential measurements and Mössbauer spectrometry of FeII adsorbed onto FeIII (oxyhydr)oxides. *Geochimica et Cosmochimica Acta* 69, 4801–4815. <https://doi.org/10.1016/j.gca.2005.06.013>
- Snoeyink, V.L., Schock, M.R., Sarin, P., Wang, L., Chen, A.S.-C., Harmon, S.M., 2003. Aluminium-containing scales in water distribution systems: Prevalence and composition. *Journal of Water Supply: Research and Technology-Aqua* 52, 455–474. <https://doi.org/10.2166/aqua.2003.0042>
- Swaringen, B.F., Gawlik, E., Kamenov, G.D., McTigue, N.E., Cornwell, D.A., Bonzongo, J.-C.J., 2022. Children’s exposure to environmental lead: A review of potential sources, blood levels, and methods used to reduce exposure. *Environmental Research* 204, 112025. <https://doi.org/10.1016/j.envres.2021.112025>
- Switzer, J.A., Rajasekharan, V.V., Boonsalee, S., Kulp, E.A., Bohannon, E.W., 2006. Evidence that Monochloramine Disinfectant Could Lead to Elevated Pb Levels in Drinking Water. *Environ. Sci. Technol.* 40, 3384–3387. <https://doi.org/10.1021/es052411r>

- Tam, Y.S., Elefsiniotis, P., 2009. Corrosion control in water supply systems: Effect of pH, alkalinity, and orthophosphate on lead and copper leaching from brass plumbing. *Journal of Environmental Science and Health, Part A* 44, 1251–1260.
<https://doi.org/10.1080/10934520903140009>
- The Cadmus Group, 2007. Review of the Interim Optimal Corrosion Control Treatment for Washington, D.C.
- Triantafyllidou, S., Edwards, M., 2012. Lead (Pb) in Tap Water and in Blood: Implications for Lead Exposure in the United States. *Critical Reviews in Environmental Science and Technology* 42, 1297–1352. <https://doi.org/10.1080/10643389.2011.556556>
- Triantafyllidou, S., Edwards, M., 2011. Galvanic corrosion after simulated small-scale partial lead service line replacements. *Journal - American Water Works Association* 103, 85–99.
<https://doi.org/10.1002/j.1551-8833.2011.tb11535.x>
- Triantafyllidou, S., Schock, M.R., DeSantis, M.K., White, C., 2015. Low Contribution of PbO₂-Coated Lead Service Lines to Water Lead Contamination at the Tap. *Environ. Sci. Technol.* 49, 3746–3754. <https://doi.org/10.1021/es505886h>
- Trueman, B.F., Bleasdale-Pollowy, A., Locsin, J.A., Bennett, J.L., Krkošek, W.H., Gagnon, G.A., 2022. Seasonal Lead Release into Drinking Water and the Effect of Aluminum. *ACS EST Water* 2, 710–720. <https://doi.org/10.1021/acsestwater.1c00320>
- Trueman, B.F., Krkošek, W.H., Gagnon, G.A., 2018. Effects of ortho- and polyphosphates on lead speciation in drinking water. *Environ. Sci.: Water Res. Technol.* 4, 505–512.
<https://doi.org/10.1039/C7EW00521K>
- Tully, J., DeSantis, M.K., Schock, M.R., 2019. Water quality–pipe deposit relationships in Midwestern lead pipes. *AWWA Water Science* 1, e1127.
<https://doi.org/10.1002/aws2.1127>

USEPA, 2021. National Primary Drinking Water Regulation: Lead and Copper Rule Revisions (LCRR).

USEPA, 1991. Lead and Copper Rule.

Vasconcelos, J.J., Rossman, L.A., Grayman, W.M., Boulos, P.F., Clark, R.M., 1997. Kinetics of chlorine decay. *Journal AWWA* 89, 54–65. <https://doi.org/10.1002/j.1551-8833.1997.tb08259.x>

Via, S., 2024. Proposed Improvements to the LCR. *Journal AWWA* 116, 5–5. <https://doi.org/10.1002/awwa.2210>

W, R.E., Baird, R.B., Eaton, A.D., Clesceri, L.S., 2012. Standard methods for the examination of water and wastewater. USA: American Public Health Association; ISBN 978-087553-013-0.

Wang, D., Bolton, J.R., Andrews, S.A., Hofmann, R., 2015. Formation of disinfection by-products in the ultraviolet/chlorine advanced oxidation process. *Science of The Total Environment* 518–519, 49–57. <https://doi.org/10.1016/j.scitotenv.2015.02.094>

Wang, Y., Wu, J., Giammar, D.E., 2012. Kinetics of the Reductive Dissolution of Lead(IV) Oxide by Iodide. *Environ. Sci. Technol.* 46, 5859–5866. <https://doi.org/10.1021/es2038905>

Wang, Y., Wu, J., Wang, Z., Terenyi, A., Giammar, D.E., 2013. Kinetics of lead(IV) oxide (PbO₂) reductive dissolution: Role of lead(II) adsorption and surface speciation. *Journal of Colloid and Interface Science* 389, 236–243. <https://doi.org/10.1016/j.jcis.2012.09.022>

Wang, Y., Xie, Y., Li, W., Wang, Z., Giammar, D.E., 2010. Formation of Lead(IV) Oxides from Lead(II) Compounds. *Environ. Sci. Technol.* 44, 8950–8956. <https://doi.org/10.1021/es102318z>

- Wasserstrom, L.W., Miller, S.A., Triantafyllidou, S., Desantis, M.K., Schock, M.R., 2017. Scale Formation Under Blended Phosphate Treatment for a Utility With Lead Pipes. *Jawwa* 109, E464–E478. <https://doi.org/10.5942/jawwa.2017.109.0121>
- Wessling, B., 1994. Passivation of metals by coating with polyaniline: Corrosion potential shift and morphological changes. *Adv. Mater.* 6, 226–228. <https://doi.org/10.1002/adma.19940060309>
- Xie, L., Giammar, D.E., 2007. Equilibrium Solubility and Dissolution Rate of the Lead Phosphate Chloropyromorphite. *Environ. Sci. Technol.* 41, 8050–8055. <https://doi.org/10.1021/es071517e>
- Xie, Y., Giammar, D.E., 2011. Effects of flow and water chemistry on lead release rates from pipe scales. *Water Research* 45, 6525–6534. <https://doi.org/10.1016/j.watres.2011.09.050>
- Xie, Y., Wang, Y., Giammar, D.E., 2010a. Impact of Chlorine Disinfectants on Dissolution of the Lead Corrosion Product PbO_2 . *Environ. Sci. Technol.* 44, 7082–7088. <https://doi.org/10.1021/es1016763>
- Xie, Y., Wang, Y., Singhal, V., Giammar, D.E., 2010b. Effects of pH and Carbonate Concentration on Dissolution Rates of the Lead Corrosion Product PbO_2 . *Environ. Sci. Technol.* 44, 1093–1099. <https://doi.org/10.1021/es9026198>
- Yan, X., Lin, T., Wang, X., Zhang, S., Zhou, K., 2022. Effects of pipe materials on the characteristic recognition, disinfection byproduct formation, and toxicity risk of pipe wall biofilms during chlorination in water supply pipelines. *Water Research* 210, 117980. <https://doi.org/10.1016/j.watres.2021.117980>
- Zhang, H., Andrews, S.A., 2012. Effects of phosphate-based corrosion inhibitors on the kinetics of chlorine degradation and haloacetic acid formation in contact with three metal materials. *Can. J. Civ. Eng.* 39, 44–54. <https://doi.org/10.1139/111-108>

Zhang, Y., Lin, Y.-P., 2011. Determination of PbO₂ Formation Kinetics from the Chlorination of Pb(II) Carbonate Solids via Direct PbO₂ Measurement. *Environ. Sci. Technol.* 45, 2338–2344. <https://doi.org/10.1021/es1039826>

Zhang, Y., Shi, B., Zhao, Y., Yan, M., Lytle, D.A., Wang, D., 2016. Deposition behavior of residual aluminum in drinking water distribution system: Effect of aluminum speciation. *Journal of Environmental Sciences* 42, 142–151. <https://doi.org/10.1016/j.jes.2015.05.010>

Zhao, J., Giammar, D.E., Pasteris, J.D., Dai, C., Bae, Y., Hu, Y., 2018. Formation and Aggregation of Lead Phosphate Particles: Implications for Lead Immobilization in Water Supply Systems. *Environ. Sci. Technol.* 52, 12612–12623. <https://doi.org/10.1021/acs.est.8b02788>

Appendix A1: Supporting Information for Chapter 2

A1.1 Lead Pipes Used in the Pipe Loop Experiments

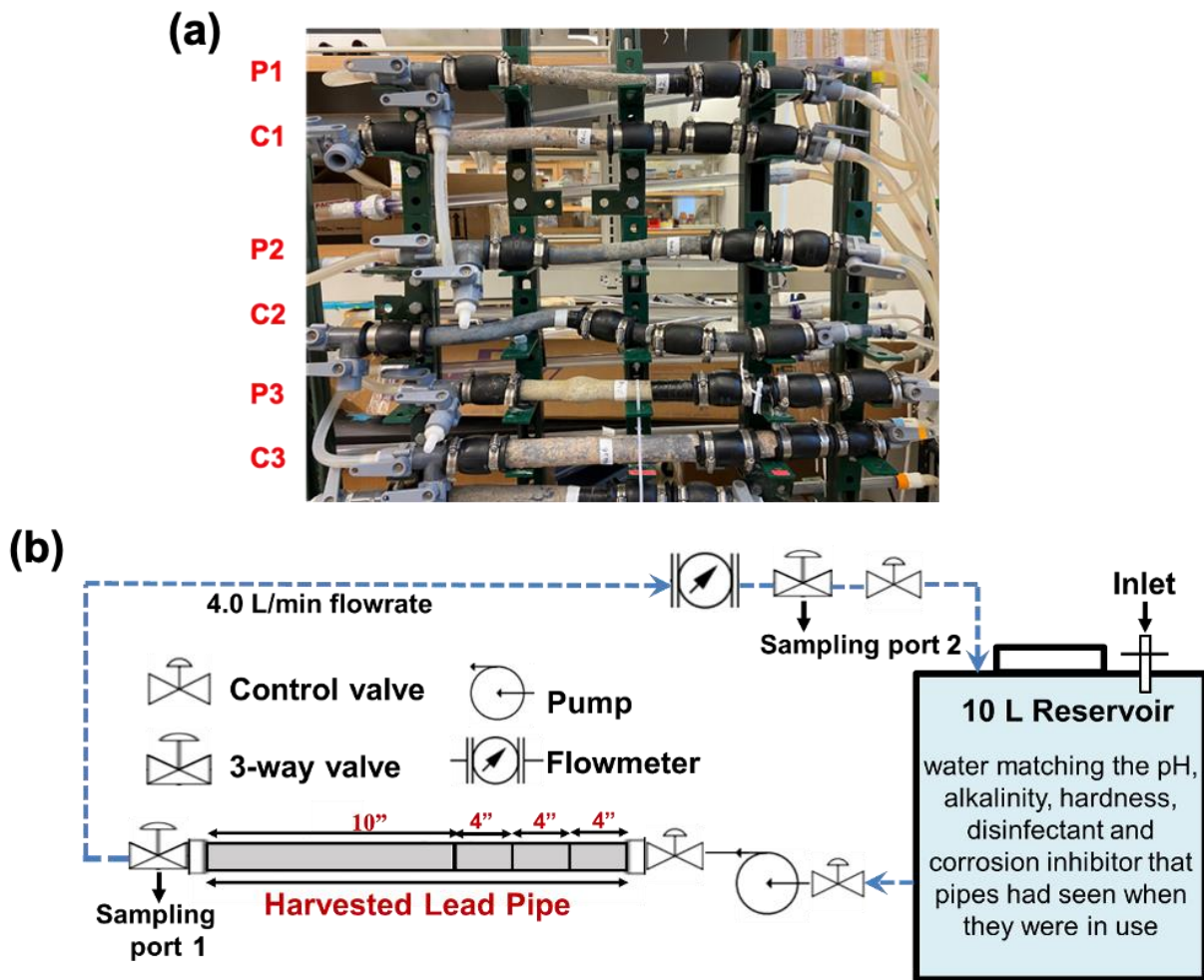


Figure A1.1 (a) Pipe loop reactors. (b) Schematic diagram of a pipe loop consisting of a pump, valves, flowmeter and reservoir. The harvested lead pipe assembly consists of one 10-inch section and three 4-inch segments that are connected with rubber connectors. The 4-inch segments allow scale analysis to be performed at different stages in the experiment while retaining the majority of the lead pipe length in the reactor and without any cutting of lead pipe.

A1.2 Flow Regime and Water Preparation

Table A1.1 Flow regime and phosphate dosing in different stages of the experiment.

Treatment	Weeks	Daily Flow ^{w2} (L/day)	Phosphate (mg/L as PO ₄)	Loop ID		
				P1	P2	P3
Treatment Stage 2	Weeks 50 to 60	Daily Flow ^{w2} (L/day)	Phosphate (mg/L as PO ₄)	1100-1500	1100-1500	1100-1500
				O:1.50 P:0.00	O:1.50 P:0.00	O:1.50 P:0.00
Treatment Stage 1	Weeks 34 to 49	Daily Flow ^{w2} (L/day)	Phosphate (mg/L as PO ₄)	1100-1500	1100-1500	1100-1500
				O:1.50 P:0.47	O:1.50 P:0.47	O:1.50 P:0.47
Conditioning	Weeks 18-32	Daily Flow ^{w2} (L/day)	Phosphate (mg/L as PO ₄)	1100-1500	1100-1500	1100-1500
				O:0.20 P:0.47	O:0.20 P:0.47	O:0.20 P:0.47
	Weeks 1-17	Daily Flow ^{w2} (L/day)	Phosphate ¹ (mg/L as PO ₄)	5000-5300	5000-5300	5000-5300
				O:0.20 P:0.47	O:0.20 P:0.47	O:0.20 P:0.47
	Time	Loop ID		P1	P2	P3
				C1	C2	C3

Notes: 1. “O” represents orthophosphate and “P” represents polyphosphate. Doses of orthophosphate and polyphosphate are both reported in units of mg/L as PO₄. 2. During all stages

of the experiment the flow rate was 4-5 L/min when the water was flowing; during the second half of conditioning and treatment stages 1 and 2, water was only flowing for 4.5 hours each day

Table A1.2 Artificial Buffalo Water composition compared to actual water composition reported by Buffalo Water.

Species	Range of Actual	Artificial Buffalo	Units
Ca ²⁺	42	36	mg/L
Na ⁺	12	44	mg/L
K ⁺			
SO ₄ ²⁻	23	21	mg/L
Cl ⁻		20	
NO ₃ ⁻	0.11	-	mg/L as NO ₃
F ⁻	0.12	0.12	mg/L
Free Chlorine	1.1	1.5	mg/L as Cl ₂
Alkalinity	94.3	92	mg/L as CaCO ₃
pH	7.7	8.0	-
Total Dissolved Solids	175.8	156	mg/L
Ca Hardness	99.2	92	mg/L as CaCO ₃
Ortho Phosphate	0.2	0	mg/L as PO ₄
Total Phosphate	0.67	0	mg/L as PO ₄

The harvesting procedures were followed to ensure minimal disruption to both the pipes and the scales on their inner surfaces: 1. Cut the lead pipe with a tube cutter or ratcheted guillotine blade (i.e., PVC cutter) and not an abrasive cutting wheel. 2. Drain the water from the pipe. 3. Insert a damp sponge into each end. Care should be taken not to disturb pipe scales. Seal both ends with duct tape (plastic wrap may be used below duct tape if ends are sealed). 4. Wrap the exterior of the pipe with one layer of bubble wrap.

Each pipe loop received freshly prepared Artificial Buffalo Water every Wednesday and the water temperature was maintained at approximately 24-26 °C. This water was prepared using ultrapure water (resistivity > 18.2 MΩ-cm) with the addition of the following chemicals: sodium bicarbonate (NaHCO₃, Sigma-Aldrich), calcium chloride (CaCl₂·H₂O, Alfa-Aesar), calcium hydroxide (Ca(OH)₂, Sigma-Aldrich), sodium hypochlorite (NaOCl, Fisher Scientific), sodium fluoride (NaF, Sigma-Aldrich), sulfuric acid (H₂SO₄, Sigma-Aldrich) and blended phosphate (Calciquest, Carus Corporation) with a 70%/30% blend of poly/ortho phosphate.

Sodium phosphate monobasic monohydrate (NaH₂PO₄·H₂O, Sigma-Aldrich) and sodium phosphate, dibasic, heptahydrate (Na₂HPO₄·7H₂O, Sigma-Aldrich) were used to make an additional orthophosphate stock solution.

A1.3 Scale Characterization and Water Sample Analysis

Scale analysis

Scale analysis involved the examination of a cross section and transverse sections of each pipe segment. To prepare a cross section, one end of the pipe was filled with a mixture of hardener and epoxy resin (18 wt.%). Once the epoxy had cured, this section was cut from the rest of the segment and polished using sandpapers of increasingly fine grit (up to 1200 grit). The polishing was done with mineral oil on the sandpaper to minimize the generation of airborne particles. The polished sample was sonicated in ethanol to remove residual mineral oil and pipe particles prior

to SEM-EDS analysis. All pipes were analyzed using a Thermo Fisher Quattro S E-SEM for imaging. Energy dispersive X-ray (EDS) spectroscopy with the SEM was used to semi-quantitatively determine the elemental composition of the pipe scales. For X-ray diffraction (XRD) and quantitative elemental analysis, portions of the scales were collected by scraping them off the pipe with a metal spatula. Two different layers of scale were collected. The top layer was material that could be removed by relatively gentle scraping, and removal of the bottom layer requiring more force and often also removed some of the underlying lead pipe at the same time. Portions of the ground up scale were analyzed by XRD on a Bruker d8 Advance X-ray diffractometer with Cu Ka radiation. MTI 1-inch low background Si sample holders were used. Scale was digested for elemental analysis by a modified aqua regia method (EPA, Method 3050B): Portions of the powdered scales were weighed and digested in concentrated hydrochloric and nitric acid (3:1 by volume) at 75°C for one hour in preparation for quantitative analysis of their elemental composition using a NexION 2000 ICP-MS.

Table A1.3 Water quality parameters measurement and scale analysis

Parameter	Matrix	Equipment	Method	Sampling
pH	Aqueous	pH meter		10-20 mL
Free chlorine	Aqueous	UV-Vis spectrometer	4500-Cl G	10 mL
Orthophosphate	Aqueous	UV-Vis spectrometer	Method 365.3, EPA	10 mL
Total phosphate	Aqueous (1% nitric acid)	ICP-MS		2 mL (diluted to 10 mL)
Lead concentration	Aqueous (1% nitric acid)	ICP-MS	Method 200.8, EPA	2 mL (diluted to 10 mL)
Scale crystalline phases	Solid	XRD		Scale powder
Scale morphology	Solid	ESEM		Pipe segments
Scale element distribution	Solid	EDS		Pipe segments
Scale element mass content	Aqueous (1% nitric acid)	ICP-MS		Acidified scale powder

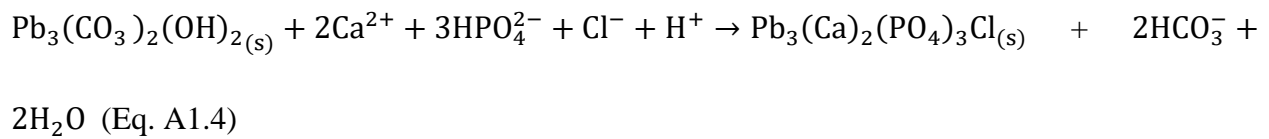
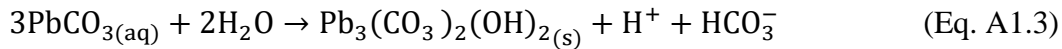
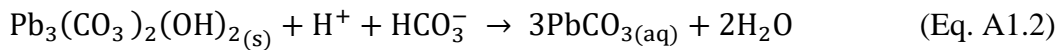
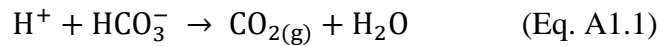
A1.4 pH and the Residual Free Chlorine Change during the Experiment

Free chlorine and pH are two important water chemistry parameters that can affect lead release in pipe loops. The pH and free chlorine were measured every weekday morning. The pH was adjusted to a target of 7.7 every Wednesday, and free chlorine was re-adjusted to the target value

(1.1 mg/L) in the morning every weekday. The pH variation of the system is shown in Figure A1.2a.

The pH change that occurs over the course of one week of stagnation and recirculation can indicate potential reactions in pipe loops during different stages. The pH always increased from the target (pH 7.7) as water flowed through the loops. Although the pipe loops were designed to minimize air-water exchange, such exchange could result in an increase in pH (Eq. A1.1). The endpoint pH was measured at the end of a week before the next water replenishment. During conditioning (Week 10 to 25), the endpoint pH of pipe loops increased substantially to 8.3 (Figure A1.2a). Dissolution of the hydrocerussite could be one of the reasons (Eq. A1.2) for the pH increase. As conditioning progressed (Week 26 to 32), the increase of pH became less substantial, and the endpoint pH became 8.1. The change in the pH increase could be due to more formation of hydrocerussite (Eq. A1.3) and its lower dissolution rate, which would offset the pH increase. During treatment stage 1 and the beginning of treatment stage 2 (Week 33 to 53), with the additional phosphate dosing to the test pipes and removal of polyphosphate, an increase in pH would be associated with the formation of phosphohedyphane (Eq. A1.4). During this stage the endpoint pH increased 8.2. At the end of treatment stage 2 (Week 54 to 60), the endpoint pH of the test pipes was at a lower level (pH 8.0) than during treatment stage 1. This lowering of the endpoint pH could be due to the lower formation rate of the phosphate-lead scale layer on pipe loop surface as well as a lower dissolution rate of hydrocerussite, which consumed

fewer protons than before. The box plots of each pipe loop during different stages (Figure A1.2b) are also consistent with the findings: the pH increased a little during treatment stage 1 and had the smallest change at the end of treatment stage 2.



The free chlorine concentration of all pipes decreased as water flowed through the loops, and the residual free chlorine in the pipe loops after 24 hours is shown in Figure A1.3a. At the beginning of the conditioning process, the residual free chlorine concentration often dropped below 0.1 mg/L, indicating essentially complete consumption of the free chlorine in the pipe loops. As the conditioning progressed, the consumption of free chlorine decreased. By the end of the conditioning stage, the residual free chlorine concentrations were around 0.5 mg/L after one day of stagnation and recirculation. During treatment stage 1, test pipes with additional phosphate showed a significant increase in the residual free chlorine concentration. These more stable free chlorine concentrations in the presence of higher orthophosphate could be due to the formation of lead-phosphate solids on lead pipe surface that serve as protective layers that prevent further

oxidation of elemental lead by free chlorine (DeSantis et al., 2020). The control pipes also showed some increase in the residual free chlorine concentrations. During treatment stage 2, the residual free chlorine concentration kept increasing, and the concentrations achieved a plateau of about 0.8 mg/L for both the control and the test pipes (Figure A1.3b). The CV of the residual free chlorine for different experiment stages (Figure A1.3c) decreased from conditioning to treatment stage 1 and to treatment stage 2, suggesting that the residual free the chlorine concentration (or free chlorine consumption of the pipe) had become more stable as treatment progressed.

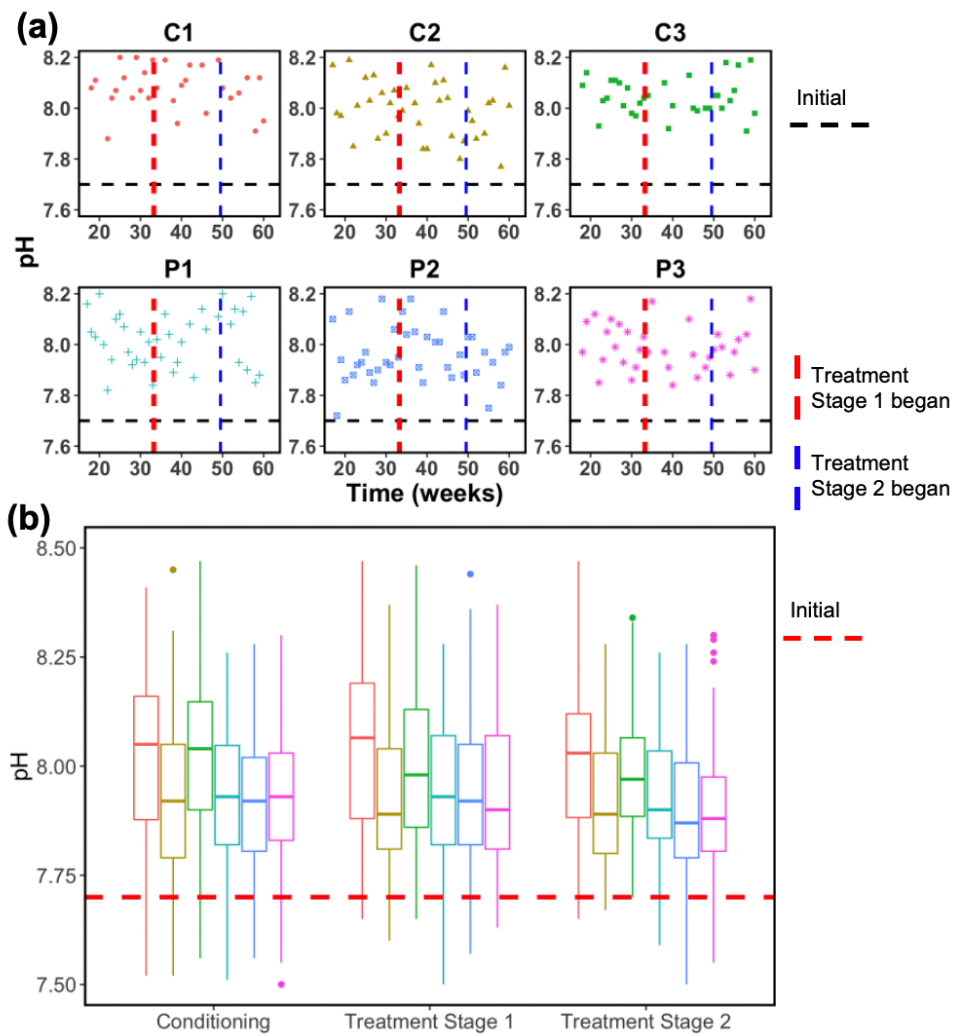


Figure A1.2 pH of the water in the pipe loops shown with (a) weekly measurements and (b) box plots of variability. The conditioning stage only includes the data starting from Week 18.

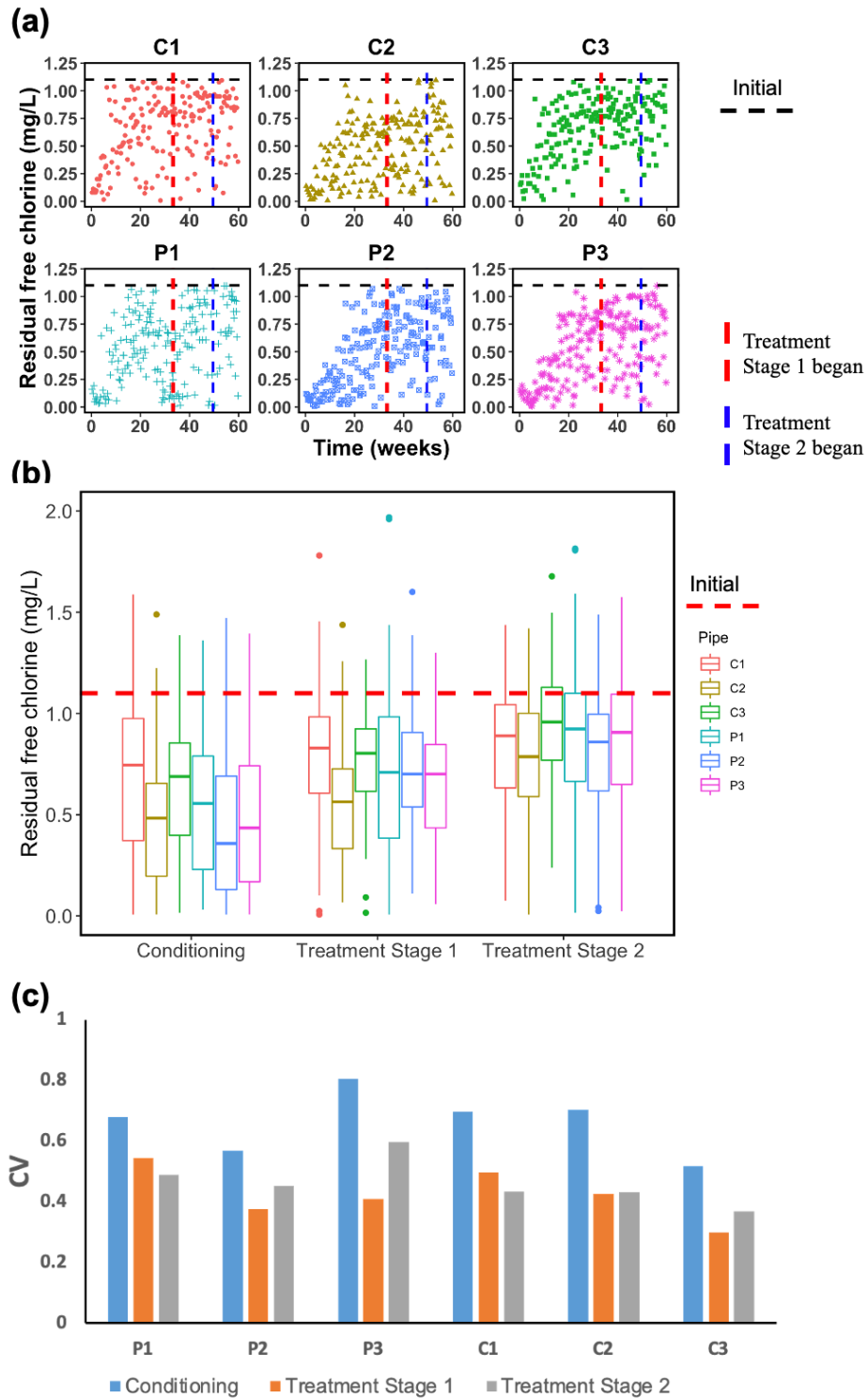


Figure A1.3 Residual free chlorine concentration in the pipe loops after 24 hours from (a) daily measurements and (b) box plots of variation and (c) coefficient of variation (CV) of measurements. The conditioning stage only includes data starting from Week 18.

A1.5 Coefficient of Variation (CV) for Total and Dissolved Lead Concentrations

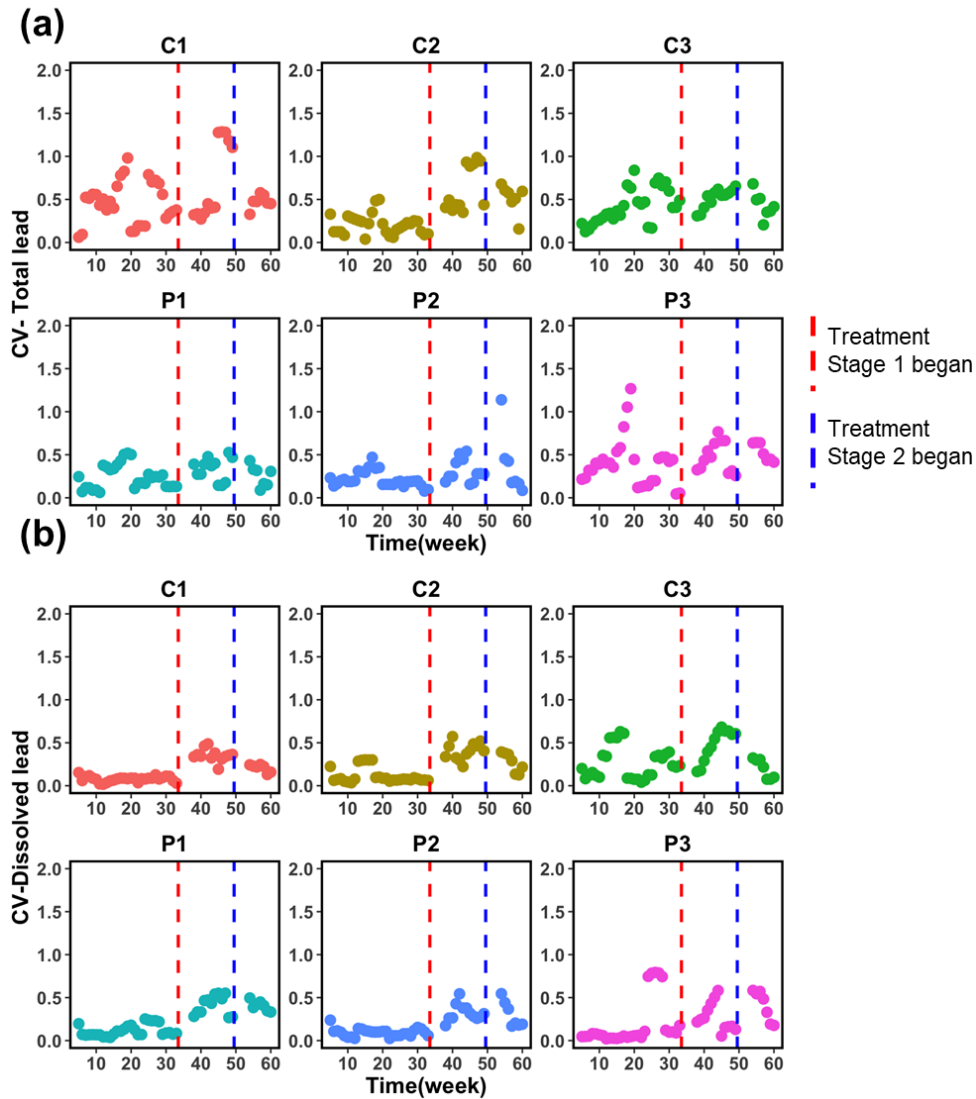


Figure A1.4 Coefficient of variation (CV) of (a) total lead and (a) dissolved lead concentrations of the pipe loops. CV was calculated for the weekly data for the preceding 5-week periods. Because the water chemistry of the test loops (P1, P2, and P3) changed when treatment stage 1 (dashed vertical red lines) and treatment stage 2 (dashed vertical blue lines) began, the CV value is not reported until five weeks after the changes in water chemistry for the test loops (P1, P2, and P3).

The total lead concentration for pipes was high and noisy (200-300 $\mu\text{g/L}$) in the beginning of the conditioning stage. By the end of Week 30 (before treatment stage 1 began), the CV of all the pipes were primarily below 1.0 (Figure A1.4a), suggesting that the total lead concentration of pipes was stable. The CV shown in Figure A1.4 for lead concentrations were calculated based on a 5-week period (e.g., the point for the CV in Week 10 is for Weeks 6 to 10). The periods that have the weeks from different treatment stages were not included (e.g., Week 30 to Week 35 not included, since Week 30 to 33 is for conditioning, and Week 34 to 35 is for treatment stage 1).

A1.6 Summary of Lead Concentrations in Different Treatment Stages

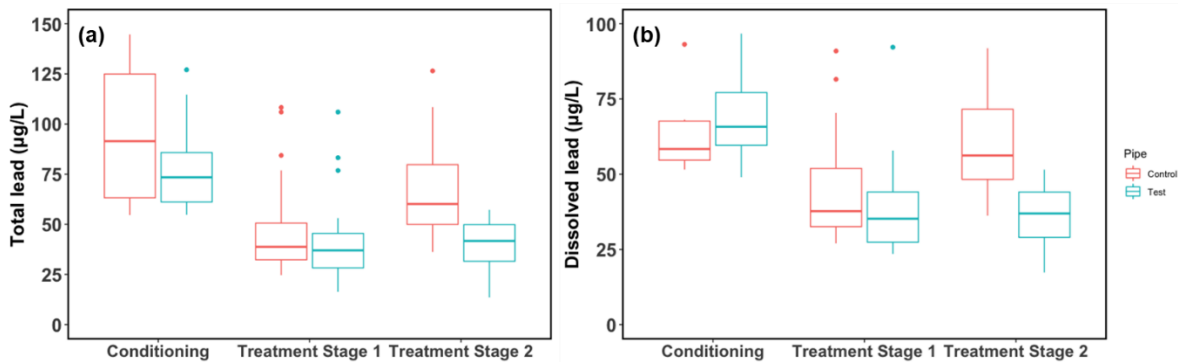


Figure A1.5 Box plots showing the variation and central tendency for (a) total lead concentration and (b) dissolved lead concentration of pipe loops.

The normality distribution assumption of the data set was checked by Shapiro-Wilk Test using R Studio.

#x is the numeric vector of data values.

shapiro.test(x)

Most of the data met the normality assumption with p value > 0.01 in Shapiro-Wilk Normal Test; however, the data during Treatment stage 1 do not satisfy the normality requirement as well (p value < 0.01). Therefore, we have employed a Wilcoxon rank-sum test, a non-parametric data analyses alternative to the t test. Both tests have the Null hypothesis (H0): There is no difference between the means of the selected two data sets ($\mu_x = \mu_y$). Alternative hypothesis (Ha): The means of the selected two data sets are different ($\mu_x \neq \mu_y$).

Using the following r codes in R studio with 40 degrees of freedom (21 + 21 - 2) and a two-tailed test, we identified each p-value associated with each certain t-value:

Set the degrees of freedom and t-value

df <- 40

t_val <- "t-value"

Calculate the p-value using pt() function, "t-value" is the input

*p_val <- 2 * (1 - pt(abs(t_val), df))*

Print the p-value

cat("p-value = ", p_val)

"p-value" is the output

Using the following r codes in R studio, we performed a two-tailed Wilcoxon rank-sum test, and the p values are shown in Table A1.6.

wilcox.test(x,y) # x and y are the numeric vector of data values in the data set.

Table A1.4 Potential dissolution-precipitation and aqueous reactions involving lead in the system.

#	Reaction	Log K
1	$PbCO_3(s)$ (Cerussite) $\rightleftharpoons Pb^{2+} + CO_3^{2-}$	-13.20
2	$Pb_3(CO_3)_2(OH)_2(s)$ (Hydrocerussite) + $2H^+$	-18.76
3	PbO (Litharge) + $2H^+$ $\rightleftharpoons Pb^{2+} + H_2O \leftrightarrow$	-12.69
4	$Pb_5(PO_4)_3OH(s)$ (Hydroxylpyromorphite) + H^+ $\rightleftharpoons 5Pb^{2+} + 3PO_4^{2-} + H_2O$	-62.79
5	$H_2CO_3(aq) \rightarrow 2H^+ + CO_3^{2-}$	-16.681
6	$HCO_3^- \rightarrow H^+ + CO_3^{2-}$	-10.329
7	$H_3PO_4(aq) \rightarrow 3H^+ + PO_4^{3-}$	-21.721
8	$H_2PO_4^- \rightarrow 2H^+ + PO_4^{3-}$	-19.573
9	$HPO_4^{2-} \rightarrow H^+ + PO_4^{3-}$	-12.375
10	$Pb^{2+} + CO_3^{2-} \rightarrow PbCO_3(aq)$	6.53
11	$Pb^{2+} + 2CO_3^{2-} \rightarrow Pb(CO_3)_2^{2-}$	9.94
12	$Pb^{2+} + CO_3^{2-} \rightarrow PbHCO_3^+$	13.23
13	$Pb^{2+} + H_2O \rightarrow PbOH^+ + H^+$	-7.597
14	$Pb^{2+} + 2H_2O \rightarrow Pb(OH)_2 + 2H^+$	-17.094
15	$Pb^{3+} + 3H_2O \rightarrow Pb(OH)_3 + 3H^+$	-28.091

Note: All reactions and constants are from Visual MINTEQ 3.1.

Table A1.5 Summary of the results from the T test performed on the dissolved and total lead concentrations in the pipe loops.

ID	Dissolved Lead	P value (P crit=0.05)	Statistically Significant	Total Lead	P value (P crit=0.05)	Statistically Significant
0-C vs 0-P		0.17	N		0.06	N
1-C vs 1-P		0.10	N		0.12	N
2-C vs 2-P		2.50E-05	Y		1.30E-06	Y
0-P vs 1-P		1.40E-08	Y		8.00E-04	Y
1-P vs 2-P		0.58	N		0.71	N
2-P vs 0-P		4.80E-11	Y		4.20E-07	Y
0-C vs 1-C		3.30E-04	Y		2.00E-03	Y
1-C vs 2-C		0.05	N		2.00E-03	Y
2-C vs 0-C		0.04	Y		0.75	N

Note: The results presented are based on an average of three distinct pipe replicates for the control and test conditions for the final seven weeks of each stage. '0', '1' and '2' indicate the Conditioning, Treatment Stage 1 and Treatment Stage 2, respectively. 'P' and 'C' indicate test and control pipes, respectively. The letters 'Y' and 'N' represent whether the results are statistically significant, with 'Y' indicating yes and 'N' indicating no.

Table A1.6 Summary of the results from the Shapiro-Wilk Test performed on the dissolved and total lead concentrations in the pipe loops.

ID	Dissolved Lead	P value (P crit=0.05)	Statistically Significant	Total Lead	P value (P crit=0.05)	Statistically Significant
0-C vs 0-P		0.80	N		0.06	N
1-C vs 1-P		0.15	N		0.24	N
2-C vs 2-P		2.92e-07	Y		1.23e-05	Y
0-P vs 1-P		1.67e-08	Y		6.89e-08	Y
1-P vs 2-P		0.90	N		0.66	N
2-P vs 0-P		4.459e-11	Y		4.46e-11	Y
0-C vs 1-C		1.1 e-4	Y		6.27e-07	Y
1-C vs 2-C		0.003	Y		2.00E-03	Y
2-C vs 0-C		0.08	N		0.015	Y

Note: The results presented are based on an average of three distinct pipe replicates for the control and test conditions for the final seven weeks of each stage. '0', '1' and '2' indicate the Conditioning, Treatment Stage 1 and Treatment Stage 2, respectively. 'P' and 'C' indicate test and control pipes, respectively. The letters 'Y' and 'N' represent whether the results are statistically significant, with 'Y' indicating yes and 'N' indicating no.

A1.7 Total Lead Concentrations After First 6-h Stagnation Period of Each Week

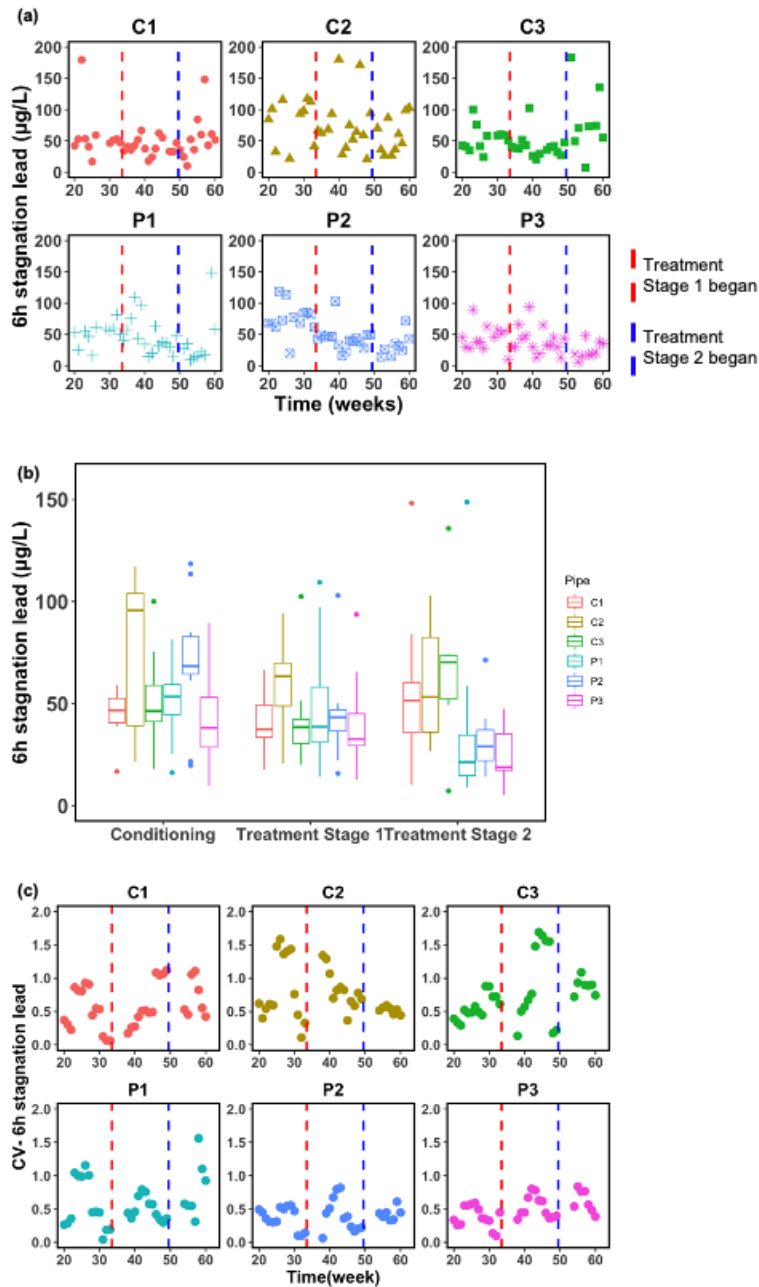
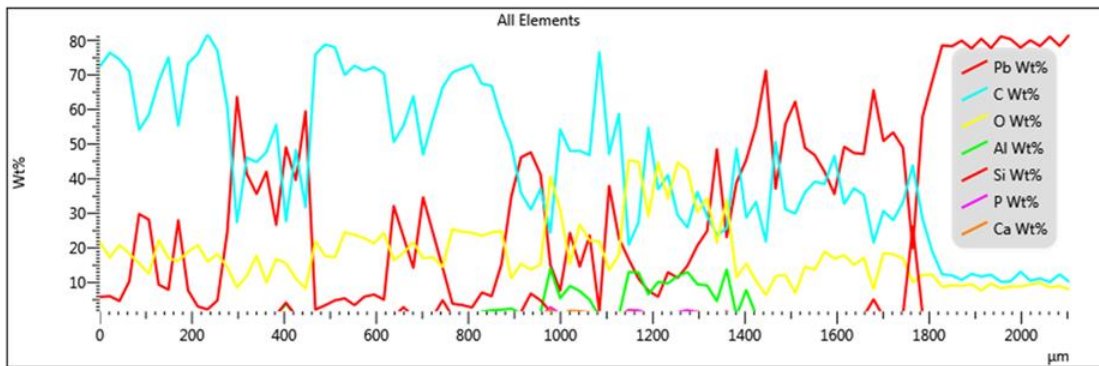
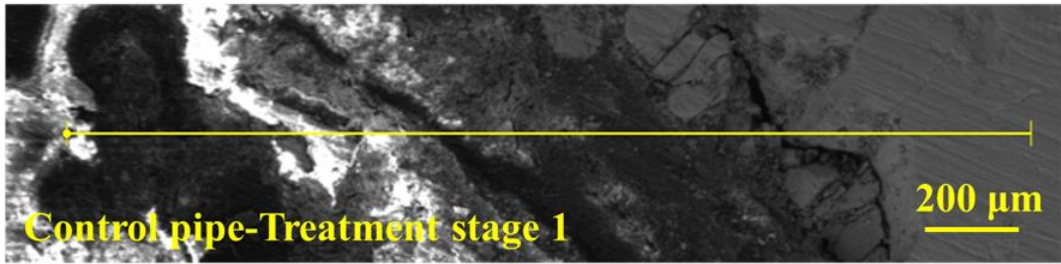
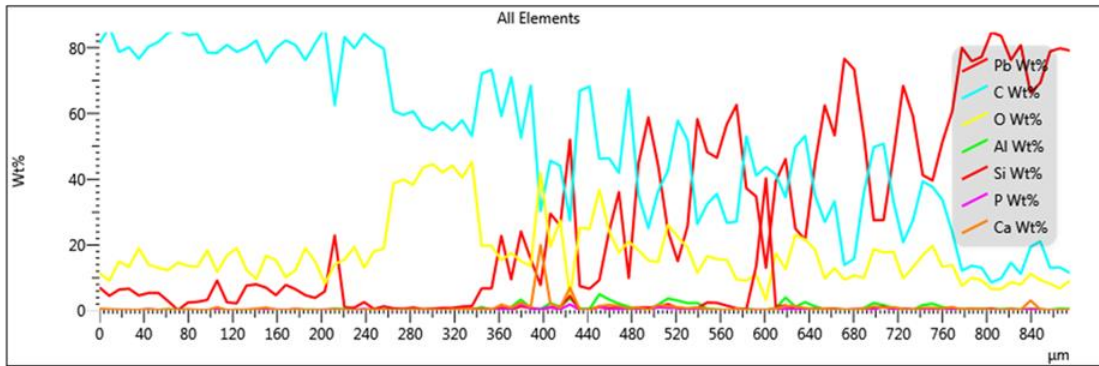
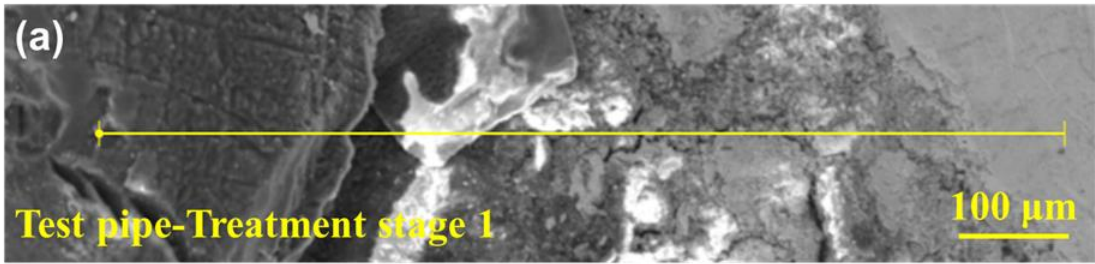


Figure A1.6 Total lead concentrations after the first 6-h stagnation period of each week shown as (a) full data series for each loop and (b) box plots of variation and (c) coefficient of variation (CV) for 6-h stagnation lead concentrations.

The lead concentrations after the first 6-h stagnation period of each week (i.e., 6h-stagnation lead) are shown in Figure A1.5a. The 6h-stagnation lead concentration was measured from Week 16 onward. It was highly variable during conditioning (50-150 $\mu\text{g/L}$), and its concentration was lower than the 168-h total lead concentrations. As conditioning progressed, the 6h-stagnation lead concentration stabilized and gradually decreased, achieving a value of about 50 $\mu\text{g/L}$ for most pipes (except C2) by the end of conditioning. The 6h-stagnation lead concentration in pipe loop C2 was still around 100 $\mu\text{g/L}$. The CV in Figure A1.5c (indicator for stability) of the 6h-stagnation lead concentration for pipe loops did not change much during conditioning. Before the beginning of treatment stage 1, the CV values for most pipes were around or below 0.5. As treatment stage 1 progressed, the 6h-stagnation lead concentration for the test pipes decreased to 35-40 $\mu\text{g/L}$. The 6h-stagnation lead concentration of the control pipes showed little change during treatment stage 1, which was still variable and high (50 $\mu\text{g/L}$). A further drop in the 6h-stagnation lead concentration in test pipes occurred in treatment stage 2 (Figure A1.5b). For the test pipes, the 6h-stagnation lead concentration was around 30 $\mu\text{g/L}$ at the end of treatment stage 2 which accounted for 80-90% of the total lead concentration after 1 week of recirculation. For the control pipes the 6h-stagnation lead concentration showed little change during this time and remained higher and more variable than for the test pipes.

A1.8 Additional Scale Analysis Results and Summary



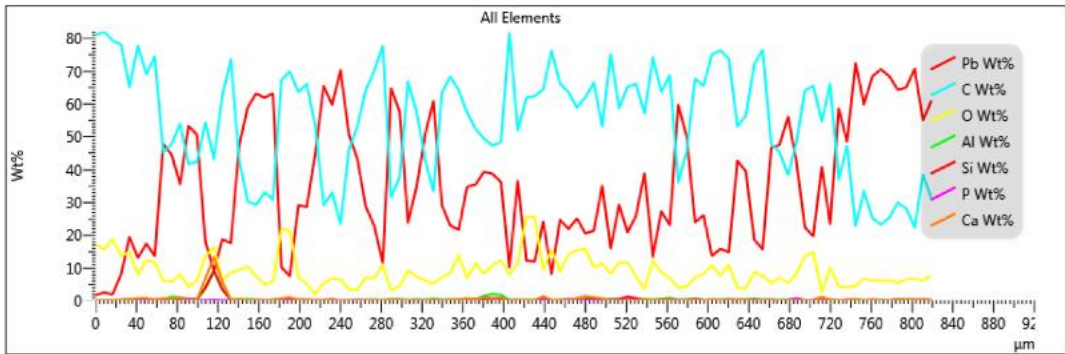
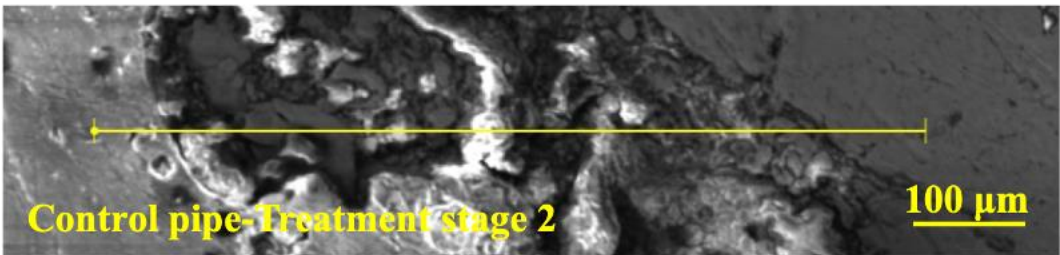
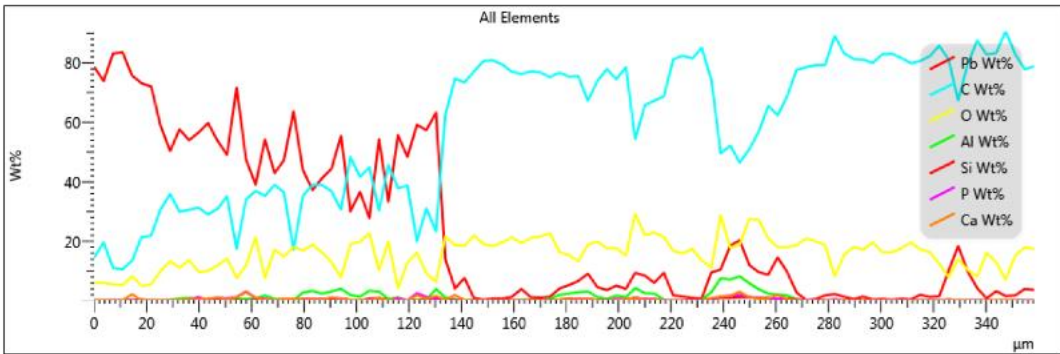
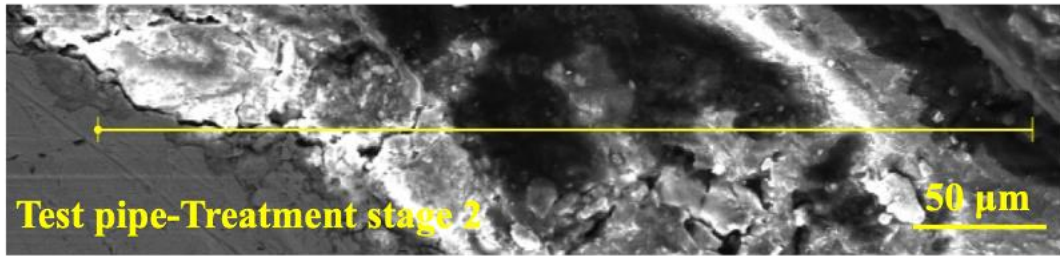


Figure A1.7 Line scans of different elements detected by EDS. (The yellow line in SEM images corresponds to the line scan); (a) for treatment stage 1 (b) for treatment stage 2.

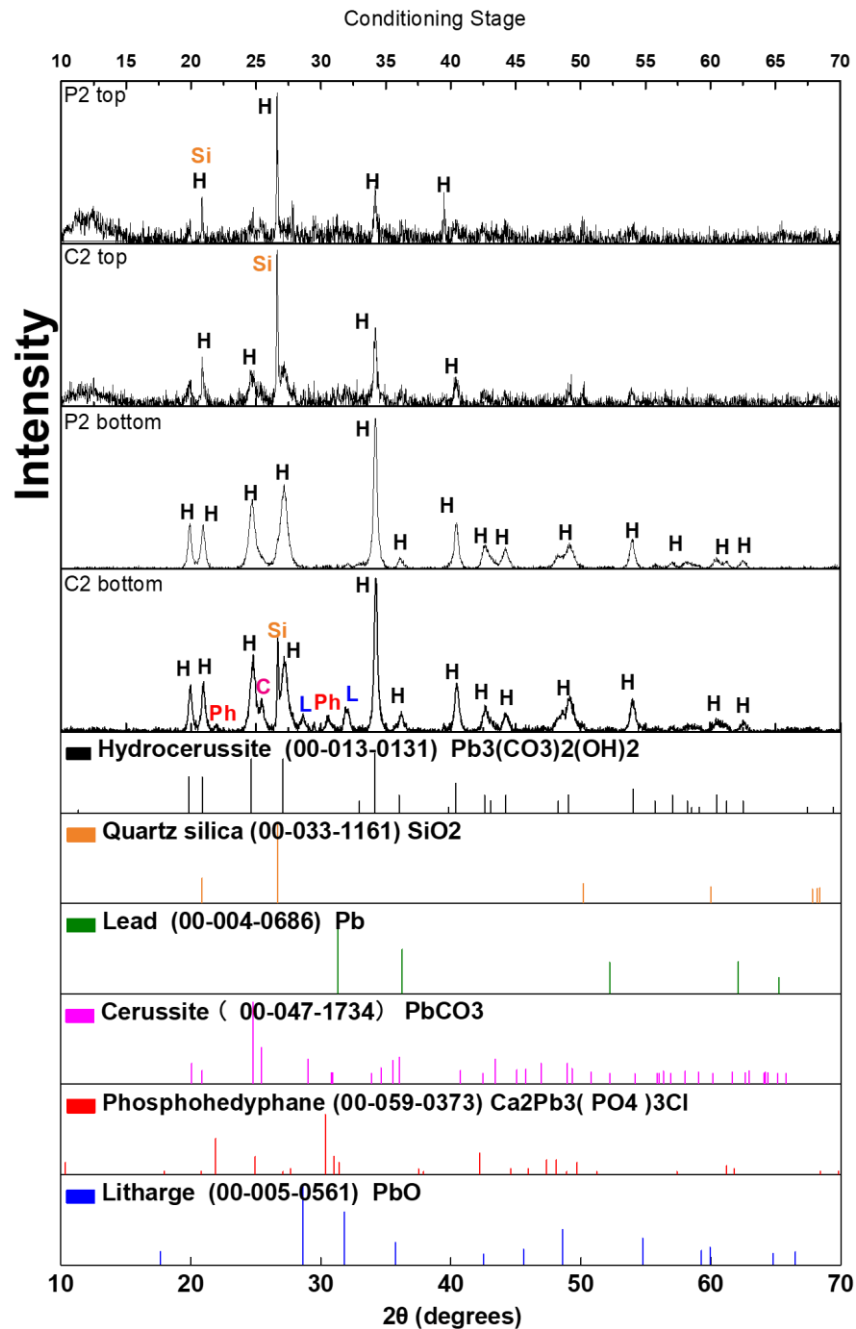


Figure A1.8 XRD patterns obtained from the two layers removed from the surfaces of two pipe assemblies (C2 and P2) at the end of conditioning. The XRD patterns (panel a) are shown together with references patterns (panel b) for hydrocerussite $Pb_3(CO_3)_2(OH)_2$, quartz (SiO_2), elemental lead (Pb), cerussite ($PbCO_3$), phosphohedyphane($Ca_2Pb_3(PO_4)_3Cl$) and litharge (PbO). Labels used throughout the patterns are peaks from corresponding solid phases abbreviated as H, Si, Pb, C, Ph and L in the same order as mentioned in the caption.

Table A1.7 Summary of XRD results for the powdered samples from the lead pipe surfaces.

Sample ID		Hydrocerussite ($\text{Pb}_3(\text{CO}_3)_2(\text{OH})_2$)	Cerussite (PbCO_3)	Phosphohedyphane ($\text{Ca}_2\text{Pb}_3(\text{PO}_4)_3\text{Cl}$)	Litharge (PbO)
P1	2-Top	+++	-	-	+
	2-Bottom	+++	+++	+++	+++
P2	0-Top	+++	-	-	-
	1-Top	++	-	+	++
	2-Top	+++	-	+	+
	0-Bottom	+++	+	+	+
	1-Bottom	+	+	+	+++
	2-Bottom	++	+	++	+++
P3	1-Top	+++	-	-	-
	2-Top	+++	+	-	-
	1-Bottom	+	+	+	+++
	2-Bottom	++	++	++	+++
C1	1-Top	+++	-	-	-
	2-Top	+++	-	-	-
	1-Bottom	++	++	?	-
	2-Bottom	+++	+	+	-
C2	0-Top	+++	-	-	-
	2-Top	+++	++	+	+
	0-Bottom	+++	-	+	+
	2-Bottom	+++	+++	++	+++
C3	1-Top	+++	++	-	-
	2-Top	++	++	-	-
	1-Bottom	++	-	++	++
	2-Bottom	++	++	++	+++

Note: '0', '1' and '2' are from pipes removed for analysis at the end the Conditioning, Treatment Stage 1 and 2, respectively. 'P' and 'C' indicate test and control pipes, respectively. '+' indicates the abundance of a certain mineral. '-' Indicates not found. '?' Indicates the uncertainty of presence.

Table A1.8 Mass concentrations (mg/g) of elements in the scales.

Sample ID		Pb	P	Al
P1	2-Top	330.6	1.5	38.6
	2-Bottom	333.3	21.7	29.0
P2	0-Top	153.9	3.3	256.5
	1-Top	71.0	41.0	107.8
	2-Top	113.5	0.7	69.6
	0-Bottom	228.8	1.2	33.3
	1-Bottom	465.2	7.9	7.1
	1-Bottom	521.2	69.1	24.8
P3	1-Top	60.4	35.2	104.7
	2-Top	91.0	1.9	103.0
	1-Bottom	391.8	10.8	8.1
	2-Bottom	302.0	10.3	47.5
C1	1-Top	85.4	18.9	54.9
	2-Top	76.0	0.6	77.0
	1-Bottom	362.1	7.2	3.91
	2-Bottom	781.9	6.6	2.5
C2	0-Top	92.0	3.8	137.5
	2-Top	251.9	0.6	54.0
	0-Bottom	134.9	2.9	113.2
	2-Bottom	435.5	7.7	51.2
C3	1-Top	66.6	26.5	14.4
	2-Top	88.1	1.1	80.4
	1-Bottom	447.6	7.7	0.27
	2-Bottom	454.0	9.6	9.7

Note: '0', '1' and '2' are from pipes removed for analysis at the end the Conditioning, Treatment Stage 1 and 2, respectively. 'P' and 'C' indicate test and control pipes, respectively.

Mass concentrations of the major elements in the scales are summarized in Table A1.8. Due to the availability of pipe segments, only P2 and C2 were analyzed at the end of the conditioning phase.

Pipe segments from pipe loops P2, P3, C1 and C3 were analyzed at the end of treatment stage 1, and materials from all pipe loops were analyzed after treatment stage 2.

By the end of conditioning, the bottom layer had higher concentrations of Pb (up to 700 mg/g) and Al (130-260 mg/g). Only a small amount of P was found in pipe scales (up to 3 mg/g). At the end of treatment stage 1, the P concentration in the top layer had increased from 3 mg/g to 40 mg/g averagely for the test pipes. Compared with the top layer, the P for the bottom layers is smaller in concentration (10 mg/g for test pipes and 7 mg/g for control pipes). According to XRD, phosphohedyphane ($\text{Ca}_2\text{Pb}_3(\text{PO}_4)_3\text{Cl}$) was mainly found in the bottom layers. The combinations of these observations suggest that during treatment stage 1 phosphorus primarily accumulated in the amorphous phase of the top layer. The increase of P concentration in the scales of the test pipes is qualitatively consistent with the observed loss of orthophosphate from the water during treatment stage 1. The presence of P in both the top and bottom scale layers indicates that the orthophosphate could be partly converted to the lead-phosphate scales as well as the amorphous layer.

Appendix A2: Supporting Information for **Chapter 3**

A2.1 Chemicals for Water Chemistry Preparation

The following chemicals were added to the water reservoir: aluminum sulfate octahydrate ($\text{Al}_2(\text{SO}_4)_3 \cdot 8\text{H}_2\text{O}$, Sigma-Aldrich) calcium chloride ($\text{CaCl}_2 \cdot \text{H}_2\text{O}$, Alfa-Aesar), magnesium chloride hexahydrate ($\text{MgCl}_2 \cdot 6\text{H}_2\text{O}$), magnesium sulfate (MgSO_4 , Sigma-Aldrich), potassium bicarbonate (KHCO_3 , Sigma-Aldrich), sodium bicarbonate (NaHCO_3 , Sigma-Aldrich), sodium fluoride (NaF , Sigma-Aldrich) and sodium nitrate (NaNO_3 , Sigma-Aldrich).

Free chlorine was prepared with sodium hypochlorite solution (NaClO , 4-6%/Laboratory, Fisher), and H_2SO_4 (0.1 M) and NaOH (0.1 M) were used to adjust the pH of the solution.

A2.2 Electrochemical Polarization

In the first step, electrochemical polarization was conducted with a potentiostat (Gamry reference 600) to generate PbO_2 on the coupons. The electrochemical polarization design consisted of a lead coupon as the anode, a platinum (Pt) electrode as the cathode, and an Ag/AgCl reference electrode in a 100 mL solution (0.1 M NaHCO_3 , pH 8.0) (Figure 3.1b). All three electrodes were connected to the potentiostat using titanium wires. The corrosion voltage for Pb(IV) was determined by the cyclic voltammetry on the lead coupons (-1~2 V, 10 mV/s, 5

cycles). Polarization was conducted by the potentiostat at the corrosion voltage for Pb(IV) for 2 hours.

A2.3 Calculations of PbO₂ Generation from Electrochemical Polarization and Chemical Conditioning

$$n_e = \frac{Q \times \eta_F}{z \times F}$$

$$Q = j \times A \times t$$

$$Q = 1 \text{ mA/cm}^2 \times 10^{-3} \text{ A/mA} \times 10.24 \text{ cm}^2 \times 7200 \text{ s} = 74 \text{ C}$$

$$n_e = \frac{74 \text{ C} \times 100\%}{4 \times 96485 \text{ C/mol}} = 1.9 \times 10^{-4} \text{ mol}$$

$$p = \frac{n_e}{n_t} \times 100\%$$

$$n_t = \frac{A \times d \times \rho}{M}$$

$$n_t = \frac{10.24 \text{ cm}^2 \times 220 \text{ } \mu\text{m} \times \frac{10^{-4} \text{ cm}}{\mu\text{m}} \times 9.38 \text{ g/cm}^3}{239 \text{ g/mol}} = 8.8 \times 10^{-3} \text{ mol}$$

$$p = \frac{1.9 \times 10^{-4} \text{ mol}}{8.8 \times 10^{-3} \text{ mol}} = 2.2 \%$$

n_e is the molar mass of the PbO₂ on one coupon produced by electro-polarization (mol); n_t is the total molar mass of the PbO₂ on one coupon at the end of test (mol); Q is the total charge passed through the system (in coulombs, C); η_F is the faraday efficiency of the electrochemical reactions which is assumed as 100% for simplification; z is the number of electrons involved in the

electrochemical reaction, which is 4 for Pb(0) oxidizing to Pb(IV); F is Faraday's constant (F=96485C/mol), which is the charge of one mole of electrons; j is the current density (in amperes per square meter, mA/cm²); A is the surface area of the electrode-coupon (in square meters, cm²); t is the time (in seconds, s) during which the current is applied; p is the percentage of PbO₂ generated by electro-polarization in total PbO₂ scale at the end test; d is the thickness of the PbO₂ scale (cm); ρ is the density of PbO₂ (9.38 g/ cm³, National Center for Biotechnology Information, assuming the scale was 100% PbO₂ after test); M is the molar mass for PbO₂ (239 g/mol).

A2.4 Changes in Residual Free Chlorine and pH during Chemical Conditioning

Figure A2.5a indicates that the coupons initially consumed a significant amount of free chlorine and that this consumption gradually decreased over time. The initial dosing of free chlorine was 40 mg/L, and the residual free chlorine was tracked daily. The residual free chlorine concentration began at 3 mg/L and ultimately stabilized at 10 mg/L after one day of contact. The pH of the solutions increased significantly from 8.0 to 10.0 over the week of conditioning (Figure A2.5b), which could be due to the oxidation of metallic lead to lead(II):

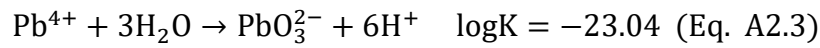
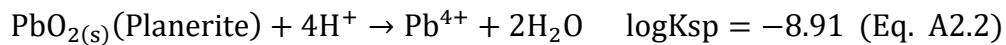


The PbCO_{3(aq)} subsequently precipitated as hydrocerussite (Pb₃(CO₃)₂(OH)₂), acting as a precursor for PbO₂ formation.¹ In parallel, solid particles settled at the jar's bottom. These settled

solids changed color from white to pink as the conditioning process advanced, corresponding to the transition between hydrocerussite and PbO₂.

A2.5 Equilibrium Solubility of Lead(IV) Oxide

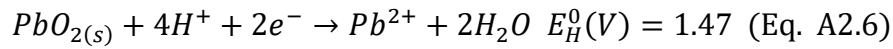
Equilibrium solubility of lead(IV) oxide was calculated from pH 6 to 9 when all dissolved lead is present as lead(IV) (Pb⁴⁺, PbO₃²⁻ and PbO₄⁴⁻) according to Eq. A 2.2-A 2.4. The total concentration of dissolved lead(IV) shown in Figure A2.8. encompasses the summation of the free metal ion Pb⁴⁺ and the hydrolysis complexes PbO₃²⁻ and PbO₄.



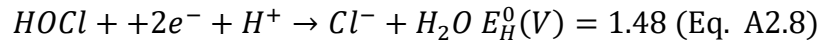
A2.6 Calculations of Threshold Free Chlorine

Two key half reactions (Eq. A 2.6 and Eq. A 2.8) in the solution govern the stability of PbO₂. In the solution that has a dissolved lead of 15 µg/L (7.2 × 10⁻⁸ mol/L), the molar concentration of Pb²⁺ is around 1.8 × 10⁻¹² mol/L (Shown in Eq. A 2.7, calculated by Minteq 5.0 with water chemistry parameters from Table A2.1). The environmental redox potential for PbO₂/Pb²⁺ at pH 8 is calculated to be 0.87 V (vs SHE) (Eq. A 2.7). For the half reaction of HOCl/Cl⁻ (shown in Eq. A 2.8), its environmental redox potential must equal the environmental redox potential of PbO₂/Pb²⁺ to prevent PbO₂ from being reduced to Pb²⁺. At the water chemistry of the

experiments with a pH of 8 and Cl^- concentration of 21 mg/L (equivalent to 6.1×10^{-4} mol/L)), the calculated threshold concentration of HOCl in the solution is 3.78×10^{-16} mol/L. According to the pK_a of the acid dissociation reaction of HOCl/OCl⁻ (Eq. A 2.10), the threshold free chlorine in the system to maintain the stability of PbO₂ is calculated to be 5.06×10^{-16} mol/L, equivalent to 3.59×10^{-11} mg/L as Cl₂.



$$E_{H1} = E_H^0 - \frac{0.059}{2} \log \frac{[Pb^{2+}]}{[H^+]^4} = 1.47 - 0.059 \log \frac{[1.8 \times 10^{-12}]}{[10^{-8}]^4} = 0.87 \text{ V} \quad (\text{Eq. A2.7})$$



$$E_{H2} = E_H^0 - \frac{0.059}{2} \log \frac{[Cl^-]}{[H^+][HOCl]} = 1.49 - \frac{0.059}{2} \log \frac{[6.1 \times 10^{-4}]}{[10^{-8}][HOCl]} \quad (\text{Eq. A2.9})$$

$$E_{H1} = E_{H2}$$

$$\rightarrow [HOCl] = 1.28 \times 10^{-16} \text{ mol/L}, \quad [OCl] = 3.78 \times 10^{-16} \text{ mol/L}$$



$$\frac{[H^+][OCl^-]}{[HOCl]} = 10^{-7.53}$$

$$[HOCl] + [OCl] = 5.06 \times 10^{-16} \text{ mol/L}$$

$$\text{Free chlorine} = 3.59 \times 10^{-11} \text{ mg/L as Cl}_2$$

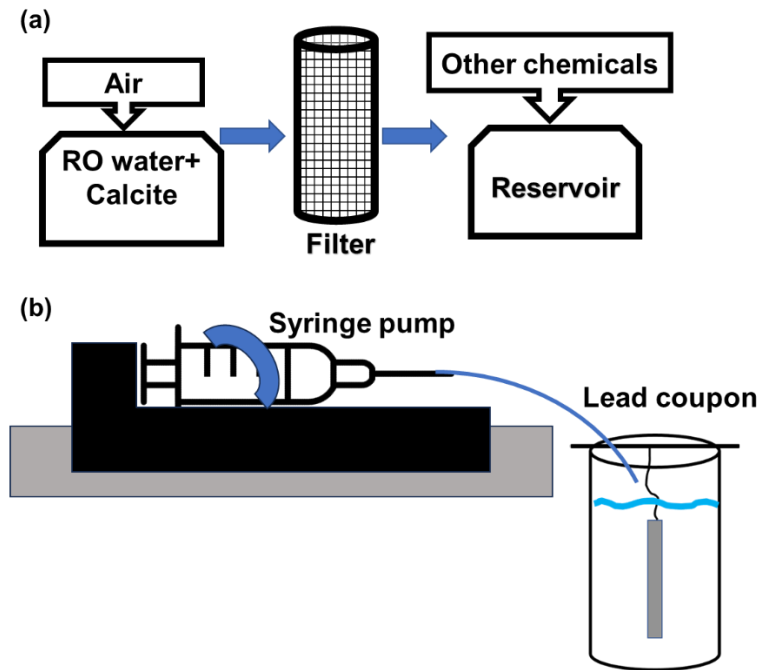


Figure A2.1 (a) Calcite contact for synthetic water preparation. (b) Syringe pump set-up for threshold free chlorine experiment.

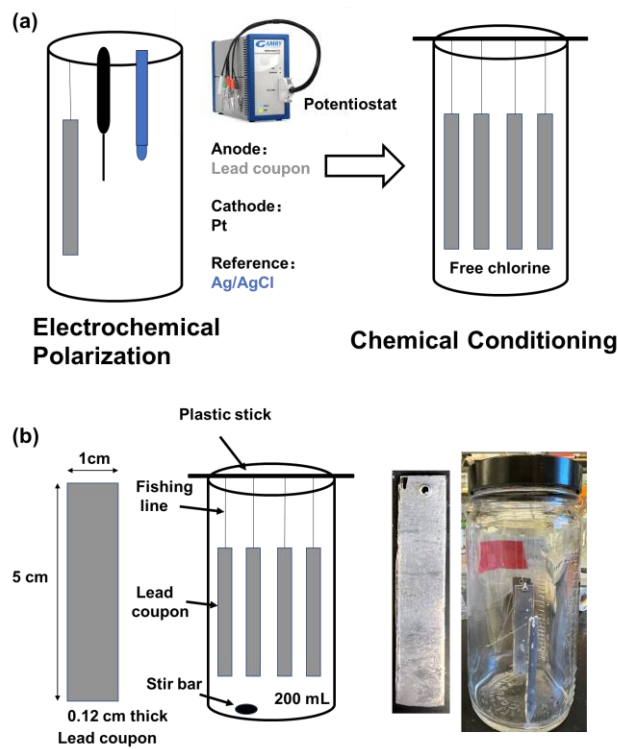


Figure A2.2 (a) Illustration of lead coupon experiment in beakers and (b) formation methods of lead(IV) PbO_2 on coupons.

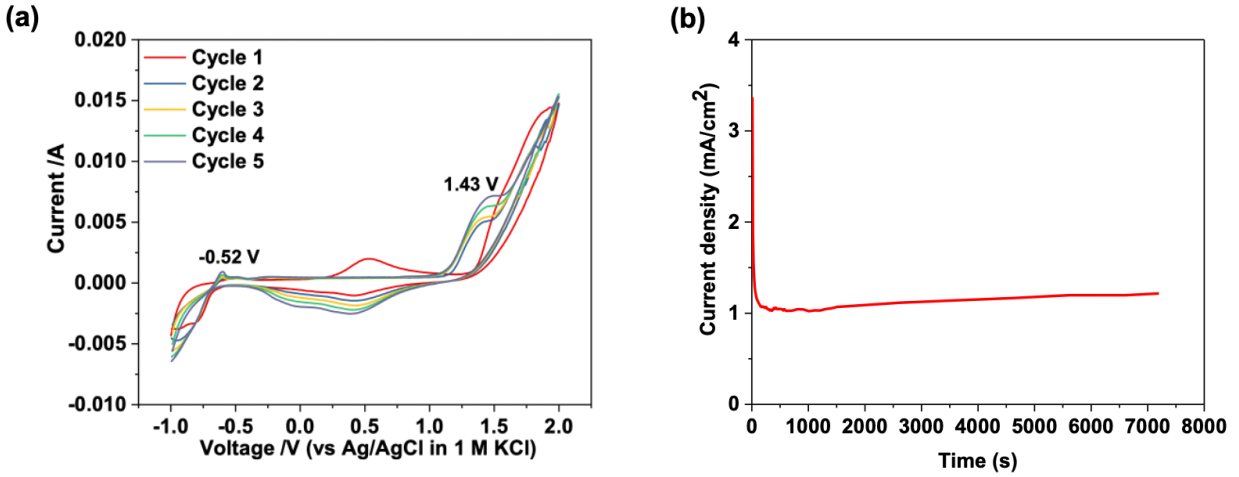


Figure A2.3 (a) Cyclic voltammety of the lead coupon in a 0.1 M NaHCO₃ solution at pH 8.0 (b) The polarization curve for the lead coupon at a constant voltage of 1.43 V (vs Ag/AgCl in 1 M KCl).

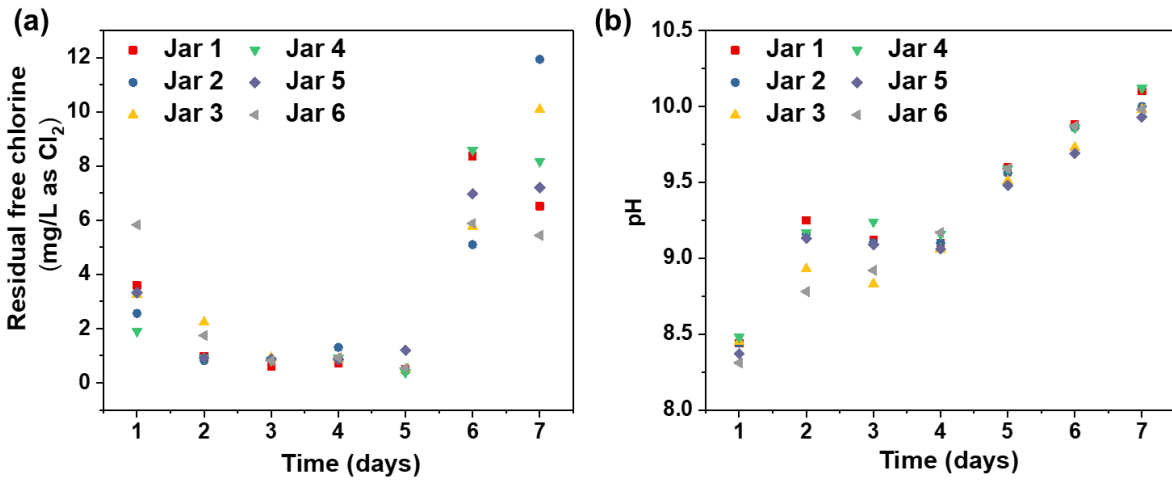


Figure A2.4 (a) Residual free chlorine concentration during chemical conditioning with an initial dosing at 40 mg/L as Cl₂ and daily readjustment (b) pH change during chemical conditioning with an initial pH of 8.

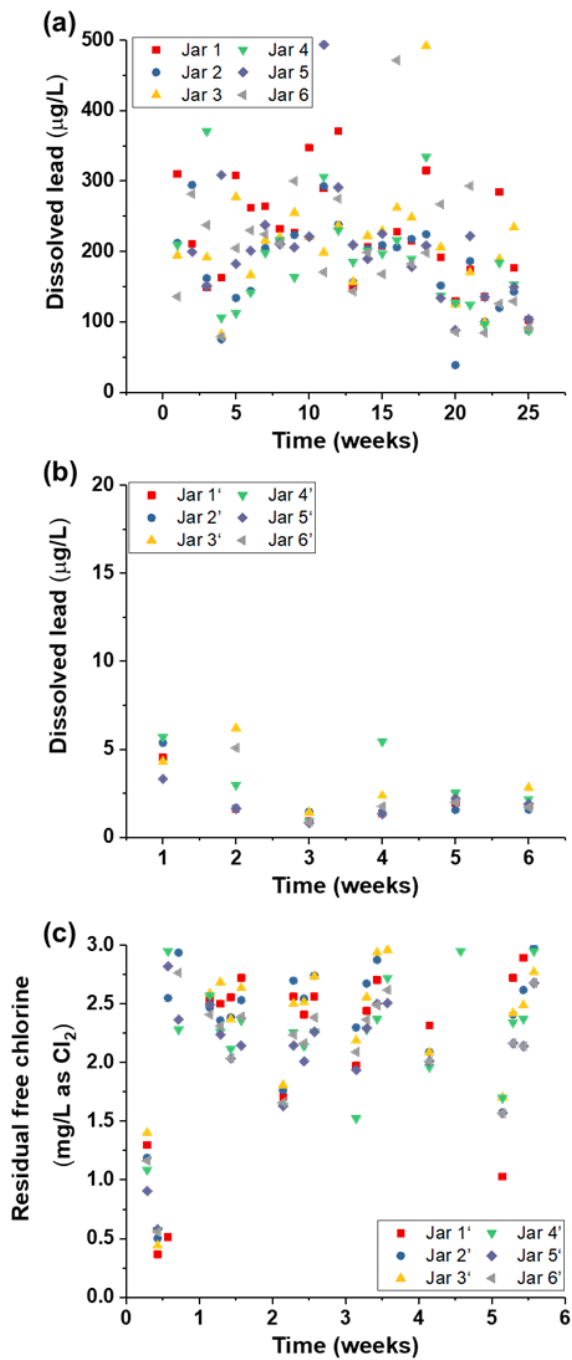


Figure A2.5 (a) Dissolved lead concentrations for Jar 1-Jar 6 during chemical conditioning at 40 mg/L free chlorine (25 weeks in total) (b) Dissolved lead concentrations and (c) residual free chlorine for Jar 1'-Jar 6' during chemical conditioning at 3 mg/L free chlorine (6 weeks in total). At the end of week 25, the best-conditioned coupon from Jar 1-Jar 6 was selected for subsequent testing, and the corresponding jars were labeled Jar 1'-Jar 6' and underwent conditioning for additional 6 weeks.

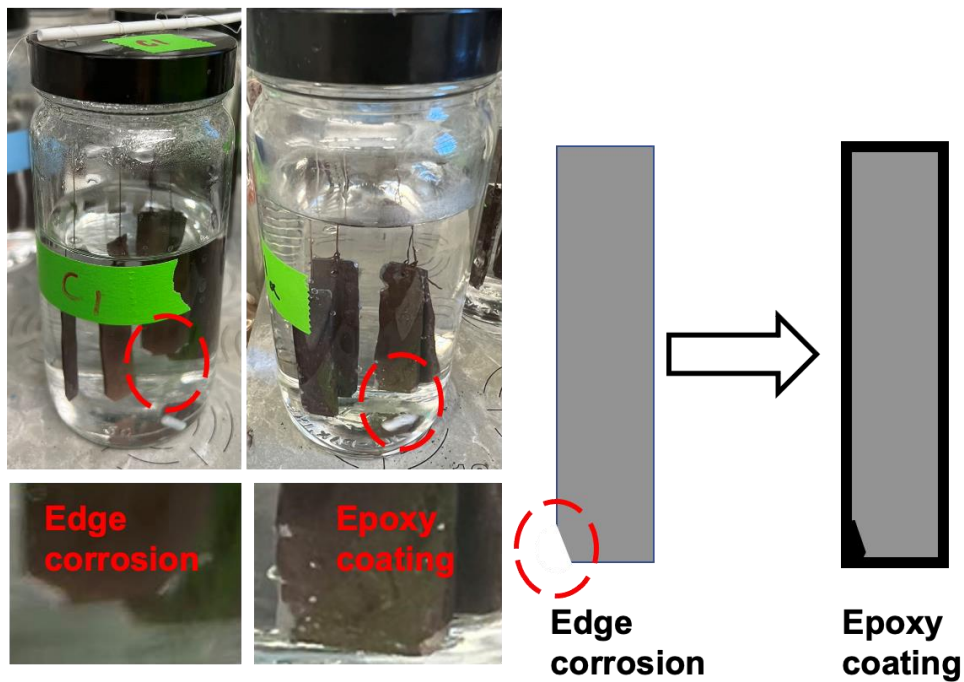


Figure A2.6 Edge corrosion on lead coupons and the application of epoxy coating to address it.

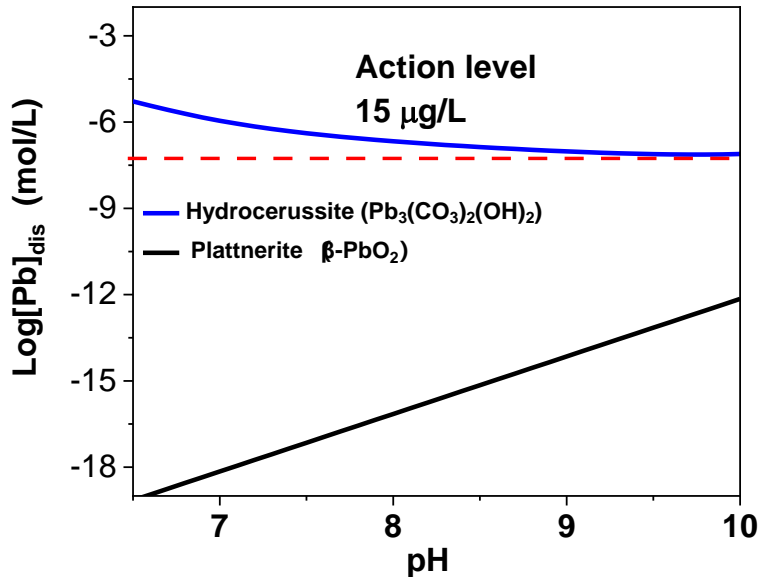


Figure A2.7 Equilibrium lead solubility for artificial water used in this study. Calculations were performed using Visual MINTEQ3.1 and its default database (relevant reactions indicated in Table A2.4). Equilibrium solubility of planerite (β - PbO_2) was calculated as the summation of the Pb^{4+} and the hydrolysis complexes PbO_3^{2-} and PbO_4^{4-} according to Table A2.5.

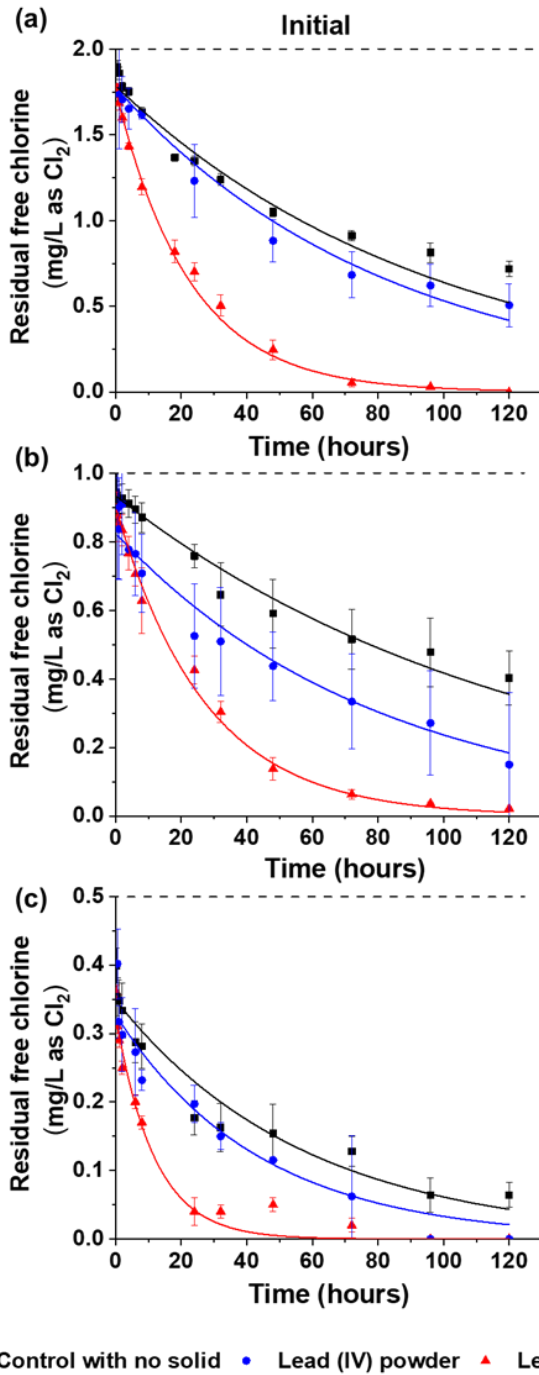


Figure A2.8 Free chlorine decay with lead coupons with PbO₂-rich scale, bare lead coupons, and without lead coupons over 5 days of stagnation at initial concentrations of (a) 2.0 mg/L (b) 1.0 mg/L and (c) 0.5 mg/L as Cl₂. The lines represent the fitted first-order kinetic model, and the error bars denote standard deviations calculated from the triplicate samples.

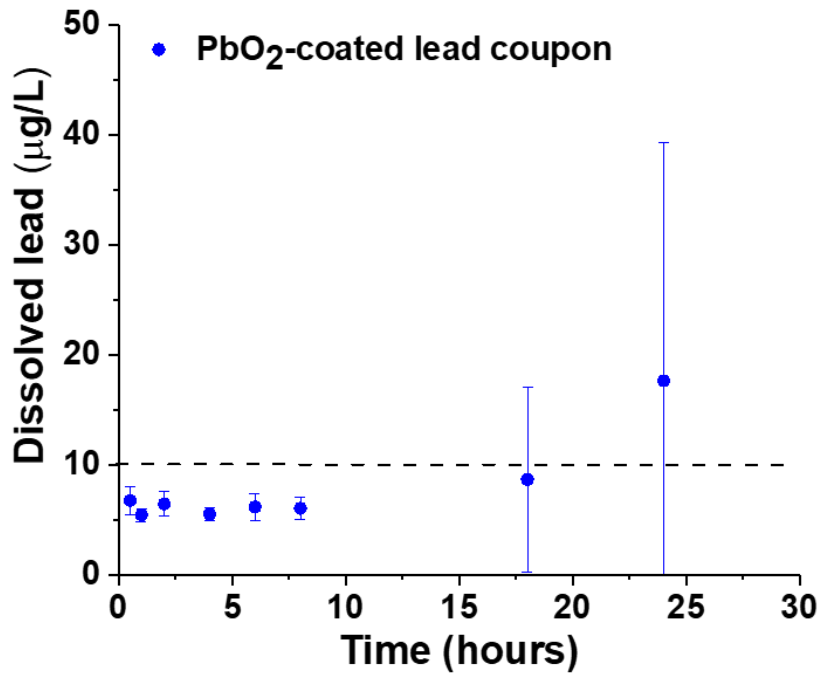


Figure A2.9 Dissolved lead concentration changes without the presence of free chlorine for PbO₂-coated lead coupon. The error bars denote standard deviations calculated from the triplicate samples.

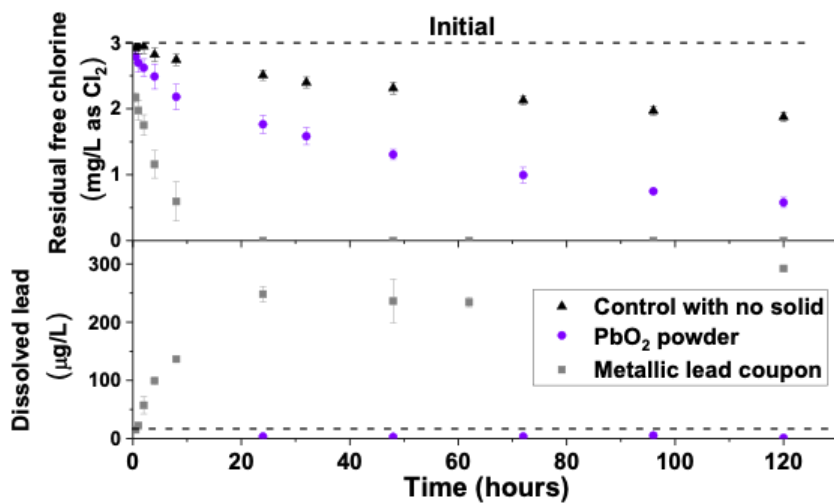


Figure A2.10 Dissolved lead concentration changes without free chlorine control at an initial concentration of 3.0 mg/L for metallic lead coupon and PbO₂ powder. The error bars denote standard deviations calculated from the triplicate samples.

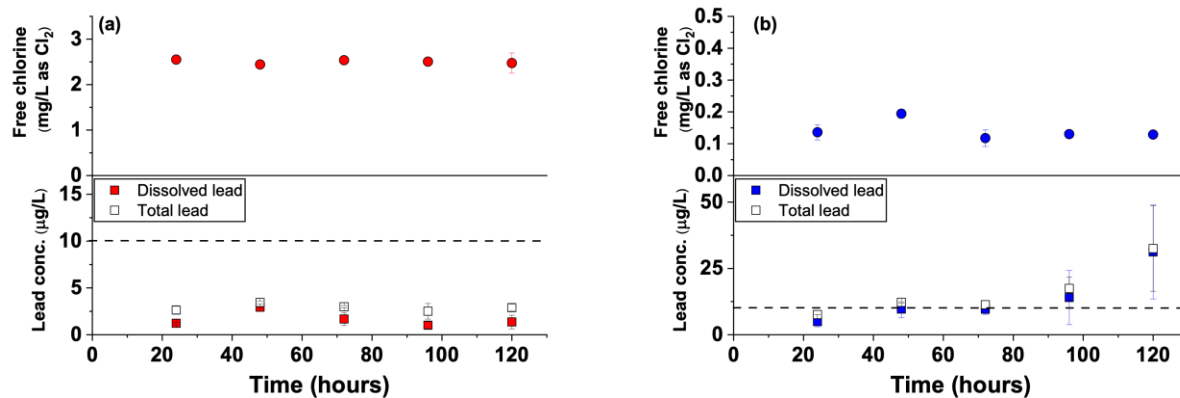


Figure A2.11 Dissolved and total lead concentrations with free chlorine controlled at constant concentrations of (a) 2-3 mg/L and (b) 0.1-0.2 mg/L. The error bars denote standard deviations calculated from the duplicate experiments.

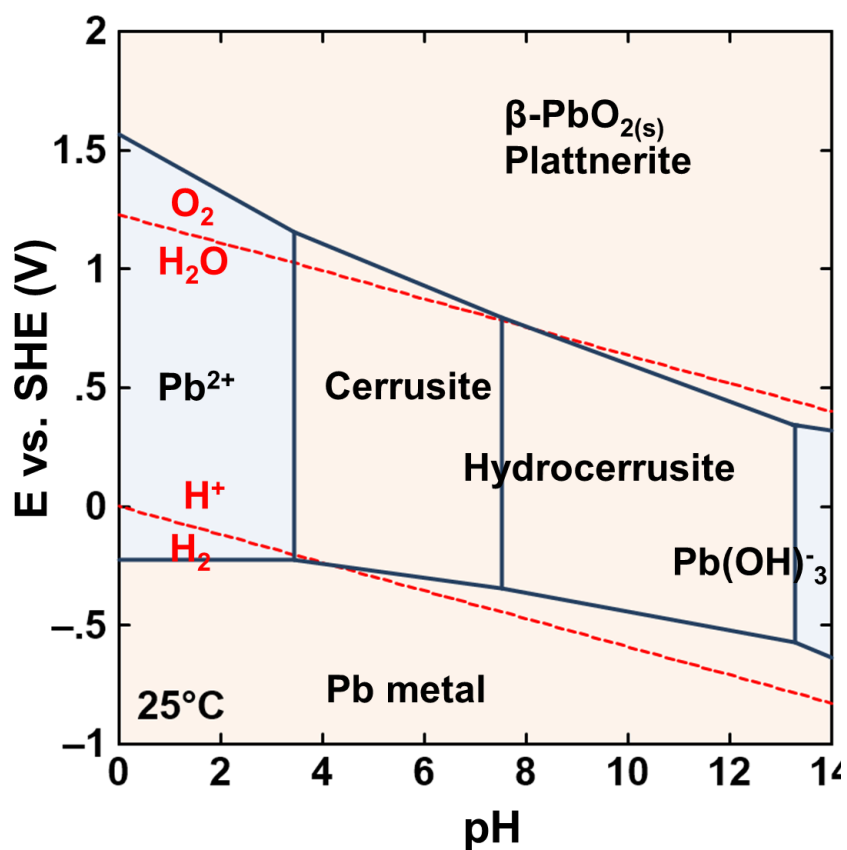


Figure A2.12. Eh-pH diagram for lead species in water system (Lead species = 0.015 mg/L, DIC= 14 mg/L as C) constructed using The Geochemist's Workbench 2023.

Table A2.1 Synthetic water composition.

Species	Synthetic Water	Units
pH	8.02	pH unit
Ca ²⁺	31.70	mg/L
Mg ²⁺	10.33	mg/L
Na ⁺	10.75	mg/L
K ⁺	18.80	mg/L
SO ₄ ²⁻	23.00	mg/L as SO ₄
NO ₃ ⁻	0.64	mg/L as NO ₃ -N
Cl ⁻	21.00	mg/L
Calcium hardness as CaCO ₃	79.25	mg/L as CaCO ₃
Alk as CaCO ₃	91.26	mg/L as CaCO ₃
DIC	22.60	mg/L as C
TDS	170.00	mg/L

Table A2.2 Syringe pump operational parameters.

Target free chlorine concentration in jars (mg/L)	Free chlorine concentration for readjustment in the syringe (mg/L)	Flow rate (μL/hour)
0.3-0.4	20	350~400
0.2-0.3	20	270~330
0.1-0.2	20	190~240

Table A2.3 Half-reactions associated with lead(IV) oxide interactions with free chlorine.

#	Reaction	E ⁰ (V vs SHE)	Log K
1	$Pb^{2+} + 2e^{-} \rightleftharpoons Pb^0$	4.25	0.13
2	PbO_2 (Plattnerite) + 4H ⁺ + 2e ⁻ \rightleftharpoons Pb ²⁺ + 2H ₂ O	1.47	49.60
3	$HOCl + H^{+} + 2e^{-} \rightarrow +Cl^{-} + H_2O$	1.48	50.20

Note: All reactions and constants are from Visual MINTEQ 3.1.

Table A2.4 Dissolution-precipitation and aqueous reactions involving lead in the system.

#	Reaction	Log K
1	$PbCO_3$ (s) (Cerussite) \rightleftharpoons Pb ²⁺ + CO ₃ ²⁻	-13.20
2	$Pb_3(CO_3)_2(OH)_2$ (s) (Hydrocerussite) + 2H ⁺ \rightleftharpoons 3Pb ²⁺ + 2CO ₃ ²⁻ + 2H ₂ O	-18.76
3	PbO (Litharge) + 2H ⁺ \rightleftharpoons Pb ²⁺ + H ₂ O \leftrightarrow	-12.69
4	PbO_2 (Plattnerite) + 4H ⁺ + 2e ⁻ \rightleftharpoons Pb ²⁺ + 2H ₂ O	49.60
5	$Pb(OH)_2$ (s) + 2H ⁺ \rightleftharpoons Pb ²⁺ + 2H ₂ O	8.15
6	$Pb^{2+} + CO_3^{2-} \rightarrow PbCO_3$ (aq)	6.53
7	$Pb^{2+} + 2CO_3^{2-} \rightarrow Pb(CO_3)_2^{2-}$	9.94
8	$Pb^{2+} + CO_3^{2-} \rightarrow PbHCO_3^{+}$	13.23
9	$Pb^{2+} + H_2O \rightarrow PbOH^{+} + H^{+}$	-7.60
10	$Pb^{2+} + 2H_2O \rightarrow Pb(OH)_2 + 2H^{+}$	-17.09
11	$Pb^{3+} + 3H_2O \rightarrow Pb(OH)_3 + 3H^{+}$	-28.09
12	H_2CO_3 (aq) \rightarrow 2H ⁺ + CO ₃ ²⁻	-16.68
13	$HCO_3^{-} \rightarrow H^{+} + CO_3^{2-}$	-10.33
14	$HOCl \rightarrow H^{+} + OCl^{-}$	-7.53

Note: All reactions and constants are from Visual MINTEQ 3.1.

Table A2.5 Reactions associated with planerite (β -PbO₂) dissolution.

#	Reaction	Log K
1	$PbO_{2(s)}(Planerite) + 4H^+ \rightarrow Pb^{4+} + 2H_2O$	-8.91
2	$Pb^{4+} + 3H_2O \rightarrow PbO_3^{2-} + 6H^+$	-23.04
3	$Pb^{4+} + 3H_2O \rightarrow PbO_4^{4-} + 8H^+$	-63.80

Table A2.6 Redox potentials corresponding to different free chlorine concentrations.

Free Chlorine Concentration (mg/L)	Measured Redox Potential (mV vs Ag/AgCl in saturated KCl)	Measured Redox Potential (mV vs SHE)	Theoretical Redox Potential (mV vs SHE)
0.1	391±11	588±11	1148
0.2	443±7	640±7	1157
0.3	486±4	683±4	1162
0.4	512±4	709±4	1166
0.5	529±5	726±5	1169
1.0	659±7	856±7	1177
2.0	710±4	907±4	1186
3.0	737±2	934±2	1192

Note: $X \pm Y$ with X as the mean of the duplicate and Y as the standard deviation.

Appendix A3: Supporting Information for

Chapter 4

A3.1 Harvesting Procedures for Pipes

The harvesting procedures were designed to minimize disruption to both the pipes and the scales on their inner surfaces:

1. Use a tube cutter or a ratcheted guillotine blade (e.g., a PVC cutter) to cut the lead pipe, avoiding abrasive cutting wheels.
2. Drain the water from the pipe.
3. Insert a damp sponge into each end of the pipe, taking care not to disturb the pipe scales. Seal both ends with duct tape; plastic wrap may be used beneath the duct tape for additional sealing.
4. Wrap the exterior of the pipe with a single layer of bubble wrap.

A3.2 Set-up of Pipe-loop Reactors

The harvesting procedures were carefully followed to ensure minimal disturbance to both the pipes and the scales lining their inner surfaces. Each pipe had an inner diameter of approximately 1.9 cm (0.75 inches) and was composed of one 45.7 cm (18-inch) section along with three 10.2 cm (4-inch) sections. These segments, originally from the same pipe, were reassembled in their initial sequence using rubber connectors, PVC pipes, and plastic tubing. To prevent contact

between cut surfaces and water, they were completely coated with epoxy (J-B Weld 8281 Professional). A magnetic drive pump and a 10-liter reservoir facilitated water recirculation in each pipe loop (Figure A3.2b), with valves and flowmeters providing control and monitoring of the flow rate.

A3.3 Preparation of Water Chemistry

Each pipe loop received freshly prepared artificial water every Monday and the water temperature was maintained at approximately 24-26 °C. This artificial water was prepared using reverse osmosis (RO) water with the addition of the following chemicals: calcium chloride dihydrate ($\text{CaCl}_2 \cdot 2\text{H}_2\text{O}$, Sigma-Aldrich), sodium bicarbonate (NaHCO_3 , Sigma-Aldrich), potassium bicarbonate (KHCO_3 , Sigma-Aldrich), magnesium chloride hexahydrate ($\text{MgCl}_2 \cdot 6\text{H}_2\text{O}$, Sigma-Aldrich), sodium nitrate (NaNO_3 , Sigma-Aldrich), magnesium sulfate (MgSO_4 , Sigma-Aldrich), aluminum chloride hexahydrate ($\text{AlCl}_3 \cdot 6\text{H}_2\text{O}$, Sigma-Aldrich), and sodium fluoride (NaF , Sigma-Aldrich). Sodium hydroxide (NaOH , Sigma-Aldrich) solutions and sulfuric acid (H_2SO_4 , Sigma-Aldrich) were used to adjust the pH. Free chlorine was prepared by diluting sodium hypochlorite (NaOCl , 4-6%/Laboratory, Fisher Scientific) to 2000 mg/L as Cl_2 .

A3.4 Scale Analysis

The harvested lead pipes were manually sectioned into two transverse segments using a hacksaw for the purpose of scale collection and analysis. Scales were collected by carefully scraping them

from the inner surface of each segment with a stainless-steel spatula. The scales removed from the inner pipe surface may comprise multiple layers, which can be differentiated by variations in color, crystalline phase, and elemental composition.

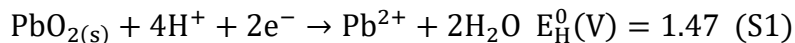
The crystalline phases in the scale were identified using X-ray diffraction (XRD) (Bruker d8 Advance). Samples were secured in an MTI 1-inch low-background Si sample holder and scanned with copper K α radiation over a 2θ range of 5 to 80° with a step size of 0.02°. The XRD patterns were analyzed by comparing the diffraction data to a reference database from the International Centre for Diffraction Data (ICDD). The elemental composition of the scale was determined using inductively coupled plasma mass spectrometry (ICP-MS) (NexION 2000). The scales were first weighed and then digested in a 3:1 mixture of concentrated hydrochloric and nitric acids at 100°C for two hours to prepare them for quantitative elemental analysis by ICP-MS.

The morphology of the scale was examined using scanning electron microscopy (SEM) (Quattro S E-SEM, Thermo Fisher). Elemental distribution within the scales was analyzed using energy dispersive X-ray spectroscopy (EDS) (AzTec, Oxford). These analyses involved examinations of both a cross section and a transverse section of the pipe segment. To prepare the cross section, one end of the pipe was filled with a mixture of hardener and epoxy resin (18 wt.%). After the epoxy had cured, the section was cut from the rest of the segment and polished with sandpapers of progressively finer grit (up to 1200 grit). Polishing was performed with mineral oil on the

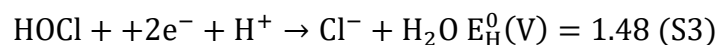
sandpaper to reduce the generation of airborne particles. The polished segment was then cleansed with ethanol to remove any residual mineral oil before characterization using SEM-EDS.

A3.5 Calculations of Equilibrium Threshold Free Chlorine for Thermodynamic Stability of PbO₂

Two key half reactions (S1 and S2) in the solution govern the stability of PbO₂. In the solution that has a dissolved lead of 15 µg/L (7.2×10^{-8} mol/L), the molar concentration of Pb²⁺ is around 1.8×10^{-12} mol/L (Shown in S7, calculated by MINEQL+ 5.0 with water chemistry parameters from Table A3.1). The redox potential for PbO₂/Pb²⁺ at pH 8 is calculated to be 0.87 V (vs SHE) (S3). For the half reaction of HOCl/Cl⁻ (shown in S4), its redox potential must equal or exceed the environmental redox potential of PbO₂/Pb²⁺ to prevent PbO₂ from being reduced to Pb²⁺. At the water chemistry of the experiments with a pH of 8 and Cl⁻ concentration of 21 mg/L (equivalent to 6.1×10^{-4} mol/L), the calculated threshold concentration of HOCl in the solution is 3.78×10^{-16} mol/L. Accounting for the pK_a of the acid dissociation reaction of HOCl/OCl⁻ (S5), the threshold free chlorine in the system to maintain the stability of PbO₂ is calculated to be 5.06×10^{-16} mol/L, equivalent to 3.59×10^{-11} mg/L as Cl₂.



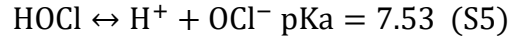
$$E_{\text{H1}} = E_{\text{H}}^0 - \frac{0.059}{2} \log \frac{[\text{Pb}^{2+}]}{[\text{H}^+]^4} = 1.47 - 0.059 \log \frac{[1.8 \times 10^{-12}]}{[10^{-8}]^4} = 0.87 \text{ V} \quad (\text{S2})$$



$$E_{H2} = E_H^0 - \frac{0.059}{2} \log \frac{[Cl^-]}{[H^+][HOCl]} = 1.49 - \frac{0.059}{2} \log \frac{[6.1 \times 10^{-4}]}{[10^{-8}][HOCl]} \quad (S4)$$

$$E_{H1} = E_{H2}$$

$$\rightarrow [HOCl] = 1.28 \times 10^{-16} \text{ mol/L}, \quad [OCl] = 3.78 \times 10^{-16} \text{ mol/L}$$



$$\frac{[H^+][OCl^-]}{[HOCl]} = 10^{-7.53}$$

$$[HOCl] + [OCl] = 5.06 \times 10^{-16} \text{ mol/L}$$

$$\text{Free chlorine} = 3.59 \times 10^{-11} \text{ mg/L as Cl}_2$$

A3.6 Calculations of the Proportion of Pb Released from Scales

Pipe scale thickness: 50 μm

Pipe diameter: 0.75 cm

Pipe length: 76.2 cm

$$\text{Area of PbO}_2 \text{ in a pipe: } \left(\frac{0.75}{2}\right)^2 \times 3.14 \times 76.2 = 34 \text{ cm}^2$$

$$\text{Volume of PbO}_2 \text{ in a pipe} = 34 \times 5 \times 10^{-3} = 0.17 \text{ cm}^3$$

$$\text{Mass of Pb in a pipe: } 0.17 \text{ cm}^3 \times 9.38 \text{ g/cm}^3 (\text{PbO}_2 \text{ density}) \times \frac{207 (\text{Molar mass of Pb})}{239 (\text{Molar mass of PbO}_2)} = 1.4 \text{ g}$$

$$\text{Mass of Pb in a water reservoir (10 L): } 100 \mu\text{g/L} \times 10 \text{ L} = 1 \text{ mg}$$

Mass percentage of Pb in a water reservoir to Pb in a pipe = $\frac{1}{1400} = 0.07\%$

Note: The scale composition was assumed to be pure PbO₂ for simplification, and a lead concentration of 100 µg/L was selected as representative of the maximum lead release.

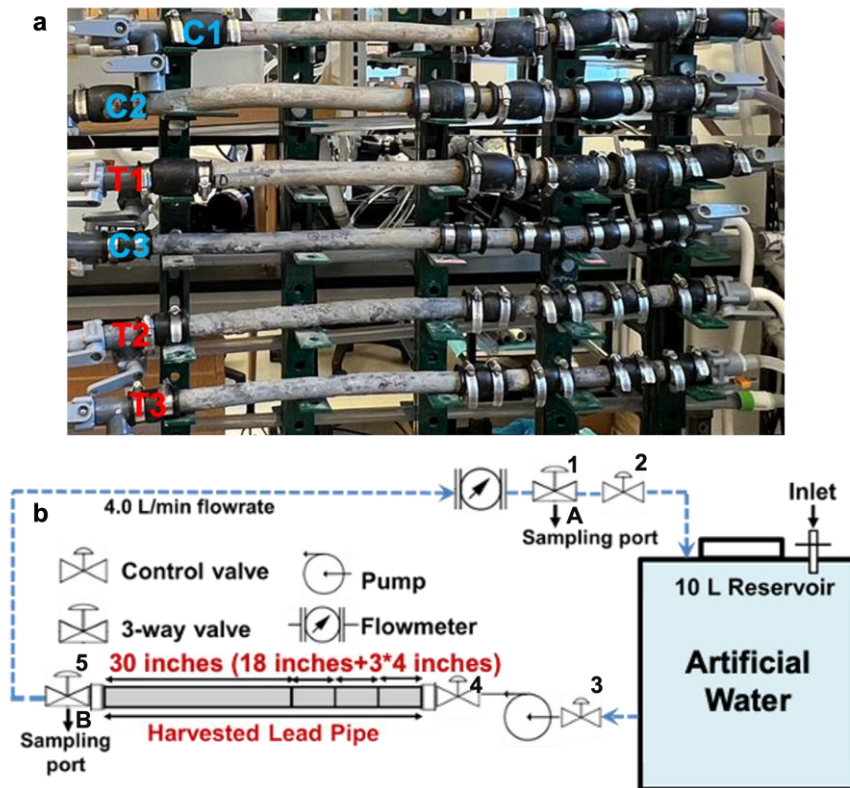


Figure A3.1 (a) Pipe loop reactors, with C for control pipes and T for test pipes. (b) Schematic diagram of a pipe loop consisting of a pump, valves, flowmeter and reservoir. The harvested lead pipe assembly consists of one 18-inch section and three 4-inch segments that are connected with rubber connectors. The 4-inch segments allow scale analysis to be performed at different stages in the experiment while retaining the majority of the lead pipe length in the reactor.

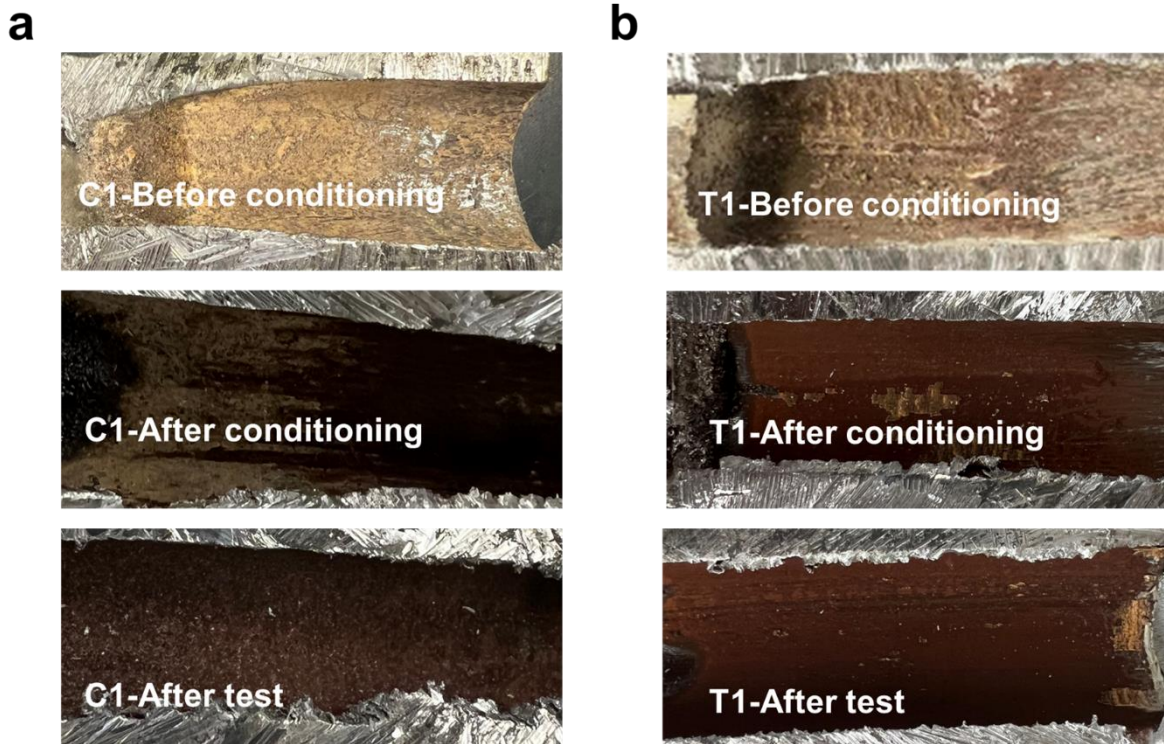


Figure A3.2 Longitudinal cross-sections of (a) control pipe C1 and (b) test pipe T1 collected before conditioning, after conditioning, and after test.

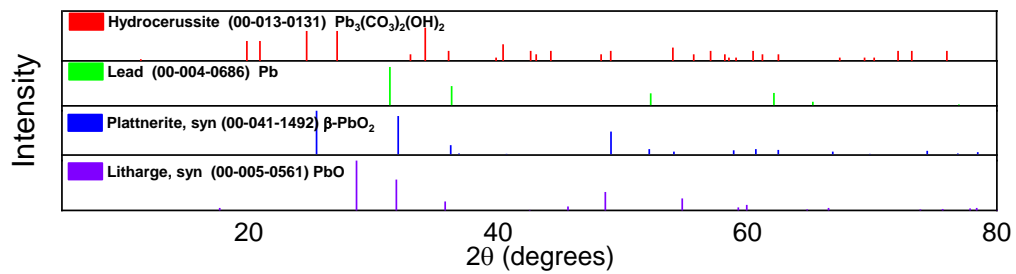


Figure A3.3 XRD Reference patterns for hydrocerussite ($Pb_3(CO_3)_2(OH)_2$), lead (Pb), plattnerite (β - PbO_2) and litharge (PbO).

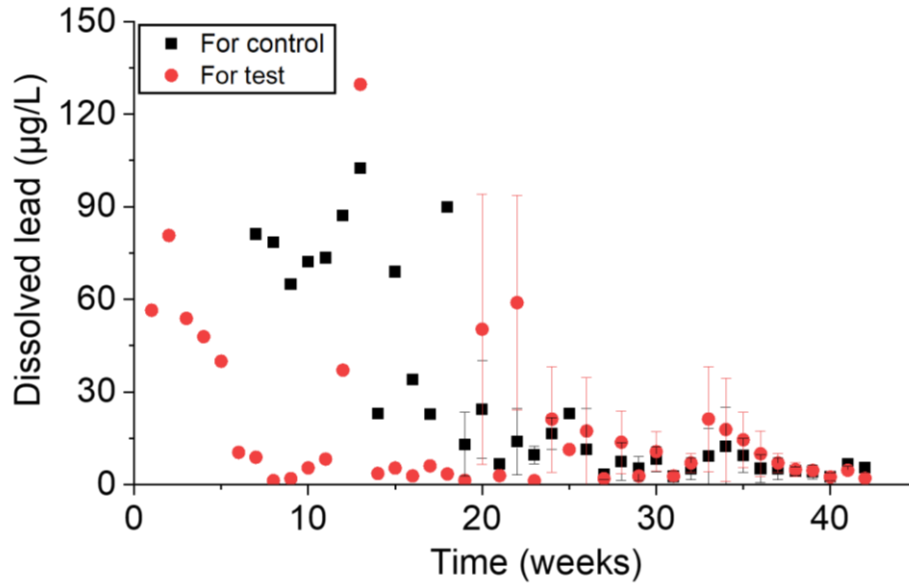


Figure A3.4 Dissolved lead concentrations during conditioning (Free chlorine: 3 mg/L as Cl₂) for pipe loops to be used as control and test groups. Error bars denote standard deviations calculated from the triplicate pipe loops. Before Week 19, only two pipes were available for conditioning, one for each group, thus no error bars are presented for that period.

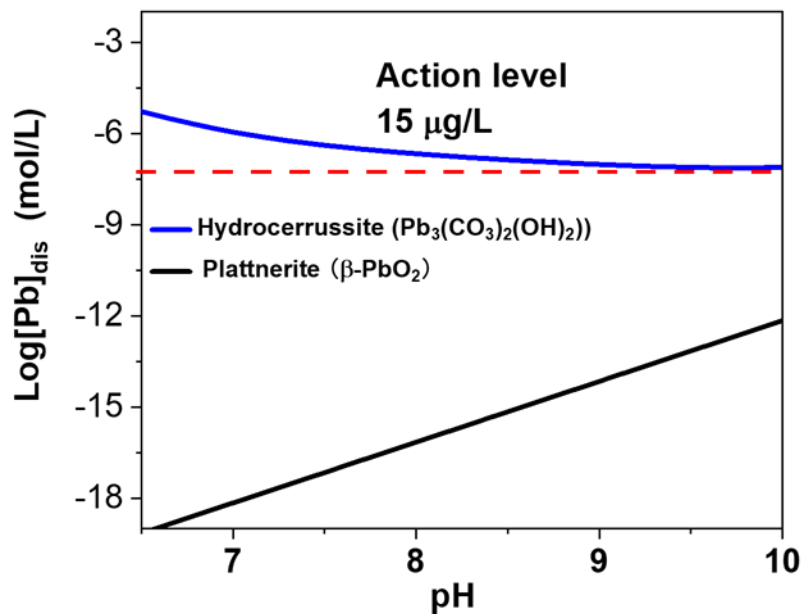


Figure A3.5 Equilibrium lead solubility for the artificial water used in this study. Calculations were performed using Visual MINTEQ3.1 and its default database (relevant reactions indicated in Table A3.4). Equilibrium solubility of plattnerite (β-PbO₂) was calculated as the summation of the Pb⁴⁺ and the hydrolysis complexes PbO₃²⁻ and PbO₄⁴⁻ according to Table A3.5.

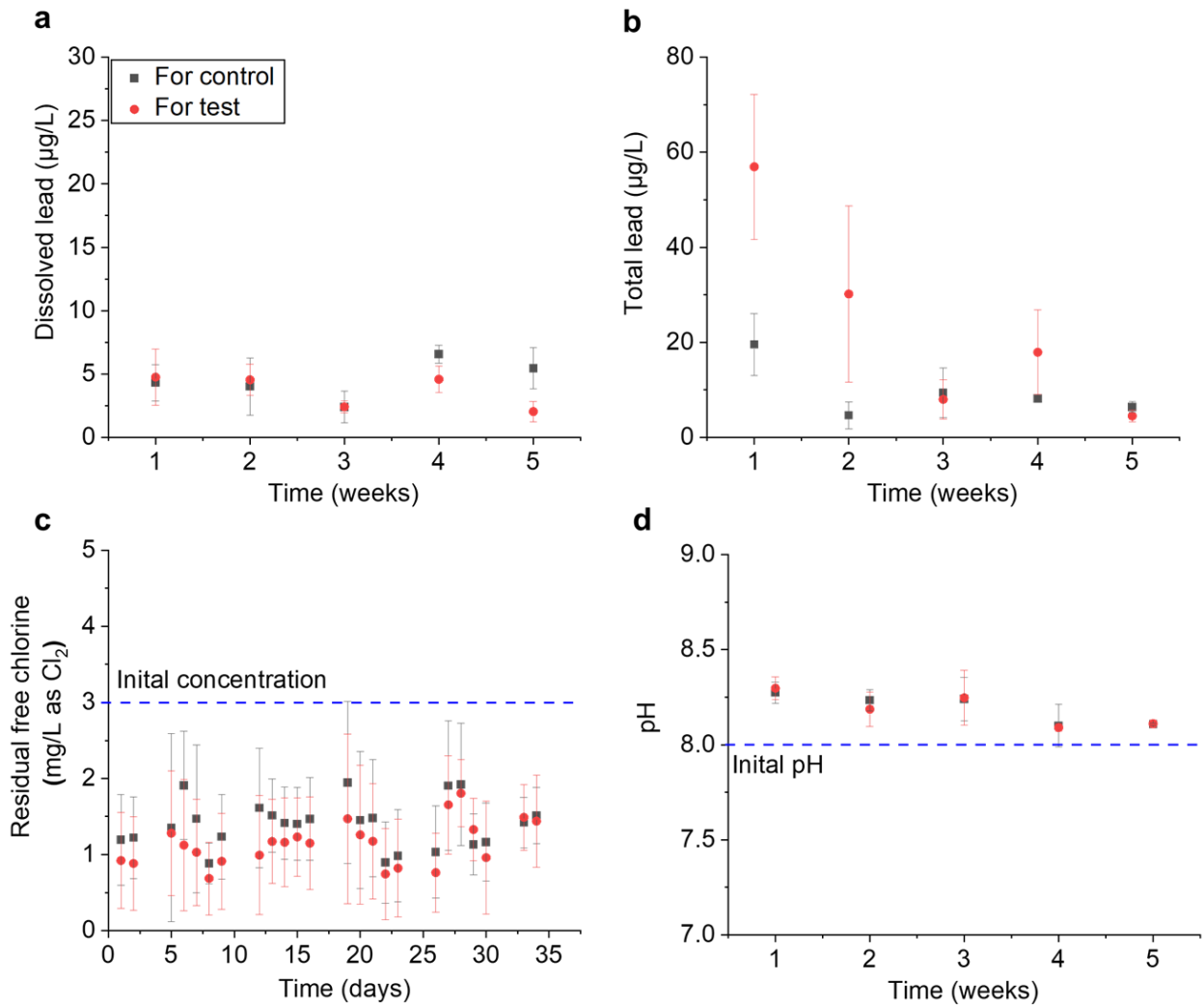


Figure A3.6 (a) Dissolved lead concentrations; (b) Total lead concentrations; (c) Residual free chlorine; and (d) pH during the last five weeks of conditioning (Weeks 38 to 42) for pipe loops to be used as control and test groups in the test phase. Free chlorine was adjusted to the initial value every day, and pH was adjusted to the initial value every week. Error bars denote standard deviations calculated from the triplicate pipe loops.

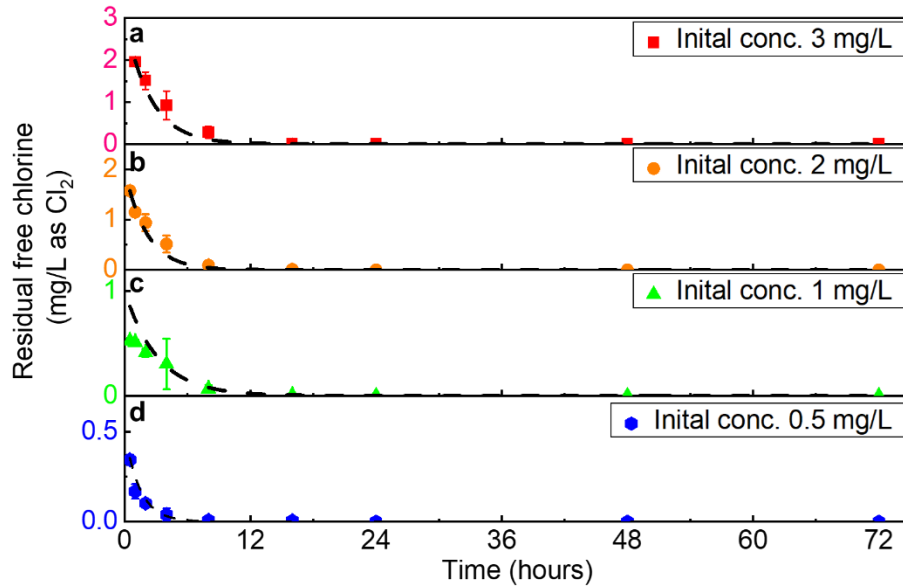


Figure A3.7 Free chlorine decay in lead pipe loops over three days of stagnation at initial concentrations of (a) 3.0 mg/L (b) 2.0 mg/L (c) 1.0 mg/L and (d) 0.5 mg/L as Cl₂. The lines represent the fitted first-order kinetic model, and the error bars denote standard deviations calculated from the triplicate pipe loops.

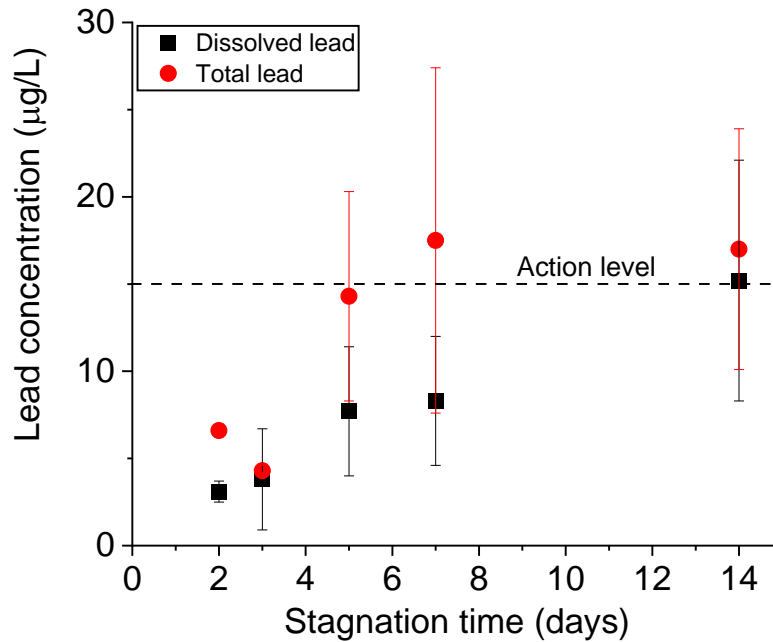


Figure A3.8 Stagnation experiment (up to 14 days) for dissolved and total lead concentrations at initial free chlorine of 3.0 mg/L. The error bars denote standard deviations calculated from triplicate experiments.

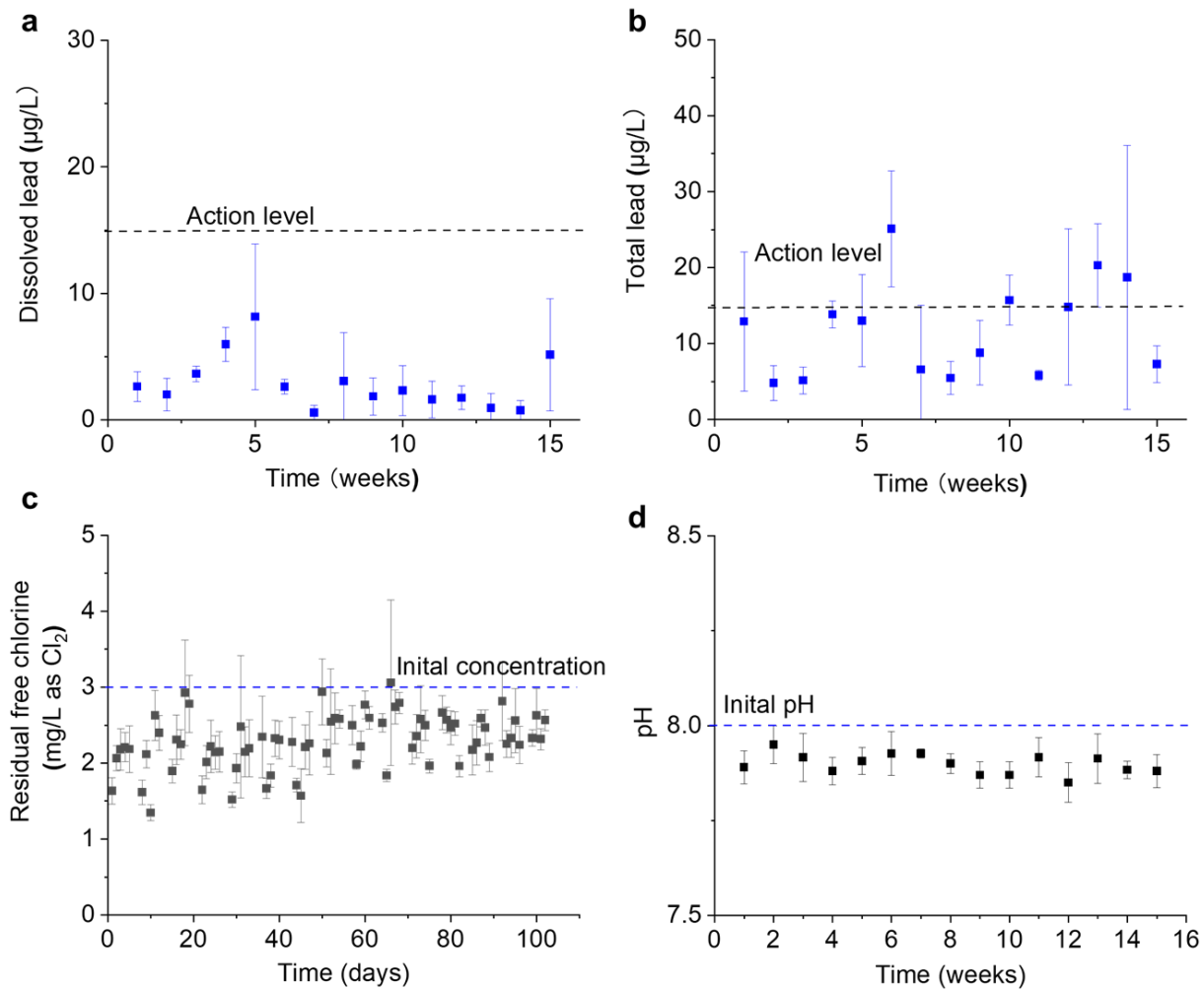


Figure A3.9 (a) Dissolved lead concentrations; (b) Total lead concentrations; (c) Residual free chlorine; and (d) pH for control pipe loops after conditioning. Free chlorine was adjusted to the initial value every day and the pH was adjusted to the initial value every week. Error bars denote standard deviations calculated from the triplicate pipe loops.

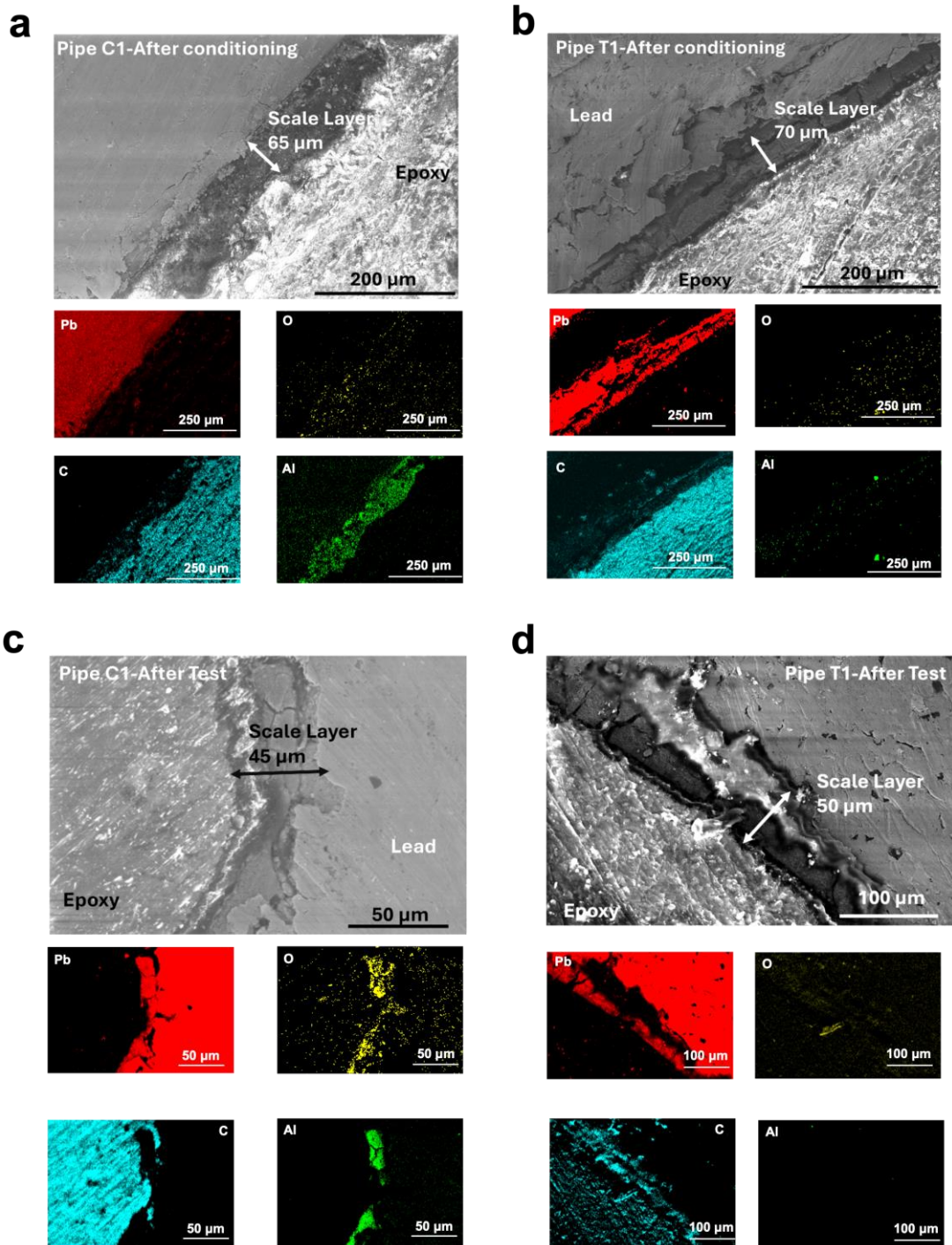


Figure A3.10 SEM images and elemental mapping of lead (Pb), oxygen (O), carbon (C), and aluminum (Al) of the cross-section of the pipes for (a) control pipe C1 after conditioning, (b) control pipe C1 after test, (c) test pipe T1 after conditioning, and (d) test pipe T1 after test.

Table A3.1 Synthetic water composition compared to actual water.

Species	Actual Water	Synthetic Water	Units
pH	8.0	8.0	mg/L
Ca ²⁺	36.0	31.7	mg/L
Mg ²⁺	9.2	10.3	mg/L
Na ⁺	13.1	10.8	mg/L
K ⁺	9.1	18.8	mg/L
SO ₄ ²⁻	21.0	23.0	mg/L as SO ₄
NO ₃ ⁻	0.5	0.6	mg/L as NO ₃ -N
Cl ⁻	21.6	21.0	mg/L
Calcium hardness as CaCO ₃	90.0	79.3	mg/L as CaCO ₃
Alk as CaCO ₃	105.0	91.3	mg/L as CaCO ₃
DIC	25.7	22.6	mg/L as C
TDS	135.8	170.0	mg/L

Table A3.2 Initial concentration and test time points during water stagnation experiments.

Initial concentrations (mg/L)	Test time points (hours)
3.0	1, 2, 4, 8, 16, 24, 48, 72
2.0	1, 2, 4, 8, 16, 24, 48, 72
1.0	1, 2, 4, 8, 16, 24, 48, 72
0.5	1, 2, 4, 8, 16, 24, 48, 72

Table A3.3 Syringe pump operational parameters.

Target free chlorine concentration in jars (mg/L)	Free chlorine concentration for readjustment in the syringe (mg/L)	Flow rate ($\mu\text{L}/\text{hour}$)
0.4-0.6	800	250~300
0.2-0.4	600	200~250
0 -0.2	600	100~150

Table A3.4 Potential dissolution-precipitation and aqueous reactions involving lead in the system.

#	Reaction	Log K
1	$PbCO_3(s) \text{ (Cerussite)} \rightleftharpoons Pb^{2+} + CO_3^{2-}$	-13.20
2	$Pb_3(CO_3)_2(OH)_2(s) \text{ (Hydrocerussite)} + 2H^+ \rightleftharpoons 3Pb^{2+} + 2CO_3^{2-} + 2H_2O$	-18.76
3	$PbO \text{ (Litharge)} + 2H^+ \rightleftharpoons Pb^{2+} + H_2O$	-12.69
4	$PbO_2 \text{ (Plattnerite)} + 4H^+ + 2e^- \rightleftharpoons Pb^{2+} + 2H_2O$	49.60
5	$Pb(OH)_2(s) + 2H^+ \rightleftharpoons Pb^{2+} + 2H_2O$	8.15
6	$Pb^{2+} + CO_3^{2-} \rightarrow PbCO_3(aq)$	6.53
7	$Pb^{2+} + 2CO_3^{2-} \rightarrow Pb(CO_3)_2^{2-}$	9.94
8	$Pb^{2+} + CO_3^{2-} \rightarrow PbHCO_3^+$	13.23
9	$Pb^{2+} + H_2O \rightarrow PbOH^+ + H^+$	-7.60
10	$Pb^{2+} + 2H_2O \rightarrow Pb(OH)_2 + 2H^+$	-17.09
11	$Pb^{3+} + 3H_2O \rightarrow Pb(OH)_3 + 3H^+$	-28.09
12	$H_2CO_3(aq) \rightarrow 2H^+ + CO_3^{2-}$	-16.68
13	$HCO_3^- \rightarrow H^+ + CO_3^{2-}$	-10.33
14	$HOCl \rightarrow H^+ + OCl^-$	-7.53

Note: All reactions and constants are from Visual MINTEQ default database: NIST Standard Reference Database 46.

Table A3.5 Reactions associated with plattnerite (β - PbO_2) dissolution.

#	Reaction	Log K
1	$PbO_{2(s)}(Plattnerite) + 4H^+ \rightarrow Pb^{4+} + 2H_2O$	-8.91
2	$Pb^{4+} + 3H_2O \rightarrow PbO_3^{2-} + 6H^+$	-23.04
3	$Pb^{4+} + 3H_2O \rightarrow PbO_4^{4-} + 8H^+$	-63.80

Table A3.6 Summary of lead concentrations (dissolved and total lead), residual free chlorine, and pH for pipes designated for control and test during the final five weeks of conditioning.

ID	Dissolved lead ($\mu\text{g/L}$)	Total lead ($\mu\text{g/L}$)	Residual free chlorine (mg/L as Cl_2)	pH
Control pipes	4.6 ± 1.8	27.8 ± 36.0	1.2 ± 0.6	8.2 ± 0.1
Test pipes	3.5 ± 1.6	23.5 ± 21.2	1.4 ± 0.6	8.2 ± 0.1
p-value (Two-tail)	0.14	0.70	0.02	0.70

Note: Dissolved lead defined as the lead concentration passing a 0.22 μm filter. This table presents an average of three distinct pipe replicates for the control and test pipes for the final five weeks of each stage. $X \pm Y$ with X as the mean and Y as the standard deviation.

Table A3.7 Mass percentage (w%) of the elements in lead solids.

Sample ID	Pb	C	O	H
Plattnerite (β -PbO ₂)	86.6	0	13.4	0
Hydrocerussite (Pb ₃ (CO ₃) ₂ (OH) ₂)	80.0	3.1	16.5	0.4
Litharge (PbO)	92.8	0	7.2	0

Table A3.8 Kinetic parameters of free chlorine decay

ID	first order rate constant (k) h ⁻¹	R ²
3-Cl ₂	0.34	0.99
2- Cl ₂	0.38	0.99
1- Cl ₂	0.34	0.86
0.5- Cl ₂	0.56	0.91

Note: “3”, “2”, “1”, and “0.5” before “-” refers to the initial free chlorine concentration (mg/L) dosed to the system; “Cl₂” refers to a condition that only have free chlorine; “PbO₂” represents laboratory PbO₂ powder; “PbO₂ coupon” represents a lead coupon coated with PbO₂; “Pb coupon” represents a metallic lead coupon.

Appendix A4: Supporting Information for **Chapter 5**

A4.1 Formation of PbO₂ on Lead Coupons

A two-step method, combining electrochemical polarization and chemical conditioning, was employed to develop a PbO₂ layer on metallic lead coupons. The electrochemical polarization treatment was conducted at a potential of 1.43 V for two hours. After polarization, the coupons were rinsed with deionized water and conditioned with 40 mg/L of free chlorine (as Cl₂) for one week. Following this, the coupons were conditioned with 3 mg/L of free chlorine (as Cl₂) for 25 weeks. Prior to the reconditioning performed for this study, the coupons had undergone experiments in our previous research for approximately three months. X-ray diffraction (XRD) analysis identified plattnerite (β -PbO₂) as the dominant scale phase on the coupons before reconditioning (Figure A4.8).

A4.2 Set up of Pipe-loop Reactors

The harvesting procedures were carefully followed to ensure minimal disturbance to both the pipes and the scales lining their inner surfaces. Each pipe had an inner diameter of approximately 1.9 cm (0.75 inches) and was composed of one 45.7 cm (18-inch) section along with three 10.2 cm (4-inch) sections. These segments, originally from the same pipe, were reassembled in their initial sequence using rubber connectors, PVC pipes, and plastic tubing. To prevent contact between cut surfaces and water, they were completely coated with epoxy (J-B Weld 8281 Professional). A magnetic drive pump and a 10-liter reservoir facilitated water recirculation in each pipe loop (Figure A4.2b), with valves and flowmeters providing control and monitoring of the flow rate.

A4.3 Preparation of Water Chemistry

Artificial Erie County water was used for each pipe and the water temperature was maintained at approximately 24-26 °C. This water was prepared to replicate the key water chemistry of actual Erie County water, based on the 2022-2023 Erie County Water Quality Report and direct measurements of local tap water chemistry (Table A4.1). The reagents used to during artificial water preparation are listed as follows:

This artificial water was prepared using reverse osmosis (RO) water with the addition of the following chemicals: calcium chloride dihydrate ($\text{CaCl}_2 \cdot 2\text{H}_2\text{O}$, Sigma-Aldrich), sodium bicarbonate (NaHCO_3 , Sigma-Aldrich), potassium bicarbonate (KHCO_3 , Sigma-Aldrich), magnesium chloride hexahydrate ($\text{MgCl}_2 \cdot 6\text{H}_2\text{O}$, Sigma-Aldrich), sodium phosphate dibasic (Na_2HPO_4 , Sigma-Aldrich), sodium phosphate dibasic heptahydrate ($\text{NaH}_2\text{PO}_4 \cdot 7\text{H}_2\text{O}$, Sigma-Aldrich), sodium nitrate (NaNO_3 , Sigma-Aldrich), magnesium sulfate (MgSO_4 , Sigma-Aldrich), aluminum chloride hexahydrate ($\text{AlCl}_3 \cdot 6\text{H}_2\text{O}$, Sigma-Aldrich), and sodium fluoride (NaF , Sigma-Aldrich). Sodium hydroxide (NaOH , Sigma-Aldrich) solutions and sulfuric acid (H_2SO_4 , Sigma-Aldrich) were used to adjust water pH. Free chlorine was prepared by diluting sodium hypochlorite (NaOCl , 4-6%/Laboratory, Fisher Scientific) to 2000 mg/L as Cl_2 .

A4.4 Scale Analysis

The harvested lead pipes were manually cut into two transverse segments using a handsaw to facilitate scale collection and analysis. Scales were collected by carefully scraping them from the surface of the coupons and inner surface of each pipe segment using a stainless-steel spatula. The scales removed from the pipe's inner surface may consist of multiple layers, distinguishable by

differences in color, crystalline phase, and elemental composition. The top layer, in direct contact with the finished water, primarily serves as a sink for deposits from the water, where amorphous materials are predominant. The bottom layer, located closer to the underlying pipe material, represents the initial stage of solids formation at the interface between the finished water and the pipe material.

The morphology of the scale was examined using scanning electron microscopy (SEM) (Quattro S E-SEM, Thermo Fisher), while elemental distribution within the scales was analyzed through energy dispersive X-ray spectroscopy (EDS) (AzTec, Oxford). Both cross-sectional and transverse sections of the pipe segment were analyzed. To prepare the cross section, one end of the pipe was filled with a mixture of hardener and epoxy resin (18 wt.%). Once the epoxy cured, the section was cut from the rest of the segment and polished using progressively finer sandpapers (up to 1200 grit). Polishing was performed with mineral oil to minimize airborne particle generation. The polished segment was then cleaned with ethanol to remove any residual mineral oil before SEM-EDS characterization.

A4.5 Statistical Analysis

Statistical significance was determined using the Wilcoxon rank-sum test, given the small sample size and non-normal distribution of the data, with a significance threshold of 0.05.

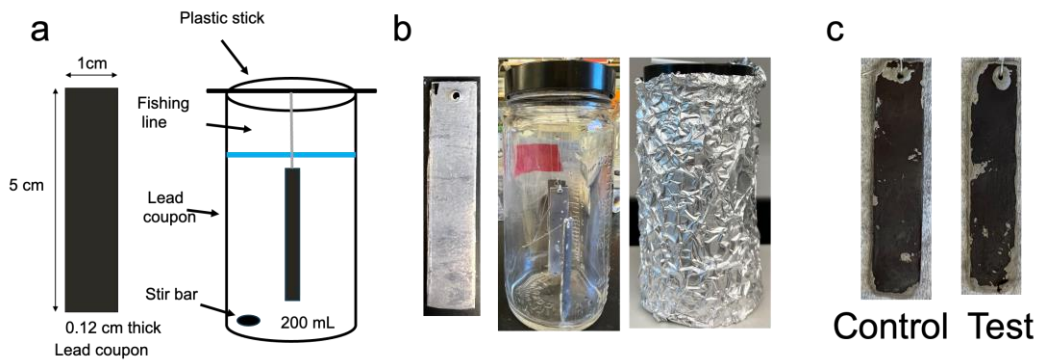


Figure A4.1 (a) Illustration of lead coupon experiments in beakers. (b) Images for a lead coupon, a jar with lead coupons and a jar covered by aluminum foil. (c) Control and test lead coupons after test.

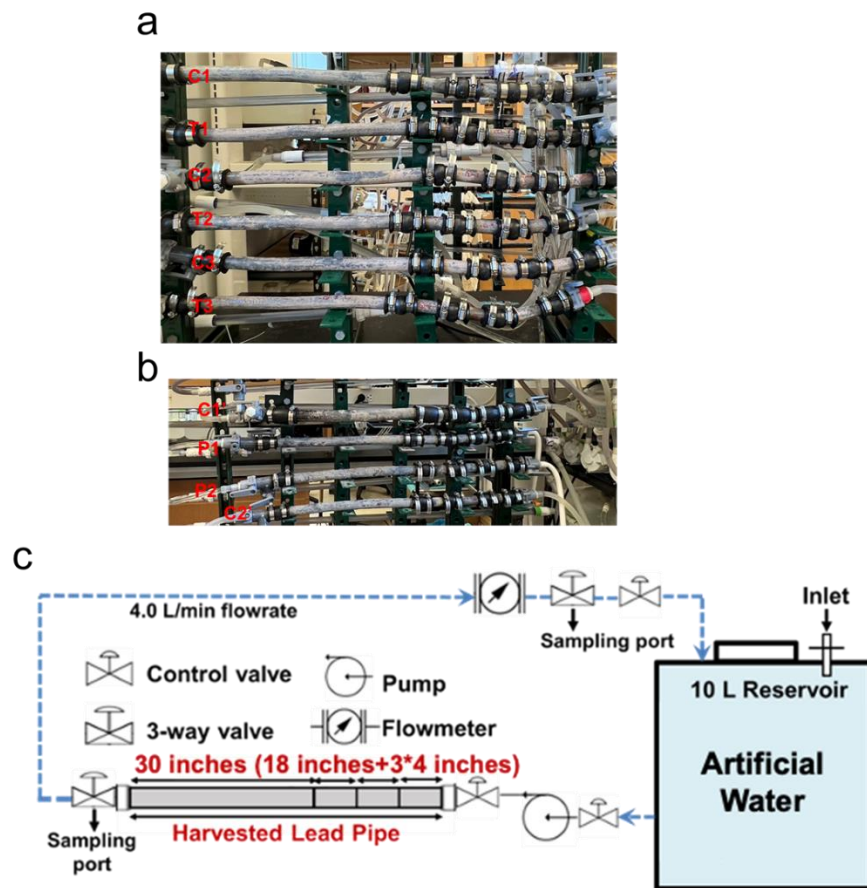


Figure A4.2 (a) Pipe loop reactors for C1-C3, and T1-T3. The pipes were used for real-world water use pattern experiments. (b) Pipe loop reactors for C1'-C2', and P1-P2. The pipes were used for stagnation and free chlorine experiments. (c) Schematic diagram of a pipe loop consisting of a pump, valves, flowmeter and reservoir. The harvested lead pipe assembly consists of one 18-inch section and three 4-inch segments that are connected with rubber connectors. The 4-inch segments allow scale analysis to be performed at different stages in the experiment while retaining the majority of the lead pipe length in the reactor.

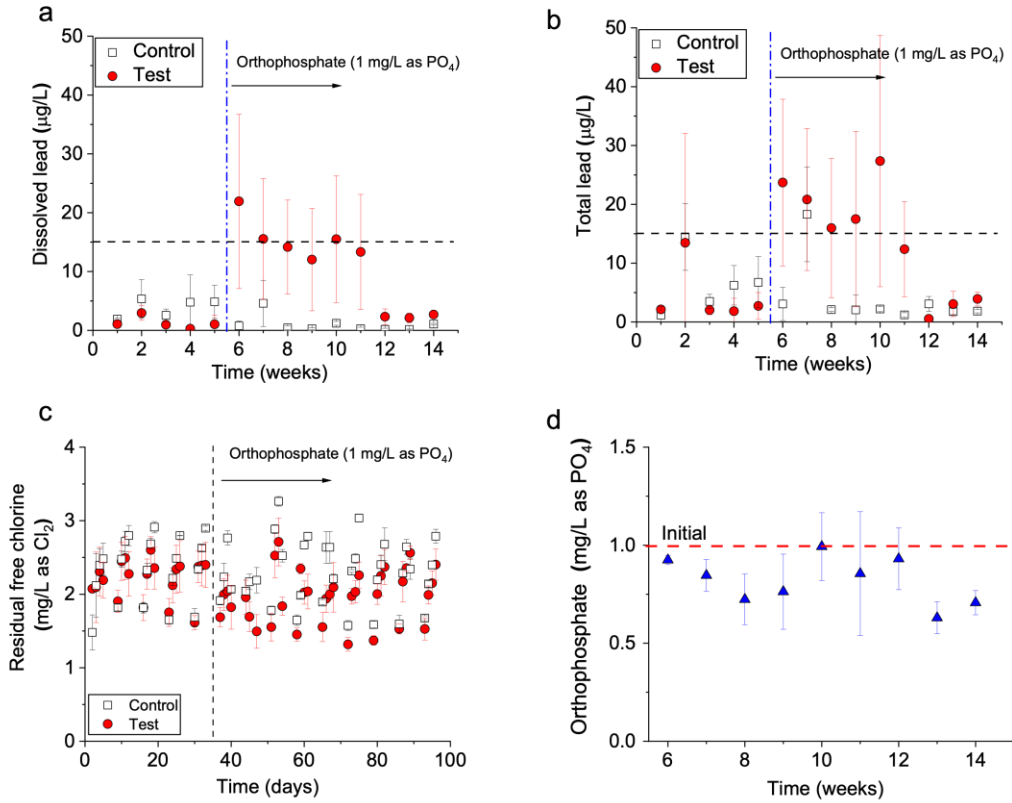


Figure A4.3 Coupon study: (a) Dissolved lead concentrations; (b) Total lead concentrations; (c) Residual free chlorine and (d) orthophosphate concentrations during conditioning (1 mg/L as PO₄ orthophosphate added to test coupons starting from Week 6). Water was refreshed every week, free chlorine was adjusted to initial value every day, orthophosphate and pH was monitored and adjusted to initial value every week. Error bars denote standard deviations calculated from the triplicate experiments.

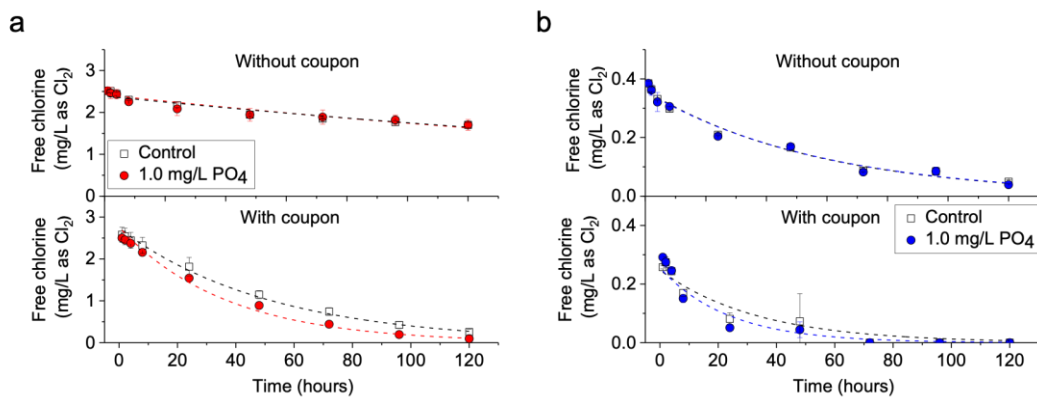


Figure A4.4 Coupon study: Free chlorine decay for lead coupons over five days of stagnation at initial concentrations of (a) 3.0 mg/L and (b) 0.5 mg/L as Cl₂. The lines represent the fitted first-order kinetic model, and the error bars denote standard deviations calculated from the triplicate experiments.

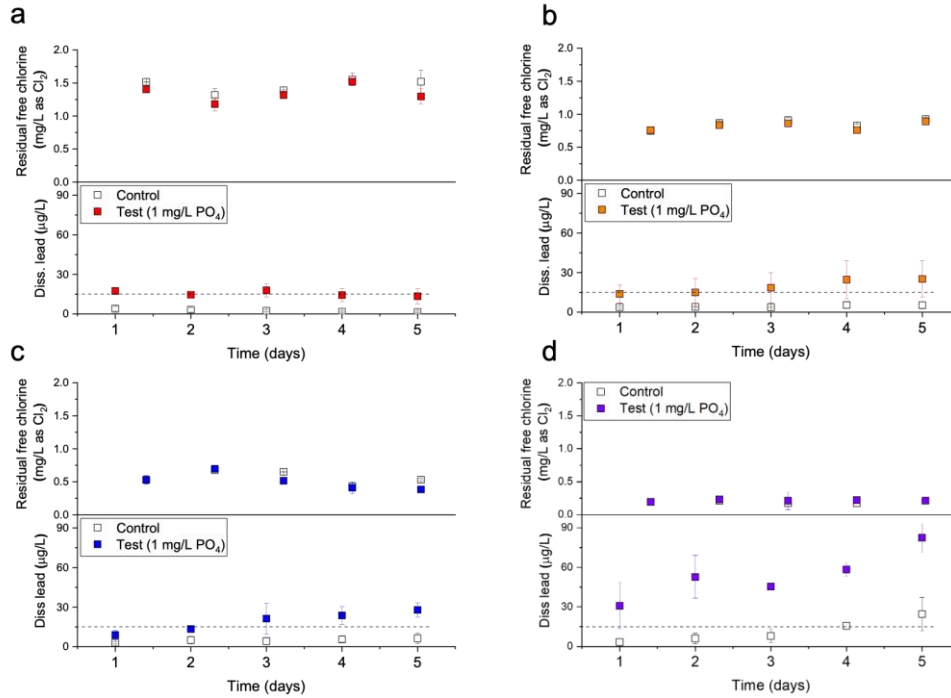


Figure A4.5 Coupon study: Dissolved lead concentrations with free chlorine controlled at concentrations of (a) 1-1.5 mg/L (b) 0.6-1 mg/L (c) 0.3-0.6 mg/L and (d) 0-0.3 mg/L. The error bars denote standard deviations calculated from the triplicate experiments.

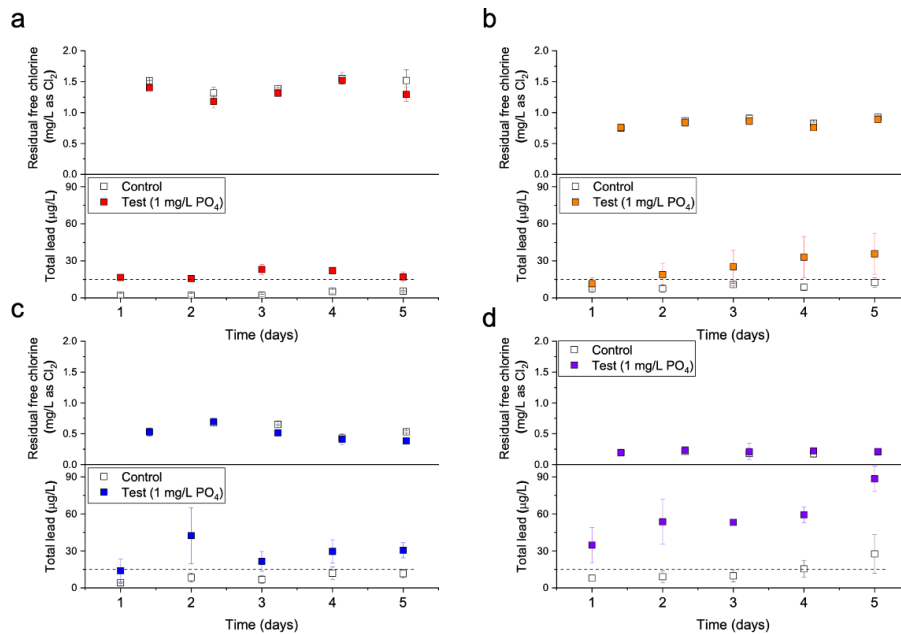


Figure A4.6 Coupon study: Total lead concentrations with free chlorine controlled at concentrations of (a) 1-1.5 mg/L (b) 0.6-1 mg/L (c) 0.3-0.6 mg/L and (d) 0-0.3 mg/L. The error bars denote standard deviations calculated from the triplicate experiments.

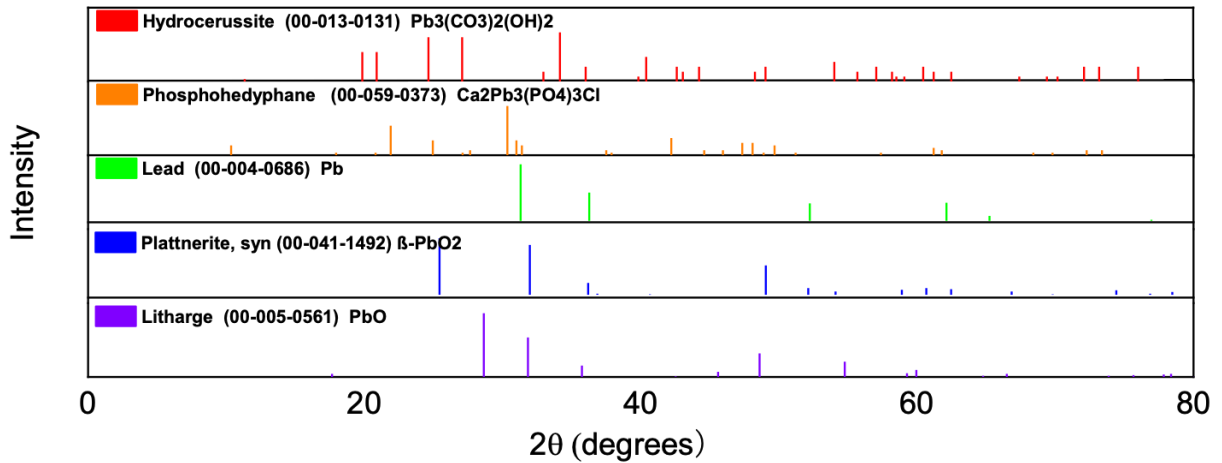


Figure A4.7 XRD Reference patterns for hydrocerussite ($Pb_3(CO_3)_2(OH)_2$), phosphohedyphane $Ca_2Pb_3(PO_4)_3Cl$, lead (Pb), plattnerite (β - PbO_2) and litharge (PbO).

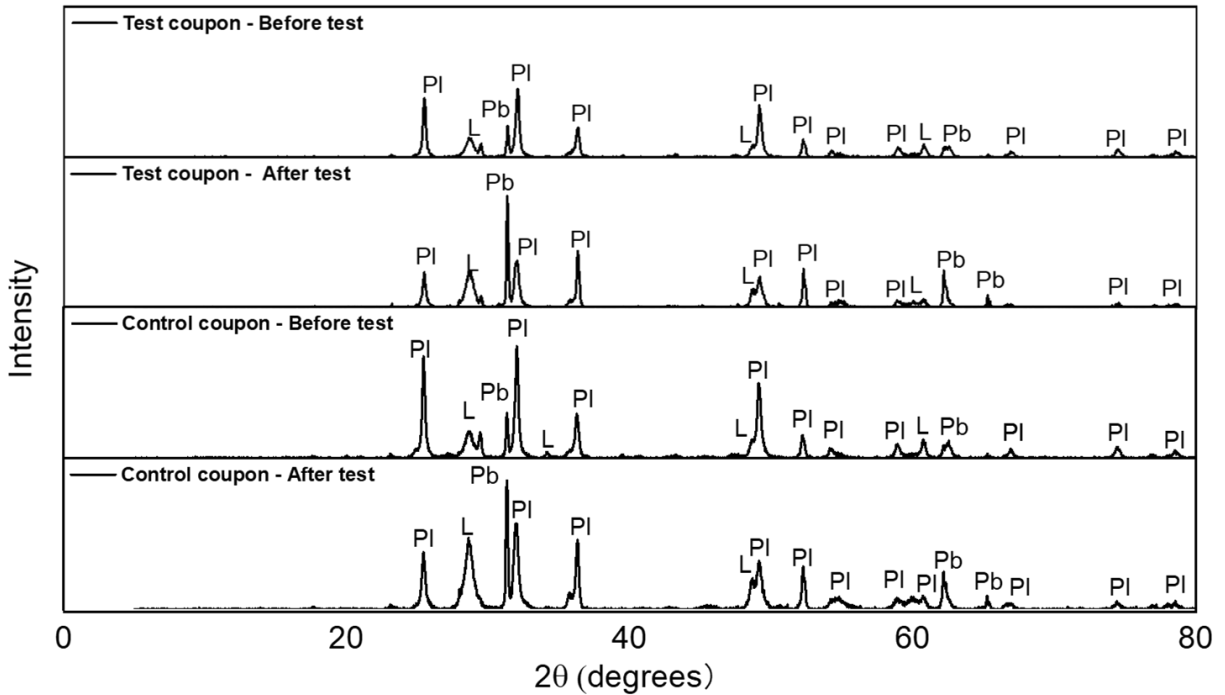


Figure A4.8 XRD patterns for corrosion products in scales of control and test coupons before and after test. Reference patterns were shown in Figure A4.7 for H: hydrocerussite ($Pb_3(CO_3)_2(OH)_2$), Ph: phosphohedyphane $Ca_2Pb_3(PO_4)_3Cl$, Pb: lead (Pb), Pl: plattnerite (β - PbO_2) and L: litharge (PbO).

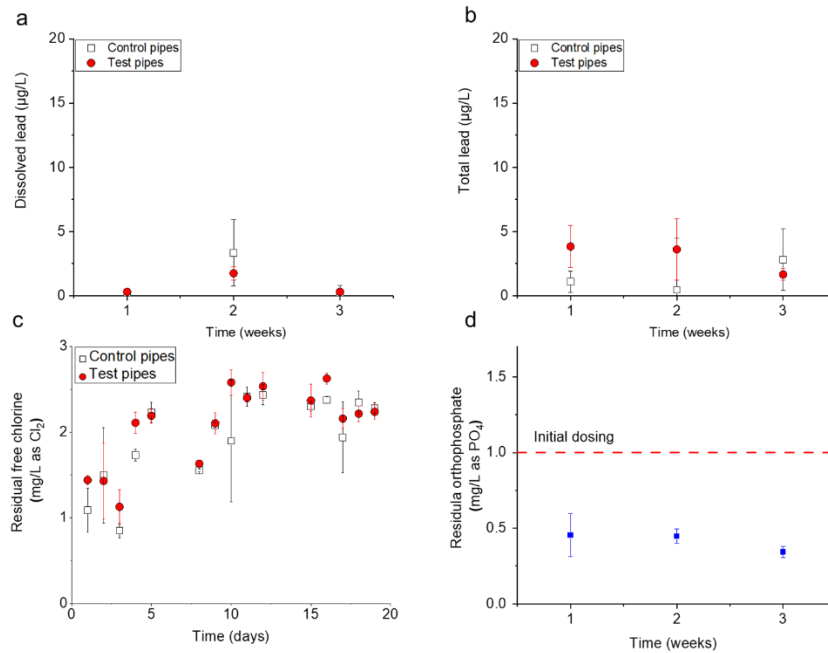


Figure A4.9 Pipe-loop study: (a) Dissolved lead concentrations; (b) Total lead concentrations; (c) Residual free chlorine and (d) orthophosphate concentrations during conditioning (1 mg/L as PO₄ orthophosphate was added to test pipes). Water was refreshed every week, free chlorine was adjusted to initial value every day, orthophosphate and pH was adjusted to initial value every week. Error bars denote standard deviations calculated from the duplicate experiments.

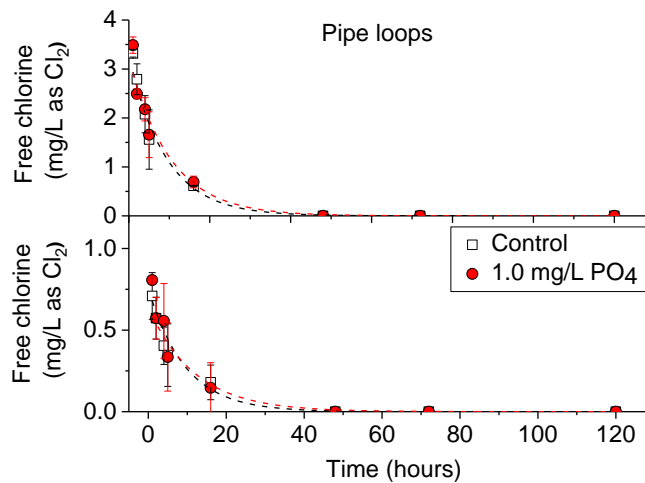


Figure A4.10 Pipe-loop study: Free chlorine decay in lead pipe loops with and without orthophosphate (1 mg/L as PO₄) over five days of stagnation at initial concentrations of 3 mg/L and 1 mg/L as Cl₂. The lines represent the fitted first-order kinetic model, and the error bars denote standard deviations calculated from the duplicate experiments.

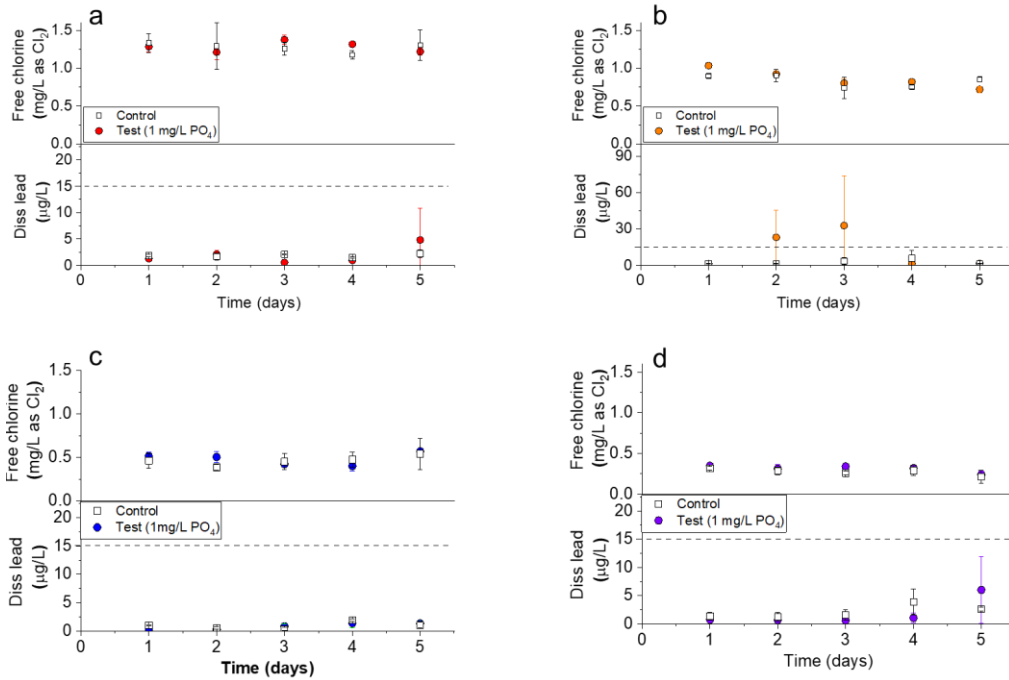


Figure A4.11 Pipe-loop study: Dissolved lead concentrations with free chlorine controlled at concentrations of (a) 1-1.5 mg/L (b) 0.6-1 mg/L (c) 0.3-0.6 mg/L and (d) 0-0.3 mg/L. The error bars denote standard deviations calculated from the duplicate experiments.

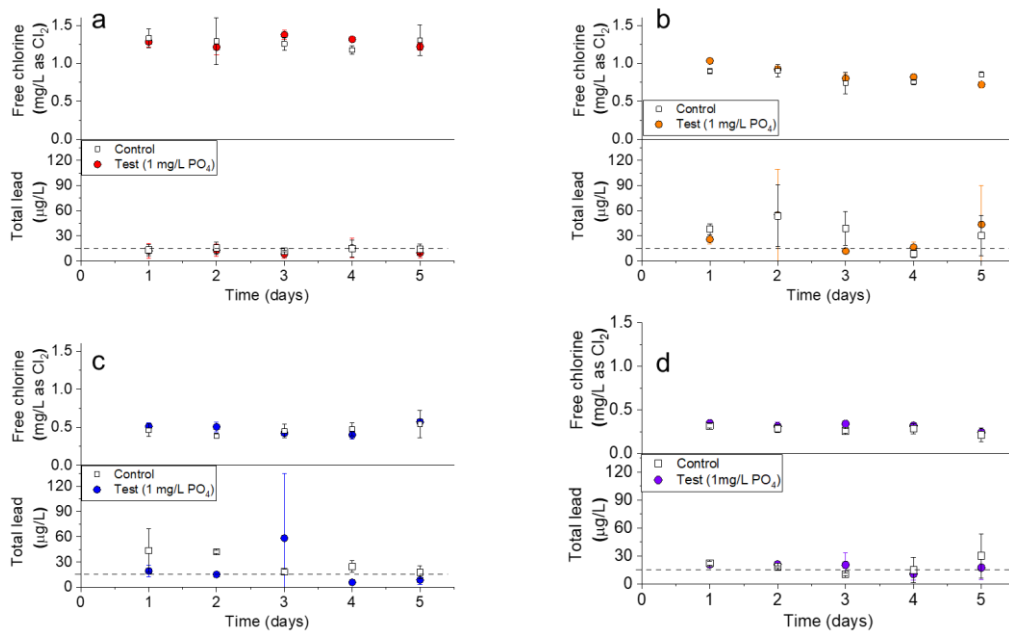


Figure A4.12 Pipe-loop study: Total lead concentrations with free chlorine controlled at concentrations of (a) 1-1.5 mg/L (b) 0.6-1 mg/L (c) 0.3-0.6 mg/L and (d) 0-0.3 mg/L. The error bars denote standard deviations calculated from the duplicate experiments.

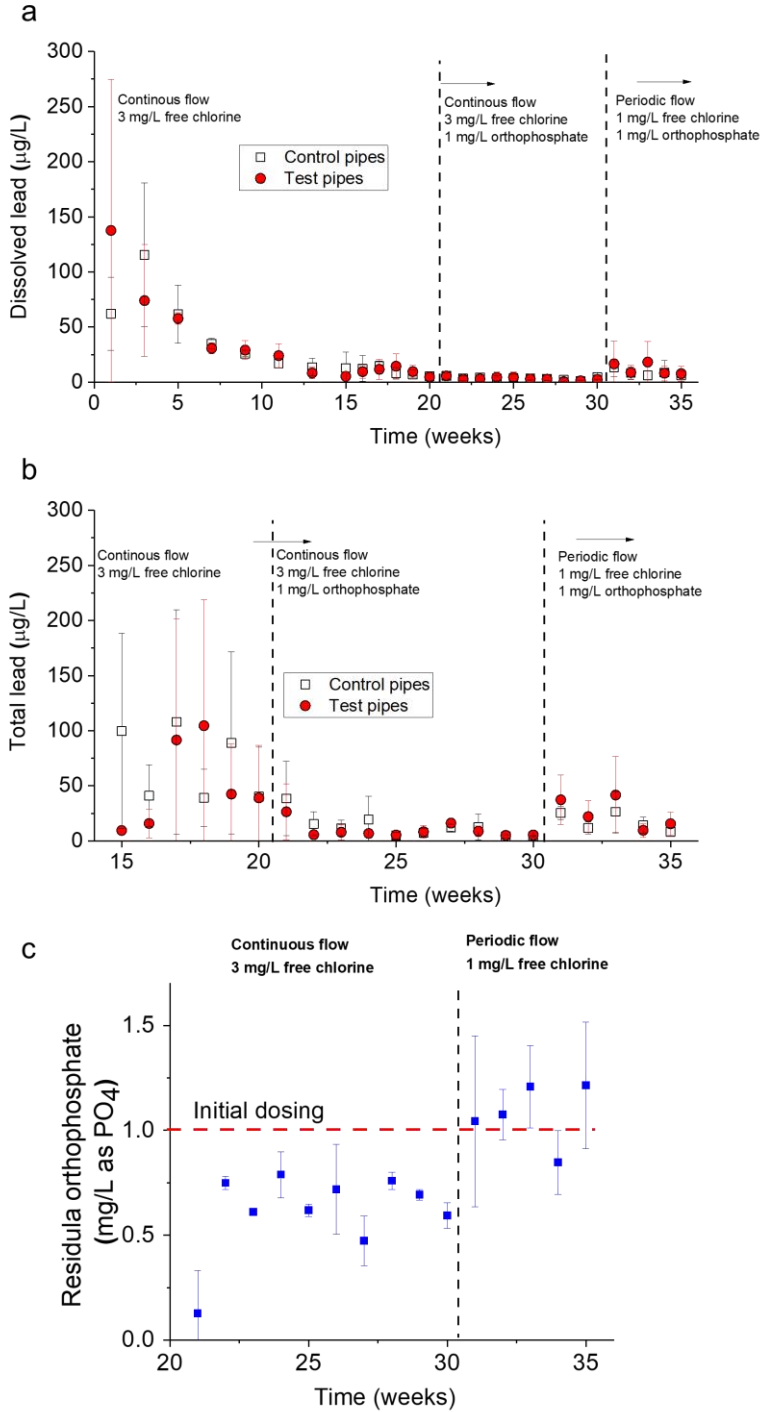


Figure A4.13 Pipe-loop study: (a) Dissolved lead concentrations, (b) total lead concentrations, and (d) orthophosphate concentrations under continuous and periodic flow conditions (1 mg/L as PO_4 orthophosphate added to test pipes). Water was refreshed every week, free chlorine was adjusted to initial value every day, orthophosphate and pH was adjusted to initial value every week. Error bars denote standard deviations calculated from the triplicate experiments.



Figure A4.14 Longitudinal cross-sections of control pipes C1', C2', and test pipes P1, P2 after test. The pipes were used for stagnation and free chlorin experiments.

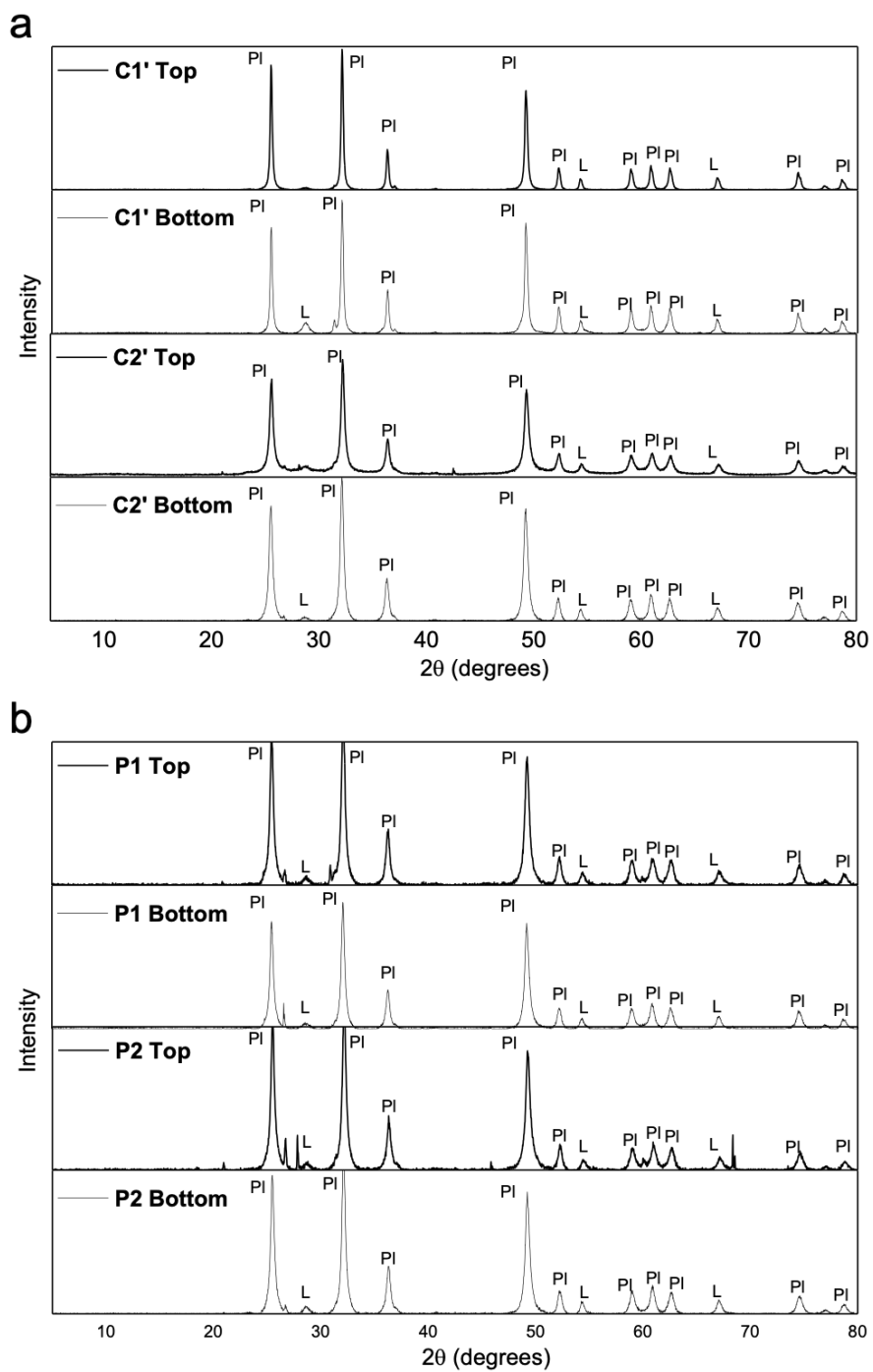


Figure A4.15 XRD patterns for control and test pipes (C' and P pipes) after test. The pipes were used stagnation and free chlorin experiments. Reference patterns were shown in Figure A4.7 for H: hydrocerussite ($\text{Pb}_3(\text{CO}_3)_2(\text{OH})_2$), Ph: phosphohedyphane $\text{Ca}_2\text{Pb}_3(\text{PO}_4)_3\text{Cl}$, Pb: lead (Pb), PI: plattnerite ($\beta\text{-PbO}_2$) and L: litharge (PbO).

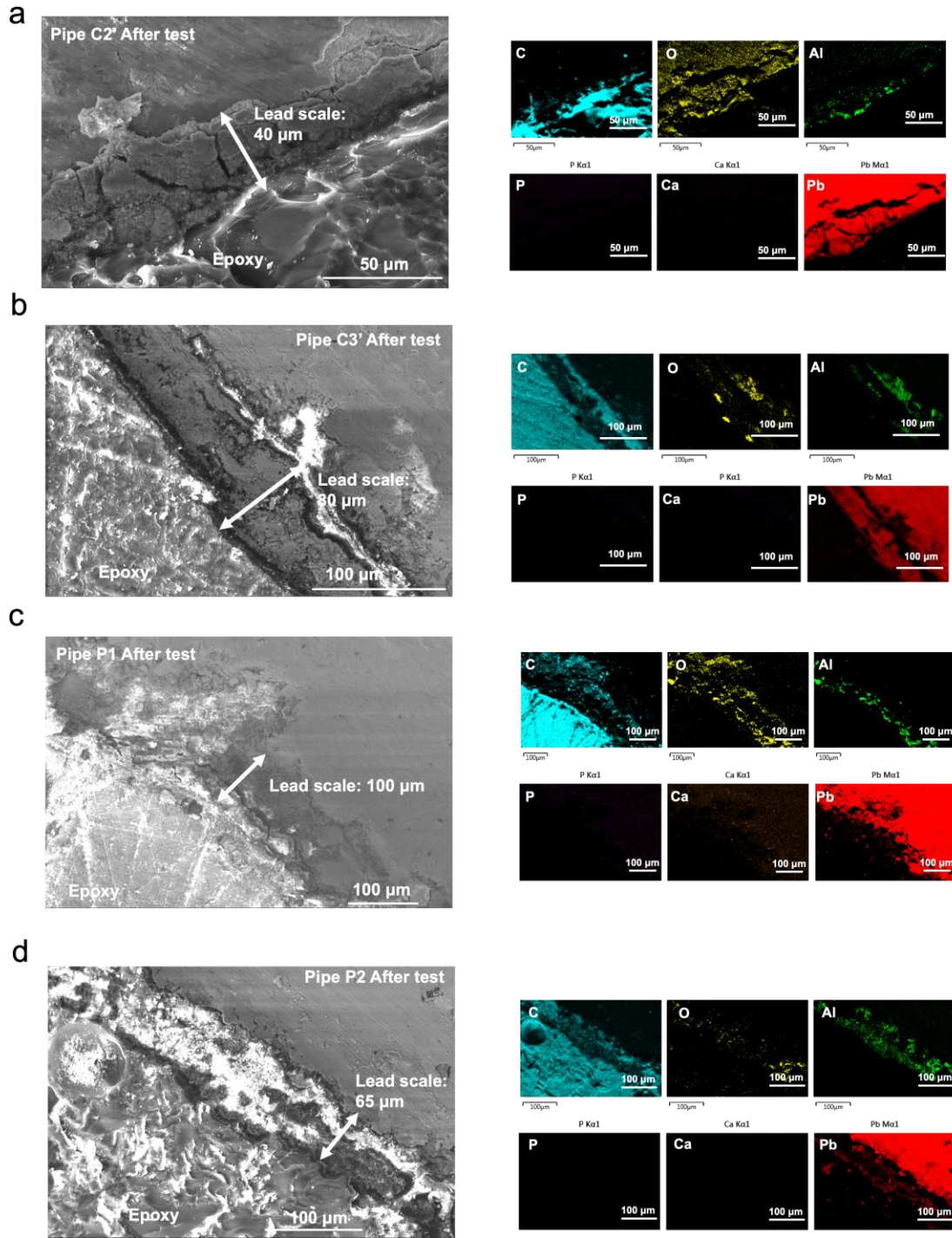


Figure A4.16 SEM images (left side) of the cross-section of the with elemental mappings (right side) of different elements detected by EDS after test for (a) Control Pipe C2' (b) Control Pipe C3' (c) Test Pipe P1, and (d) Test Pipe P2. The pipes were used for stagnation and free chlorin experiments.

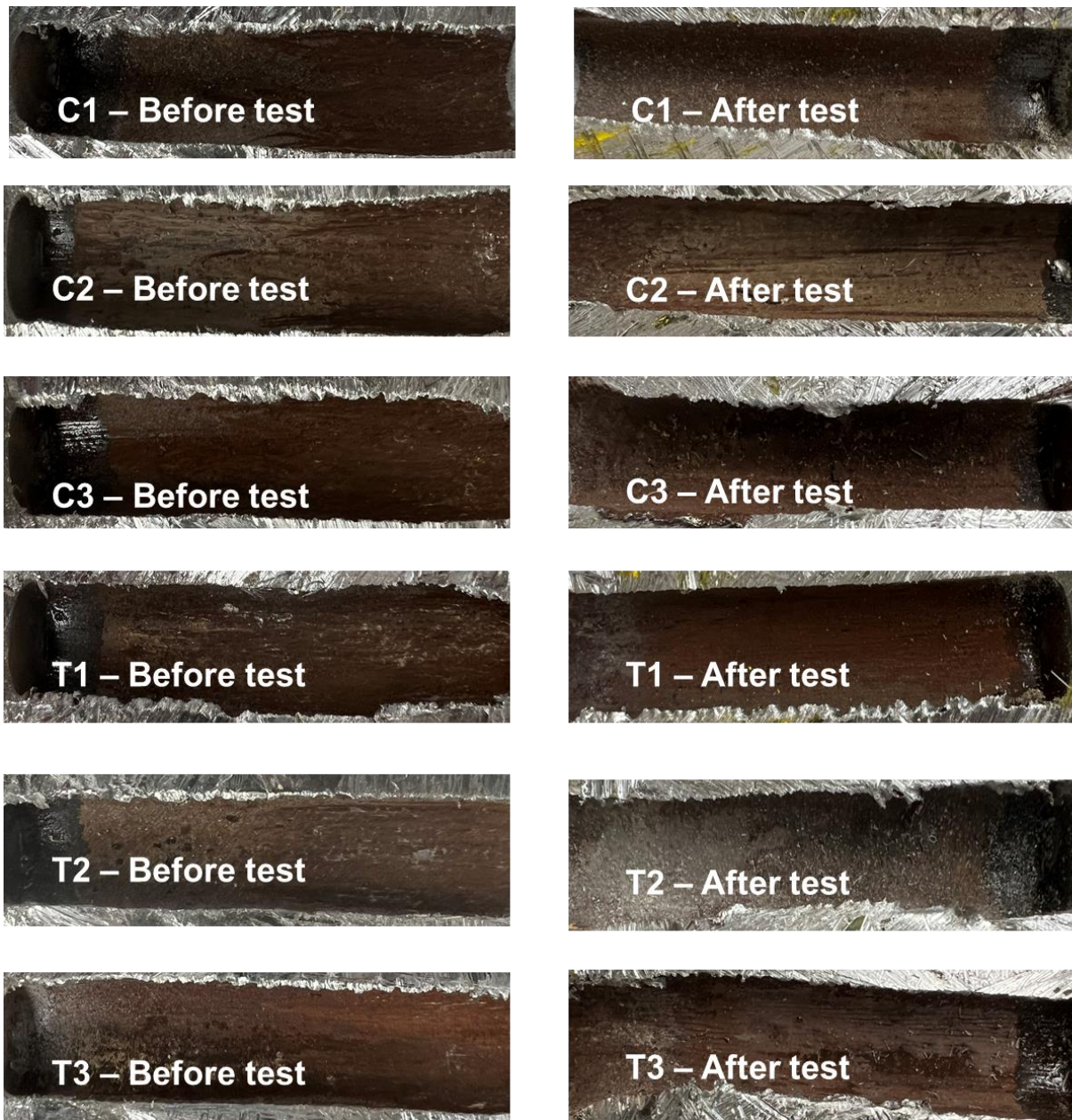


Figure A4.17 Longitudinal cross-sections of control pipes C1-C3, and test pipes T1-T3 before and after test. The pipes were used for real-world water use pattern experiments.

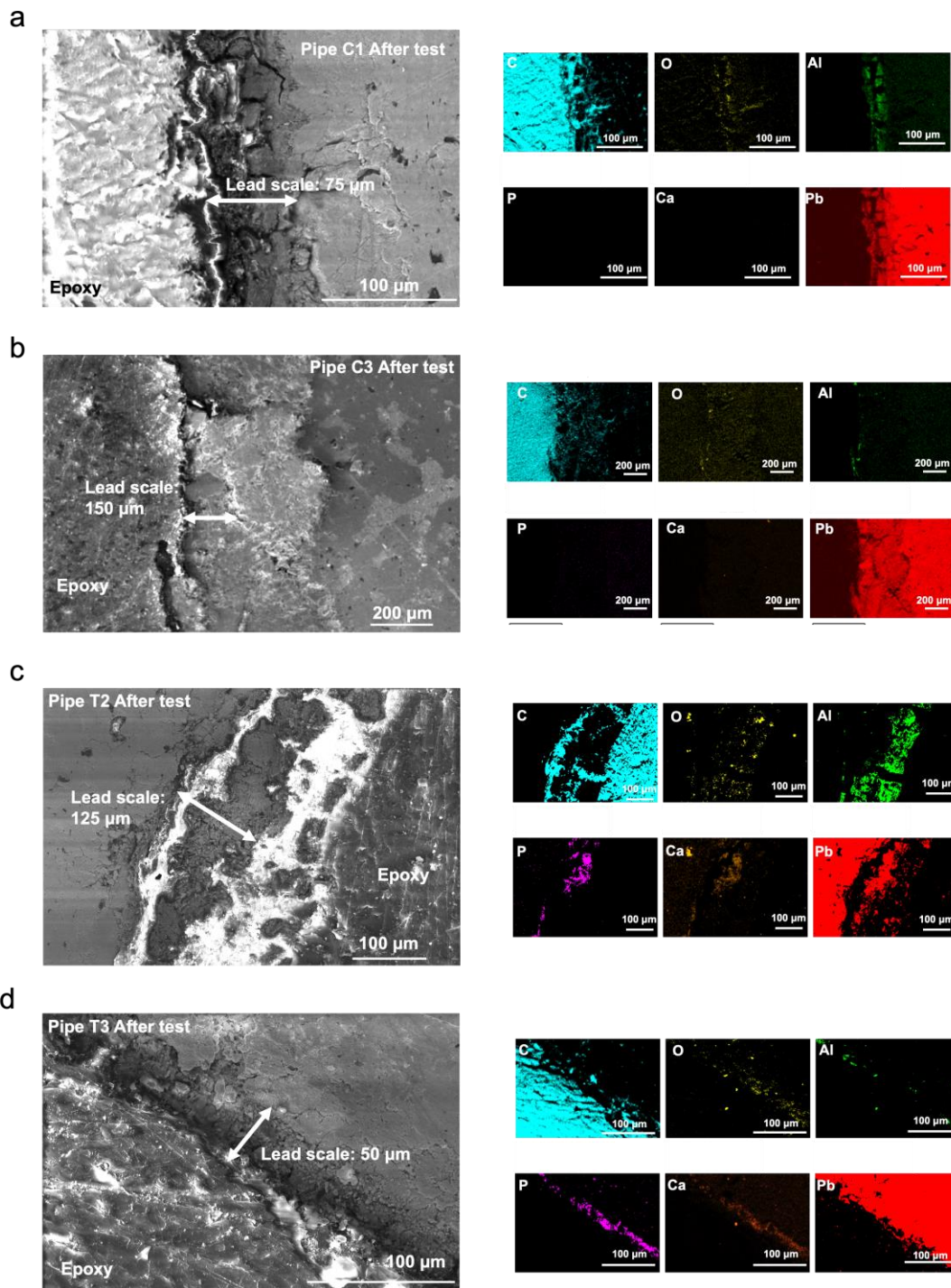


Figure A4.18 SEM images (left side) of the cross-section of the with elemental mappings (right side) of different elements detected by EDS after test for (a) Control Pipe C1 (b) Control Pipe C3 (c) Test Pipe T2, and (d) Test Pipe T3. The pipes were used for real-world water use pattern experiments.

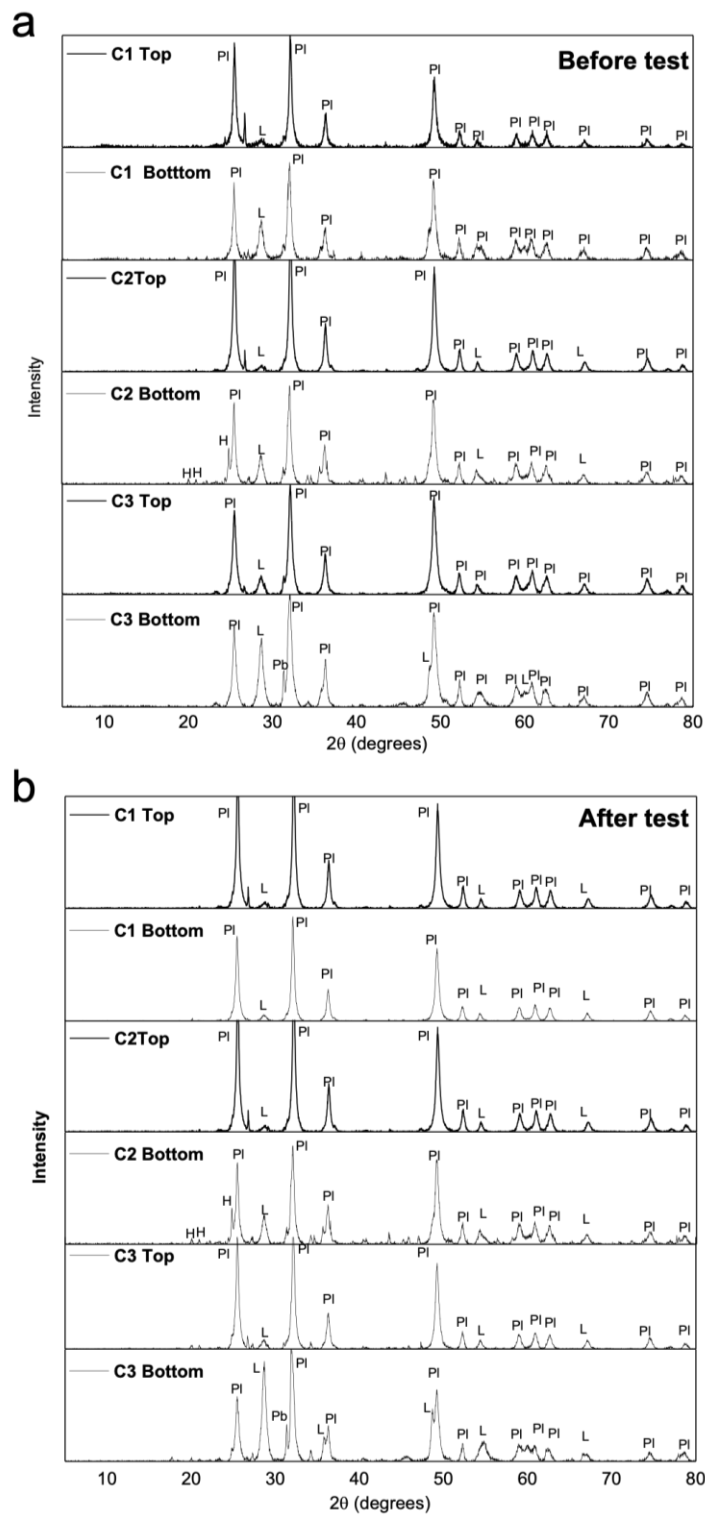


Figure A4.19 XRD patterns for control pipes C1-C3 before and after test. The pipes were used for real-world water use pattern experiments. Reference patterns were shown in Figure A4.7 for H: hydrocerussite ($\text{Pb}_3(\text{CO}_3)_2(\text{OH})_2$), Ph: phosphohedyphane $\text{Ca}_2\text{Pb}_3(\text{PO}_4)_3\text{Cl}$, Pb: lead (Pb), Pl: plattnerite ($\beta\text{-PbO}_2$) and L: litharge (PbO).

Table A4.1 Water composition of ECWA water and artificial water.

Species	ECWA Water	Artificial water	Units
Ca ²⁺	36.0	31.7	mg/L
Na ⁺	13.0	10.7	mg/L
K ⁺	9.0	18.8	mg/L
SO ₄ ²⁻	21.0	23.0	mg/L
Cl ⁻	19.5	21.0	mg/L
NO ₃ ⁻	0.5	0.6	mg/L as NO ₃ -N
F ⁻	0.1	0.1	mg/L
Alkalinity	90.0	92.0	mg/L as CaCO ₃
pH	8.0	8.0	pH unit
Total Dissolved Solids	156.0	170.0	mg/L
Ca Hardness	92.0	80.0	mg/L as CaCO ₃

Table A4.2 Identification for pipe loops assigned to different tests.

ID	Pipe type	Orthophosphate	Test
C1	Control pipe	/	Real-world water use pattern
C2	Control pipe	/	Real-world water use pattern
C3	Control pipe	/	Real-world water use pattern
T1	Test pipe	1 mg/L as PO ₄	Real-world water use pattern
T2	Test pipe	1 mg/L as PO ₄	Real-world water use pattern
T3	Test pipe	1 mg/L as PO ₄	Real-world water use pattern
C1'	Control pipe	/	Stagnation and residual free chlorine
C2'	Control pipe	/	Stagnation and residual free chlorine
P1	Test pipe	1 mg/L as PO ₄	Stagnation and residual free chlorine
P2	Test pipe	1 mg/L as PO ₄	Stagnation and residual free chlorine

Table A4.3 Kinetic parameters of free chlorine decay for lead coupons and lead pipes.

ID	first-order rate constant (k) /h ⁻¹	R ²
0.5-Cl ₂	0.02	0.95
0.5-Cl ₂ (P)	0.02	0.93
3-Cl ₂	0.003	0.94
3-Cl ₂ (P)	0.003	0.91
0.5-Pb coupon	0.34	0.86
0.5-Pb coupon (P)	0.56	0.91
3-Pb coupon	0.02	0.99
3-Pb coupon (P)	0.03	0.99
0.5-Pb pipes	0.11	0.93
0.5-Pb pipes (P)	0.09	0.91
3-Pb pipes	0.11	0.97
3-Pb pipes (P)	0.10	0.96

Note: “3” and “0.5” represent the initial free chlorine concentrations; “Pb coupon” and “Pb pipes” represent experiments with PbO₂-coated lead coupons and in pipe loops; “(P)” means that 1.0 mg/L as PO₄ orthophosphate was added; Control experiments with free chlorine only were conducted in 200 mL jars.

Table A4.4 Summary of XRD results for the powdered samples from the lead coupons and lead pipes.

Sample ID		Hydrocerussite ($\text{Pb}_3(\text{CO}_3)_2(\text{OH})_2$)	Plattnerite ($\beta\text{-PbO}_2$)	Phosphohedyphane ($\text{Ca}_2\text{Pb}_3(\text{PO}_4)_3\text{Cl}$)	Litharge (PbO)
Control coupons	Before test	-	+	-	+
	After test	-	+	-	+
Test coupons	Before test	-	+	-	+
	After test	-	+	-	+
Pipe C1	1-Top	-	+	-	+
	1-Bottom	-	+	-	+
	2-Top	-	+	-	+
	2-Bottom	-	+	-	+
Pipe C2	1-Top	-	+	-	+
	1-Bottom	+	+	-	+
	2-Top	-	+	-	+
	2-Bottom	+	+	-	+
Pipe C3	1-Top	-	+	-	+
	1-Bottom	-	+	-	+
	2-Top	-	+	-	+
	2-Bottom	-	+	-	+
Pipe T1	1-Top	-	+	-	+
	1-Bottom	-	+	-	+
	2-Top	-	+	-	+
	2-Bottom	+	+	+	+
Pipe T2	0-Top	+	+	-	+
	0-Bottom	+	+	-	+
	1-Top	-	+	-	+
	1-Bottom	-	+	-	+
	2-Top	-	+	-	+

	2-Bottom	+	+	+	+
Pipe T3	1-Top	-	+	-	+
	1-Bottom	-	+	-	+
	2-Top	+	+	+	+
	2-Bottom	+	+	+	+
Pipe C1'	0-Top	+	+	-	+
	0-Bottom	+	+	-	+
	1-Top	-	+	-	+
	1-Bottom	-	+	-	+
	2-Top	+	+	+	+
	2-Bottom	+	+	+	+
Pipe C2'	1-Top	-	+	-	+
	1-Bottom	-	+	-	+
	2-Top	-	+	-	+
	2-Bottom	-	+	-	+
Pipe P1	1-Top	-	+	-	+
	1-Bottom	-	+	-	+
	2-Top	-	+	-	+
	2-Bottom	-	+	-	+
Pipe P2	1-Top	-	+	-	+
	1-Bottom	-	+	-	+
	2-Top	-	+	-	+
	2-Bottom	-	+	-	+

Note: '0', '1' and '2' are for analysis before conditioning, at the end of conditioning and at the end of test, respectively. '+' indicates the presence of a certain mineral. '-' Indicates not found.

Table A4.5 Mass concentrations (mg/g) of elements in the scales determined by acid digestion of solids followed by analysis with ICP-MS.

Sample ID	Pb	Al	Fe	Mg	P
Control Coupons-AC	778	9	BDL	BDL	BDL
Test Coupons -AC	697	13	BDL	BDL	BDL
Control Coupons -AT	820	5	BDL	BDL	BDL
Test Coupons -AT	787	5	BDL	BDL	BDL
C1-AC					
Top	667	35	21	BDL	BDL
Bottom	696	36	18	BDL	BDL
C2-AC					
Top	866	64	27	BDL	BDL
Bottom	895	29	25	BDL	BDL
C3-AC					
Top	881	34	19	BDL	BDL
Bottom	883	29	22	BDL	BDL
T1-AC					
Top	688	70	23	BDL	BDL
Bottom	545	12	14	BDL	BDL
T2-AC					
Top	606	46	28	BDL	BDL
Bottom	848	26	25	BDL	BDL
T3-AC					
Top	720	53	26	BDL	BDL
Bottom	851	25	21	BDL	BDL
C1-AT					
Top	685	13	8	4	BDL
Bottom	754	BDL	BDL	BDL	BDL
C2- AT					
Top	418	40	9	BDL	BDL
Bottom	608	9	BDL	BDL	BDL
C3- AT					
Top	335	27	9	2	BDL
Bottom	383	BDL	BDL	BDL	BDL
T1-AT					
Top	317	32	5	BDL	3
Bottom	627	14	BDL	2	3
T2- AT					
Top	304	35	12	4	11
Bottom	393	18	10	BDL	4
T3- AT					
Top	544	14	8	6	28
Bottom	658	BDL	BDL	4	9
C1'-AT					
Top	503	7	17	5	BDL
Bottom	513	40	14	7	BDL
C2'-AT					
Top	253	14	BDL	6	BDL
Bottom	459	24	BDL	6	BDL
P1-AT					
Top	510	28	12	14	9
Bottom	373	13	BDL	10	19
P2-AT					
Top	250	30	5	8	24
Bottom	163	15	BDL	10	11
Detection limit	10	5	5	5	1

Note: "C1": Control pipe 1; "T1": Test pipe 1; "BC": Before conditioning; "AC": After conditioning; "AT": After tests. "BDL" represents below the detection limit.

Appendix A5 Effect of Water Blending on Lead Release from PbO₂-coated Lead Pipes

A5.1 Introduction

Lead(IV) oxide (PbO₂) is an important component of lead corrosion products found on lead service lines (LSLs). There are two different crystalline phases of PbO₂, scrutinyite (α -PbO₂) and plattnerite (β -PbO₂) (Lytle and Schock, 2005), and both have an extremely low solubility compared with lead(II) carbonate and even lead(II) phosphate solids (Triantafyllidou et al., 2015). The formation of lead oxide (PbO₂) on the surface of lead pipes can potentially provide good protection and a passivating layer for the lead pipe surface that could minimize the release of lead to water (Zhang and Lin, 2011).

The stability of PbO₂ on the surface of lead pipes can control lead release into water flowing through or stagnating in lead pipes. However, lead is not stable in the +IV oxidation state in which it is present in PbO₂ in the absence of a strong oxidant like free chlorine (Pan et al., 2022). PbO₂ is a strong oxidant, and it is susceptible to changes in water chemistry with respect to pH, disinfectant type and concentration (Edwards and Dudi, 2004; Lin and Valentine, 2008b), and the presence of chemical reductants (e.g., Fe(II), natural organic matter) (Dryer and Korshin, 2007). Blending water from various sources is a common practice in drinking water systems. These sources often differ in water chemistry and corrosion inhibitors, which may affect the stability of existing PbO₂ pipe scales. However, previous research has not specifically addressed the stability and dissolution of PbO₂ pipe scales when exposed to variations during water blending.

In this study, a pipe-loop experiment was conducted using six harvested pipes from the Erie County Water Authority (ECWA) to examine the effects of water blending on the stability of existing PbO₂ pipe scales. Initially, all pipes were supplied with artificial ECWA water, after which three test pipes received a 50%:50% blend of ECWA and an artificial water representing that of the public water system for the city of Buffalo, NY. These two water systems have interconnections through which they can provide treated water from one system into the distribution system of the other. The water from Buffalo has a lower pH than ECWA and contains a blended-phosphate corrosion inhibitor, while ECWA currently has no phosphate-based chemicals added. Lead concentrations in the water, both dissolved and total, were monitored before and after the water blending. Additionally, scale analysis was performed on the control and test pipes following the experiment.

A5.2 Materials and Methods

A5.2.1 Set-up of Pipe Loops

Six harvested lead pipes from Erie County Water Authority (ECWA) were used in a recirculating pipe loop system for this study (Figure A5.1). Each pipe had an inner diameter of approximately 1.9 cm (0.75 inches) and was composed of one 45.7 cm (18-inch) section along with three 10.2 cm (4-inch) sections. These segments, originally from the same pipe, were reassembled in their initial sequence using rubber connectors, PVC pipes, and plastic tubing. To prevent contact between cut surfaces and water, they were completely coated with epoxy (J-B Weld 8281 Professional). A magnetic drive pump and a 10-liter reservoir facilitated water recirculation in each pipe loop, with valves and flowmeters providing control and monitoring of the flow rate.

Three pipes served as the test ones (B1, B2, B3) and the remaining three pipes were the control pipes (C1, C2, C3).

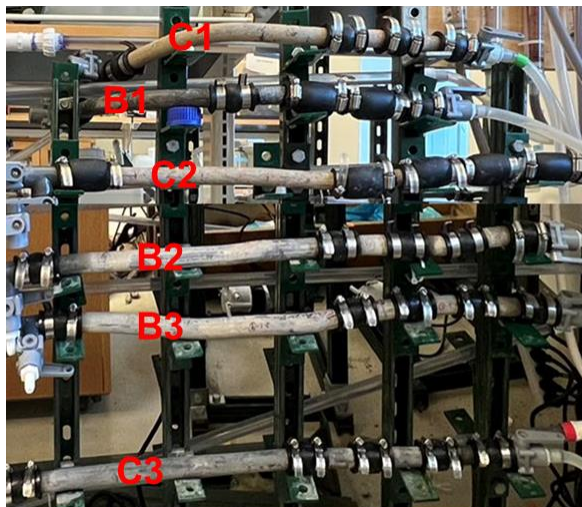


Figure A5.1 Pipe loop reactors for C1-C3, and B1-B3. The harvested lead pipe assembly consists of one 18-inch section and three 4-inch segments that are connected with rubber connectors. The 4-inch segments allow scale analysis to be performed at different stages in the experiment while retaining the majority of the lead pipe length in the reactor.

A5.2.2 Water Preparation and Blending

Artificial ECWA water was prepared the same as described in Chapter 5. Artificial water was prepared using calcite contact and blended phosphate (Calciquest) from Table A5.1. Test pipes received a blend of 5 L of Buffalo and 5 L of ECWA water. The waters were thoroughly mixed before being flowed through the pipes via a peristaltic pump. The reagents used to prepare the artificial water were the same as in Chapter 5.

Table A5.1 Water composition of Artificial Buffalo and ECWA Water.

Species	Buffalo Water	ECWA Water	Units
Ca ²⁺	42.0	36.0	mg/L
Na ⁺	12.0	13.0	mg/L
K ⁺	9.0	9.0	mg/L
SO ₄ ²⁻	23.0	21.0	mg/L
Cl ⁻	20.0	19.5	mg/L
NO ₃ ⁻	0.1	0.5	mg/L as NO ₃ -N
F ⁻	0.1	0.1	mg/L
Free Chlorine	1.1	1.5	mg/L as Cl ₂
Alkalinity	94.3	92.0	mg/L as CaCO ₃
pH	7.7	8.0	pH unit
Total Dissolved Solids	169.0	156.0	mg/L
Ca Hardness	99.2	92.0	mg/L as CaCO ₃
Ortho Phosphate	0.2	0	mg/L as PO ₄
Total Phosphate	0.7	0	mg/L as PO ₄

A5.2.3 Scale Analysis Methods

Scale analysis includes the characterization of crystalline minerals present, elemental composition, and morphology. The crystalline phases in the scale were identified using X-ray diffraction (XRD, Bruker d8 Advance). The elemental composition of each scale was characterized by inductively coupled plasma mass spectrometry (ICP-MS, NexION 2000) after acid digestion. The morphology of the scale was characterized by scanning electron microscopy of pipe cross sections (SEM, Thermo Fisher Quattro S E-SEM). The element distribution within the scales was characterized by energy dispersive X-ray spectroscopy (EDS, Oxford AzTec). The detailed scale analysis procedures and protocols are the same as described in Chapter 5.

A5.2.4 Conditioning

Conditioning was conducted on each pipe receiving a continuously recirculating flow of ECWA artificial water containing 3 mg/L as Cl₂ of free chlorine for more than 40 weeks. Daily free chlorine adjustments and weekly water replacement was carried out. Weekly monitoring tracked total and dissolved lead. The flow regime for all pipes was adjusted to a daily pattern consisting of three periods of stagnation (6.5 hours) and three periods of flow (1.5 hours) at a flow rate of 4–5 L/min, with free chlorine concentrations decreasing to 1.5 mg/L and then to 1 mg/L prior to water blending test (each concentration lasted for three weeks).

A5.2.5 Water Blending Experiments

Water blending impacts were assessed over five duration times: 8 h, 1 d, 3 d, 5 d, 7 d, 10 d and 14 d. Experiments were done in one experiment in which samples were collected at different times. Within each duration, test pipes received a 50%:50% blend of ECWA and Buffalo water. The flow regime for all pipes consisted of three periods of flow (1.5 h) and three periods of stagnation (6.5 h) per day at a flow rate of 4-5 L/min, and stagnation started at the beginning of each duration. Residual free chlorine concentrations and pH were monitored and adjusted daily throughout each duration. Water was refreshed once at the end of Day 7. At the conclusion of each duration, dissolved and total lead were sampled and measured from the water reservoir.

A5.2.6 Statistical Analysis Methods

Statistical significance was determined using the t-test for independent samples (two-tailed), with a significance threshold of 0.05. Normality and variance assumptions were verified by the Shapiro-Wilk Test and Levene's Test.

A5.3 Results and Discussion

A5.3.1 Lead Release during Conditioning

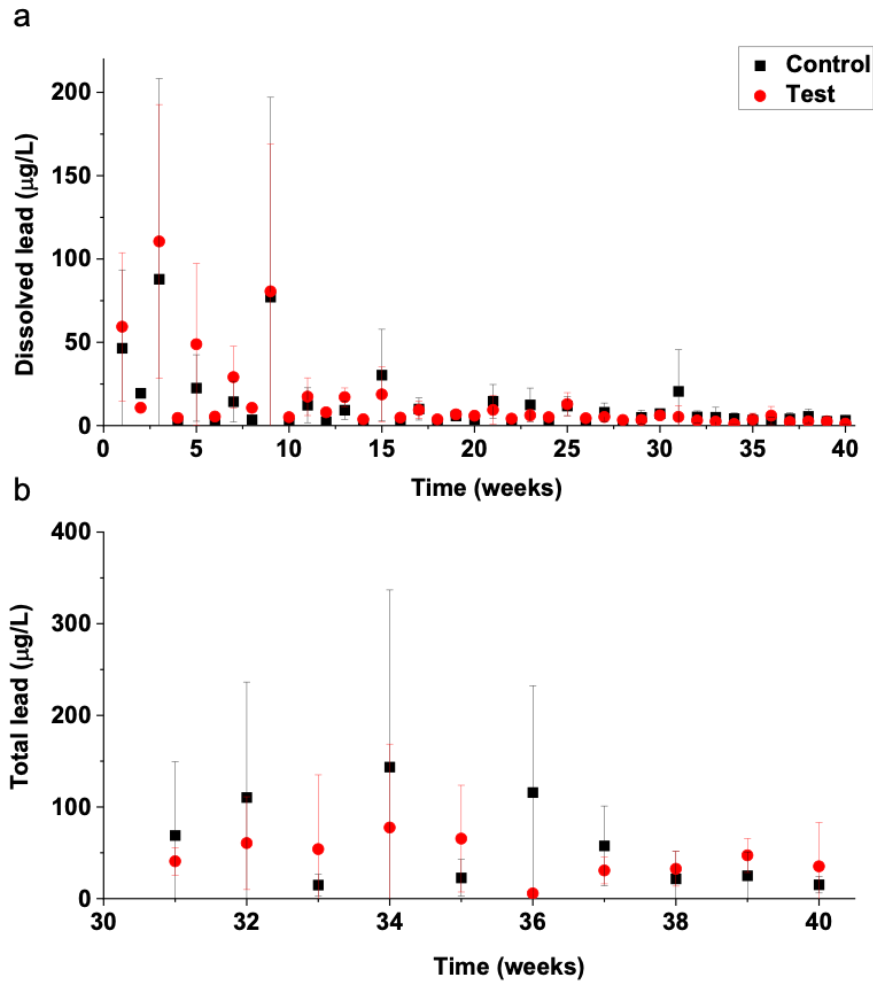


Figure A5.2 (a) Dissolved lead concentrations and (b) total lead concentrations during conditioning treated by artificial ECWA water with 3 mg/L as Cl_2 . Error bars denote standard deviations calculated from the triplicate experiments.

During conditioning, all pipes received artificial ECWA water with 3 mg/L as Cl_2 . The concentrations of dissolved lead gradually decreased from approximately 100 $\mu\text{g/L}$ to below 15 $\mu\text{g/L}$ over the course of ten weeks of conditioning (Figure A5.2a). Thereafter, the dissolved lead concentrations remained consistently low, below 10 $\mu\text{g/L}$, throughout the remainder of the 40-week conditioning period. We began monitoring the total lead concentrations beginning from

week 30. Total lead dropped from 100 $\mu\text{g/L}$ to below 20 $\mu\text{g/L}$ as conditioning progressed, and mostly remained below 15 $\mu\text{g/L}$ during the final three weeks of conditioning (Figure A5.2b). Furthermore, no significant difference was noticed between control and test pipe groups, indicating that they were comparable and prepared for the experimental phase.

A5.3.2 Lead Release during Experimental Phase

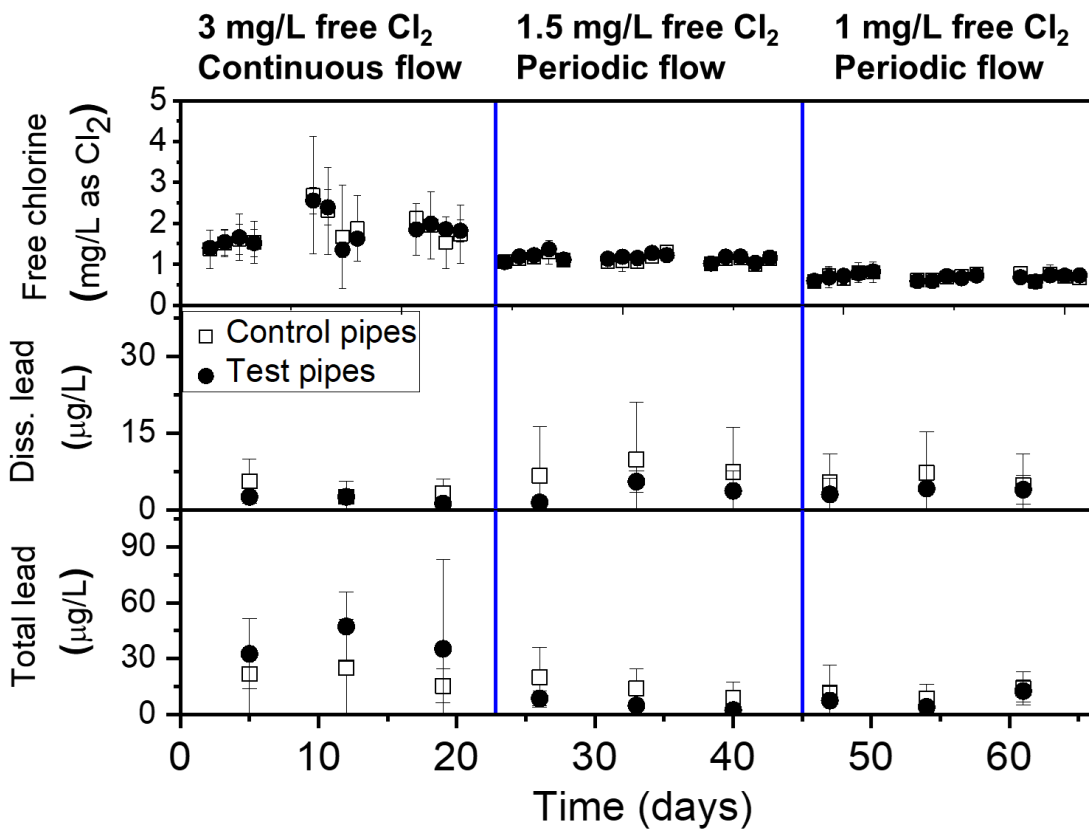


Figure A5.3 Free chlorine concentrations (top part of the panel), dissolved lead (middle part of the panel) and total lead concentrations (bottom part of the panel) for pipes assigned to control and test groups before water blending. Both the control and test pipes had identical conditions, as described above the figure, prior to water blending. The results from the final three weeks of the previous stage of conditioning with 3 mg/L Cl₂ and continuous flow (beginning at week 38 in Figure A5.2 and denoted here as days 0-22) are included for comparison with the concentrations once the free chlorine concentration and flow regime were adjusted.

After conditioning, the concentration of free chlorine decreased from 3 mg/L to 1.5 mg/L, and eventually to 1.0 mg/L as Cl₂. Each concentration was maintained and tested for three weeks to

simulate lower free chlorine concentrations that more closely match those found in real lead service lines (LSLs). As the free chlorine concentration decreased, dissolved lead levels increased slightly from below 5 $\mu\text{g/L}$ to approximately 10 $\mu\text{g/L}$ (Figure A5.3). However, this change was not statistically significant, and the concentrations in both the control and test pipes remained comparable to each other. The total lead concentrations in both the control and test pipes remained stable and low (below 15 $\mu\text{g/L}$) throughout the changes in free chlorine concentration.

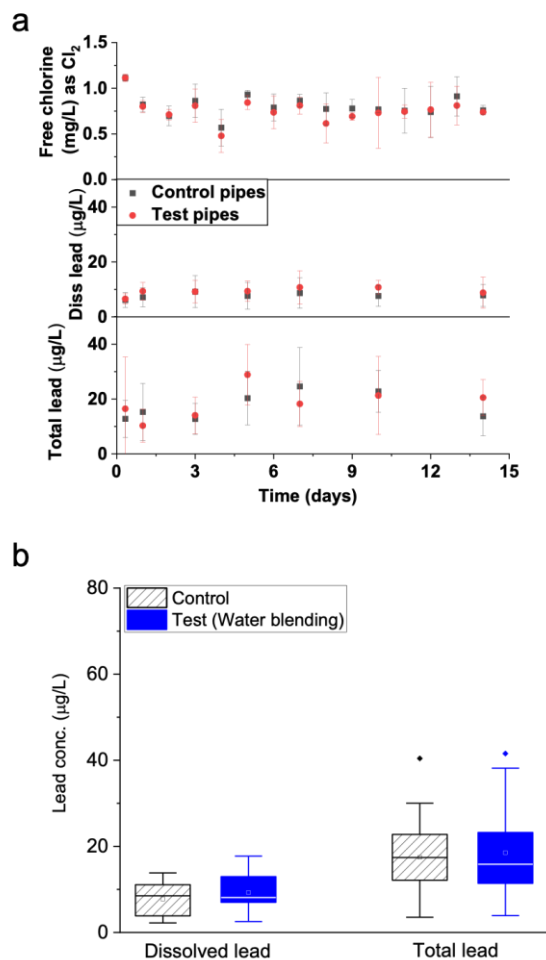


Figure A5.4 (a) Free chlorine, dissolved lead and total lead concentrations during water blending for test pipes. Here day 0 indicates the first day in which blended water was introduced to the test pipes. (b) Box plots for dissolved and total lead concentrations for control and test (water blending) pipe loops

After being treated with 1.0 mg/L of free chlorine (as Cl₂) using continuously recirculating artificial ECWA water for three weeks, the flow pattern was switched to periodic flow. The test pipes then began receiving a 50%:50% blend of ECWA and Buffalo water for 14 days. The shift in flow pattern from continuous to periodic flow resulted in a slight increase in total lead concentrations in both the test and control pipes (Figure A5.4). This increase was potentially due to water stagnation, which may have caused reductive dissolution in the absence of sufficient free chlorine and contributed to the detachment of particulate lead (Arnold and Edwards, 2012; Masters et al., 2016). No statistically significant difference was observed between the control and test pipes. The dissolved lead concentrations in the control and test pipes were 8 ± 4 µg/L and 9 ± 4 µg/L, respectively, and the total lead concentrations were 17 ± 9 µg/L and 18 ± 11 µg/L, respectively (Table A5.2).

Table A5.2 Summary of average lead concentrations (dissolved and total lead) and p-value for control and test pipes in water blending tests.

ID	Flow pattern	Free chlorine (mg/L as Cl ₂)	Dissolved lead (µg/L)	Total lead (µg/L)
Control pipes	Periodic	1	8 ± 4	17 ± 9
Test pipes	Periodic	1	9 ± 4	18 ± 11
p-value			0.2	0.7

Note: Dissolved lead defined as the lead concentration passing a 0.22 µm filter. This table presents an average of three distinct pipe replicates for the control and test pipes. X ± Y with X as the mean and Y as the standard deviation.

A5.3.3 Scale Analysis

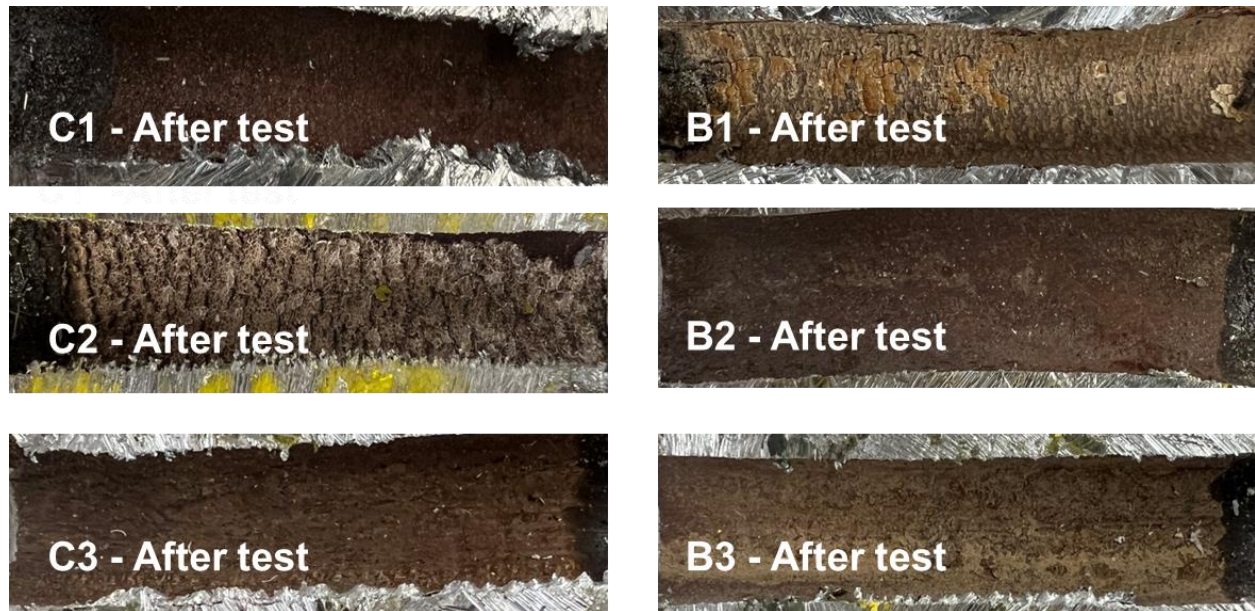


Figure A5.5 Cross-sections of control pipes C1-C3, and test pipes B1-B3 after test.

Scale analysis was conducted on the pipe segments following all experiments. Both the control and test pipes had dark red scales (Figure A5.5), a color characteristic of PbO_2 -dominated scales. X-ray diffraction (XRD) patterns indicated that plattnerite ($\beta\text{-PbO}_2$) was the dominant component in the scale of both control and test pipes, with litharge (PbO) also being detectable. In the test pipes treated with blended water, no lead-phosphate solids were observed (Figure A5.5), which aligned with the phosphorus mass concentrations in the test pipes being below the detection limit.

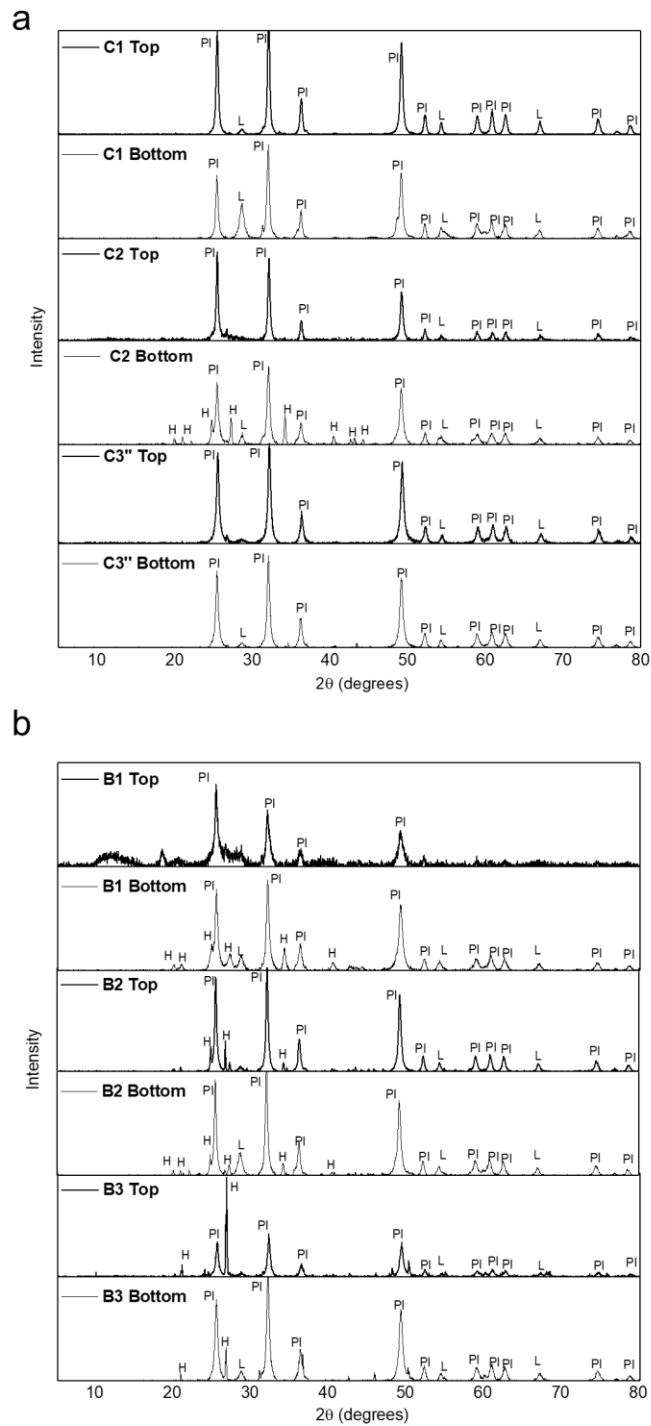


Figure A5.6 XRD patterns for control and test pipes (C1-C3 and B1-B3 pipes) after the test stage when blending was done for the test pipes. Reference patterns were shown in Figure A4.7 for H : hydrocerussite ($Pb_3(CO_3)_2(OH)_2$), Ph: phosphohedyphane $Ca_2Pb_3(PO_4)_3Cl$, Pb: lead (Pb), PI: plattnerite (β - PbO_2) and L: litharge (PbO).

Table A5.3 Mass concentrations (mg/g) of elements in the scales after test determined by acid digestion of solids followed by analysis with ICP-MS.

Sample ID		Pb	Al	Fe	Mg	P
C1	Top	557	9	BDL	8	BDL
	Bottom	645	11	BDL	8	BDL
C2	Top	227	105	BDL	8	BDL
	Bottom	313	68	BDL	9	BDL
C3	Top	440	46	BDL	11	BDL
	Bottom	511	32	BDL	6	BDL
B1	Top	170	107	BDL	10	BDL
	Bottom	413	59	BDL	10	BDL
B2	Top	465	13	BDL	9	BDL
	Bottom	522	10	BDL	7	BDL
B3	Top	502	21	BDL	9	BDL
	Bottom	460	21	BDL	4	BDL
Detection limit		10	5	5	5	1

Note: “BDL” represents below the detection limit. “Top” represents the top scale layer and “bottom” represents the bottom scale layer .

The thickness of the scales was similar between the control and test pipes (Figure A5.7), ranging from 70 μm to 170 μm . Furthermore, aluminum was present in the scale layers according to both EDS mapping and ICP-MS, with concentrations varying from 9 to 107 mg/g (Table A5.3).

Previous research has also indicated that amorphous materials rich in aluminum are common in LSLs (Kvech and Edwards, 2001; Li et al., 2020). No significant difference in elemental distribution was noticed between the control and test pipes.

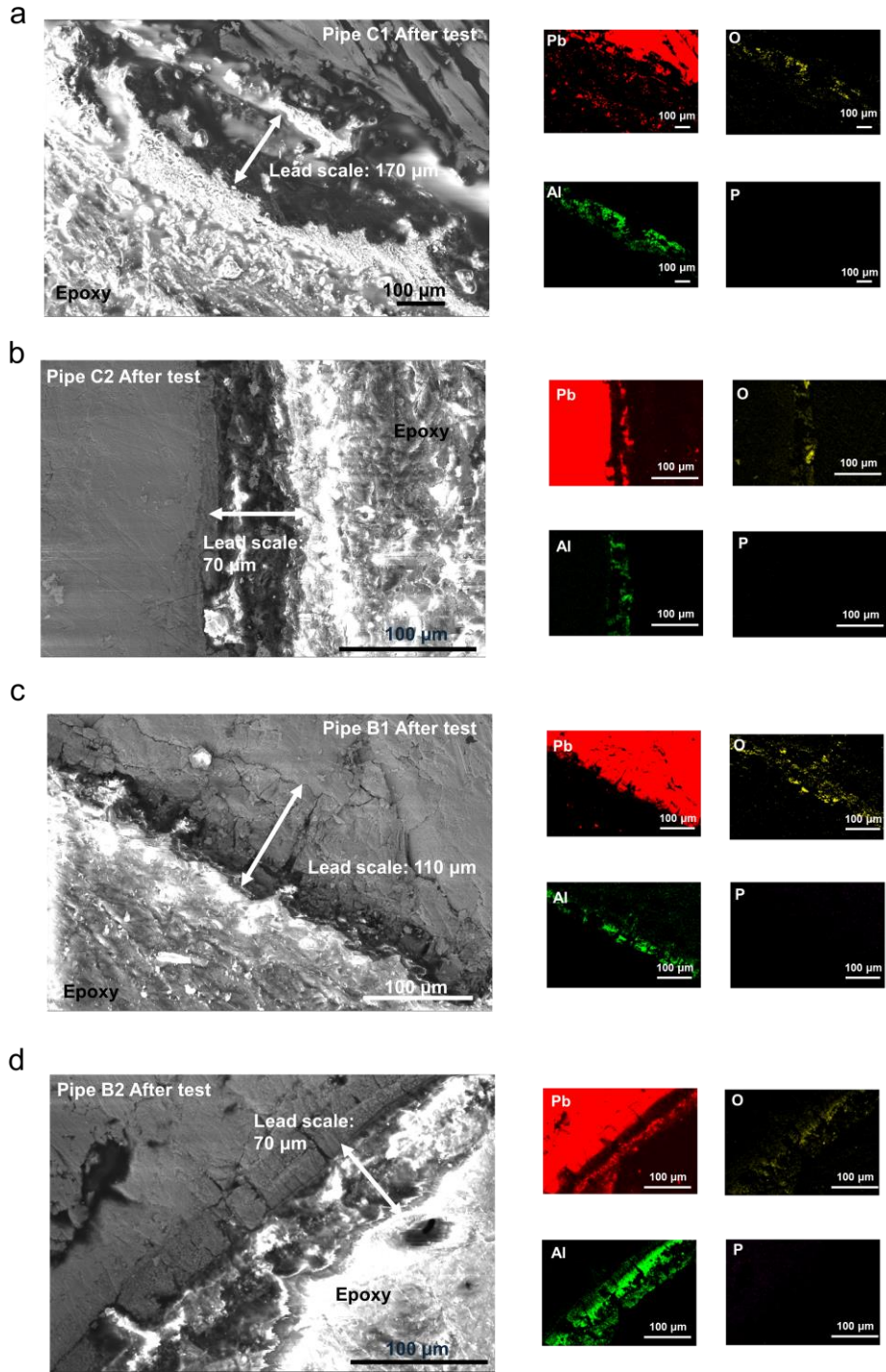


Figure A5.7 SEM images (left side) of the cross-section of the with elemental mappings (right side) of different elements detected by EDS after test for (a) Control Pipe C1, (b) Control Pipe C2, (c) Test Pipe B1, and (d) Test Pipe B2.

A5.3 Conclusions

Water blending from ECWA and Buffalo water (50%:50%) was tested on pipes over a 14-day period, with 1 mg/L of free chlorine as Cl_2 and under periodic flow conditions. All the pipes had PbO_2 -rich layers in their scales and were stabilized with low lead release prior to tests. Compared to ECWA water, Buffalo water has a lower pH of 7.7 and uses blended phosphate as a corrosion inhibitor. The results indicated that the water blending had minimal impact on lead release from the test pipes. PbO_2 remained the dominant component in the pipe scale, and no lead-phosphate solids were detected in the test pipes. Further tests could be conducted on lead release during longer durations of water blending.

Appendix A6: Supporting Information for **Chapter 6**

A6.1 Lead Pipe Harvesting Protocols

Harvesting procedures were followed to ensure minimal disruption to both the pipes and the scales on their inner surfaces: The lead pipe was cut using a tube cutter or ratcheted guillotine blade to avoid abrasive cutting wheels. After draining the pipe, a damp sponge was inserted into each end to avoid disturbance of the scales. Both ends of pipes were sealed with duct tape and often plastic wrap as well, and the pipe was wrapped with a single layer of bubble wrap.

A6.2 Scale Analysis Methods

The harvested lead pipes were manually cut open into two transverse sections using a hacksaw. Scales were collected by gently scraping them from the inner surface of a transverse section using a stainless-steel spatula. The scale removed from the inner pipe surface may consist of multiple layers distinguished by their color, crystalline phase, and elemental composition differences.

The mineral solid phase of the scale was identified using X-ray diffraction (XRD, Bruker d8 Advance). Samples were held in place using an MTI 1-inch low background Si sample holder and scanned under copper $K\alpha$ radiation from 5 to 80° 2 θ with a 0.02° step size. XRD patterns were analyzed by comparing diffraction data to a reference database of the International Centre for Diffraction Data (ICDD). Element composition of scale was characterized by inductively coupled plasma mass spectrometry (ICP-MS, NexION 2000). The scales were weighed and then

digested in a mixture of concentrated hydrochloric and nitric acids (3:1 by volume) at 100°C for two hours. After digestion, the solution was diluted 10,000-fold with deionized water, followed by a quantitative analysis of its elemental composition using ICP-MS.

The morphology of the scale was characterized by scanning electron microscopy (SEM, Thermo Fisher Quattro S E-SEM). The element distribution within the scales was characterized by energy dispersive X-ray spectroscopy (EDS, Oxford AzTec). These analyses involved the examination of a cross section and transverse section of the pipe segment. To prepare a cross section, one end of the pipe was filled with a mixture of hardener and epoxy resin (18 wt.%). Once the epoxy had cured, this section was cut from the rest of the segment and polished using sandpapers of increasingly fine grit (up to 1200 grit). The polishing was done with mineral oil on the sandpaper to minimize the generation of airborne particles. The polished segment was cleansed with ethanol to eliminate any residual mineral oil prior to its characterization using SEM-EDS.

A6.3 Model Predication for Crystalline Lead Phase

For systems where parameters remained almost consistent, average values were input. For systems with substantial variability in water chemistry, a computational titration method was adopted to thoroughly assess key parameters, including pH, free chlorine dosing, and orthophosphate addition. For all computations, a total input lead concentration of 0.1 mg/L was used, and the temperature was fixed at 25°C, with ionic strength calculated by the software based on the inputs. Predictions regarding lead-carbonate solids included cerussite (PbCO_3), hydrocerussite ($\text{Pb}_3(\text{CO}_3)_2(\text{OH})_2$) and plumbonacrite ($\text{Pb}_{10}(\text{CO}_3)_6\text{O}(\text{OH})_6$). Due to limitations in available thermodynamic constants for alternative lead-phosphate solids and lead(IV) oxide

solids (PbO_2) in the software, hydroxylpyromorphite ($\text{Pb}_5(\text{PO}_4)_3(\text{OH})$) and plattnerite ($\beta\text{-PbO}_2$) were chosen as their model solids, respectively. Other lead solids were not considered in our computations.

To predict the presence of lead-carbonate and lead-phosphate solids, the output for the Saturation Index was examined (Saturation Index = $\log \text{IAP} - \log \text{Ksp}$, where IAP is the ion activity product and Ksp is the solubility product). For lead(IV) oxide solids, the system's redox potential, calculated by the software, was compared with the theoretical redox potential derived from reduction half-reactions in Table S6.

A6.4 Lead-phosphate Solids: Phosphate Inhibitors and Water Chemistry

Pb-P solids have various crystalline phases reported in LSLs including phosphohedyphane ($\text{Ca}_2\text{Pb}_3(\text{PO}_4)_3\text{Cl}$), calcium lead phosphate hydroxide ($\text{Ca}_x\text{Pb}(5-x)(\text{PO}_4)_3\text{Cl}$) and hydroxylpyromorphite ($\text{Pb}_5(\text{PO}_4)_3\text{OH}$). The primary phosphate-based corrosion inhibitors used include orthophosphate, blended-phosphate and zinc phosphate. Half of the PWSs involved in our study use phosphate-based inhibitors as their corrosion control method, while the remaining primarily rely on pH and alkalinity adjustment (Figure A6.7a). Orthophosphate and blended-phosphate are the two major phosphate-based inhibitors.

The calculated threshold orthophosphate concentration needed to form Pb-P solids often sits below 0.8 mg/L PO_4 , a level achievable by most PWSs (Table A6.9). Those PWSs where a required higher orthophosphate concentration is predicted correlate with either very high DIC levels, such as iPWS 17-MI (DIC 9.4 mM), or high pH, as seen in PWS A-2 (pH 10.2). PWSs

containing Pb-P solids showed no significant difference in DIC levels compared to those without Pb-P solids (1.7 ± 1.6 mM versus 2.5 ± 1.5 mM, Figure A6.7e, p-value=0.33), nor in pH levels between the two (8.1 ± 0.7 versus 8.0 ± 0.6 , Figure A6.7f, p-value=0.51).

A6.5 Amorphous Material: Elements in Scale Phase and Finished Water

The role of amorphous material in corrosion control is complex. It can serve as a protective barrier for metal corrosion and sequester metals like Al, Fe, and Mg (Li et al., 2018; Lobo et al., 2022). Meanwhile, its vulnerability to fluctuations in water dynamics and chemistry poses a risk of detachment of the bound metals (Li et al., 2020).

There is a significant linear relationship between P concentrations in finished water and P weight concentrations from scale analysis (Pearson correlation coefficient $r = 0.56$) (Figure A6.8a).

There is no significant relationship between finished water concentrations and scale weight percentage for either Ca or Mg (Pearson correlation coefficient $r = -0.15$ and 0.39 for Ca and Mg respectively, Figures A6.8b and A6.8c). This may require further investigation, as the primary mechanisms for calcium and magnesium incorporation into scales are likely due to deposits from treated water.

A6.6 Applications of Scale Analysis Techniques and Their Limitations

An overall challenge in scale analysis is the physical disturbance during segment excavation, transportation, and sample preparation. Scales may fall off as a result of external physical forces.

Therefore, scale analysis may not provide information on the original pipe scales but altered ones. Key parameters such as morphology, elemental distribution and solid compositions can all change consequently. Loosely attached amorphous materials are especially prone to this loss. Another main barrier involves the choice of segment to be analyzed. Pipe systems are not homogenous, underlying material compositions and flow characteristics are not constant at different parts of the distribution systems. Selection of segments should include considerations on whether they are representative of the overall system.

XRD techniques are only able to identify crystalline solids. However, in actual water systems, amorphous solids can be present and even abundant (Tables A6.3 and A6.4). XRD can be used to determine if amorphous solids are present, but it cannot characterize amorphous materials. In addition, several common lead solids found in drinking water have similar or even overlapping major peaks. For example, cerussite and hydrocerussite can be distinguished by their exclusive peaks (e.g. $2\theta=25^\circ$ and 43° for cerussite and $2\theta=27^\circ$ and 35° for hydrocerussite), but they also share similar XRD patterns (Figure A6.9a), and so as peaks between lead-phosphate solids (Figure A6.9c). This similarity among XRD patterns poses another challenge in identifying solid phases. To accurately identify the crystalline phase in practical analysis, it is essential to combine XRD results with additional factors such as water chemistry, scale color, and the mass concentration of different elements. Another limitation of employing XRD is the almost inevitable incorporation of elemental lead. During sample preparation, shavings and scratching of underlying unaltered pipe materials can all contribute to the detection of elemental lead by XRD (Figure A6.9a). Elemental lead patterns can make solid phase identification more difficult due to its overlapping peaks with other crystal solids. Other solids at a low weight concentration may not be identified.

The main limitation of ICP-MS is its detection limits. Trace elements, such as arsenic, cadmium and chromium, may not be detected by ICP-MS due to their relatively low contents. In addition, undesired elemental lead from sample preparations may overestimate lead concentration and underestimate other elements. Additionally, ICP-MS is primarily used for measuring metal concentrations, but it is not effective for most non-metals, including carbon and oxygen, which are often abundant in the scale. Moreover, without the use of hydrofluoric acid for digestion ICP-MS does not provide quantification of silicon in the scale.

SEM image on the morphology of scale layers may be biased by physical distortion during sample preparation. Scale layer thickness reported by SEM may be thinner than visual inspection. This difference could be attributed to detachment of loose layers when carbon epoxy is used to solidify samples. Future work is needed to reduce the physical impact of carbon epoxy on SEM samples or alternative techniques should be explored.

EDS is a semi-quantitative tool, which only reports relative weight distribution of elements selected for analysis. It can be utilized to gain a general understanding on the spatial distribution and relative abundance of different elements. However, one should be cautious on the exact concentrations provided by EDS.

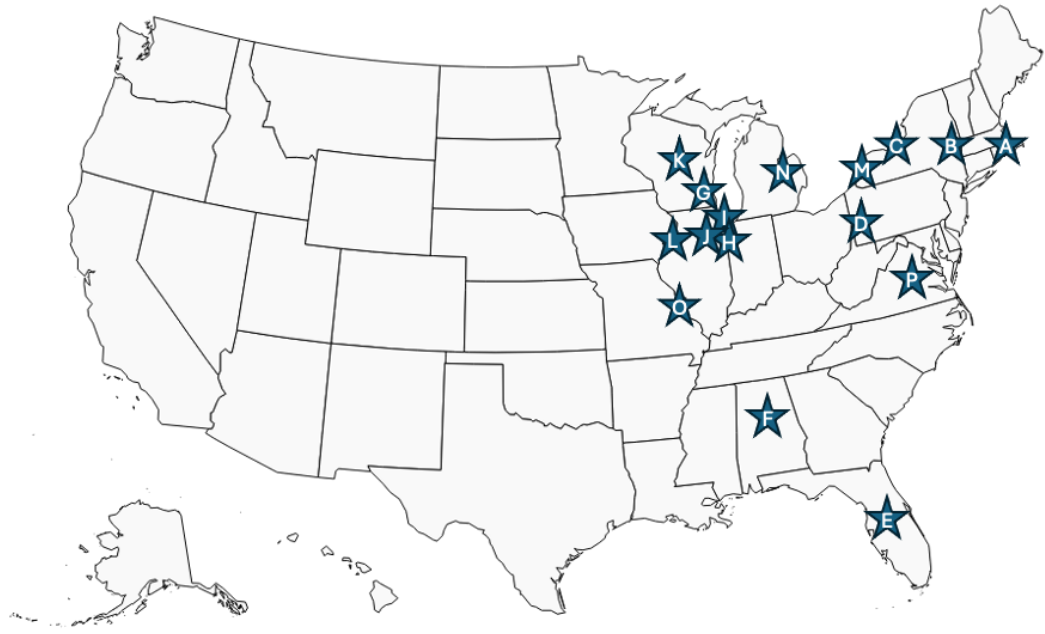


Figure A6.1 Locations for PWSs with laboratory pipe scale analysis by this study.

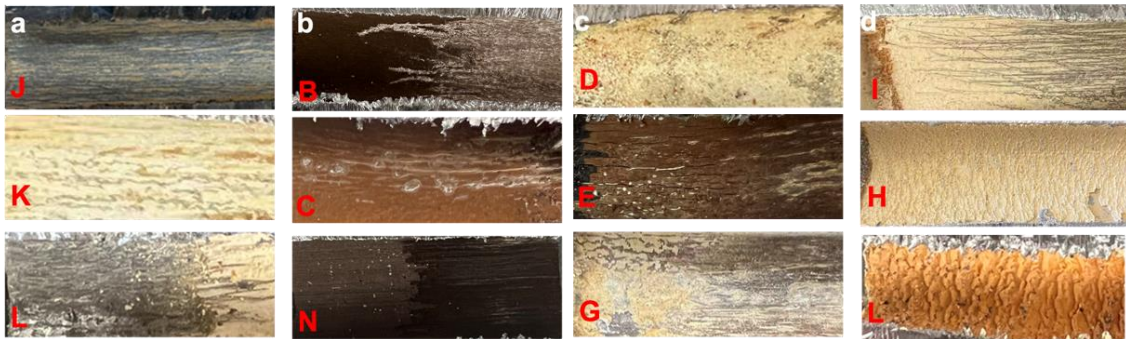


Figure A6.2 Longitudinal cross-sections of LSLs dominated by different phases: (a) Pb-C solids from PWSs J, K, L. (b) PbO₂ solids from PWSs B, C, N. (c) Pb-P solids from PWSs D, E, G. (d) Amorphous layers from PWSs I, H, L.

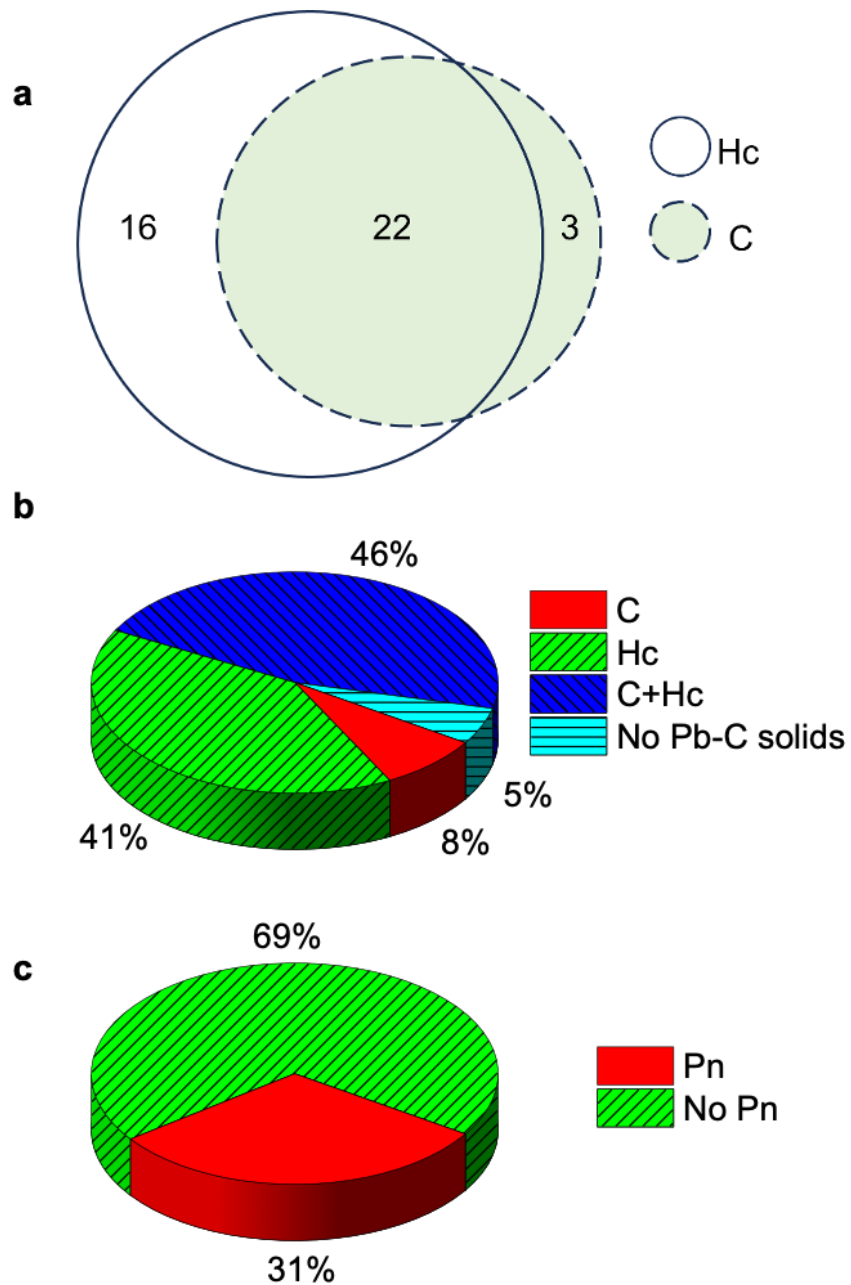


Figure A6.3 (a) Venn diagram of the presence of different Pb-C solids in pipe scales. (b) Percentage of PWSs with Pb-C solids: cerussite (C), hydrocerussite (Hc), cerussite and hydrocerussite (C+Hc) and no Pb-C solid. (c) Percentage of PWSs with and without plumbonacrite (Pn).

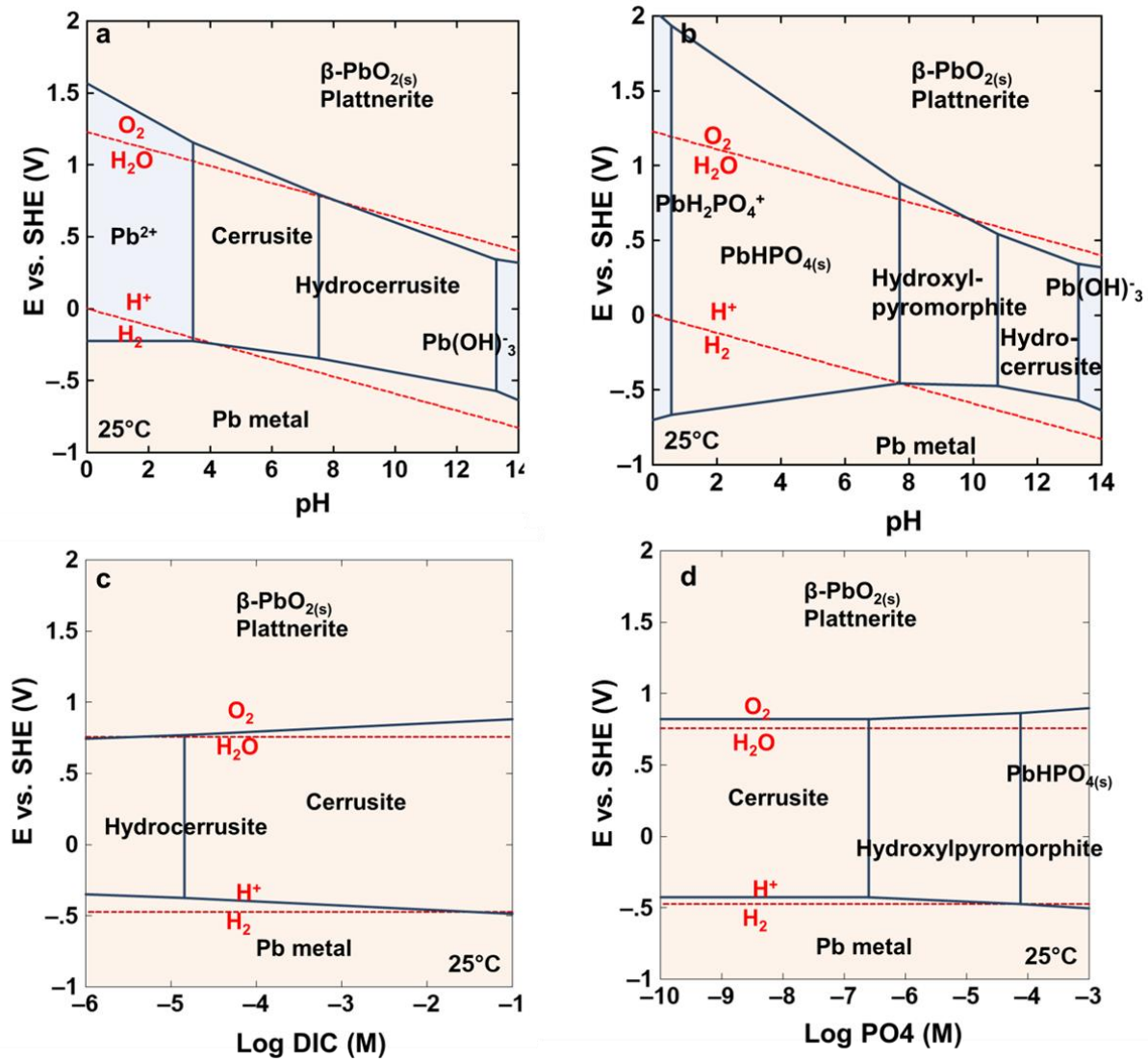


Figure A6.4 Eh-pH diagram for lead species in water system constructed using the Geochemist's Workbench 2023 using MINTEQA2 database (Table A6.5). (a) Lead species = 0.01 mg/L, DIC = 12 mg/L as C. (b) Lead species = 0.01 mg/L, DIC = 20 mg/L as C, orthophosphate = 1.0 mg/L as PO₄. (c) Eh-Log DIC diagram for lead species (Lead species = 0.01 mg/L, pH = 8). (d) Eh-Log PO₄ diagram for lead species (Lead species = 0.01 mg/L, pH = 8, DIC = 12 mg/L).

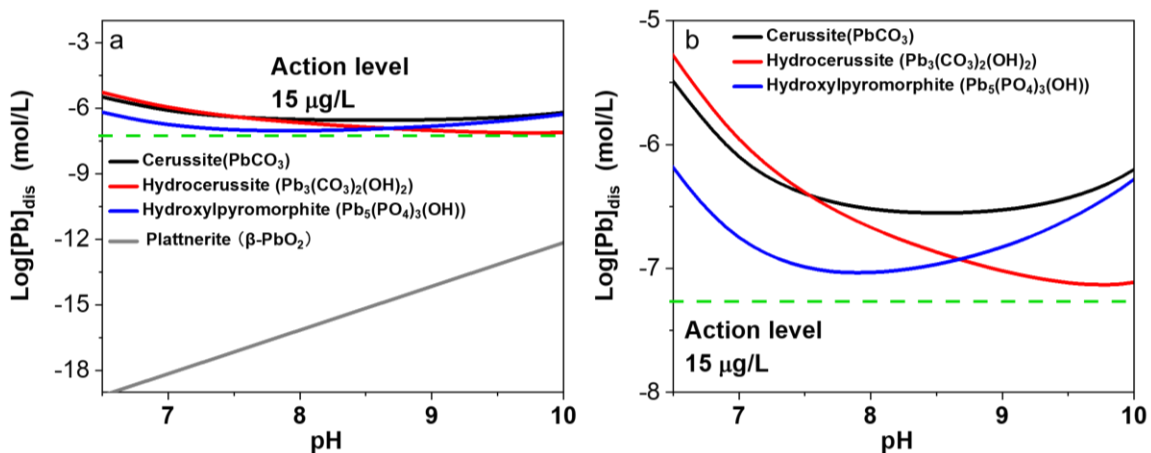


Figure A6.5 Equilibrium lead solubility for water (a) with free chlorine and without (b) free chlorine. (Lead species = 0.01 mg/L, DIC = 12 mg/L as C, orthophosphate = 1.0 mg/L as PO_4 .) Calculations were performed using Visual MINTEQ3.1 and its default database (relevant reactions indicated in Table A6.5). This database does not include any reactions for dissolved lead complexation with polyphosphate. Equilibrium solubility of plattnerite (β - PbO_2) was calculated as the summation of the Pb^{4+} and the hydrolysis complexes PbO_3^{2-} and PbO_4^{4-} according to Table A6.6 and Table A6.7.

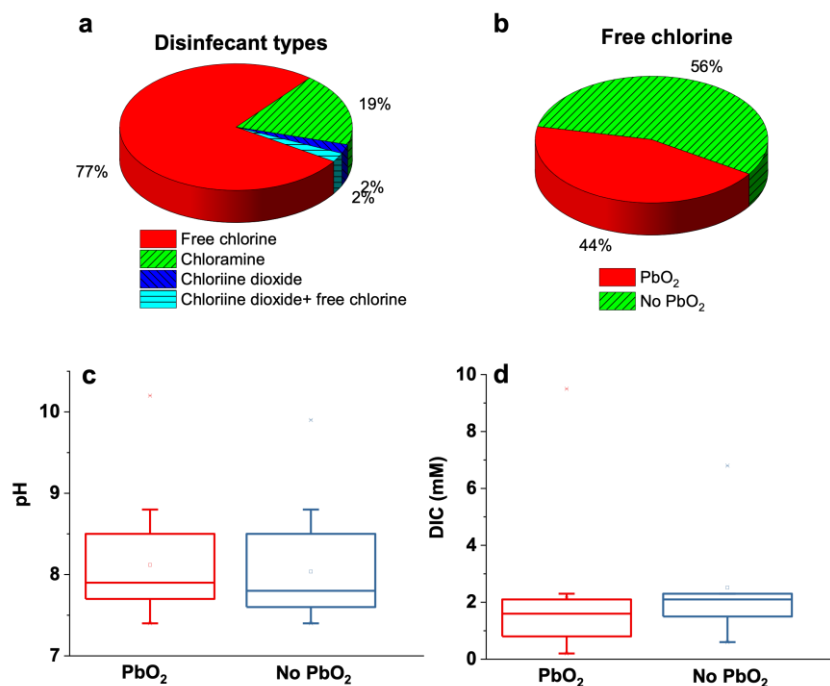


Figure A6.6 (a) Disinfectant types in PWSs included in this research. (b) Percentage of PWSs using free chlorine with and without PbO_2 solids. (c) pH of PWSs with and without PbO_2 solids. (d) DIC of PWSs with and without PbO_2 solids.

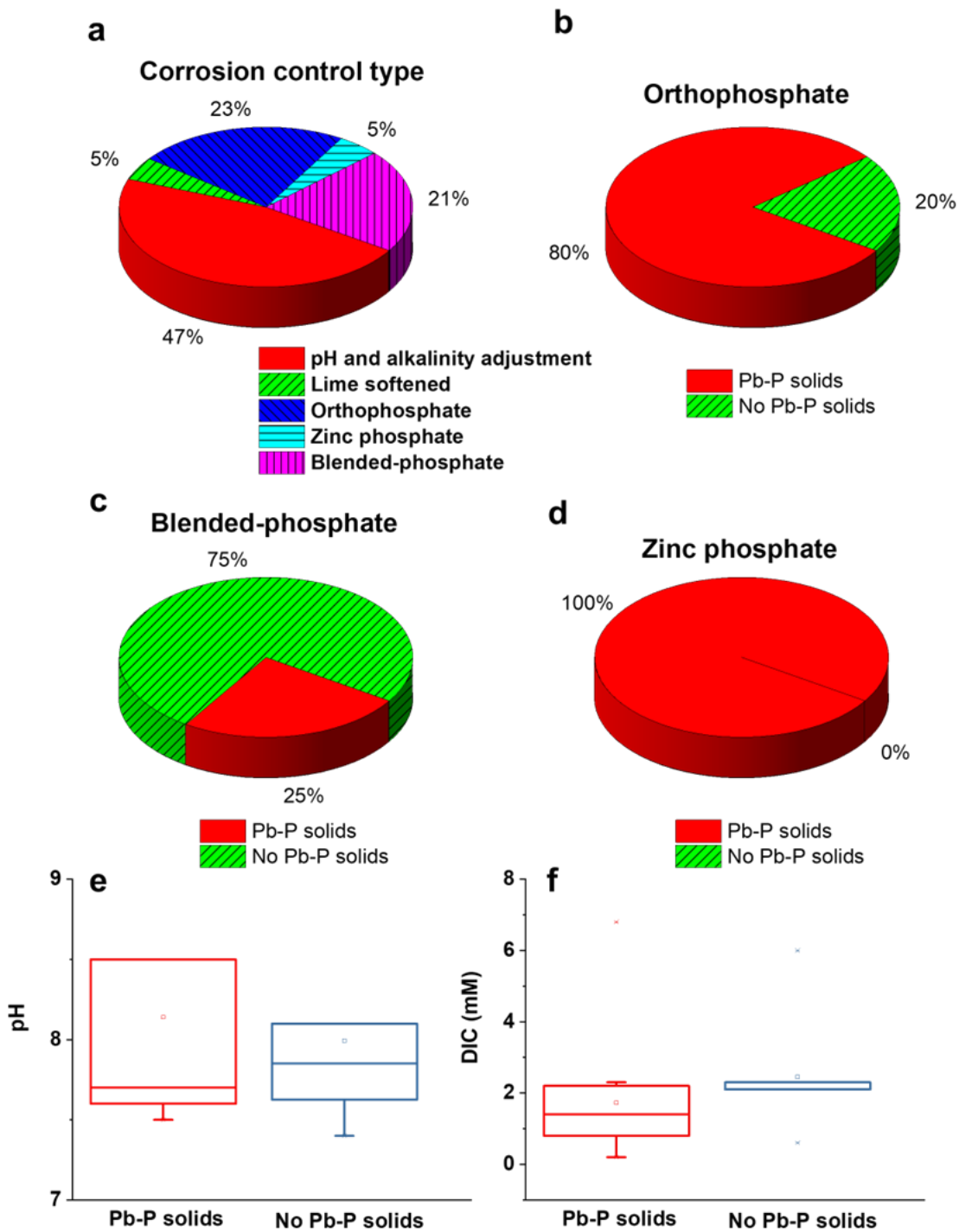


Figure A6.7 (a) Corrosion control treatment methods in PWSs included in this research. Presence of Pb-P solids in PWSs using (b) orthophosphate (c) blended-phosphate and (d) zinc phosphate. (e) pH and (f) DIC of PWSs with and without Pb-P solids.

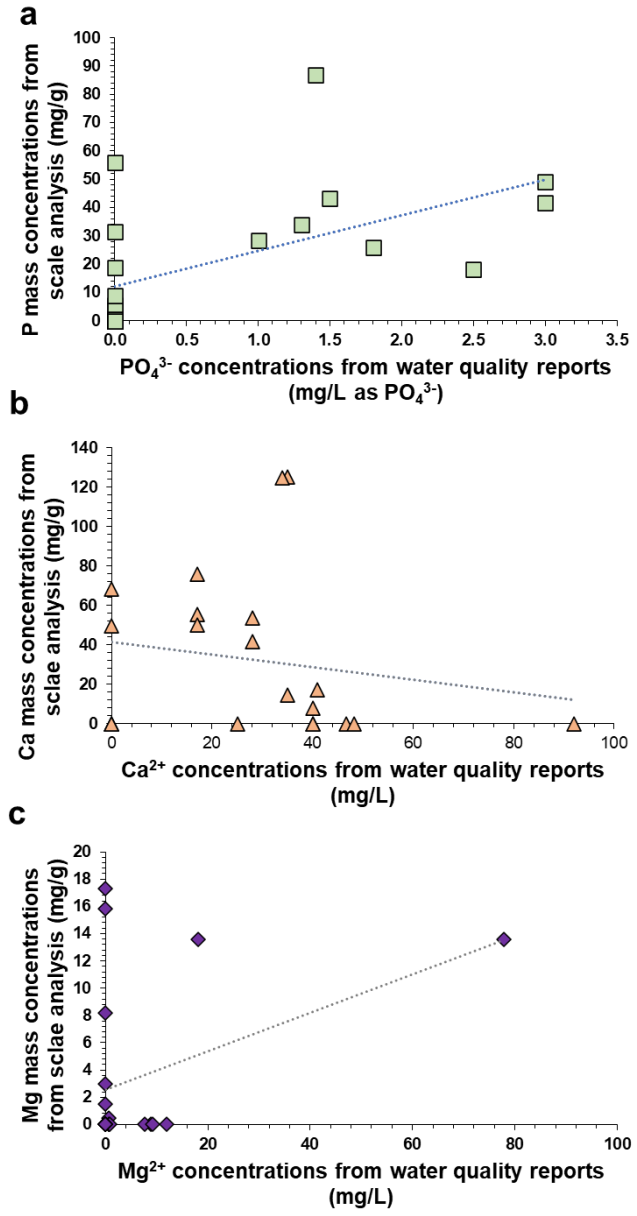
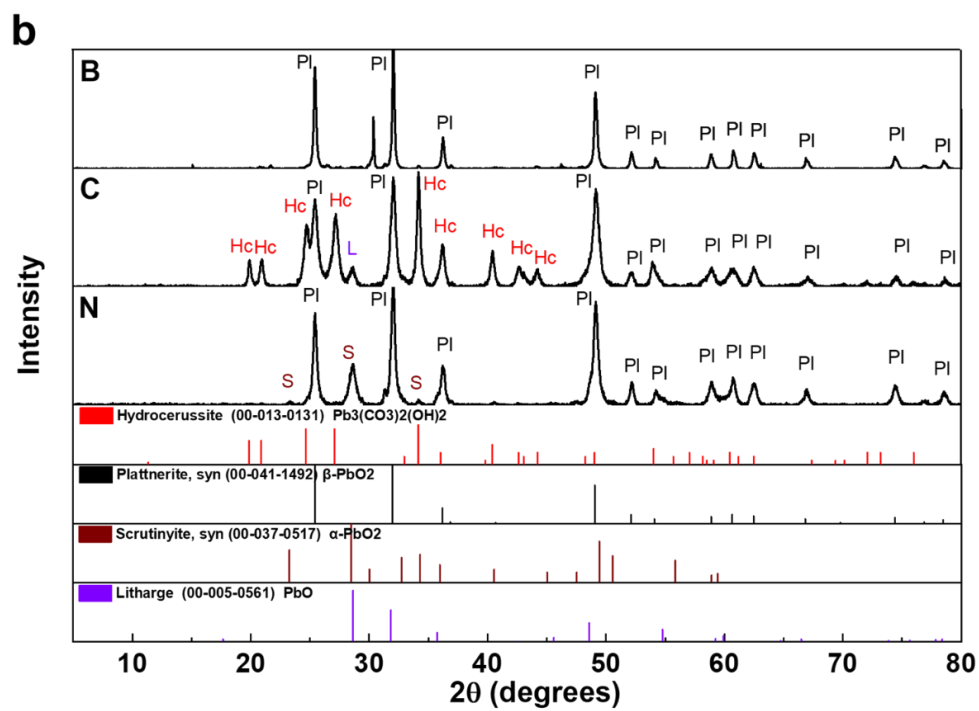
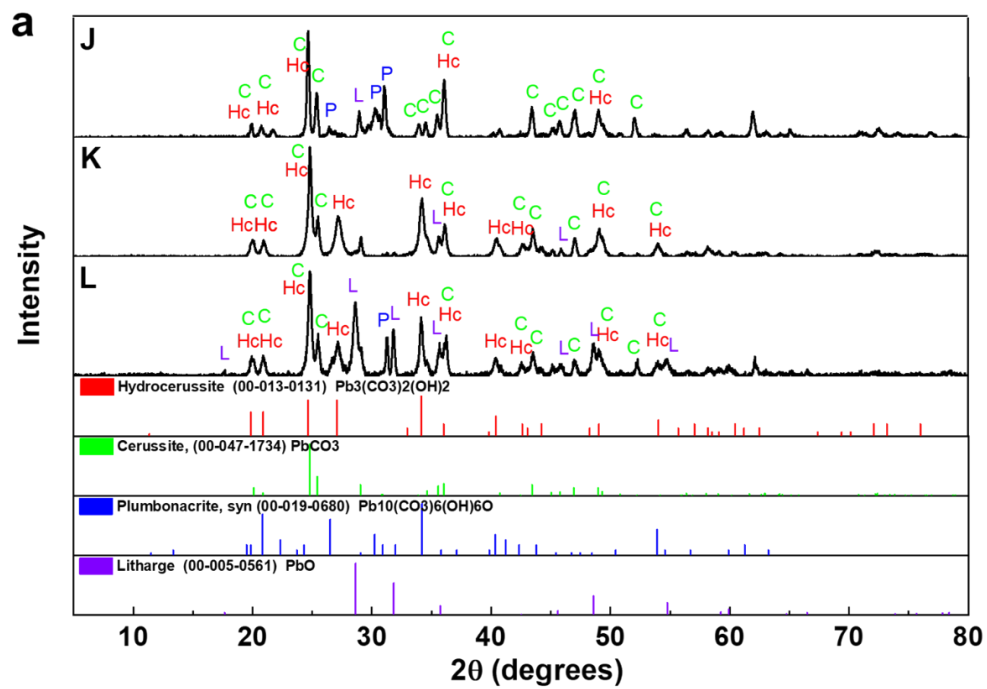


Figure A6.8 Correlations between mass concentrations in pipe segment scales and concentrations in finished water for (a) P, (b) Ca, and (c) Mg



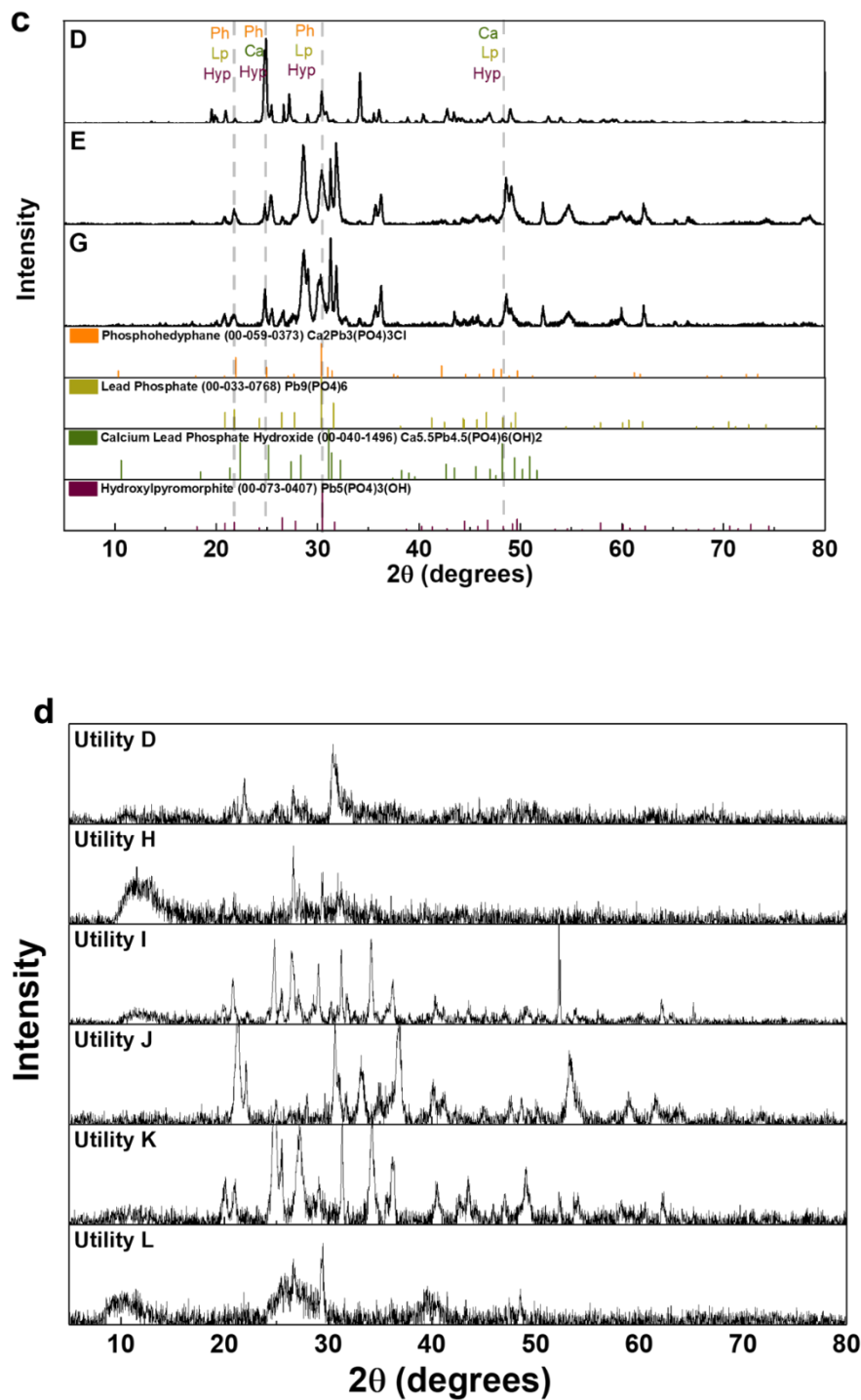


Figure A6.9 XRD patterns pipe scales from different PWSs. (a) Pb-C solids scale; (b) PbO_2 solids scale; (c) Pb-P solids scale; (d) Amorphous material. The patterns at the bottom are the reference patterns for H : hydrocerussite ($\text{Pb}_3(\text{CO}_3)_2(\text{OH})_2$), C: cerussite (PbCO_3), P: plumbonacrite ($\text{Pb}_{10}(\text{CO}_3)_6(\text{OH})_6\text{O}$), L: litharge (PbO), Pl: plattnerite ($\beta\text{-PbO}_2$), S: scrutinyite ($\alpha\text{-PbO}_2$), Ph: phosphohedyphane ($\text{Ca}_2\text{Pb}_3(\text{PO}_4)_3\text{Cl}$), Lp: lead phosphate ($\text{Pb}_9(\text{PO}_4)_6$), Ca: calcium lead phosphate hydroxide ($\text{Ca}_2\text{Pb}_8(\text{PO}_4)_6(\text{OH})_2$), and Hyp: hydroxylpyromorphite ($\text{Pb}_5(\text{PO}_4)_3(\text{OH})$).

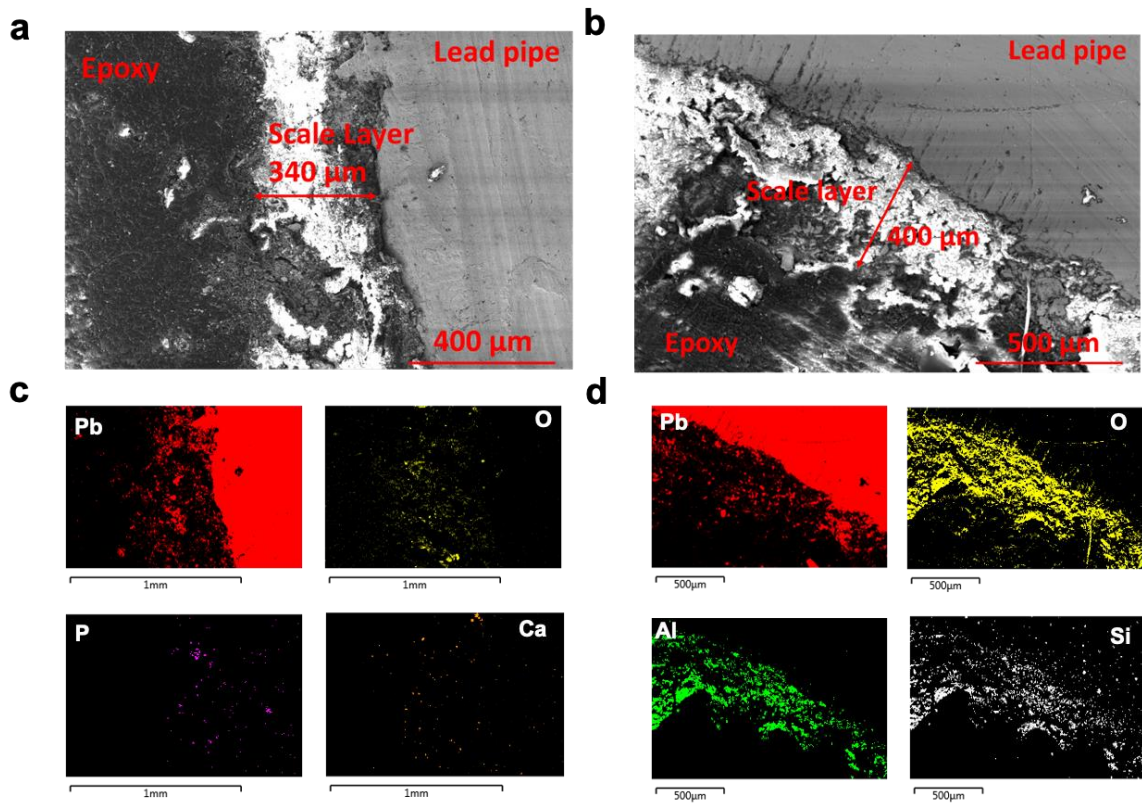


Figure A6.10 SEM image of the cross-section of the pipe for (a) PWS-D and (b) PWS-L. Elemental mapping of different elements detected by EDS for (c) PWS-D and (d) PWS-L.

Table A6.1 Finished water chemistry from different PWSs.

PWSs ID	pH	Alkalinity (mg/L)	DIC (mM)	Disinfectant	Free chlorine (mg/L as Cl ₂)	Corrosion control	Orthophosphate (mg/L)
A-1 (4)	10.2	17.0	0.2	Free chlorine	1.0	pH/alkalinity	/
A-2 (5)	10.2	17.0	0.2	Free chlorine	1.0	Orthophosphate	1.0-1.5
A-3 (6)	10.2	17.0	0.2	Free chlorine	1.0	Orthophosphate	2.0-3.0
B (4)	8.5	42.7	0.8	Free chlorine	0.8	pH/alkalinity	/
C (13)	7.7	77.5	1.6	Free chlorine	0.9	pH/alkalinity	/
D-1(4)	8.5	37.8	0.8	Free chlorine	1.3	Orthophosphate	1.5-2.0
D-2 (2)	8.5	37.8	0.8	Free chlorine	1.3	Orthophosphate	3.0
E (3)	7.9	88.8	1.8	Free chlorine	2.4	Orthophosphate	0.2
F (1)	8.1	54.0	1.1	Free chlorine	1.8	pH/alkalinity	/
G (4)	7.7	108.0	2.2	Free chlorine	1.3	Blended phosphate	0.7
H-1 (6)	8.1	106.5	2.1	Free chlorine	1.4	Blended phosphate	1 (60%)
H-2 (2)	8.1	106.5	2.1	Free chlorine	1.4	Orthophosphate	1-2
H-3 (2)	8.1	106.5	2.1	Free chlorine	1.4	Orthophosphate	3
I (1)	7.6	96.0	2.0	Free chlorine	1.0	Blended phosphate	0.3 (40%)
J (1)	8.9	71.0	1.5	Chloramine	/	pH/alkalinity	/
K (1)	8.7	83.0	1.6	Chloramine	/	pH/alkalinity	/
L (1)	8.5	163.0	3.3	Chloramine	/	pH/alkalinity	/
M (4)	8.0	92.0	1.6	Free chlorine	1.1	pH/alkalinity	/

N (3)	8.5	90.0	1.8	Free chlorine	1.3	pH/alkalinity	/
O (1)	9.6	58.0	1.0	Chloramine	/	pH/alkalinity	/
P (2)	7.8	43.4	0.9	Chloramine	/	Zinc orthophosphate	1.4
1-OH	9.9	64	0.9	Free chlorine	1.72	Lime softened	/
2-OH	8.1-9.5	42-102	1.4	Free chlorine	0.78-1.48	pH/alkalinity	0.08-0.18
3-OH	8.8	31.5	0.6	Chlorine dioxide	0.12-0.48	Lime softened	0.038
4-IN	8.8	35.78	0.7	Chloramine	/	pH/alkalinity	/
5-OH	8.5	74.5	1.5	Chlorine dioxide + free	0.8	pH/alkalinity	/
6-IN	7.7-8.0	/	2.1	Chloramine	1.1-1.4	pH/alkalinity	/
7-IL	7.8	193	4.0	Free chlorine	1.3	pH/alkalinity	/
8-WI	7.6-7.9	100-130	2.3	Free chlorine	0.52	pH/alkalinity	/
9-IL	7.5	448	9.5	Free chlorine	0.18	pH/alkalinity	0.91
10-WI	7.1-7.6	259-336	6.5	Free chlorine	0-0.4	pH/alkalinity	/
11-WI	7.3-7.9	225-266	5.2	Free chlorine	0.1-0.35	pH/alkalinity	/
12-OH	7.5	85	1.8	Free chlorine	0.9	pH/alkalinity	/
13-IL	7.7-7.8	98-108	2.1	Free chlorine	0.70-0.9	Blended phosphate	0.51
14-IL	7.8	101	2.1	Free chlorine	0.8	Blended phosphate	0.3
15-IL	7.4	276	6.0	Free chlorine	/	Blended phosphate	0.28
16-MI	7.5	109	2.3	Free chlorine	1.3	Blended phosphate	1.1
17-MI	9.4	35	0.6	Chloramine		Orthophosphate	0.2
18-MI	7.5	71.3	1.4	Free chlorine	0.67	Orthophosphate	3.1
19-OH	7.7	55	1.1	Free chlorine	/	Zinc phosphate	1.2

20-WI	7.9	110.8	2.3	Free chlorine	0.49	Blended phosphate	0.19
21-WI	7.5	322.5	6.8	Free chlorine	0.61	Blended phosphate	0.22
22-WI	7.7	106.1	2.2	Free chlorine	0.78	Orthophosphate	0.5-0.55

Note: PWSs “A” to “H” were analyzed by this research and the data are collected from their latest water quality reports. PWSs “A-1”, “A-2”, “A-3” were from the same area but with different corrosion control treatment conditions denoted by -1, -2 and -3; The values in parentheses “()” after PWSs “A” to “H” indicate the number of pipes analyzed. Any value in this table without a range is reported in average; “/” means the value was missed in the water quality report. PWSs “1-OH” to “22-WI” are sourced from Tully et al. (2019).

Table A6.2 Finished water element concentrations from different PWSs

PWSs	Ca	Fe	Mg	Mn	PO ₄ ³⁻	Cl ⁻	SO ₄ ²⁻
A-1 (4)	17.0	/	0.7	0.0008	0	30	28.9
A-2 (5)	17.0	/	0.7	0.0008	1.3	30	28.9
A-3 (6)	17.0	/	0.7	0.0008	2.5	30	28.9
B (4)	/	0.02	0.84	0.03	/	21.2	19.1
C (13)	35.0	0.3	8.9	/	/	25.5	26.0
D-1(4)	28.0	/	/	/	1.8	20.0	/
D-2 (2)	28.0	/	/	/	3	20.0	/
E (3)	/	/	/	/	/	22.0	1.9
F (1)	46.7	/	7.7	/	/	9.0	74.3
G (4)	35.0	0.3	/	/	/	18.0	22.0
H-1 (6)	40.0	/	/	/	1.0	20.0	27.1
H-2 (2)	40.0	/	/	/	1.5	20.0	27.1
H-3 (2)	40.0	/	/	/	3.0	20.0	27.1
I (1)	34.0	/	12.0	/	/	15.0	25.0
J (1)	48.2	/	77.9	/	/	113.0	33.1
K (1)	/	/	/	/	/	28.0	9.0
L (1)	41.0	/	/	/	/	/	/
M (4)	92.0	/	9.2	/	/	20.0	21.0
N (3)	/	/	/	/	/	20.0	/
O (1)	25.1	/	18.1	0.20	/	27.5	151.3
P (2)	/	/	/	<0.01	1.4	12.0	31.6
1-OH	37.0	/	5.0	/	0.5	/	/
2-OH	48.5	<0.05	8.9	<0.01	/	32.5	72.5
3-OH	31.7	0.0	20.8	/	/	64.5	109.3
4-IN	28.2	0.0	6.9	0.0	/	30.6	56.7
5-OH	/	<0.04	/	<0.05	/	/	/
6-IN	/	<0.1	/	<0.01	/	/	24.9

7-IL	62.0	/	34.0	/	/	34.0	56.0
8-WI	34.5	0.0	11.5	/	/	14.5	22.5
9-IL	25.0	0.0	11.0	/	0.6	17.0	0.4
10-WI	81.0	0.12	43.0	/	/	40.9	56.1
11-WI	93.3	0.26	31.8	/	/	39.8	100.3
12-OH	32.0	/	8.2	<0.002	<0.010	19.0	26.0
13-IL	36.5	<0.005	/	<0.003	0.3	18.5	29-30
14-IL	35.0	/	12.0	/	/	14.0	20.3
15-IL	87.0		40.2	/	/	/	/
16-MI	39.0	<0.02	10.5	/	0.6	17.3	24.0
17-MI	20.0	0.2	10.0	/	0.8	46.0	70.0
18-MI	34.8	0.0	5.5	/	/	13.4	/
19-OH	37.0	0.1	6.0	<0.0005	/	40.0	110.0
20-WI	39.0	/	13.0	/	0.1	23.1	28.0
21-WI	59.0	0.2	44.5	0.0	0.5	4.8	11.0
22-WI	36.0	/	17.0	/	0.5	19.0	23.0

Note: PWSs “A” to “H” were analyzed by this research and the data are collected from their latest water quality reports. PWSs “A-1”, “A-2”, “A-3” were from the same area but with different corrosion control treatment conditions denoted by -1,-2 and -3; All values in this table are reported in average, and “/” means the value was missed in the water quality report. PWSs “1-OH” to “22-WI” are sourced from Tully et al. (2019).

Table A6.3 Identification of lead crystalline solids in pipe scales

PWSs	Cerussite (PbCO ₃)	Hydrocerussite (Pb ₃ (CO ₃) ₂ (OH) ₂)	Litharge (PbO)	Plattnerite (β-PbO ₂)	Pb-P solids	Plumbonacrite (Pb ₁₀ (CO ₃) ₆ O(OH) ₆)	Scrutinyite (α-PbO ₂)	Amorphous Materials
A-1	-	+	+	+	-	+'	-	-
A-2	-	+	+	+	+'	+'	-	-
A-3	-	+	+	+	+'	+'	-	-
B	+'	+	+	+	-	+'	+'	-
C	+'	+	+	+	-	-	+'	-
D-1	+'	+'	+'	-	+	+'	-	+'
D-2	-	-	+'	-	+	-	-	+'
E	-	+	+	+	+	-	-	-
F	-	-	+	+	-	-	-	-
G	+	+	+	-	+'	-	-	-
H-1	+'	+	+'	-	-	-	-	+'
H-2	+'	+	+'	-	-	-	-	+
H-3	+	+	+	-	+	-	-	+
I	-	+	+	-	+'	-	-	+
J	-	+	+	-	-	+	-	+
K	+	+	+	-	-	-	-	+
L	+	+	+	-	-	-	-	+
M	-	+	+	+	-	-	-	-
N	+'	+	+'	+	-	-	+	-
O	+	+	+	-	-	-	-	-
P	+	+	+'	-	+'	-	-	+

Note: “ - ” indicates that the phase was not identified in any analyzed pipe in the system; “ +' ” indicates that the phase was identified in some pipes in the system but not all; ; “ + ” indicates that the phase was identified in all of the pipes in the system; Pb-P solids include phosphohedyphane(Ca₂Pb₃(PO₄)₃Cl), calcium lead phosphate hydroxide (Ca_xPb(5-x)(PO₄)₃Cl) and hydroxylpyromorphite (Pb₅(PO₄)₃OH).

Table A6.4 Identification of lead mineral solids in pipe scales based on Tully et al. (2019)

PWSs ID	Cerussite (PbCO ₃)	Hydrocerussite (Pb ₃ (CO ₃) ₂ (OH) ₂)	Plattnerite (β-PbO ₂)	Litharge (PbO)	Pb-P solid	Plumbonacrite (Pb ₁₀ (CO ₃) ₆ O(OH) ₆)	Amorphous layer
1-OH	-	+	-	-	-	+	-
2-OH	-	+	+	+	-	-	-
3-OH	-	+	-	+	-	-	+
4-IN	-	+	-	+	-	+	-
5-OH	-	+	-	+	-	-	+
6-IN	+	+	-	+	-	+	-
7-IL	+	-	-	+	-	-	-
8-WI	+	+	-	+	-	+	+
9-IL	+	+	+	+	-	-	-
10-WI	+	-	+	+	-	-	+
11-WI	+	+	-	+	-	-	-
12-OH	-	+	-	+	-	+	-
13-IL	+	+	+	+	-	-	+
14-IL	+	+	-	-	-	+	-
15-IL	+	-	-	+	-	-	-
16-MI	+	+	-	+	-	-	-
17-MI	-	+	-	+	-	-	+
18-MI	+	+	+	+	+	-	+
19-OH	-	+	+	+	+	-	-
20-WI	+	+	-	+	-	+	+
21-WI	+	+	-	+	+	+	+
22-WI	+	+	-	+	+	-	-

Note: “ - ” indicates that the mineral was not identified in the system; “ + ” indicates that the mineral was identified in the system; Pb-P solids include tertiary lead phosphate (Pb₃(PO₄)₂), lead phosphate (Pb₉(PO₄)₆), calcium lead phosphate hydroxide (Ca_xPb_(5-x)(PO₄)₃Cl) and hydroxylpyromorphite (Pb₅(PO₄)₃OH).

Table A6.5 Dissolution-precipitation and aqueous reactions involving lead in the model calculations.

#	Reaction	Log K
1	$\text{Pb}(\text{CO}_3)_2^{2-} + 2\text{H}^+ \rightarrow \text{Pb}^{2+} + 2\text{HCO}_3^-$	10.72
2	$\text{Pb}(\text{OH})_2(\text{aq}) + 2\text{H}^+ \rightarrow \text{Pb}^{2+} + 2\text{H}_2\text{O}$	17.09
3	$\text{Pb}(\text{OH})_3^- + 3\text{H}^+ \rightarrow \text{Pb}^{2+} + 3\text{H}_2\text{O}$	28.09
4	$\text{Pb}_2\text{OH}^{3+} + \text{H}^+ \rightarrow 2\text{Pb}^{2+} + \text{H}_2\text{O}$	6.40
5	$\text{Pb}_3(\text{OH})_4^{2+} + 4\text{H}^+ \rightarrow 3\text{Pb}^{2+} + 4\text{H}_2\text{O}$	23.89
6	$\text{Pb}_4(\text{OH})_4^{4+} + 4\text{H}^+ \rightarrow 4\text{Pb}^{2+} + 4\text{H}_2\text{O}$	20.89
7	$\text{PbCO}_3(\text{aq}) + \text{H}^+ \rightarrow \text{Pb}^{2+} + \text{HCO}_3^-$	3.80
8	$\text{PbHCO}_3^+ \rightarrow \text{Pb}^{2+} + \text{HCO}_3^-$	-2.90
9	$\text{PbOH}^+ + \text{H}^+ \rightarrow \text{Pb}^{2+} + \text{H}_2\text{O}$	7.60
10	$\text{PbCO}_3(\text{cerussite}) + \text{H}^+ \rightarrow \text{Pb}^{2+} + \text{HCO}_3^-$	-2.87
11	$\text{Pb}_3(\text{CO}_3)_2(\text{OH})_2(\text{hydrocerussite}) + 4\text{H}^+ \rightarrow 3\text{Pb}^{2+} + 2\text{H}_2\text{O} + 2\text{HCO}_3^-$	1.90
12	$\text{PbO}(\text{litharge}) + 2\text{H}^+ \rightarrow \text{Pb}^{2+} + \text{H}_2\text{O}$	12.69
13	$\text{PbO}(\text{massicot}) + 2\text{H}^+ \rightarrow \text{Pb}^{2+} + \text{H}_2\text{O}$	12.89
15	$\text{Pb}(\text{OH})_2 + 2\text{H}^+ \rightarrow \text{Pb}^{2+} + 2\text{H}_2\text{O}$	8.15
16	$\text{Pb}_{10}(\text{OH})_6\text{O}(\text{CO}_3)_6 + 14\text{H}^+ \rightarrow 10\text{Pb}^{2+} + 7\text{H}_2\text{O} + 6\text{HCO}_3^-$	53.21
17	$\text{Pb}_2\text{O}(\text{OH})_2 + 4\text{H}^+ \rightarrow 2\text{Pb}^{2+} + 3\text{H}_2\text{O}$	26.19
19	$\text{Pb}_2\text{OCO}_3 + 3\text{H}^+ \rightarrow 2\text{Pb}^{2+} + \text{H}_2\text{O} + \text{HCO}_3^-$	9.77
20	$\text{Pb}_3\text{O}_2\text{CO}_3 + 5\text{H}^+ \rightarrow 3\text{Pb}^{2+} + 2\text{H}_2\text{O} + \text{HCO}_3^-$	21.34
21	$\text{PbO} \cdot 0.3\text{H}_2\text{O} + 2\text{H}^+ \rightarrow \text{Pb}^{2+} + 1.33\text{H}_2\text{O}$	12.98
23	$\text{PbH}_2\text{PO}_4^+ \rightarrow \text{Pb}^{2+} + 2\text{H}^+ + \text{PO}_4^{3-}$	-21.07
24	$\text{PbHPO}_4(\text{aq}) \rightarrow \text{Pb}^{2+} + \text{H}^+ + \text{PO}_4^{3-}$	-15.48
25	$\text{Pb}_5(\text{PO}_4)_3(\text{OH})(\text{hydroxylpyromorphite}) + \text{H}^+ \rightarrow 5\text{Pb}^{2+} + \text{H}_2\text{O} + 3\text{PO}_4^{3-}$	-62.79
26	$\text{Pb}_3(\text{PO}_4)_2 \rightarrow 3\text{Pb}^{2+} + 2\text{PO}_4^{3-}$	-43.53
27	$\text{PbHPO}_4 \rightarrow \text{Pb}^{2+} + \text{H}^+ + \text{PO}_4^{3-}$	-23.81

Note: All reactions and constants are from Visual MINTEQ default database: NIST Standard Reference Database 46.

Table A6.6 Reduction half-reactions associated with lead(IV) oxide interactions with free chlorine.

#	Reaction	E ⁰ (V vs SHE)	Log K
1	$\text{Pb}^{2+} + 2\text{e}^{-} \rightleftharpoons \text{Pb}^0$	4.25	0.13
2	$\text{PbO}_2 \text{ (Plattnerite)} + 4\text{H}^{+} + 2\text{e}^{-} \rightleftharpoons \text{Pb}^{2+} + 2\text{H}_2\text{O}$	1.47	49.60
3	$\text{HOCl} + \text{H}^{+} + 2\text{e}^{-} \rightarrow +\text{Cl}^{-} + \text{H}_2\text{O}$	1.48	50.20
4	$\text{NH}_2\text{Cl} + \text{H}_2\text{O} + 2\text{e}^{-} \rightarrow +\text{Cl}^{-} + \text{OH}^{+} + \text{NH}_3$	0.69	23.303

Note: All reactions and constants are from Visual MINTEQ default database: NIST Standard Reference Database 46.

Table A6.7 Reactions associated with planerite (β - PbO_2) dissolution

#	Reaction	Log K
1	$\text{PbO}_{2(\text{s})} \text{ (Planerite)} + 4\text{H}^{+} \rightarrow \text{Pb}^{4+} + 2\text{H}_2\text{O}$	-8.91
2	$\text{Pb}^{4+} + 3\text{H}_2\text{O} \rightarrow \text{PbO}_3^{2-} + 6\text{H}^{+}$	-23.04
3	$\text{Pb}^{4+} + 3\text{H}_2\text{O} \rightarrow \text{PbO}_4^{4-} + 8\text{H}^{+}$	-63.80

Note: The solubility and hydrolysis constants were calculated by Gibbs free energies from Pourbaix, (1996).

Table A6.8 DIC, pH for PWSs and their calculated values for Pb-C solids formation.

PWSs	DIC	pH	Pb-C solids	Pb-C solids
A-1	0.2	10.2	Hc	Hc
A-2	0.2	10.2	Hc	Hc
A-3	0.2	10.2	Hc	Hc
B	0.8	8.5	Hc	C and Hc
C	1.6	7.7	C	C and Hc
D-1	0.8	8.5	Hc	C and Hc
E	1.8	7.9	Hc	Hc
G	2.2	7.7	C	Hc
H-1	2.1	8.1	Hc	C and Hc
H-2	2.1	8.1	Hc	C and Hc
H-3	2.1	8.1	Hc	C and Hc
I	2.0	7.6	C	Hc
J	1.5	8.9	Hc	Hc
K	1.6	8.7	Hc	C and Hc
L	3.3	8.5	Hc	C and Hc
M	1.6	8.0	Hc	Hc
N	1.8	8.5	Hc	C and Hc
O	1.0	9.6	Hc	C and Hc
P	0.9	7.8	Hc	C and Hc
1-OH	0.9	9.9	Hc	Hc
2-OH	1.4	8.8	Hc	Hc
3-OH	0.6	8.8	Hc	Hc
4-IN	0.7	8.8	Hc	Hc
5-OH	1.5	8.5	Hc	Hc
6-IN	2.1	7.9	Hc	C and Hc
7-IL	4.0	7.8	C	C
8-WI	2.3	7.8	C	C and Hc
9-IL	9.5	7.5	C	C and Hc
10-WI	6.5	7.4	C	C
11-WI	5.2	7.6	C	C and Hc
12-OH	1.8	7.5	C	Hc
13-IL	2.1	7.8	C	C and Hc
14-IL	2.1	7.8	C	C and Hc
15-IL	6.0	7.4	C	C
16-MI	2.3	7.5	C	C and Hc
17-MI	0.6	9.4	Hc	Hc
18-MI	1.4	7.5	C	C and Hc
19-OH	1.1	7.7	Hc	Hc
20-WI	2.3	7.9	Hc	C and Hc
21-WI	6.8	7.5	C	C and Hc
22-WI	2.2	7.7	C	C and Hc

Note: "C" represents cerussite and "Hc" represents hydrocerussite.

Table A6.9 Free chlorine concentration for PWSs and the required and calculated Eh for PbO₂ formation

PWSs ID	Free chlorine concentrations (mg/L)	Eh required to form PbO ₂ (mV)	Calculated Eh (mV)	PbO ₂ solids Prediction	PbO ₂ solids Formation
A-1	1.0	582	1052	Y	Y
A-2	1.0	582	1052	Y	Y
A-3	1.0	582	1052	Y	Y
B	0.8	723	1053	Y	Y
C	0.9	866	1222	Y	Y
D-1	1.3	728	1162	Y	N
D-2	1.3	728	1162	Y	N
E	2.4	795	1199	Y	Y
F	1.8	765	1202	Y	Y
G	1.3	814	1203	Y	N
H-1	1.4	776	1182	Y	N
H-2	1.4	776	1182	Y	N
H-3	1.4	776	1182	Y	N
I	1.0	878	1232	Y	N
M	1.1	809	1199	Y	Y
N	1.3	878	1231	Y	Y
1-OH	1.7	612	1081	Y	N
2-OH	1.1	708	1134	Y	Y
3-OH	0.3	698	1109	Y	N
5-OH	0.8	738	1153	Y	N
7-IL	1.3	806	1189	Y	N
8-WI	0.5	786	1192	Y	N
9-IL	0.2	847	1172	Y	Y
10-WI	0.2	855	1185	Y	Y
11-WI	0.2	829	1175	Y	N
12-OH	0.9	829	1207	Y	N
13-IL	0.8	807	1195	Y	Y
14-IL	0.8	802	1196	Y	N
16-MI	1.3	827	1211	Y	N
18-MI	0.7	827	1207	Y	Y
20-WI	0.5	798	1180	Y	N
21-WI	0.6	843	1220	Y	N
22-WI	0.8	816	1198	Y	N

Note: “Y” indicates that the mineral was identified in prediction or in the system; “N” indicates that the mineral was not identified in prediction or in the system.

Table A6.10 Phosphate type, dosing concentration for PWSs and the calculated orthophosphate threshold for Pb-P solids formation.

PWSs ID	Phosphate type	Orthophoto dosing concentration	Orthophosphate to form Pb-P solid	Pb-P solids Prediction	Pb-P solids Formation
A-2	Orthophosphate	1.3	1.1	Y	Y
A-3	Orthophosphate	2.5	1.1	Y	Y
D-1	Orthophosphate	1.8	0.1	Y	Y
D-2	Orthophosphate	3.0	0.1	Y	Y
E	Orthophosphate	0.2	0.1	Y	Y
G	Blended phosphate	0.7	0.2	Y	Y
H-1	Blended phosphate	1.0	0.7	Y	N
H-2	Orthophosphate	1.5	0.7	Y	N
H-3	Orthophosphate	3.0	0.7	Y	Y
I	Blended phosphate	0.3	0.3	Y	Y
P	Zinc phosphate	1.4	0.1	Y	Y
13-IL	Blended phosphate	0.5	0.4	Y	N
14-IL	Blended phosphate	0.3	0.4	N	N
15-IL	Blended phosphate	0.3	2.4	N	N
16-MI	Blended phosphate	1.1	0.4	Y	N
17-MI	Orthophosphate	0.2	2.7	N	N
18-MI	Orthophosphate	3.1	0.2	Y	N
19-OH	Zinc phosphate	1.2	0.2	Y	Y
20-WI	Blended phosphate	0.2	0.5	N	N
21-WI	Blended phosphate	0.2	3.0	N	Y
22-WI	Orthophosphate	0.5	0.4	Y	Y

Note: “Y ” indicates that the mineral was identified in prediction or in the system; “ N ” indicates that the mineral was not identified in prediction or in the system.